INVESTIGATION INTO THE MOLECULAR MECHANISMS OF IMPORT OF MITOCHONDRIAL SMALL TIM PROTEINS

A thesis submitted to the University of Manchester for the degree of

Ph.D.

in the Faculty of Life Sciences

2012

Romina Durigon

CONTENTS

LIST OF FIGURES

LIST OF TABLES

ABSTRACT

"Investigation into the molecular mechanisms of import of mitochondrial small Tim proteins"

2012-09-27

Protein import is essential for the biogenesis of mitochondria, as the majority (99%) of mitochondrial proteins are synthesised in the cytosol and thus, have to be imported into mitochondria for their function. The biogenesis of many cysteine-containing proteins of the mitochondrial intermembrane space (IMS), such as members of the small TIM and Cox17 families, is regulated by their thiol-disulphide redox state. Only the Cys-reduced precursors can be imported into mitochondria, whereas oxidised forms cannot. Their import and oxidative folding in the IMS is driven by the IMS disulphide relay system, known as mitochondrial import and assembly (MIA) pathway, whose central components are the oxidoreductase Mia40 and the sulphydryl oxidase Erv1.

Currently, little is known about how the MIA precursors are maintained in the cytosol in an import-competent form, and whether they interact with the translocase of the outer membrane (TOM complex) to enter the IMS. In addition, the MIA-mediated protein folding events occurring in the IMS that lead to the generation of fully oxidised substrates are still under investigation. Using Tim9 and yeast as models, studies presented in this thesis showed that Tim9 binding to the mitochondrial outer membrane (OM) does not depend on the receptors of the TOM complex, and occurs without regard to the redox state of the precursor proteins. In addition, it is shown that the oxidised and reduced precursors share the same binding site on the OM, and that this binding site is not important for the translocation process across the OM (Chapter 3). Studies in this thesis investigated the role of the cytosolic thioredoxin and glutaredoxin systems in the biogenesis of mitochondria. Firstly, *in vivo* studies provided the evidence that the cytosolic thioredoxin system but not the glutaredoxin system is required for growth of yeast cells under respiratory conditions. Secondly, *in vivo* studies provided the first proof that the Trx system is required for the biogenesis of small Tim proteins. *In vitro* studies confirmed that the Trx1 system facilitates import of small Tim proteins into isolated mitochondria by maintaining the precursors in a reduced and therefore competent form (Chapter 5). Finally, *in vitro* studies showed that Mia40 is able to promote the full oxidation of Tim9. Efficient release of Tim9 from Mia40 required the presence of all cysteine residues of Tim9, as effective oxidation and concomitant release from Mia40 failed upon mutation of single cysteine residues. Finally, the study showed that reduced glutathione resolved rapidly the Mia40-Tim9 mixed-disulphide complexes, probably accelerating and/or promoting the Tim9 oxidative (Chapter 4).

DECLARATION

No portion of the work referred to in this thesis has been submitted in support of an application for another degree or qualification of this or any other university or other institute of learning.

COPYRIGHT STATEMEMENT

I. The author of this thesis (including any appendices and/or schedules to this thesis) owns certain copyright or related rights in it (the "Copyright") and s/he has given The University of Manchester certain rights to use such Copyright, including for administrative purposes.

II. Copies of this thesis, either in full or in extracts and whether in hard or electronic copy, may be made only in accordance with the Copyright, Designs and Patents Act 1988 (as amended) and regulations issued under it or, where appropriate, in accordance with licensing agreements which the University has from time to time. This page must form part of any such copies made.

III. The ownership of certain Copyright, patents, designs, trade marks and other intellectual property (the "Intellectual Property") and any reproductions of copyright works in the thesis, for example graphs and tables ("Reproductions"), which may be described in this thesis, may not be owned by the author and may be owned by third parties. Such Intellectual Property and Reproductions cannot and must not be made available for use without the prior written permission of the owner(s) of the relevant Intellectual Property and/or Reproductions.

IV. Further information on the conditions under which disclosure, publication and commercialisation of this thesis, the Copyright and any Intellectual Property and/or Reproductions described in it may take place is available in the University IP Policy (see http://documents.manchester.ac.uk/DocuInfo.aspx?DocID=487), in any relevant Thesis restriction declarations deposited in the University Library, The University Library's regulations (see http://www.manchester.ac.uk/library/aboutus/regulations) and in The University's policy on Presentation of Theses.

ACKNOWLEDGEMENTS

I would like to thank my supervisor Dr. Hui Lu for offering me a Ph.D. studentship in her Lab at the Faculty of Life Sciences of The University of Manchester. I want to thank her for all the help, support and guidance she gave me throughout the project. I also thank Hui for her precious teachings that I will keep with me forever.

I would like to thank all past and present members of the Lu Lab, particularly Efrain, Liang, Michael, Peter, Qi and Swee Kim for the time we spent together, your help and our Monday-journal clubs. A special thank goes to Michael for proof-reading all my thesis! Thanks also to Swee Kim who gave me helpful comments on the 4th chapter.

A particular thank goes to the BBSRC for funding my Ph.D. project, and for giving me the opportunity to attend the "2011 Enterprise Programme" in Cambridge. I would like also to thank my advisor Dr. Martin Pool for his helpful advices and comments on my project. I would like to thank also everyone in the Bayat, Bella, Bulleid, Eyers, Flitsch, Golovanov, Grant, Hayes, High, Pool, Swanton, Schwappach and Turner groups, for letting me to use their instruments, for their help and the lovely time spent together. Thanks to the Faculty of Life Sciences for being an Institution of high scientific impact and giving me the opportunity to attend a wide range of scientific seminars. Thanks also to Dr. John Hughes, Senior experimental officer for the radioactive works in the MIB (Manchester Institute of Biotechnology).
A special thank goes to Prof Sally Temple, who is one of the best person I have ever met in my life.

Finally, thank to Who inspired and inspire my days every day, and to my big family: papá, mamma, Ulisse, Milena, Vanessa, Julian, Attila, Elisa, Davide, Anna, Alberto, Melissa, Maddalena, Jacopo, Jonathan and Ginevra, for their love and support even if thousands of miles far from me! I thank Vanessa and Julian for proof-reading my thesis. I thank my friends

This work is dedicated to my family and my grandparents.

LIST OF ABBREVIATIONS

A_{600}: Optical density measured at 600 nm
AAC: ATP/ADP Carrier
AMS: 4-acetomido-4'-maleimidylstilbene-2,2-disulphonic acid
ADP: Adenosine diphosphate
ATP: Adenosine triphosphate
Ahp1: Alkyl hydroperoxide reductase
ALR: Augmenter of liver regeneration
ATP: Adenosine 5^{I}-triphosphate
BSA: Bovin serum albumin
Ccs1: Copper chaperone superoxide dismutase 1
COX: Cytochrome c oxidase family
CCHL : Cytochrome c heme lyase
Cytb2: Cytochrome b2
Cytc: Cytochrome c
Ccp1: Cytochrome c peroxidase 1
Cpn10: mitochondrial Chaperonin10
DDP1: Deafness dystonia peptide 1
Dsb: disulphide bond formation protein
DTT: Dithiothreitol
EDTA: Ethylenediaminetetracetic acid
ER: Endoplasmic reticulum
Ero1: Endoplasmic reticulum oxidoreductin 1
Erv1: Essential for respiration and vegetative growth 1
FAD: Flavin adenine dinucleotide
F1-β: Subunit F1-β of the F1-ATPase complex
G-6-PDH: Glucose-6-phosphate dehydrogenase
Grx: Glutaredoxin
Glr1: Glutathione reductase 1
GSH: Reduced glutathione
GSSG: oxidised glutathione
GIP: General insertion pore
Hot13: Helper of Tims of 13 kDa
Hsp70: heat shock protein 70
IAA: 2-Iodoacetamide
IM: Inner membrane
IMS: Intermembrane space
ITS: IMS-targeting signal
MIA: Mitochondrial import assembly
Mia40: Mitochondrial import assembly 40
HLH: Helix-loop-helix
LM: Lactate medium
MDH: Malate dehydrogenase
MIM: Mitochondrial import of the outer membrane
MISS: Mitochondrial intermembrane space sorting
MPP: Mitochondrial=processing peptidase
mtHsp60/70: Matrix heat shock protein 60/70
MST: mitochondrial stimulating factor
MTS: Mohr-Tranebjaerg syndrome

NADH: reduced Nicotinamide adenine dinucleotide
NADP: reduced Nicotinamide adenine dinucleotide phosphate
NEM: N-ethylmaleimide
OM: Outer membrane
Oxa1: Oxidase assembly 1
PAM: Presequence translocase-associated motor
PAPS: 3^{I}-phosphoadenosine 5^{I}-phosphosulphate
PDI: Protein disulfide isomerase
PMSF: Phenyl methane sulphonyl fluoride
ROS: Reactive oxygen species
RT: room temperature
SAM: Sorting assembly machinery
SBTI: Soya-bean trypsin inhibitor
SDS: Sodium dodecyl sulphate
SDS-PAGE: Sodium dodecyl sulphate-polyacrylamide gel electrophoresis
SOD1: Superoxide dismutase 1
Su9-DHFR: Subunit 9-dihydrofolate reductase
TCEP: Tris(2-carboxyethyl)phosphine hydrochloride
TIM: Translocase of the IM
TOB: Topogenesis of mitochondrial OM β-barrel proteins
TOM: Translocase of the OM
Trx: Thioredoxin
Trr: Thioredoxin reductase
Tsa1: Thioredoxin peroxidase
yAP-1: Yeast activator protein- 1
YPD: Yeast extract, peptone, dextrose
YPEG: Yeast extract, peptone, ethanol, glycerol
YPG: Yeast extract, peptone, glycerol
WT: Wild type

1. INTRODUCTION

The mitochondrion (from Greek *mitos*, warp thread, and *khondrion,* grain or granule, meaning “small grain”), also called “*chondrosome*”, is considered a universal organelle within the eukaryotic kingdom, though mature erythrocytes and the protist *Entamoeba histolytica* lack it. According to Margulis’s endosymbiotic theory, mitochondria are direct descendants of a α-protobacterium that inhabited the cytosol of a nucleus-containing proto-eukaryotic host cell (Margulis 1970; Gray *et al.,* 1999).

Mitochondria are involved in many cellular processes. In addition to the generation of ATP (adenosine triphosphate) through oxidative phosphorylation, they house a large number of biosynthetic pathways (i.e. synthesis of amino acids, lipids and heme), and are involved in iron-sulfur cluster biogenesis, calcium homeostasis, generation and detoxification of reactive oxygen species (ROS), as well as in the control of cell growth and apoptosis. Thus, not surprisingly, mitochondrial dysfunction is associated with a broad range of human diseases, including diabetes, cardiovascular diseases and Parkinson’s disease, as well as process of ageing and cancer.

1.1. Mitochondrial structure

Mitochondria are generally described as static, rod-shaped structures ranging from 2 to 8 micrometres scattered throughout the cytoplasm. Mitochondrial morphology and abundance in cells usually depends on the specialized energy needs. For example, animal myocardic cells contain more mitochondria than cells of the kidney’s parenchyma. Mitochondrial morphology can also vary during the cell cycle: the yeast *Saccharomyces cerevisiae* contains a single

long tubular mitochondrion when cells divide or numerous small round mitochondria when cells are mature (Yaffe 2003).

Mitochondria are characterized by two membranes, the outer and the inner membrane (OM and IM, respectively). The two membranes delimit two aqueous compartments, the intermembrane space (IMS) between the OM and the IM and the matrix enclosed by the IM (Figure 1.1).

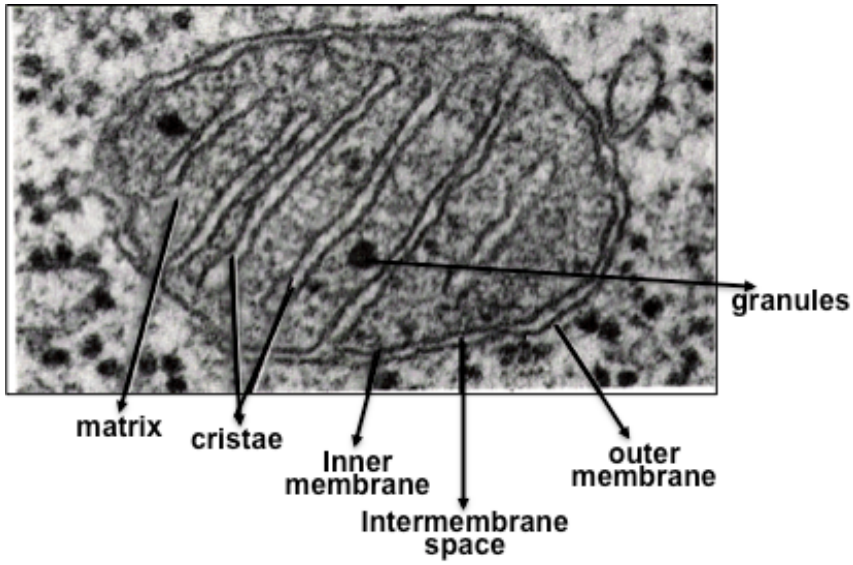

Figure 1.1: The structural features of mitochondria.

Electron micrograph *in situ* showing the major structural characteristics of a mitochondrion: the size of the organelle can vary form 0.5 micrometers to 10 micrometers. It generally presents a pair of double lipid by-layers, the OM and the IM, which enclose the narrow aqueous sub-compartment named IMS. The IM delimits the innermost space, known as matrix, and is highly folded into this space creating structures named cristae. The matrix is a solute-rich environment containing the mitochondrial DNA and granules. *Mitochondrial structure.* Digital image. Lecture Outline on line by Professor James Nishiura. Web. <*http://academic.brooklyn.cuny.edu/biology/bio4fv/page/mito.htm* >.

The OM is a semipermeable barrier prevalently enriched by porins that allow the free passage from/to cytosol of ions or up to 5-6 kDa small molecules.

The IMS occupies 5% of the total mitochondrial volume, and it originated from the periplasm of bacteria. It houses proteins involved in the assembly of respiratory chain components, in apoptotic signalling and protein import. The solute environment of the IMS is thought be similar to that of the cytosol due to the semipermeability of the OM.

The IM has a very high protein to phospholipids ratio (3:1) and is impermeable to molecules and even small ions. Thus, it contains multi-subunit complexes involved in solute and protein transport, in the generation of ATP (ATP synthase) and in electron transport (cytochromes). The peculiarity of the IM is the folding into the *cristae mitochondrialis*, which enhance its surface area and thus the ability to produce ATP. The matrix contains about one third of the total amount of mitochondrial proteins, since the majority of mitochondrial processes occur in the matrix (e.g. oxidation of pyruvate, of fatty acids, and Krebs' cycle). The matrix is also the storage space for cellular calcium, contains one to ten copies of the circular mitochondrial DNA (mtDNA) and the machinery for RNAs biosynthesis. The solute environment of the matrix is dependent on the solutes and proteins transported across the IM.

1.2 Mitochondrial biogenesis

According to the endosymbiotic theory, during the gradual transformation from bacterial endosymbiont to intracellular organelle, the symbiont transferred most of its genes into the host nucleus. As a result, the actual mitochondrial genome is severely reduced in size in comparison to their α-proteobacterial ancestors

(Burger *et al.*, 2003; Perry *et al.*, 2008). To date, it has been estimated that the mtDNA encodes for ~1% of the 800 or 1500 yeast or human mitochondrial proteins respectively, whilst the remaining ~99% of mitochondrial proteins is encoded by the nuclear DNA (McKenzie *et al.*, 2004; Mokranjac and Neupert, 2008). Hence, mitochondrial biogenesis requires the integration of various processes and machineries enabling the transport of precursor proteins from the cytosol to the specific mitochondrial sub-compartments (Figure 1.2). The process begins with synthesis of mitochondrial mRNAs on free cytosolic ribosomes. Based on the mitochondrial targeting signal present in the primary sequence, the precursor proteins (or precursors) associate with specific cytosolic factors that prevent their aggregation and degradation. For example, the 70 kDa Heat-shock protein (Hsp70) or the mitochondrial stimulating factor (MSF) bind to the matrix- or IM-targeted proteins, respectively (Hachiya *et al.*, 1993; Young *et al.*, 2003). Both chaperones and mitochondrial targeting signals mediate the targeting and binding of the precursors to the mitochondrial OM. Import and subsequent intra-mitochondrial sorting are mediated by membrane-protein machineries, called translocases, of the OM and IM and by soluble factors of the IMS and the matrix (Neupert 1997; Pfanner and Geissler, 2001; Neupert and Herrmann, 2007). Once they have reached their final destination, proteins fold and acquire their native conformations. A few studies have suggested that mitochondrial precursor proteins are imported in a co-translational manner; in this case, mechanisms exist that direct the mitochondrial mRNAs to the surface of mitochondria where they are translated by OM-bound ribosomes and at the same time imported into the organelle (Corral-Debrinski *et al.*, 2000; Marc *et al.,* 2002).

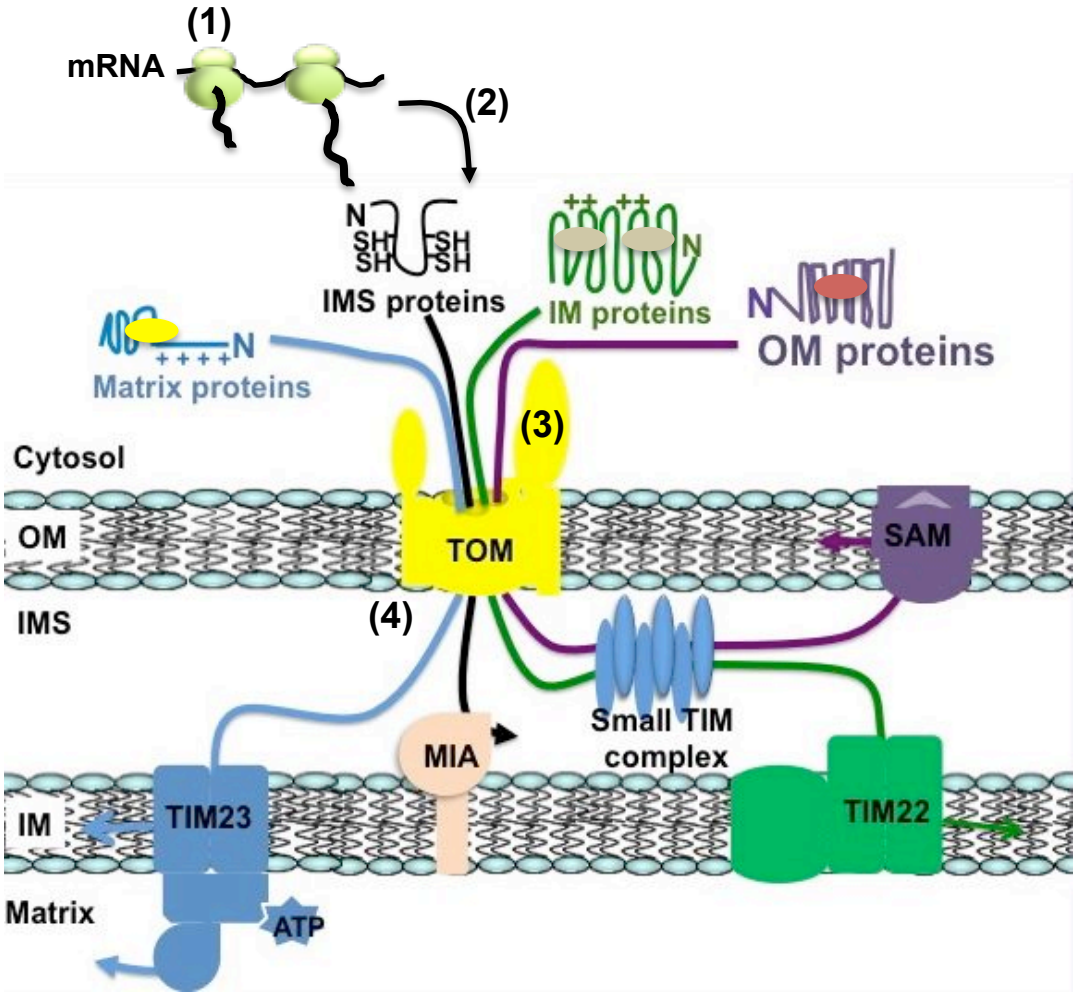

Figure 1.2: General overview about the mitochondrial protein biogenesis.

About 99% of mitochondrial proteins are synthesized on cytosolic ribosomes (1). After their translation, cytosolic chaperones and/or factors bind to the precursor proteins escorting them to the mitochondrial OM (2). The precursors then interact with the receptors of the translocase of the OM, the TOM complex and use the channel of the TOM complex as main entry gate into mitochondria (3). Once crossed the OM, there exist four different sorting pathways directing the preproteins into their final mitochondrial sub-compartments (4): precursor proteins destinated to the matrix use the TIM23 translocase; preproteins destinated to the IM use the soluble IMS small TIM complex that chaperones them to the TIM22 machinery; preproteins of the OM use both the small TIM complex and the SAM complex of the OM for insertion into the OM; lastly, small cysteine-rich preproteins of the IMS use the MIA machinery to be imported into the IMS. (TOM, Translocase of the OM; TIM23, Translocase of the IM built around Tim23; small TIM complex, small Translocase of the IM; TIM22, Translocase of the IM built around Tim22; SAM, Sorting and Assembly Machinery; MIA, Mitochondrial Import and Assembly). Figure adapted from Mokranjac and Neupert (2009).

1.2.1 The mitochondrial targeting signals

Mitochondrial precursors carry in their primary sequences a targeting signal that directs them to mitochondria. On the basis of the mitochondrial-targeting signal, mitochondrial precursors are typically divided into two main groups:

1) ~70% of mitochondrial precursors contain the cleavable *N-terminal targeting presequence* that is an extension of about 10-80 amino acids rich in basic and hydroxylated amino acids (Pfanner and Geissler, 2001). The N-terminal presequence is usually cleaved by the mitochondrial matrix peptidase (MPP) as soon as the precursors reach the matrix. Nearly all matrix-, some IM- and IMS-precursor proteins carry an N-terminal presequence.

2) ~30 % of precursor proteins do not contain a cleavable presequence, but contain distinct and multiple segments known as *multiple internal targeting signals* within their mature sequence. Such proteins include the polytopic IM proteins (e.g. ATP/ADP and metabolite carriers), most of the IMS proteins (e.g. small Tim proteins, Cytochrome c heme lyase) and all the OM proteins (e.g. Tom40, Tom5, Bcl2 and Porin).

Without regard to the type of mitochondrial targeting signal, all mitochondrial precursors enter mitochondria trough the translocase of the OM, the TOM complex (translocase of the OM), and then they make use of their specific sorting pathways to reach the final destination (Hoogenraad and Ryan, 2001; (Neupert 1997). Most of the knowledge about mitochondrial protein import derives from studies in the fungi *Neurospora crassa* and *S. cerevisiae*, but similar mechanisms and components are conserved in animals and plants. In

the next sections, the TOM complex and the different mitochondrial sorting pathways present in the yeast *S.cerevisiae* will be briefly described.

1.2.2 The TOM complex: the translocase of the outer membrane

The TOM complex is the main entry gate for all nuclear-encoded mitochondrial precursors into mitochondria. It interacts with chaperones and associated precursors to allow translocation into mitochondria. The TOM complex is composed of at least 7 components, and is commonly subdivided into two functional parts, the receptors and the pore components (Figure 1.3).

Receptor components include Tom70, Tom20 and Tom22 (70-kDa, 20-kDa and 22-kDa, respectively). Tom70 and Tom20 are both integrated into the OM with a single N-terminal transmembrane domain and expose their receptor domains to the cytosol. Tom22 exposes its N-terminal domain to the cytosol and a short C-terminus to the IMS. The N-terminal presequence preproteins bind to Tom20, whereas precursors with multiple internal targeting signal bind to Tom70. Both Tom20 and Tom70 pass the precursors to Tom22, which assists the transfer of the precursors from the receptors to the pore of the TOM complex (Kiebler *et al.*, 1993; van Wilpe *et al.,* 1999; Saitoh *et al.,* 2007; Chacinska *et al.,* 2009).

The pore-components of the TOM complex are Tom40 and the three small subunits Tom5, Tom6 and Tom7 (Dekker *et al.,* 1998). Tom40 is probably a β-barrel, and is the only subunit of the TOM complex to be essential for cell viability (Baker *et al.,* 1990). The small subunits Tom5, Tom6 and Tom7 have a single α-transmembrane domain and are tightly associated with Tom40.

Together with Tom22, they form the 400 kDa conducting channel, called the general insertion pore (GIP; van Wilpe *et al*., 1999; Wiedemann *et al*., 2003; Meisinger *et al*., 2004). Tom40 forms the pore of the complex whose estimated diameter (~20 Å) is large enough to allow the passage of two polypeptide segments in a loop conformation (Künkele *et al.,* 1998). Tom6 and Tom7 mediate channel dynamics, while Tom5 promotes assembly of the TOM complex and functions as a linker between the receptors and the GIP of the complex (Alconada *et al*., 1995; Dietmeier *et al*., 1997; Kurz *et al*., 1999).

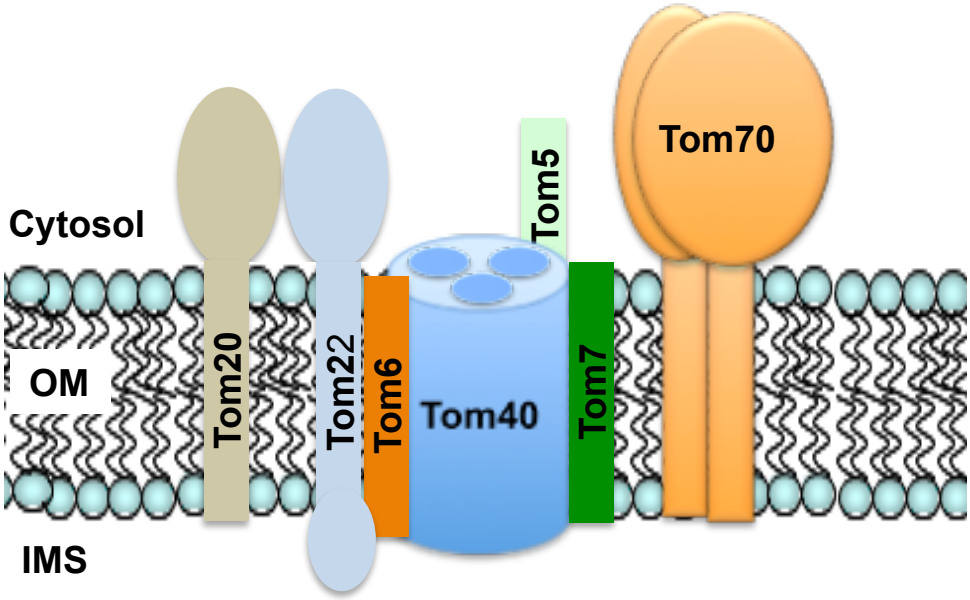

Figure 1.3: Composition of the TOM complex of the OM.

The TOM complex consists of the pore components and of the receptors subunits Tom70, Tom20 and Tom22. The channel-forming subunit Tom40 and three low molecular weight Tom5, Tom6 and Tom7 subunits are the pore components. Tom70 and Tom20 are integrated in the OM with a single N-terminal transmembrane domain and expose their receptor domains into the cytosol. Tom22 exposes also its short C-terminal domain to the IMS. Adapted from Neupert and Herrmann (2007).

Based on the “binding chain hypothesis”, the driving force allowing the translocation of precursors trough the TOM complex is mediated by the

presence of a chain of binding sites (Komiya *et al.,* 1998; Kanamori *et al.,* 1999; Esaki *et al.,* 2003, 2004; Chacinska *et al.,* 2005). The cytosolic domains of Tom70, Tom20 and Tom22 represent the so-called *cis*-binding sites, which promote the further passage of the precursors into the Tom40 channel, perhaps via Tom5 (Rapaport *et al.,* 1997). Inside the channel, Tom40 may interact via hydrophobic interactions with the translocating precursors, favouring unfolding and further passage to the *trans*-binding site of the complex. Tom40, the IMS domains of Tom22 and Tom7 may contribute to the *trans*-binding site (Mayer *et al.,* 1995). In this way, the TOM complex functions as chaperone that prevents unfolding and aggregation of the precursors and promotes their translocation across the OM (Rapaport *et al.,* 1998; Esaki *et al.,* 2003).

1.2.3 The import of matrix proteins

Matrix-targeted precursor proteins with the classical N-terminal presequence follow the TIM23 pathway. Being one of the most complicate import pathways, the molecular mechanisms of action of the TIM23 pathway are still under investigation. It requires the cooperation of the IM translocase TIM23 (translocase of the IM built around Tim23 subunit) with the TOM complex, the mitochondrial respiratory chain, as well as two different energy sources: the electrochemical potential (Δψ) across the IM and the hydrolysis of ATP.

The TIM23 complex is formed by 2 separate subgroups: the $TIM23_{core}$ embedded in the IM that forms the channel of the complex, and the import motor or presequence translocase-associated motor (PAM) that drives the translocation into the matrix. Tim23, Tim17 and Tim50 are the three essential proteins of $TIM23_{core}$, whilst Tim21 is dispensable (Chacinska *et al.,* 2005).

Tim50, the receptor subunit of the $TIM23_{core}$, interacts with the incoming precursors as they reach the *trans*-side of the TOM complex and, helps to pass them to the channel of the TIM23 complex formed by Tim23 and Tim17 subunits (Chachinska *et al.,* 2005; Meinecke *et al.,* 2006; Gevorkyan-Airapetov *et al.,* 2009; Mokkranjac *et al.,* 2009; Tamura *et al,* 2009). The translocation of the presequence into the matrix requires Δψ, whereas the inward movement of the precursor proteins themselves is driven by the PAM complex and requires ATP.

In the matrix, the motor subunit Tim44, which is peripherally associated with the channel, recruits to the import site the ATP-bound form of the chaperone heat shock protein mtHsp70, which binds to the translocating chains (Hutu *et al.,* 2008; D'Silva *et al.,* 2004). Upon ATP hydrolysis mediated by the subunit Tim14 of the motor complex, ADP-bound mtHsp70 tightly binds to the preprotein and dissociates from Tim44 (Schneider *et al.,* 1996; Liu *et al.,* 2003; Mokranjac *et al.,* 2003). Finally, mtHsp70 is released from the chain upon exchange of the bound ADP with ATP, mediated by the nucleotide exchange factor Mge1 (Schneider *et al.,* 1996; Liu *et al.,* 2003). Repeated mtHsp70-binding cycles drive the complete translocation of the precursors into the matrix, where the presequence is proteolytically removed by the mitochondrial-processing peptidase (MPP; Braun and Schmitz, 1997; Gakh *et al.,* 2002; Figure 1.4). Other components of the PAM complex are Pam16, which associates with Tim14 to regulate its activity, and Pam17 that participates in the organization of the TIM23-PAM interaction before the arrival of the incoming precursor proteins (Kozany *et al.,* 2004; Frazier *et al.,* 2004; Hutu *et al.,* 2008).

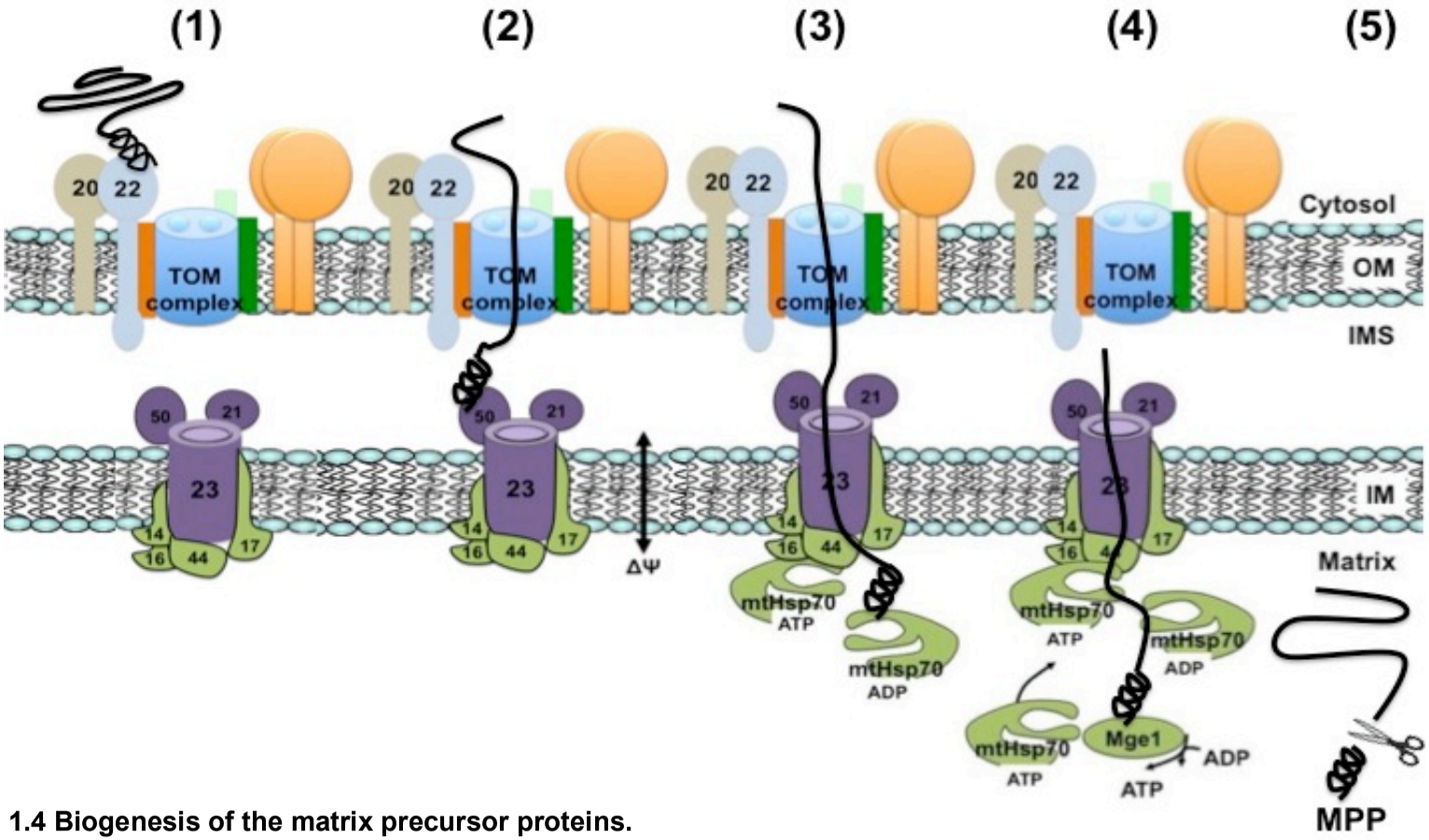

Figure 1.4 Biogenesis of the matrix precursor proteins.

Matrix precursor proteins are recognized by Tom20 and Tom22, which transfer them to Tom40 for the translocation across the OM **(1)**. As the preproteins emerge from the GIP of the TOM complex, they serially bind to the IMS domains of Tom7, Tom22, Tom40 and Tim50, and are then transferred to the channel of the TIM23 complex. Preprotein initiates to cross the IM in a membrane potential-dependent manner **(2)** . As soon as the preproteins reach the matrix, the motor subunit Tim44 recruits to the import site the ATP-bound form of mtHsp70, which associates with the incoming precursors **(3)** . ATP hydrolysis causes mtHsp70 release from Tim44 and tight association of mtHsp70 with the preproteins. Mge1 promotes the dissociation of ADP from mtHsp70 allowing binding of a new molecule of ATP to mtHsp70, and thus a new cycle of the ATP-dependent translocation process. Repeated cycles of mtHsp70 binding and release from Tim44 help to complete import of the preproteins into the matrix **(4)** . Finally once into the matrix, the N-terminal presequence is cleaved by MPP (Matrix Processing Peptidase) **(5)**. Adapted from Neupert and Herrmann (2007).

1.2.4 The import of inner membrane proteins

Import and insertion of the IM precursors is believed to follow three different pathways based on the type of mitochondrial targeting signal present in the precursors:

i) The Stop-transfer pathway: substrates of this pathway include IM preproteins containing a presequence followed by one transmembrane domain and adopting a N_{in}-C_{out} topology in the IM (Duhl *et al.,* 1990). The pathway is considered as a variation of the TIM23 import pathway, as the substrates are halted in the TIM23 translocase and inserted laterally into the IM in a Δψ-dependent manner via a mechanism not currently understood in detail. The transmembrane domain functions as a critical sorting signal that arrests the precursors in the IM. Examples are the yeast Mia40, subunit 5a of the cytochrome oxidase (Cox5a) and Tim50 (Glaser *et al.,* 1990; Miller and Cumsky, 1993; Gärtner *et al.,* 1995; Chacinska *et al.,* 2008; Figure 1.5, A).

ii) The conservative pathway: substrates of this pathway are the IM precursors with the presequence followed by multiple membrane spanning domains. They are imported into the matrix via the TIM23 pathway, and from the matrix they are re-exported to the IM by the OXA1 complex of the IM (Hell *et al*., 1998; Hell *et al*., 2001; Figure 1.5, B) in a reaction that is still poorly defined. Because the direction of this pathway resembles that of the prokaryotic ancestors of mitochondria, this pathway is called the *Conservative sorting* pathway. Examples are Cox18 and Yta10 (for details see review by Hermann and Neupert, 2003).

iii) The TIM22 pathway: all known substrates of this pathway lack the presequence, contain even-numbered transmembrane segments and expose both the N- and C-termini in the IMS The TIM22 pathway uses the TOM complex, the soluble IMS small TIM complexes and the translocase of the IM TIM22 (translocase of the IM built around Tim22 subunit) in successive steps, and depends on the Δψ. The TIM22 translocase is a 300kDa complex that consists of the three IM embedded proteins Tim22, Tim54 and Tim18, and the peripheral bound Tim9-Tim10-Tim12 complex (Sirrenberg *et al.,* 1996; Sirrenberg *et al.,* 1998; Lionaki *et al.,* 2008). Tim54 and Tim18 are not essential for the function of the complex and their precise function is still unclear. Tim22, Tim12, Tim9 and Tim10 are all essential for yeast cell viability (Kovermann *et al.*, 2002; Hwang *et al*., 2007). The soluble IMS complex Tim9-Tim10 receives the polytopic precursors emerging from the TOM complex. Then, the loaded Tim9-Tim10 complex associates with Tim12 to transfer the precursor to the TIM22 machinery. The translocation and insertion into the IM depends on the Δψ, but the mechanisms are unknown (Figure 1.5, C). Examples are members of the metabolite carrier family (at least 34 in yeast *S. cerevisiae*) and the membrane-embedded subunits of the TIM machineries Tim17, Tim22, and Tim23 (Sirrenberg *et al.,* 1998; Káldi *et al.,* 1998; Endres *et al.,* 1999; Luciano et al, 2001; Zara *et al.,* 2001; Truscott *et al,* 2002). Although import of the TIM subunits is less well characterized, their import makes use of the IMS soluble Tim8-Tim13 complex instead of the Tim9-Tim10 complex (Leuenberger *et al.,* 1999; Davis *et al.,* 2000).

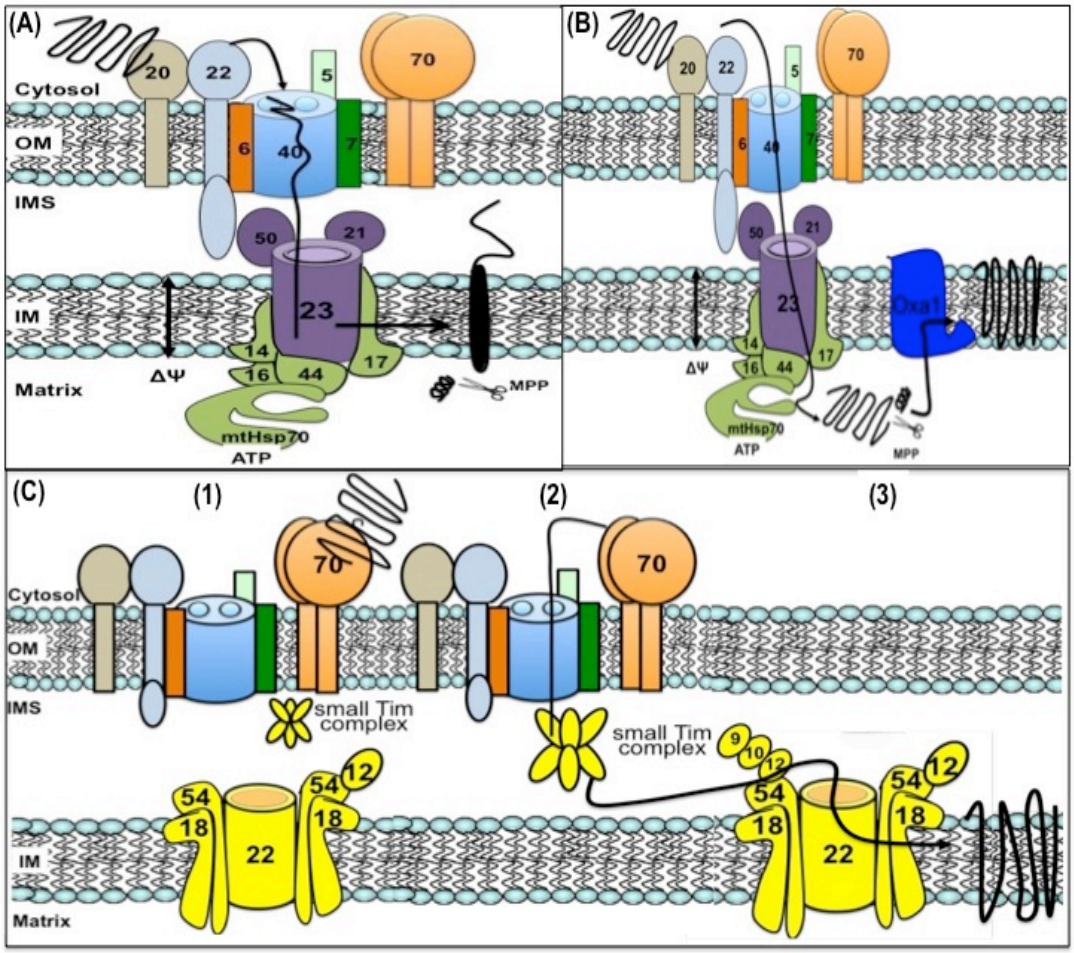

Figure 1.5 Biogenesis of the IM precursor proteins.

(A) IM preproteins containing the N-terminal presequence followed by only one transmembrane domain use a variation of the TIM23 pathway, named the Stop-Transfer pathway, to be inserted into the IM. The substrate is halted at the level of the TIM23 translocase and then laterally inserted into the IM in a membrane potential-dependent manner.
(B) IM preproteins containing a presequence followed by multiple membrane spanning domains follow the Conservative pathway, which includes the complete TIM23 pathway and the OXA1 complex. Once in the matrix, they are re-exported into the IM, whose insertion is facilitated by the OXA1 complex of the IM.
(C) All the other IM preproteins lacking a presequence and containing even-numbered transmembrane segments use the TIM22 pathway. The IM preproteins bind to the Tom70 receptor of the TOM complex, which transfers them to Tom40 (1). Once reached the IMS side of the TOM complex, the precursors bind to the IMS soluble small TIM complex, which escorts them across the IMS to the TIM22 translocase of the IM (2). The TIM22 complex inserts the preproteins laterally into the IM in a membrane-potential dependent manner (3) Figure adapted from Neupert and Herrmann (2007).

1.2.5 The import of outer membrane proteins

Proteins of the OM can be subdivided mainly into two classes that, as far as we know, use different pathways to be inserted into the OM. One class of the OM proteins is the β-barrel proteins, which are present exclusively in the membranes of mitochondria, chloroplasts and gram-negative bacteria. They use the TOB/SAM (topogenesis of mitochondrial OM β-barrel proteins/sorting and assembly machinery) import route. Examples of β-barrel proteins are Tom40 and porin. Precursors of the β-barrel proteins move through the TOM pore to insert into the membrane from the IMS site. Once in the IMS, they interact with the soluble small TIM complex, which guides them from the TOM to the TOB/SAM machinery of the OM (Wiedemann *et al.*, 2004). The TOB/SAM complex mediates then the insertion and assembly in the OM (Figure 1.6, A) (Paschen *et al.,* 2003; Wiedemann *et al.,* 2003, Becker *et al*., 2009).

The second class includes proteins that contain a single α-helical transmembrane domain (TMD). The TMD can be either at the C-terminus in a tail-anchored domain (e.g. Tom5 and Tom6), or at the N-terminus in a signal-anchored domain, or spanning across the OM (e.g. Tom70 and Tom20). The mechanisms that mediate import of these proteins are ill defined, although some of them depend on the SAM complex and MIM (mitochondrial import) complex of the OM (Figure 1.6, B; Stojanovski *et al.,* 2007; Becker *et al.*, 2008; Popov-Celeketić *et al.*, 2008; Dimmer *et al.,* 2012).

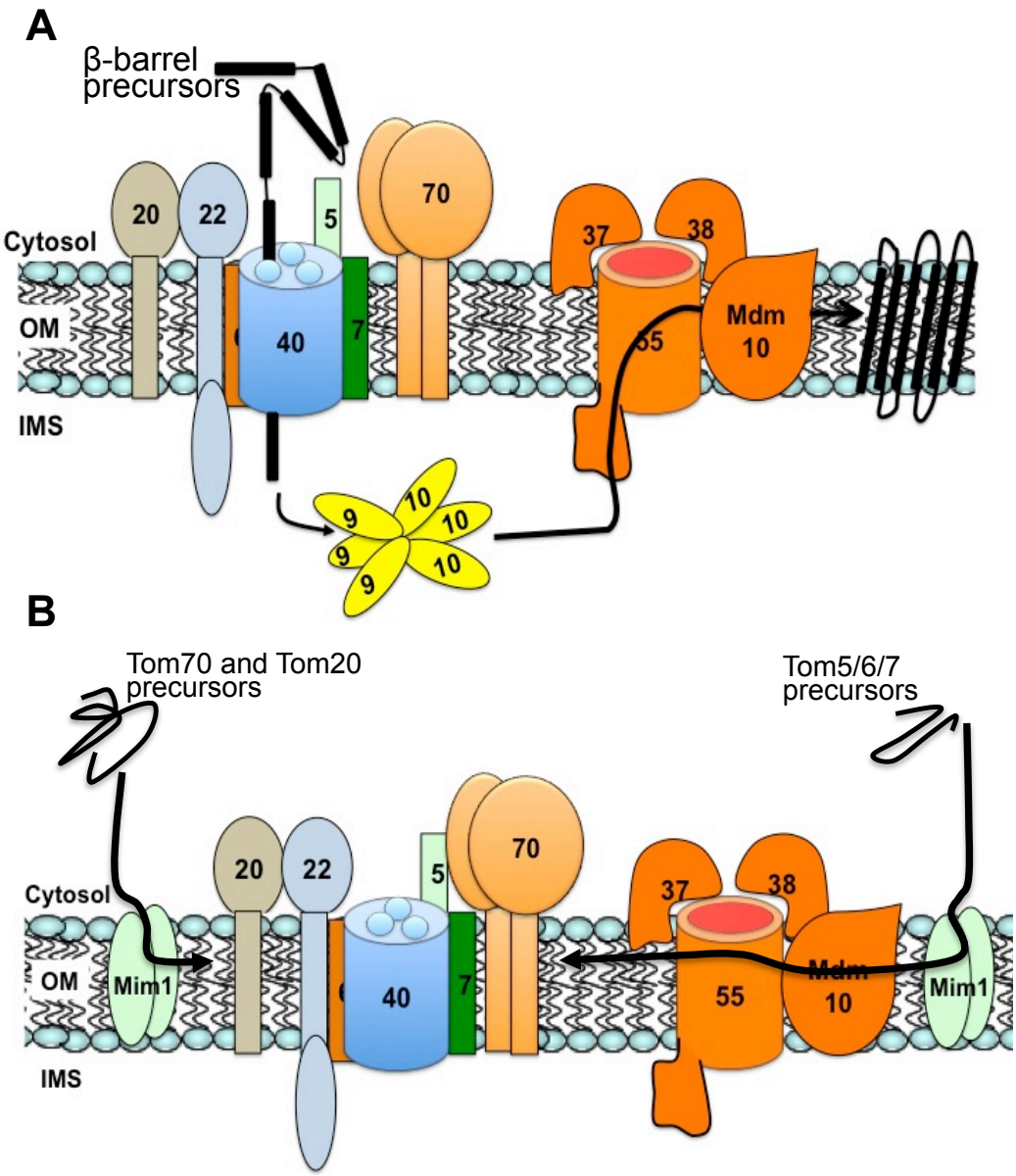

Figure 1.6 Biogenesis of the OM precursor proteins.

(A) The precursors of the β-barrel proteins (e.g. Tom40 and porin) translocate the OM by the TOM complex. Once at the IMS side of the TOM complex, they bind to the small TIM complex of the IMS, that chaperone them across the IMS to the SAM complex of the OM. Tom55 and the two peripheral associated subunits Tom37 and Tom38 form the core of the SAM complex, and together they insert the precursors into the OM. Mdm10 is an OM protein that associating with the SAM complex mediates the final steps of the TOM complex assembly.
(B) The biogenesis of the OM precursor proteins with a single α-helical transmembrane, such as the small Tom subunits Tom5, Tom6 and Tom7, use Mim1 and the SAM complex for their insertion and assembly into the TOM complex. Mim1 is also crucial for import of Tom20 and Tom70. Figure adapted from Becker *et al* (2009).

1.2.6 The import of intermembrane space proteins

The import of the 50-100 IMS precursors is believed to follow three different pathways (Figure 1.7).

i) Import of IMS proteins with bipartite presequence: the IMS precursors with a bipartite presequence are so named because they contain a canonical N-terminal cleavable sequence followed by a hydrophobic sorting sequence (Glick *et al.,* 1992). The import pathway is a variation of the stop-transfer pathway. Therefore, they embark on a stop-transfer pathway route to the IM and once they reach the TIM23 translocase, their hydrophobic region is arrested at the level of the IM and laterally integrated into the IM. This sorting intermediate is then recognized and cleaved by the IM peptidase complex, which separates the transmembrane domain from the mature, IMS soluble C-terminal part of the protein (Glick et al., 1992; Jan et al., 2000; Gakh et al., 2002; Mossmann *et al*, 2011). Examples of this group of proteins include Cytochrome b2 and Cytochrome c peroxidase (Figure 1.7A; Daum *et al,* 1982b).

ii) Import of IMS proteins via affinity binding sites: substrates belonging to this pathway lack a presequence. Their import does not depend on ATP nor on Δψ; instead these preproteins associate permanently with binding sites on the IMS side of the OM or the IM and the affinity for these factors seems to guide their net import across the OM (Neupert and Hermann, 2007). An example is cytochrome c lyase (Steiner *et al.,* 1995; Figure 1.7B).

iii**) Import of IMS proteins via the folding trap:** substrates of this pathway have small molecular weight (typically 7-22 kDa), lack a N-terminal

presequence and contain conserved cysteine (Cys) residues. Their translocation into the IMS does not depend on Δψ or ATP, and their small size may enable them to diffuse through Tom40 into the IMS where they interact with specific receptors. These receptors stimulate either binding of cofactors or formation of disulfide bonds enabling the folding and therefore the trapping of the mature proteins in the IMS (Figure 1.7C). The first characterized example is the IM embedded receptor cytochrome c heme lyase (CCHL), which is responsible for the biogenesis of cytocrome c (cytc). CCHL binds transiently to the newly imported cytc and catalyses the covalent attachment of the heme cofactor to the protein. Cytc then folds in its mature soluble form (Nargang *et al.,* 1998; Diekert, *et al.,* 2001). Small Cys-containing IMS precursors, such as the small Tim proteins, follow the MIA (mitochondrial import and assembly) pathway to be imported into the IMS. The major components of the MIA pathway are Mia40 and Erv1, which are responsible for catalysing the formation of disulphide bonds in the substrates (Allen *et al.*, 2005; Lutz *et al.*, 2003; Chacinska *et al.*, 2004, Milenkovic *et al*., 2007, 2009; Sideris and Tokatlidis, 2007). A detailed description of the MIA machinery will be reported in Section 1.4.

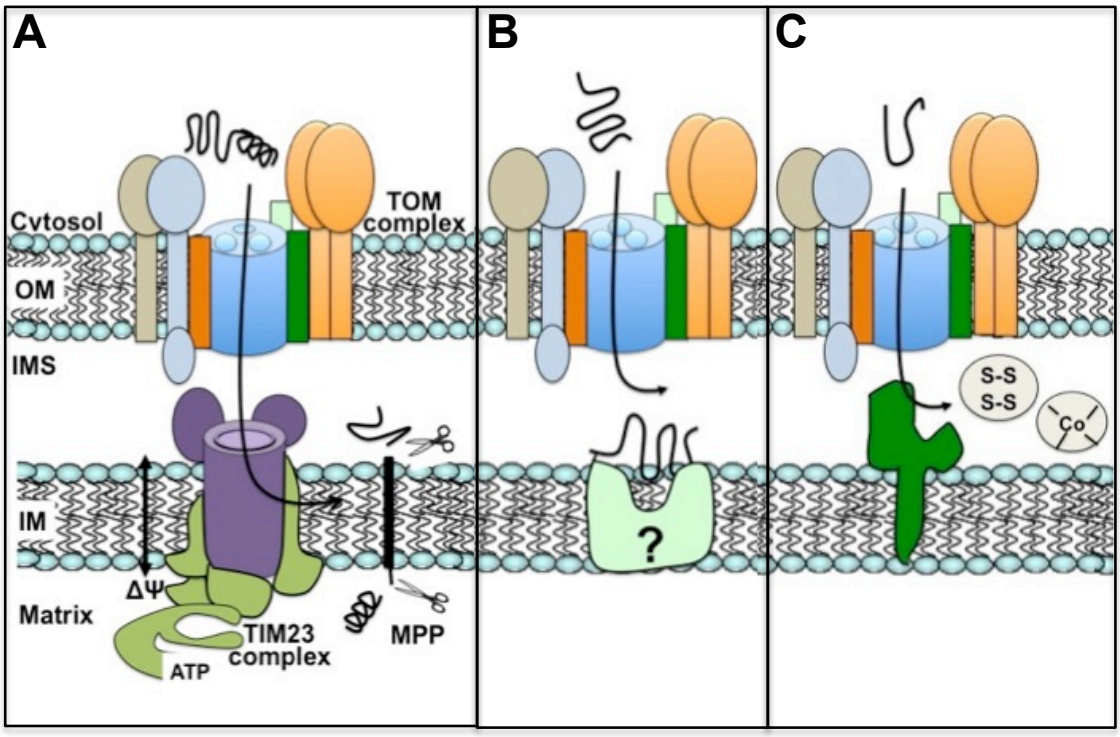

Figure 1.7 Biogenesis of the IMS precursor proteins.

(A) IMS preproteins with bipartite pre-sequences embark on a Stop-transfer import route, followed by cleavage of both bipartite sequences and release of the mature part of the protein in the IMS.
(B) IMS preproteins lacking a presequence require for their net import into the IMS binding to affinity sites in the IMS.
(C) Import of IMS precursor proteins of small size depends on IMS factors, that promote their oxidative folding and/or metal acquisition. Formation of disulphide bonds or coordination of metal ions trap the proteins in the IMS. Figure adapted from Mokranjac and Neupert (2008).

1.3 The small TIM protein family

My studies focused on the biogenesis of the nuclear-encoded mitochondrial small Tims (translocase of the innermembrane) proteins or small Tims. While it is known that mature small Tims in the IMS assemble in the soluble chaperone-like complexes to escort highly hydrophobic proteins across the IMS aqueous environment to the IM or OM (Koehler 2000; Paschen and Neupert, 2001; Rehling *et al.,* 2003), little is still known about the early steps of their biogenesis.

Small Tims were first identified in 1996-1998 in yeast whose genome encodes for five members that, according to their molecular weight in kilodaltons, are named Tim8, Tim9, Tim10, Tim12 and Tim13 (Jarosch *et al.*, 1996; Koehler *et al.*, 1998; Sirrenberg *et al*., 1998). They are characterized by a unique arrangement of the highly conserved Cys residues: the twin CX_3C motif in which two Cys are separated by three amino acids and the spacing between each motif varies from 11 to 16 amino acids (Koelher 2004).

The small TIM family is highly conserved throughout the eukaryotic kingdom and not found in prokaryotes (Bauer *et al.*, 1999). The number of small Tim proteins among eukaryotes ranges from 1 in the early eukaryote *Cryptosporidium parvum* to 6 in mammals *Homo sapiens* and *Mus musculus* (Gentle *et al.,* 2007). The only small Tim present in *C. parvum* has a chaperone-like function and is a hybrid protein with characteristics of both Tim8 and Tim13.

Based on the “primitive condition of small TIMs” hypothesis, the duplication of this gene gave rise to both the Tim10- and Tim13-like chaperones in the IMS. Further gene duplications and codependent mutations created then the Tim9- and Tim8- type subunits, and, much more recently, gene duplication events

gave rise to the Tim12- type subunits as component of the TIM22 machinery of the IM (Gentle *et al.,* 2007).

1.3.1 The yeast small TIM proteins

Yeast Tim8, Tim9, Tim10, Tim12 and Tim13 are 25% identical and 40-50% similar. Tim9, Tim10 and Tim12 are essential for cell viability, whereas Tim8 and Tim13 are dispensable (Koehler *et al.*, 1998; Koehler *et al.,* 1999). In the IMS, three subunits of Tim9 partner with three molecules of Tim10 forming the soluble 70kDa $\alpha_3\beta_3$ Tim9-Tim10 complex. In addition, one subunit of Tim12 substitutes one molecule of Tim10 in the Tim9-Tim10 complex to form the Tim9-Tim10-Tim12 complex, that then assembles with the TIM22 machinery (Koehler *et al.*, 1998; Adam *et al.*, 1999; Luciano *et al.*, 2001; Curran *et al.*, 2002a; Lu *et al.*, 2004; Lu and Woodburn, 2005). Similarly, three subunits of Tim8 also combine with three subunits of Tim13 to form the $\alpha_3\beta_3$ 70kDa soluble complex (Curran *et al.*, 2002b). In addition, Tim8 and Tim13 form a complex with a small fraction of Tim9 giving the 70kDa soluble Tim9-Tim8-Tim13 complex. Although the Tim8-Tim13 complex is not essential for viability, the Tim9-Tim8-Tim13 complex appears to be more important than the Tim8-Tim13 complex as it is indispensable for the temperature sensitive *tim10-1* mutated yeast strain viability (Koehler *et al.,* 1999).

1.3.2 The human small TIM proteins and the Mohr-Tranjaeberg syndrome

Humans contain a single homologue of each Tim9 and Tim13 (human Tim9 and Tim13) and two homologues of each Tim10 (human Tim10a, Tim10b) and Tim8 (DDP1 and DDP2, Deafness-Dyastonia Peptide 1 and 2; Bauer *et al.,* 1999). Human Tim10b might be the functional homolog of yeast Tim12, as it was exclusively found in a large 300kDa complex associated to the IM (Bauer *et al*., 1999; Mühlenbein *et al.,* 2004). All six homologues of human small Tims appear to be ubiquitously expressed at the mRNA level in human adult tissues with the highest steady-state levels in heart, liver, skeletal muscle and kidney, whereas in foetal tissues Tim10 and DDP1 seem to be the most expressed isoforms (Bauer *et al.,* 1999; Jin *et al.,* 1999).

In human mitochondria small Tims are organized into three different complexes (Mühlenbein *et al.,* 2004). One complex consisting of Tim9 and Tim10a subunits have a molecular weight of 70kDa and represents the homologue of yeast Tim9•Tim10 complex (Figure 1.8, C). The second complex containing Tim9, Tim10a and Tim10b subunits is part of a higher molecular weight complex of about 450kDa that resembles the yeast Tim9•Tim10•Tim12 complex (Mühlenbein *et al.,* 2004). The third complex is composed by three subunits of DDP1 and three subunits of Tim13 forming the 70kDa hetero-oligomeric complex identical to the yeast Tim8•Tim13 complex. The DDP1•Tim13 complex specifically assists the import of Tim23 precursors in the inner membrane.

Unlikely to yeast, deletions and/or mutations in the gene encoding for the human homologue Tim8, DDP1 are the underlying cause of the X-linked Mohr-

Tranebjaerg Syndrome (MTS), a rare and progressive neurodegenerative disease characterized by progressive hearing loss, dystonia, spasticity, mental retardation, myopia and cortical blindness (Koelher *et al.,* 1999; Jin *et al.,* 1996). Mutations in DDP1 were also seen to be the cause of other MTS-related clynical phenotypes such as the Jensen syndrome characterized by optico-acoustic nerve atrophy and dementia (Tranebjaerg *et al.,* 1995; Jin *et al*., 1996; Koelher *et al*., 1999).

The absence of a functional DDP1•Tim13 complex may be the cause of a defective import and insertion of Tim23 in the IM, which in turn may cause both a decreased import into the matrix of the precursors that rely on the TIM23 machinery and a decrease in oxidative phosphorylation and energy production. Thus, it has been suggested that an impaired mitochondrial preprotein import is the molecular pathogenetic basis of the MTS syndrome (Rothbauer *et al.,* 2001). The MTS syndrome represents the first example of a disorder derived from mitochondrial import defect. It is hard to understand why the loss and/or mutation of DDP1/Tim8 have dramatic effects on mammals but not on yeast. DDP1 is ubiquitously expressed in human tissues indicating that it plays an important role in basic cellular processes and its loss may manifest itself differently in selected tissue types because of their different energy requirement. This could also explain why the MTS syndrome affects only neural tissues, particularly the basal ganglia, the optical nerve and hair cells of the ear (Tranjaegberg *et al.,* 1995; Jin *et al.,* 1996).

1.3.3 The twin Zinc finger CX_3C motif

In the late 1990s there was some debate on the *in vivo* oxidation state of the Cys of the twin CX_3C motif. Whilst a group of studies showed that the recombinant monomer small Tims bind a zinc ion in a 1:1 ratio by forming a zinc-finger like structure (Sirrenberg *et al.,* 1998; Adam *et al.,* 1999; Lutz *et al.,* 2003), a different set of studies showed that the recombinant and native small Tim complexes do not coordinate zinc, but instead harbour intra-molecularly juxtaposed disulphide bonds (Curran *et al.*, 2002a; Curran *et al.*, 2002b; Allen *et al.*, 2003; Lu *et al.,* 2004a).

The conflicting results over the *in vivo* redox state of the Cys residues in small Tims has been resolved recently with two important discoveries. Firstly, studies showed that only oxidised subunits assemble in the Tim9-Tim10 complex with the inner thiol-linkage playing a crucial role for folding and chaperone activity, whilst the reduced apo- and Zn- bound forms are unable to assemble (Allen *et al.*, 2003; Lu *et al.,* 2004a). Subsequently, the crystal structure of both yeast and human homologue Tim9-Tim10 complexes revealed that each monomer has a helix-loop-helix (HLH) fold with the anti-parallel helices connected by two intrachain disulphides via an inner (C2-C3) and outer (C1-C4) disulphide bonds (Figure 1.8; Webb *et al.,* 2006; Beverly *et al.,* 2008; Baker *et al.,* 2009).

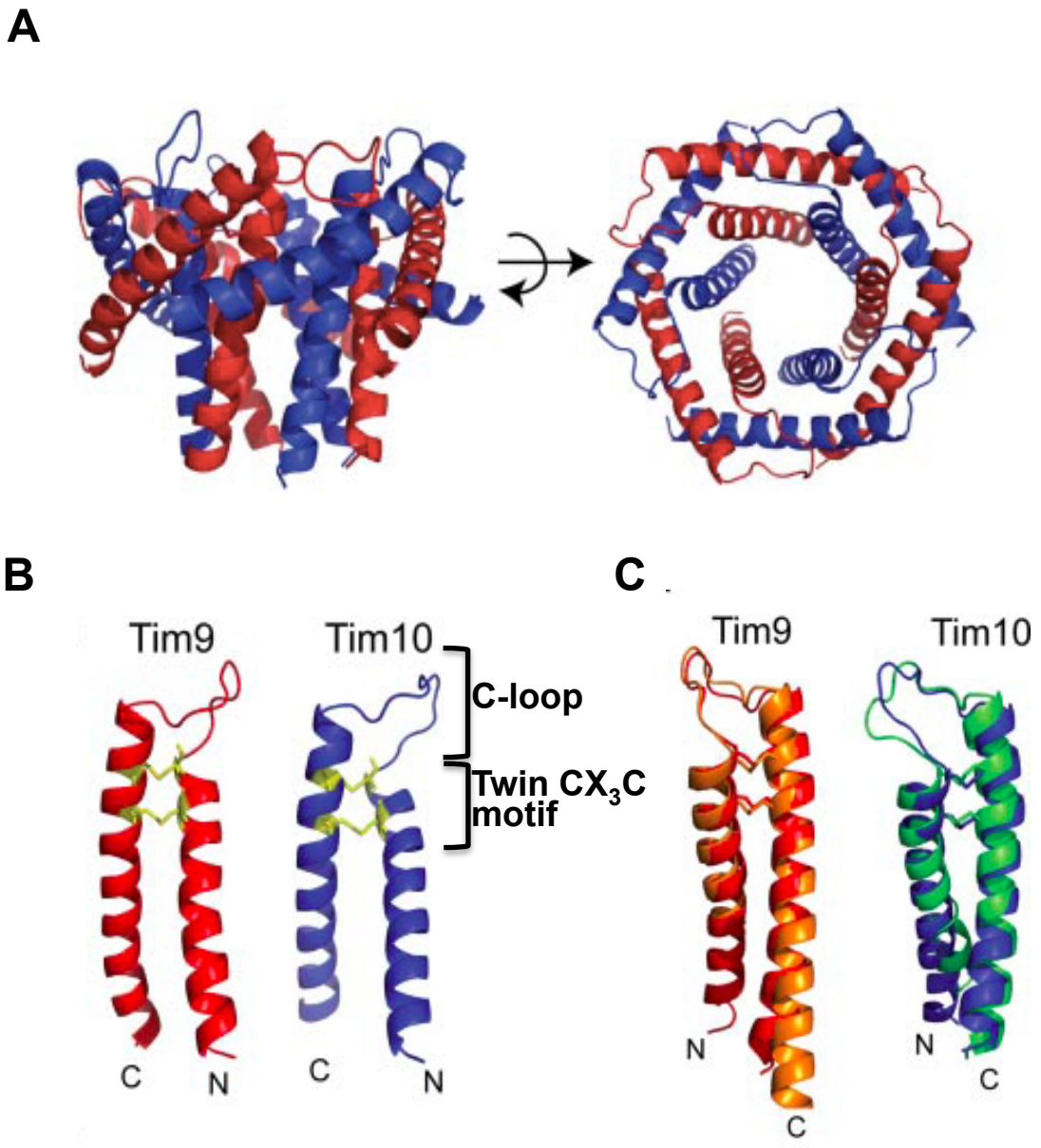

Figure 1.8 The crystal structure of small Tim proteins.

(A) Ribbon diagram of the yeast Tim9-Tim10 complex with a side view (left) and on aerial view (right). Tim10 is in blue and Tim9 in red. Alternating subunits of Tim9 and Tim10 assemble into a six-bladed, α-propeller structure.
(B) Ribbon diagrams showing the structure of the individual yeast Tim19 and Tim10 subunits. Each subunit have a helix-loop-helix conformation connected by a C-loop and the two intrachain disulphide bonds (shown in yellow) among the outermost and innermost cysteine pairs.
(C) Fold comparison of the human Tim9 (orange) and yeast Tim9 (red) and between the human Tim10 (green) and the yeast Tim10 (green). Figure adapted from Webb *et al*. (2006).

Secondly, the identification in the mitochondrial IMS of a new disulphide relay system, the MIA machinery, responsible for the oxidative folding of newly imported small Tims, clarified the relevance of the twin CX_3C motif in the biogenesis of small Tims (Allen *et al.,* 2005; Mesecke *et al.,* 2005; Tokatlidis, 2005).

It is now clear that only the cytosolic reduced form of small Tims is mitochondrial import-competent, whereas the oxidised form is not (Chacinska *et al.*, 2004; Naoe *et al.*, 2004; Terziyska *et al.*, 2005; Lu *et al.*, 2004b; Morgan and Lu, 2008). At the same time, *in vitro* studies showed that zinc-binding may stabilise the proteins in a reduced and import-competent form under cellular glutathione conditions (Lu and Woodburn, 2005; Morgan *et al.*, 2009). Thus, these studies demonstrated that the redox state of the Cys residues in small Tims is not permanently fixed and that this redox state is crucial both for the assembly of a functional chaperone-like complex in the IMS and for the maintenance in the cytosol of mitochondrial import-competence.

1.4 The disulphide bond formation in the cell

Cysteines are the least abundant amino acids in proteins (Pe'er *et al.,* 2004; Hansen *et al.,* 2009). If conserved, they serve in stabilising protein structure by forming disulphide bonds or coordinating metal ions. In addition, due to their peculiarity and high reactivity, they can be key catalytic components of enzymes, or present in protein motifs as regulatory redox-regulated switches. The formation of disulphide bonds in protein folding (or oxidative protein folding) is a rate-limiting step, and failure to form or position the disulphide bonds correctly leads to protein misfolding.

Biochemically, the formation of a disulphide bond results from an oxidation (loss of electrons) of two cysteine thiol groups with the concomitant release of two electrons that must be transferred to an oxidant. In cells the formation of disulphide bonds is enzymatically catalysed. *In vivo* the most common mechanism for formation of a disulphide bond into folding proteins is typically achieved by enzyme pairs.

Enzymes known as sulfhydryl oxidases catalyse *de novo* generation of disulphide bond transferring the electrons to molecular oxygen with the aid of catalysts (i.e. transition metals or flavins). The sulfhydryl oxidases then initiate inter- or intra-molecular dithiol/disulphide relays to pass the disulphides onto their substrates. The second type of enzymes acquires disulphides from the sulfhydryl oxidases and transfers the disulphide to free thiols of substrate proteins.

DsbB and DsbA (disulphide bond formation B and A, respectively) in the periplasm of gram-negative bacteria, whilst Ero1 (endoplasmic reticulum oxidoreductin 1) and PDI (protein disulfide isomerase) in the endoplasmic reticulum (ER), and Erv1 (essential for respiration and vegetative growth 1) and Mia40 (mitochondrial import and assembly 40) in the IMS of eukaryotic cells are examples of this partnership (Figure 1.9; Goldberger *et al*., 1963; Bardwell *et al.,* 1991; Akiyama *et al.*, 1992; Mesecke *et al.*, 2005). Notoriously, the bacterial periplasm, the ER and the IMS of eukaryotic cells are the extra-cytosolic compartments harbouring complex oxidative machineries that mediate the oxidative protein folding of newly imported precursors.

1.4.1 The MIA pathway

The IMS of mitochondria is evolutionarily descendent of the bacterial periplasm and has been recently identified as an intracellular compartment accommodating sulfhydryl oxidation (Allen *et al.*, 2003; Lu *et al.*, 2004a; Mesecke *et al.,* 2005; Webb *et al.*, 2006). It had long been thought that the IMS of mitochondria is inhospitable to thiol-disulphide exchange reactions due to the permeability of the OM that allows free passage of reduced glutathione (GSH) from the cytosol to the IMS.

However, the identification of stable disulphide bonded proteins in the IMS led to the discovery in 2005 of the MIA machinery as the disulphide relay system mediating the acquisition of disulphide bonds in newly imported IMS proteins (Mesecke *et al*., 2005).

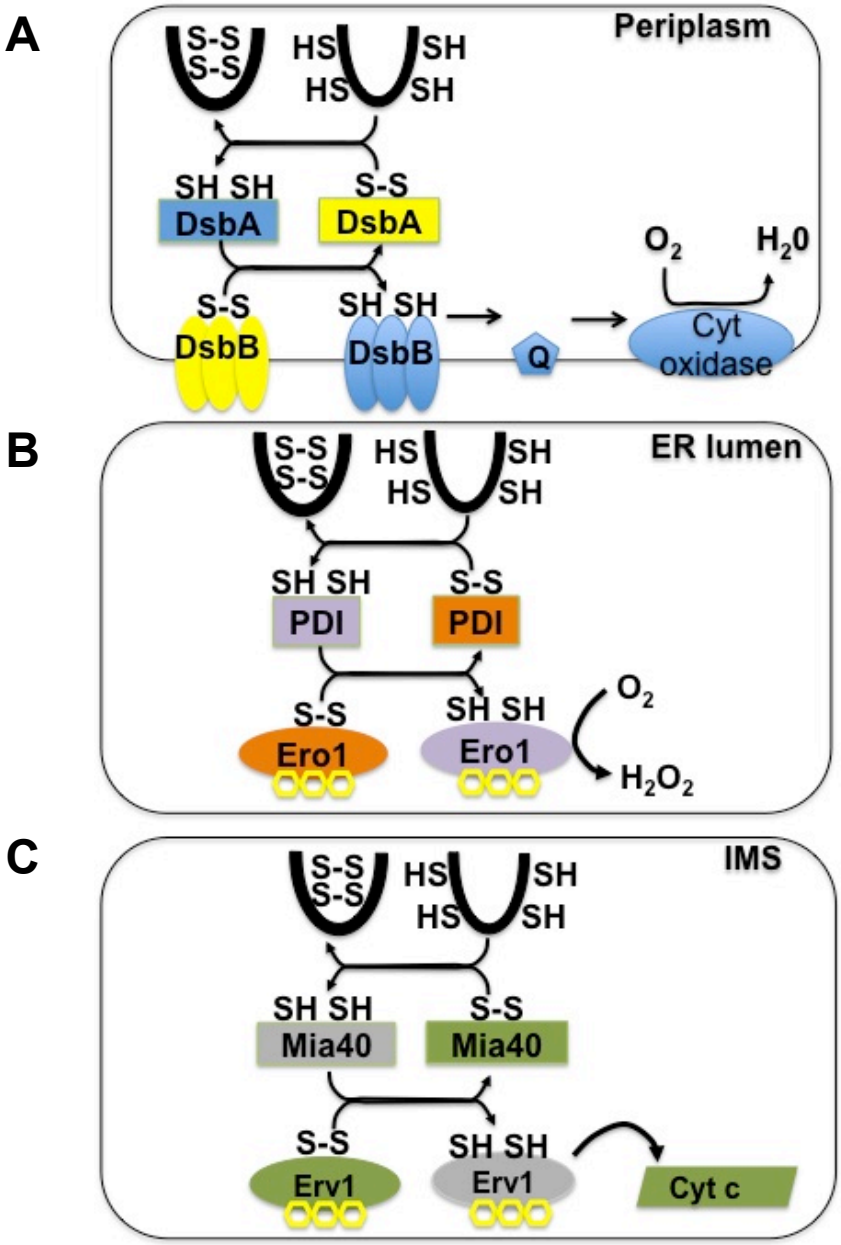

Figure 1.9 The disulphide relay machineries in cells.

(A) In the periplasm of gram-negative bacteria the soluble oxidoreductase DsbA introduces oxidising equivalents into the newly imported protein substrates. DsbA is then re-oxidised by the cytoplasmic membrane protein DsbB, which in turn is oxidised by a quinone cofactor (Q), that transfers the electrons to oxygen.
(B) In the ER of the eukaryotic cells already during their translocation in the ER proteins are oxidised by PDI. PDI is then re-oxidised by the FAD-dependent sulphydryl oxidase Ero1, which passes the electrons to O_2, generating H_20_2 (the FAD cofactor is indicated by the yellow hexagons).
(C) In the IMS of eukaryotic cells the oxidoreductase Mia40 oxidises newly imported IMS proteins. Mia40 is then re-oxidised by the FAD-dependent sulphydryl oxidase Erv1, which transfers the electrons to Cyt c.

In addition, the MIA machinery contributes to the direction of the transport of the MIA substrates into the IMS, as the MIA-dependent oxidation locks the newly imported proteins in a folded state in which they cannot traverse the OM.

The two major players of the MIA machinery are the oxidoreductase Mia40 and the sulphydryl oxidase Erv1. The IMS disulphide relay system consists of four steps (Figure 1.10):

Step 1: Import and substrate recognition by Mia40: reduced and unfolded MIA substrate enters the IMS where it interacts with oxidised Mia40 to form a mixed disulphide (Chacinska *et al.,* 2004, Mesecke *et al.,* 2005; Sideris and Tokatlidis*,* 2007; Müller *et al.,* 2008).

Step2: Oxidation and release of substrate proteins: upon interaction with Mia40, the substrate undergoes oxidative folding in a dedicated reaction scheme not fully understood. The oxidised substrate is released from Mia40 and Mia40 is reduced (Mesecke *et al*., 2005; Milenkovic *et al.,* 2007; Sideris and Tokatlidis*,* 2007; Tienson *et al.,* 2009).

Step 3: Reoxidation of Mia40: reduced Mia40 passes the electrons to the oxidised CXXC motif of the flexible N-terminal domain of Erv1 enabling Mia40 to participate in another cycle (Mesecke *et al.,* 2005; Rissler *et al.,* 2005; Grumbt *et al*., 2007; Tienson *et al*., 2009; Lionaki *et al*., 2010).

Step 4: Reoxidation of Erv1: the reduced N-terminal domain of Erv1 passes the electrons intermolecularly to the CXXC motif of the second molecule of Erv1 dimer, which is close to the FAD cofactor. $FADH_2$ is then re-oxidised by Cytc, connecting the MIA pathway to the respiratory chain (Bihlmaier *et al.*, 2007;

Dabir *et al.*, 2007; Daithankar *et al.*, 2009; Tienson *et al.*, 2009). A better description of the downstream of the MIA pathway is given in section 1.4.6.

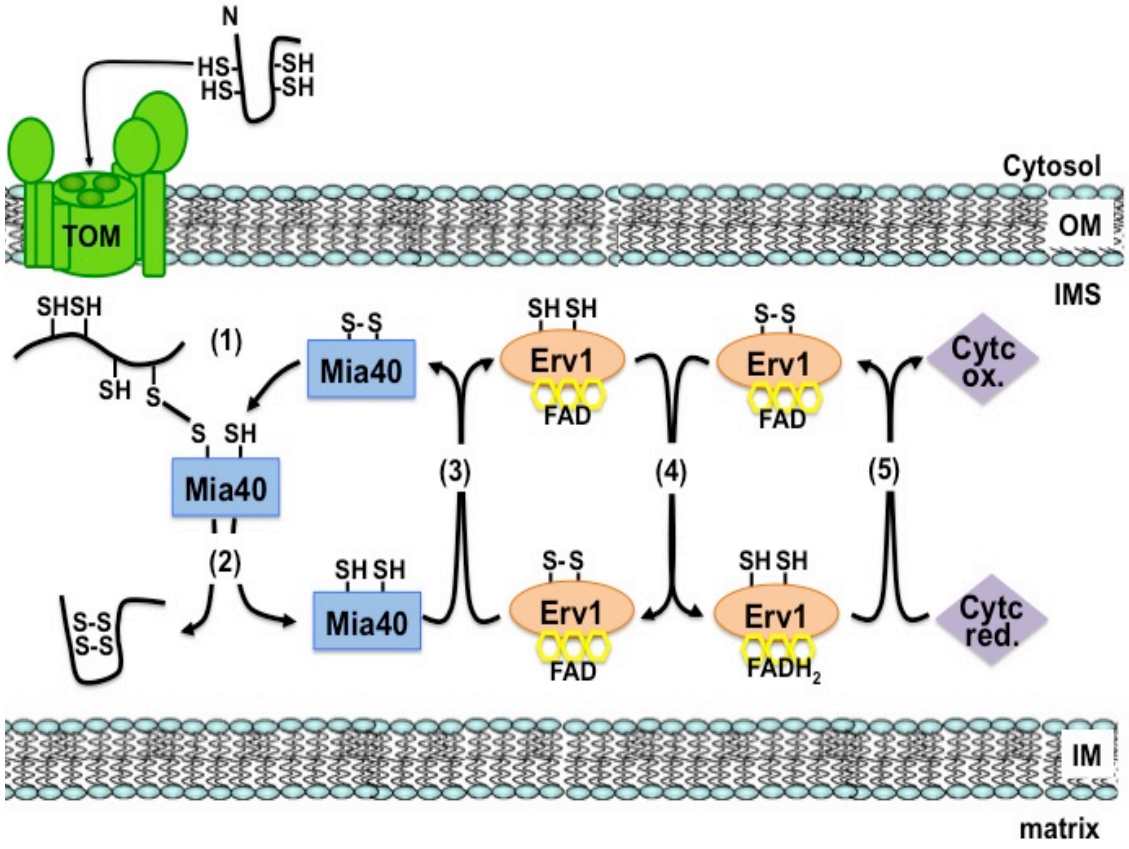

Figure 1.10 The MIA pathway.

Step 1: Substrates of the MIA pathway translocate into the IMS in a reduced and unfolded conformation. Upon channelling through the TOM complex, they are recognized and bind to Mia40 via a mixed disulphide bond.
Step 2: The interaction with Mia40 results in the oxidation of the substrates and the reduction of the CPC motif of Mia40.
Step 3: Reduced Mia40 is then re-oxidised by the FAD-dependent sulphydryl oxidase Erv1. Mia40 is ready to participate to another cycle.
Step 4: the electrons are then shuttled intermolecularly from the N-domain of one molecule of Erv1 to the CXXC motif of the second molecule of Erv1 dimer, and then to the close FAD cofactor. Reduced $FADH_2$ is then re-oxidised by Cytc, thus connecting the MIA machinery to the respiratory chain of mitochondria. Alternatively, Erv1 can be oxidised by O_2 generating H_2O_2 (not shown). Figure adapted from Dabir *et al*. (2009).

1.4.2 Substrates of the MIA pathway

At the moment 15 out of the 50-100 IMS proteins are known to be substrates of the MIA machinery (Gabriel *et al.,* 2007). All MIA substrates are nuclear encoded, synthesised in the cytosol, of small size (about 10-23 kDa) and harbour highly conserved Cys residues, which play either structural or catalytic roles. Based on the arrangements of their Cys residues, MIA substrates are grouped into three main categories: (1) proteins containing the twin CX_3C motif; (2) proteins containing the twin CX_9C motif; and (3) proteins containing conserved Cys but lacking a typical twin CXnC motif.

(1) Proteins with the twin CX_3C motif: to this group belong members of the small TIM family described in section 1.3.

(2) Proteins with the twin CX_9C motif: the second group of MIA substrates includes proteins with the twin CX_9C motif, where nine residues separate the two cysteines of each motif.

In yeast 14 twin CX_9C motif-containing proteins have been identified to date, and most of them have homologues in mammals. In addition, 7 of these proteins contain additional cysteines besides the four of the twin CX_9C motif. This group includes members of the COX17 family, such as Cox17 and Cox19, and Cox23, Cmc1 and Cmc2, that are involved in the assembly of Cytochrome oxidase (Cco), and Mia40, the oxidoreductase of the MIA machinery (Longen *et al.,* 2009; Horn *et al.,* 2012; Nobrega *et al.,* 2002).

Like the small Tim proteins, Cox17 has a helix-loop-helix (HLH) fold within the two helixes connected by two juxtaposed disulphide bonds. The HLH fold is

shared by other substrates involved in the Cco assembly, such as Cox19, Cox23 and Cox12 (Arnesano *et al.,* 2005).

Mia40 harbours a twin CX_9C motif and two additional cysteine residues at the N-terminal arranged as CXC. In its oxidised state Mia40 harbours 3 disulphide linkages: two juxtaposed disulphide bonds between the outermost and innermost pair of cysteines of twin CX_9C motif that have a structural role, and one disulphide bond connecting the pair of cysteines of the catalytic CPC motif. Yeast Mia40 differs from its mammalian counterpart in being IM anchored and having a N-terminal presequence signal. Thus, yeast Mia40 can utilise both the TIM23 and MIA pathways to be imported into the IM, whereas in higher eukaryotes Mia40 import may specifically depend on the MIA machinery (Chacinska *et al.,* 2008).

(3) Other MIA substrates: this group includes IMS proteins containing conserved cysteines not arranged in a twin CXnC motif, such as Erv1, Sod1 (Superoxide dismutase 1), its copper chaperone Ccs1 (Gabriel *et al.,* 2007; Terziyska *et al.,* 2007; Kawamata and Manfredi, 2008; Reddehase, *et al.,* 2009).

Ccs1 is a 23 kDa protein and, to date, represents the biggest substrate of the MIA machinery. The copper chaperone Ccs1 promotes import and maturation of Sod1 into the IMS by introducing a disulphide bond and incorporating a copper ion in newly imported Sod1 (Sturtz *et al.,* 2001). Studies demonstrated that retention in the IMS of Sod1 and Css1 depends on the MIA machinery, as their IMS levels diminish in mitochondria depleted of Erv1 and Mia40. It has been suggested that upon formation of a mixed-disulphide with Css1, Mia40

introduces a disulphide bond into Ccs1 that then passes it onto the newly imported Sod1, resulting in maturation and IMS retention of Sod1 (Kawamata and Manfredi, 2008; Reddehase *et al.,* 2009).

1.4.3 Mia40, the import receptor of the MIA pathway

Mia40 acts as a redox-regulated receptor for the MIA substrates: like PDI in the ER (Scheren *et al.,* 1991; Holst *et al.,* 1997) and DsbA in the bacterial periplasm (Zapun *et al.,* 1993), Mia40 interacts with the incoming reduced and unfolded substrates via a transient mixed-disulphide bond. During this interaction the substrates undergo oxidative folding and is released from Mia40 in an oxidised form. In contrast to PDI and DsbA, Mia40 does not contain the typical thioredoxin-fold (TRX-fold) domain (consisting of 4 β-stranded sheets sandwiched by 3 α-helices, and the catalytic CXXC site; Martin 1995; Qi and Grishin, 2005), and has no similarity with any other known cellular oxidoreductase. Thus, Mia40 more likely may represent a new type of oxidoreductase.

Mia40 is essential for cell viability and is ubiquitously present in eukaryotes (Naoé *et al.,* 2004; Chacinska *et al.,* 2004; Terziyska *et al.,* 2005). However, the length of Mia40 primary sequence among species varies substantially: yeast Mia40 (yMia40) and its human counterpart (hMia40) are respectively 45 kDa and 16 kDa. Moreover, yMia40 is anchored to the IM through its N-terminal hydrophobic segment and exposes its long C-terminal domain to the IMS, whereas hMia40 lacks the N-terminal hydrophobic segment and is a soluble IMS protein.

The C-terminal domain of yMia40 is highly conserved among eukaryotes and includes the invariant C_1PC_2-$C_3X_9C_4$-$C_5X_9C_6$ motif. Mia40 contains three disulphide bonds when it is in its oxidised state: one connecting the Cys in between the CPC motif, and two juxtaposed disulphides linking C_3-C_6 and C_4-C_5 of the twin CX_9C motif. The CPC disulphide is redox-sensitive, with the second cysteine being the catalytic residue that participates in the dithiol/disulphide exchange reaction with the incoming substrates. The other two disulphides play a structural role (Figure 1.11, A; Terziyska *et al.,* 2009).

The crystal structure of yMia40 revealed that Mia40 has a fruit-dish-shape consisting of 2 regions: 1) a long N-terminal lid containing the CPC motif and several hydrophobic residues that form a binding cleft; and 2) a HLH fold consisting of two helices with anti-parallel orientation connected by the two juxtaposed disulphides C_3-C_6 and C_4-C_5 (Figure 1.11, B and C; Kawano *et al.,* 2009). The hydrophobic cleft, mainly formed by phenylalanine residues, serves as binding-site for the substrates, as substitution of any hydrophobic residues with charged residues strongly interferes with the substrate binding activity of Mia40 (Kawano *et al.,* 2009). The second cysteine of the CPC motif is slightly exposed to the hydrophobic cleft, supporting its role in substrate docking via mixed-disulphide formation (Terziyska *et al.,* 2009; Tienson *et al.,* 2009).

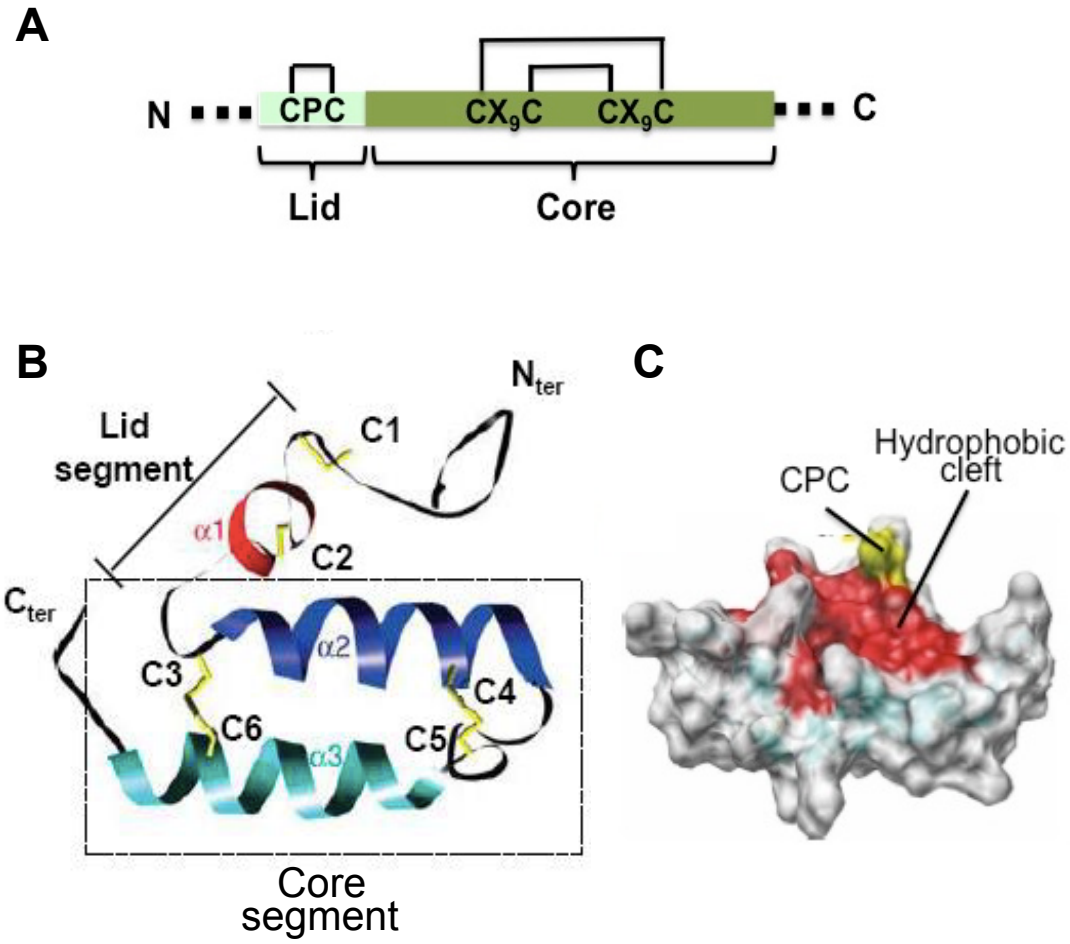

Figure 1.11 The structural characteristics of human Mia40.

(A) Primary structure of the functional domain of Mia40. Mia40 contains six cysteine residues arranged in the CPC-CX_9C-CX_9C motif. The functional domain of Mia40 consists of a lid segment containing the CPC redox active site, and of a core segment harbouring the twin CX_9C motif.
(B) Ribbon diagram of the central region of human Mia40: the helix α1 of the lid segment (red) contains the two cysteine residues of the CPC motif (indicated in yellow) in a reduced form. Helices α2 (blue) and α3 (cyan) of the core segment form an anti-parallel α-hairpin structure kept together by two disulphide pairings among the cysteines of the twin CX_9C motif (shown in yellow; figure adapted from Banci et al. 2009).
(C) Surface representation of Mia40 structure as in (B). The hydrophobic cleft of Mia40 is shown in red. The second cysteine of the CPC motif closer to the hydrophobic cleft is indicated in yellow. The structural core segment is depicted as a ribbon diagram coloured in transparent cyan. Figure adapted from Banci *et al.* (2009).

Furthermore, both *in vivo* and *in vitro* studies suggested that Mia40 recognizes specifically distinct hydrophobic residues in its substrates, namely called **MISS** (Mitochondrial Intermembrane Space Sorting) or **ITS** (IMS-Targeting Signal) signals. In both cases the MISS/ITS signal consists of one aromatic and one hydrophobic residue at positions 4 and 7 respectively upstream or downstream of the critical Cys that attacks the CPC motif of Mia40 (C1 for Tim9 and C4 for yeast Cox17 respectively; Milenkovic *et al.,* 2009; Sideris *et al.,* 2009). The MISS/ITS sequence forms an amphipathic helix with the aromatic and hydrophobic residues located on the same side of the docking cysteine, and the charged residues located at the opposite side (Figure 1.12).

The nature of the aromatic and hydrophobic residues may allow the accommodation of the ITS helix in the substrate-binding cleft of Mia40 through hydrophobic interactions. This then leads to the docking of the substrate to the CPC motif of Mia40 and subsequent disulphide bond formation between Mia40 and the substrate (Figure 1.13). Mia40 then oxidises the substrate in a dedicated reaction scheme, which however, is not fully mechanistically understood. Once oxidised, the substrate is released from Mia40, which in turn is now reduced. Mia40 is then re-oxidised by the sulphydryl oxidase Erv1. The oxidation of substrates by Mia40 is thermodynamically favoured with both CX_3C and CX_9C containing substrates having more reducing redox potentials (-340 mV and -310 mV, respectively) than the redox potential of the CPC motif of Mia40 (-290 mV) (Lu and Woodburn, 2005; Morgan and Lu, 2008; Kawano *et al.*, 2009; Tienson *et al*., 2009).

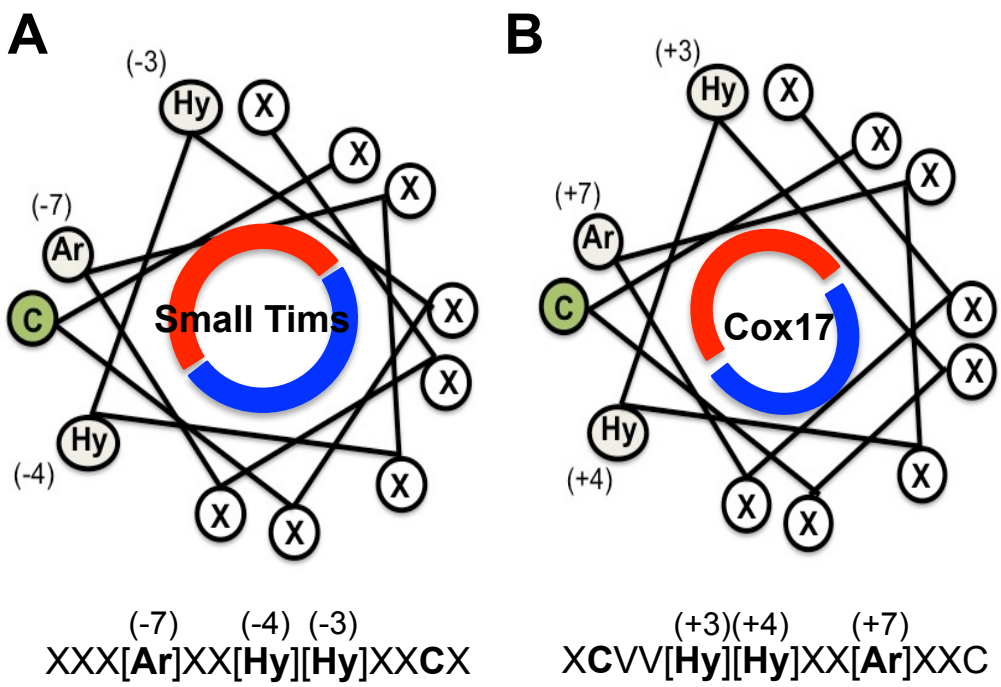

Figure 1.12 Helical wheel representation of the MISS/ITS signal.

Helical wheel representation of the MISS/ITS targeting signal for yeast small Tim proteins **(A)** and Cox17 **(B)**: the MISS/ITS signal forms an amphipathic α-helix with the docking cysteine (green) located next to the two hydrophobic residues at positions ±3 and ±4 and the aromatic residue at position ±7, respectively. The docking cysteine and the three hydrophobic residues form the hydrophobic face (red) of the helix, whereas the other amino acids are located at the opposite side of the helix forming the hydrophilic face of the sequence (blue). Figure adapted from Sideris *et al*. (2009).

1.4.5 Erv1, the sulphydryl oxidase of MIA pathway

Erv1 was identified as the first sulfhydryl oxidase in mitochondria (Lee *et al.,* 2000). Erv1 is conserved among fungi, plants and animals, but not found in prokaryotes. In yeast Erv1 is essential for viability (Lisowsky 1992). The human homolog of Erv1 is called Alr (Augmenter of Liver Regeneration) for its function in increasing hepatocyte proliferation (Hagiya *et al.,* 1994). Erv1 and the ER oxidase Erv2 belongs to the Erv/quiescin sulfhydryl oxidase family of flavoproteins, whose members share a common flavin adenine dinucleotide (FAD)-binding domain that harbours a conserved CXXC motif adjacent to the FAD cofactor (Coppock and Thorpe, 2006; Fass 2008). In addition to the FAD-domain, Erv1 contains a second domain, called N-domain, which is very flexible and harbours a second set of CXXC motif.

Erv1 is a soluble homodimeric protein, in which each subunit cooperates in the electron transfer. It has been proposed that the second cysteine of the CPC motif of Mia40 forms a mixed disulphide with the second cysteine in the initially oxidised CXXC motif of the flexible N-domain of Erv1 (Bien *et al.,* 2010). After interaction with Mia40, the N-domain of one of the two subunits of Erv1 is reduced, and it then passes the electrons intermolecularly to the CXXC motif of the FAD-domain of the second subunit of the homodimer. Electrons can then be passed from the CXXC motif to the close FAD cofactor (Bien *et al.,* 2010).

1.4.6 The downstream of the MIA pathway

Subsequently, the reduced flavin cofactor $FADH_2$ of Erv1 has to be reoxidised for Erv1 to be able to participate to another cycle. Both *in vitro* and *in vivo* studies supported Cytochrome c (Cytc) as direct oxidizing agent for reduced

Erv1, indicating that the MIA pathway is linked to the mitochondrial respiratory chain, similarly to the DsbA/DsbB oxidative system in the bacterial periplasm. Subsequently, reduced Cytc can be reoxidised by Cytochrome c peroxidase 1 (Ccp1, Allen *et al.,* 2005; Bihlmaier *et al.,* 2007; Dabir *et al.,* 2007, Bien *et al,* 2010). Alternatively, both *in vitro* and *in vivo* studies showed that reduced Erv1 can also use O_2 as electron acceptor with the subsequent release of hydrogen peroxide (H_2O_2; Bilhmaier *et al.,* 2007; Dabir *et al.,* 2007; Ang and Lu, 2009; Daithankar *et al.,* 2009; Tienson *et al.,* 2009). In the IMS, H_2O_2 is then reduced by Ccp1 to H_2O, and oxidised Ccp1 is in turn reduced and recycled by reduced Cytc (Dabir *et al.,* 2007). Either way, the transfer of electrons from Erv1 to Cytc leads to the final production of water instead of the harmful H_2O_2. Dabir *et al.* (2007) proposed that both pathways might occur in the IMS, depending on, for example, the aerobic/anaerobic state of cells. The yeast genome encodes two genes for Cytc, CYC1 and CYC7, which are expressed respectively under high and low oxygen concentrations. Thus, it could be that under different O_2 concentrations different forms of Cytc may dictate Erv1 function (Dabir *et al.,* 2007). This model is further supported by the observation that, in yeast deleted for both CYC1 and CYC7 genes, the Mia40 redox state shifted towards its reduced form under oxygen-limiting conditions (Bihlmaier *et al.,* 2007). In addition, in contrast to Mia40 and Erv1, Cytc is not essential for cell viability, and since the MIA pathway is strictly essential under fermentative growth conditions, other unidentified oxidizing agents may be responsible for the *in vivo* oxidation of Erv1 (Stojanoski *et al.,* 2008a).

1.4.7 Hot13

Beside Mia40 and Erv1, another soluble IMS proteins, named Hot13 (Helper of Tims of 13 kDa), has been proposed as another component of the MIA machinery (Curran *et al.,* 2004; Mesecke *et al.,* 2008). Hot13 is not essential for yeast cell viability, but is conserved among yeast and prokaryotes. Being a member of the zf-CHY domain family, Hot13 contains a RING finger motif that can coordinate two Zn^{2+} ions and facilitate protein-protein interactions. The first study on Hot13 suggested that small Tim assembly into the hexameric complex is inhibited in mitochondria lacking Hot13. Thus, this suggests that Hot13 might be required only after that small Tims have interacted with Mia40 (Curran *et al.,* 2004). A recent study showed that Hot13 may work as a zinc chaperone that transfers zinc ions from Mia40 to an unknown IMS acceptor, resulting in efficient oxidation of Mia40 by Erv1. Since zinc-binding to both Mia40 and Erv1 has an overall inhibitory effect on the MIA machinery (Mesecke *et al.,* 2008; Morgan *et al.,* 2009), Hot13 may act as a zinc chelator to improve the MIA machinery. Hence, this might explain why assembly of small Tims were impaired in the absence of Hot13.

1.4.8 Spatial organization of the MIA machinery

Since most MIA substrates contain at least two disulphide bonds and the CPC motif of Mia40 can only donate one disulphide, the actual protein folding events that lead to the generation of a fully oxidised substrate and the role of Mia40 in these remain unknown. Currently, two models have been proposed based on *in vitro* studies. The first model suggests an alternating association of Mia40 with the substrate (reduction of Mia40) and Erv1 (reoxidation of Mia40; Mesecke *et*

al., 2005; Sideris and Tokatlidis, 2007). Studies from several groups reported that Mia40 alone was able to introduce both disulphide bonds in yeast Cox19 and human Cox17, indicating that Erv1 is not necessary for the complete oxidative folding of Cox19 (Bien *et al.,* 2010; Banci *et al*., 2010).

Alternatively, the second model implies that the oxidative protein folding involves also Erv1 in a ternary complex with Mia40 and the substrate, where electrons flow from the substrate to Erv1 through Mia40. In the ternary complex, during the shuffling of electrons, the substrate remains associated with Mia40 while both disulphides are formed. In this way, the oxidative folding of the substrates will require fewer binding and release steps than the first model. A ternary complex including imported Tim9, Mia40 and Erv1 has been detected in mitochondria (Stojanoski *et al.,* 2008b). The imported Tim10 and twin CX_9C Cmc1 proteins were also shown to form a ternary complex with Mia40 and Erv1 (Stojanoski *et al.,* 2008; Bouress *et al.,* 2012).

1.4.9 The role of glutathione in the MIA pathway

In the ER and bacterial periplasm there exist oxidation/isomerisation machineries counteracting the formation of non-native disulphide bonds introduced by PDI or DsbA, respectively. In both cases, the electrons flow from the cytosol either through a membrane specific shuttle system (DsbB in the periplasm) or by transport into the ER of reduced glutathione (GSH). There is a possibility that a reduction/isomerisation pathway is not required in the IMS, as MIA substrates are small with only one or two disulphides. However, recently it has been shown that the *in vitro* reconstituted mitochondrial disulphide relay is also prone to release proteins containing non-native disulphides (Bien *et al.,*

2010). These unproductive intermediates can be counteracted by GSH (Bien et al., 2010). It still remains to be shown to what extent such non-native disulphides are formed *in vivo*, and the precise role of GSH in the MIA pathway.

1.5 The reducing power of the cytosol

Due to the versatility of cysteine residues, cells use several mechanisms to avoid oxidative modifications of this amino acid. For example, translocation and disulphide bond formation in the lumen of the ER occurs typically in a co-translational manner, whereas thiol groups of periplasmic proteins of bacteria are maintained reduced in the cytosol by oxidoreductases (Pollitt and Zalkin, 1983; Derman and Beckwith, 1991; Dutton *et al.,* 2008; Dutton *et al.,* 2010). The cytosol is considered a reducing environment due to the presence of a high concentration of GSH (10 to 14 mM) and of oxidoreductases (Østergaard *et al.,* 2004). Although several thermophilic archaea harbour a large fraction of disulphide bonded cytoplasmic proteins, stable disulphide bonded proteins are usually rare in the cytosol of prokaryotes and eukaryotes (Mallick *et al.,* 2002).

Using small Tims as models, it has been shown that the oxidised forms of these proteins are thermodynamically stable under cellular glutathione redox conditions (Lu and Woodburn 2005; Morgan *et al.,* 2008; Tienson *et al.,* 2009). Small Tim proteins have a standard redox potential of -310 mV to -330 mV, which is more negative than that of the glutathione redox conditions in both the cytosol (-290 mV) and IMS (-255 mV; Østergaard *et al.,* 2004; Hu *et al.,* 2008). Such a redox potential for small Tims is consistent with their oxidised state in the IMS, but not with their reduced state in the cytosol. Thus, cytosolic factors are required to prevent the oxidative folding of MIA substrates. The two major

oxidoreductases responsible for maintaining cytosolic proteins in a reduced state are the thioredoxin (Trx) and GSH-dependent glutaredoxin (Grx) enzymes.

1.5.1 The Thioredoxin and Glutaredoxin systems

Trxs and Grxs are heat-stable oxidoreductases present from archaea to human. Both proteins belong to the Thioredoxin superfamily and contain the typical active site CXXC and TRX-fold domain (Holmgren 1989). In addition to classical Trxs and Grxs, most genomes encode for monocysteinic Grxs with a CXXS motif (a cysteine and a serine separated by two amino acids), whereas monocysteinic Trxs are found only in plants (Meyer *et al.,* 2009).

The Trxs and Grxs were originally identified as hydrogen donor for ribonucleotide reductase (Holmgren 1976), but they are involved in the regulation of many other metabolic enzymes that form disulphides during their catalytic cycle. Roles have been proposed for them in many cellular processes including protein folding and regulation, repair of oxidative damaged proteins, oxidative stress defence, sulfur metabolism and control of apoptosis (Holmgren 1989; Wells *et al.*, 1993; Rietsch and Beckwith, 1998; Lillig *et al.,* 1999; Nordberg and Arner, 2001; Gromer and Becker, 2004; Arner and Holmgren, 2006; Lillig and Holmgren, 2007; Lu and Holmgren, 2012).

The major function of the Trxs and Grxs is to catalyse the reversible reduction of disulphide bridges in target proteins by a dithiol-disulphide exchange reaction that takes place in two steps (Figure 1.14; Holmgren, 1989; Brandes *et al.,* 1993):

1) the N-terminal thiol of the CXXC motif within the oxidoreductase attacks the disulphide bond in the substrate, resulting in the release of a free thiol and

concomitant formation of an intermolecular disulphide bond with the target protein.

2) the C-terminal thiol of the CXXC motif breaks the mixed-disulphide, resulting in the reduction of the substrate and oxidation of the enzyme.

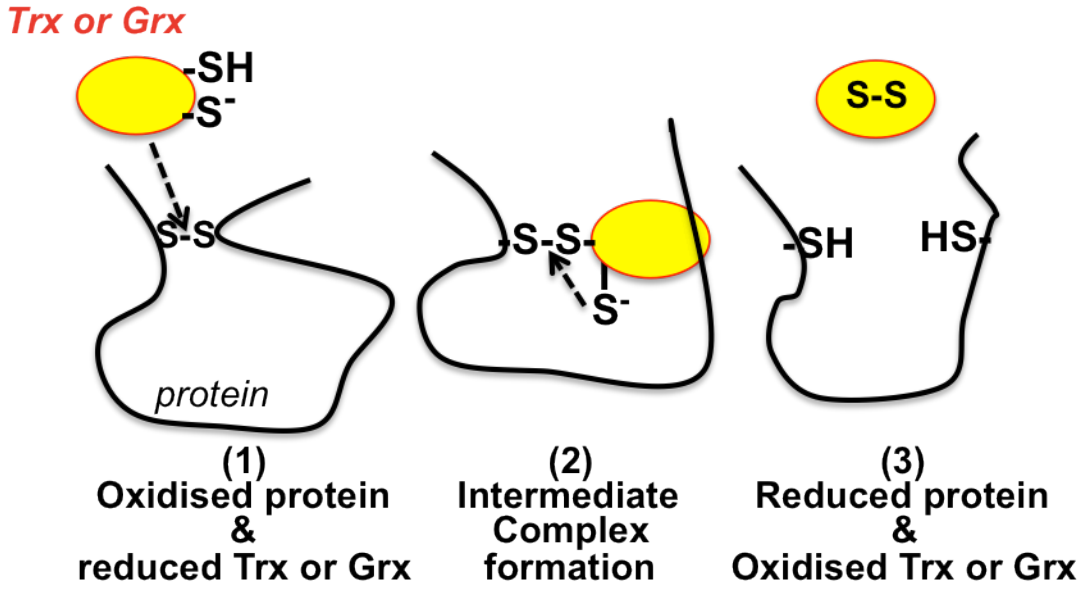

Figure 1.14 Mechanisms for reducing disulphide bonds in protein targets of the Trxs and Grxs.

Reduced Trx or Grx attacks the disulphide bridge of the target protein (1), resulting in the release of a free thiol and a formation of an intermolecular disulphide (2). Then, the C-terminal thiol of the oxidoreductase attacks the inter-disulphide bond, releasing the reduced substrate and oxidised redoxin protein (3). Figure adapted from Meyer *et al.* (2009).

Despite similarity in structure and activity, the Trxs and Grxs are regulated differentially: oxidised Trx is reduced by the thioredoxin reductase (Trr) and NADPH (reduced nicotinamide adenine dinucleotide phosphate), whilst oxidised Grx is reduced by GSH, and the resulting oxidised glutathione (GSSG) is in turn

reduced by the glutathione reductase (Glr) and NADPH (Holmgren 1989; Toledano *et al.,* 2007).

Trxs are more electronegative than the Grxs enabling the Trx have specific substrates (i.e. insulin, PAPS, Tsa1 and Tpx1, Ahp1 (alkyl hydroperoxide reductase; Holmgren 1979; Vignols *et al.*, 2005; Meyer *et al.,* 2009; Day *et al.,* 2012; Lian *et al.*, 2012) and /or to perform unique functions. Knockout mice for cytosolic Trx1 induces early embryogenic lethality, whereas knockout mice for Grx1 did not display any defect during development and grew as the wild-type counterpart, indicating that Trx1 fulfils an essential function which cannot be performed by other redoxins (Matsui *et al.,* 1996; Ho *et al.,* 2007). On the other hand, the Trxs are considered proto-oncogenes as numerous studies suggested that their over-expression was associated with cell proliferation in various types of tumours, drug-resistance and aggressive tumour phenotype (SeunJin *et al.,* 2005; Changping *et al.,* 2012).

Grxs are far more efficient to reduce mixed disulphides that have been formed by nucleophilic attack of GSH on disulphide bonds (Holmgren 1979; Collison *et al.,* 2002), protect against selenium toxicity both in human and yeast cells (Wallenberg *et al.,* 2010; Izquierdo *et al.,* 2010), and are involved in iron-sulphur biosynthesis (Lillig *et al.,* 2005; Rouhier *et al.,* 2007; Feng *et al.,* 2006).

1.5.2 The cytosolic Trx and Grx systems in yeast

The yeast S. *cerevisiae* contains two cytoplasmic Trx systems including the two homologs Trx1 and Trx2 and a single Trr1, and two Grx systems including the two classical Grx1 and Grx2 and the glutathione reductase Glr1. Grx2 and Glr1

also localised to the mitochondrial matrix (Figure 1.15; Muller, 1991; Luikenhuis *et al.,* 1998; Porras *et al.,* 2006).

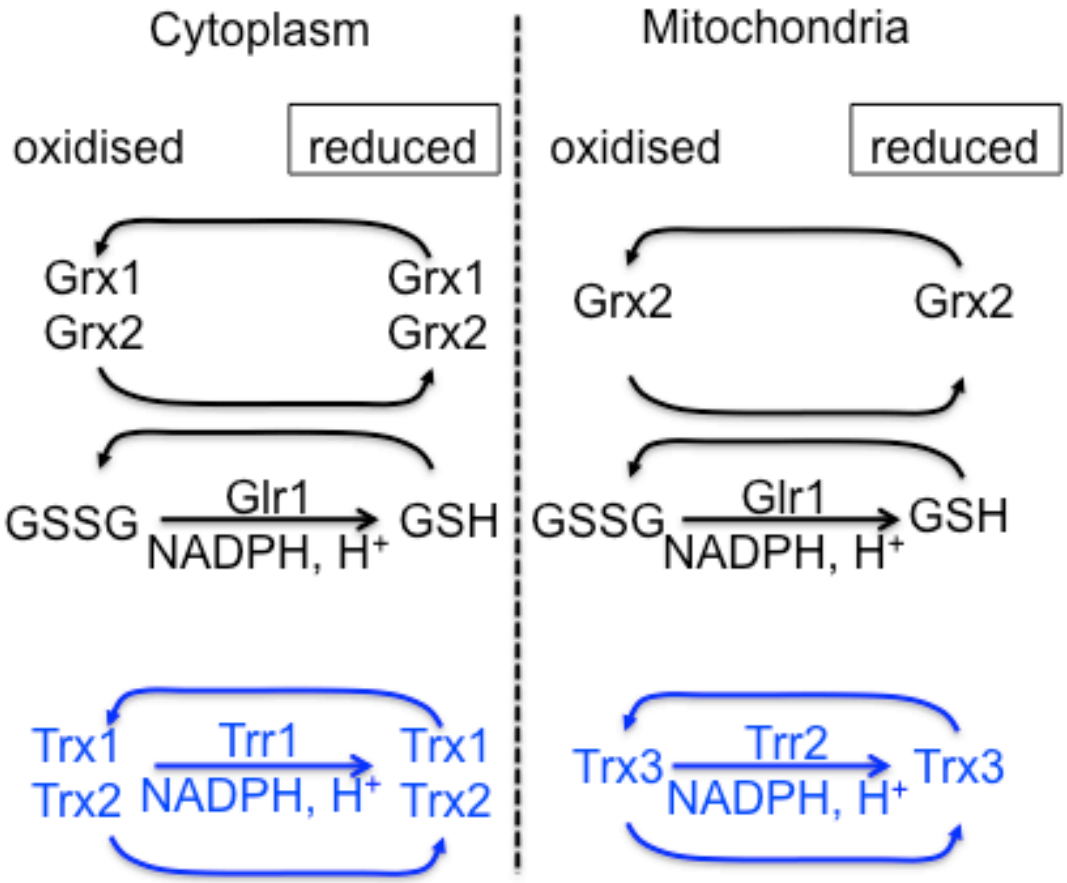

Figure 1.15 The Trx and Grx systems in the yeast.

Yeast contains two gene pairs encoding for two cytosolic glutaredoxin homologs (Grx1 & Grx2) and two thioredoxin homologs (Trx1 & Trx2). Oxidised Grx1 and Grx2 are reduced non enzymatically by GSH, and GSSG is reduced in a NADPH-dependent reaction by the GSH reductase (Glr1). The oxidised forms of Trx1 and Trx2 are, in turn, reduced by the the thioredoxin reductase (Trr1) in a NADPH-dependent reaction. Yeast also contains a mitochondrial thioredoxin system, which includes Trx3 and Trr2. Grx2 and Glr1 colocalize both to the cytosol and mitochondria. Adapted from Trotter and Grant (2005).

Many *in vivo* studies showed that the Trx and Grx systems are functionally redundant (Table 1). For example, in yeast, as well as in bacteria, the quadruple *trx1 trx2 grx1 grx2* is inviable, and a single Grx or Trx is required for cell viability

(Prinz *et al.,* 1997, Draculic *et al.,* 2000). This indicates that the remaining Grx or Trx can provide all functions required for cell viability, most importantly the ribonucleotide reductase activity. Further evidence of the functional link between the two systems was provided when both *trr1 glr1* and *trx1 trx2 glr1* mutants were shown to be non-viable, and from the finding that loss of both TRX1 and TRX2 results in elevated levels of GSSG and GSH (Muller 1996; trotter and Grant, 2002). Recently, it was demonstrated that both Trx1 and Trx2 are able to reduce GSSG *in vivo*, indicating that also the cytosolic Trxs can reduce GSSG (Bao *et al.,* 2009; Tan *et al.,* 2010). The contribution of the cytosolic thioredoxin systems for reduction of GSSG *in vivo* becomes particularly important under stress conditions (e.g. oxidative stress), where the glutathione-glutaredoxin system is over-loaded and accumulation of GSSG may occur (Grant *et al*., 1996; Grant *et al.,* 1998; Ng *et al.,* 2008; Tan *et al.,* 2009).

Grx1 and Grx2 share 40-52% identity and 61-75% similarity with those from bacterial and mammalian species (Luikenhuis *et al*., 1998). Grx1 and Grx2 are not essential for growth under normal aerobic conditions (Luikenhuis *et al.,* 1998). The cytosolic Grx1 and Grx2 have general activity as GSH-dependent oxidoreductases and for protection against ROS (reactive oxygen species) (Luikenhuis *et al.,* 1998; Collinson *et al.,* 2002; Collinson and Grant, 2003; Eckers *et al*., 2009). *In vivo* studies showed that Grx1 is efficient against the superoxide anion, whereas Grx2 is specific for hydroperoxides (Luikenhuis *et al.,* 1998). This indicates that, despite their high degree of homology, the two Grxs have different sets of substrates or different ability to detoxify ROS (Grant *et al.,* 2000).

Trx1 and Trx2 are highly homologous (74% identity) and thus, have redundant functions (Muller 1991; Muller 1996). Many *in vitro* studies suggested that the Trxs have a more general function than Grxs. Both Trx1 and Trx2 are dispensable under normal growth conditions, but deletion of both genes affects the cell cycle, resulting in a shortened G1 interval and prolonged S phase (Muller 1991). It has been shown that this growth defect was not due to the alterations in the levels of deoxyribonucleotides, but to a redox-dependent activity (Muller 1995). In addition, in yeast thioredoxin and not glutaredoxin was shown to be the sole hydrogen donor for phosphoadenyl-sulphate reductase (PAPS reductase), the enzyme catalysing the reduction of PAPS to sulphite at expenses of one molecule of NADPH (Muller 1991).

Several lines of evidences showed that Trx1 and Trx2 work as anti-oxidants. Firstly, overexpression of both Trx1 and Trx2 led to an increased resistance against hydroperoxides. Secondly, both Trx1 and Trx2 act as cofactors for the thioredoxin-peroxidase (Tsa-1) mediated resistance to hydroperoxides. And thirdly, the *trx2* mutant is sensitive to H_2O_2 during stationary phase, but not during exponential phase (Garrido and Grant, 2002; Wheeler and Grant, 2004). In addition, in contrast to the Grxs, the cytosolic Trxs normally functions *in vivo* to maintain the intracellular GSH/GSSG ratio in a growth-dependent manner: exponential-phase *trx1 trx2* cells displayed increased GSSG levels resulting in altered cellular GSH/GSSG redox balance (Muller 1996; Luikenhuis *et al.,* 1998; Dardalhon *et al.,* 2012). In contrast, in stationary-phase the GSH/GSSG ratio of *trx1 trx2* cells was restored to WT levels, because of the induction of various cellular antioxidants whose expression increases during stationary phase (e.g. GLR1, Grx1 and Grx2, Catalase 1 and Superoxide Dismutase 2; Garrido and

Grant, 2002). However, stationary-phase *trx1 trx2* cells were unable to maintain the redox ratio GSH/GSSG in response to a challenge with H_2O_2, suggesting that the TRXs are primarily involved in the protection against H_2O_2 (Garrido and Grant, 2002). Additionally, the loss of TRX1 and TRX2 determines the constitutively activation of yAP-1, the transcription activator protein which regulates the activation of many stress-responses genes (Izawa *et al,* 1999; Delaunay *et al.,* 2000; Garrido and Grant, 2002). Thus, this indicates that the thioredoxin system helps control the oxidative stress during normal growth of yeast. In contrast, this function seems not to be linked to the glutaredoxin system as in the *grx1 grx2* mutants no YAP-1 activation was seen. It has been also shown that both Trx1 and Trx2 are required for proper nuclear accumulation of Msn2 and Msn4, transcription factors of the general response to stress, as the two transcriptional regulators failed to accumulate into the nucleus in response to a challenge with H_2O_2 (Boysnard *et al.,* 2000). Finally, the recent discovery that GSSG is also substrate of the cytosolic thioredoxins may indicate that the thioredoxin systems work as back-up systems to protect cells against oxidative stress (Ng *et al.,* 2008; Tan *et al.,* 2009).

Due to the diverse occurrence of the Trxs and Grxs in all genomes, the identification of the specific functions and/or target proteins of each oxidoreductase is one of the major tasks for the redox biology scientists. Here, this study investigated the role of these cytosolic redoxins in mitochondrial protein biogenesis making use of both *in vivo* and *in vitro* approaches.

1.6 Aims and objectives

Although in recent years many developments in the understanding of the biogenesis of the small Tim proteins have been achieved, numerous facets of this process need still to be elucidated. Using the yeast *S. cerevisiae* and Tim9 as model, the main objectives of this study were:

1) to identify the OM proteinaceous factors interacting with Tim9 during its binding to the OM and translocation across the OM (Chapter 3).

2) to understand the molecular mechanisms of Tim9 oxidative folding in the presence of Mia40 both *in vitro* and *in organello*. In addition, studies to identify the role of GSH in the import and the Mia40-mediated oxidative folding of Tim9 were conducted (Chapter 4).

3) to identify the cytosolic factor/s involved in the biogenesis of small Tim proteins (Chapter 5).

2. Materials and Methods

2.1 Cell biology methods

2.1.1 Yeast strains

The *Saccharomyces cerevisiae* strains used in this study are indicated in table 2.1:

Table 2.1: List of the yeast strains used in this study.

Strains	Genotype	Ref/source
D273-10B	MAT a mal	Fred Sherman, 1962
BY4742	MATα his3Δ1 leu2Δ0 lys2Δ0 ura3Δ0	
BY4742 *tom5*Δ	MATa his3Δ1 leu2Δ0 lys2Δ0 ura3Δ0 YPR133w-a::kanMX4	
CY4	MATa ura3-52 leu2-3,112 trp1-1ade2-1 his3-11 can1-100	Luikenhuis et al., 1997/ Chris Grant (Manchester)
CY117	As in strain CY4 but grx1::LEU2 grx2::HIS3	Luikenhuis et al., 1997/ Chris Grant (Manchester)
CY302a	As in strain CY4 but trx1::TRP1 trx2::URA3	Draculic et al. 2000/ Chris Grant (Manchester)
CY303α	As in strain CY302 but MATα	Garrido and Grant, 2002/ Chris Grant (Manchester)
CY476	As in strain CY4 but trr1::HIS3	Garrido and Grant, 2002/ Chris Grant (Manchester)
CY524	As in strain CY4 but trx1::TRP1 trx2::URA3 trr1::HIS3	Chris Grant (Manchester)

2.1.2 Media for the cultivation of the yeast strains

Types of media for yeast culture were YPD (2% w/v glucose, Fisher Scientific; 2% w/v bactopeptone, Melford; 1% w/v yeast extract, Melford); YPG (2% v/v glycerol, Fisher chemical; 2% w/v bactopeptone; 1% w/v yeast extract); and YPEG (1% v/v ethanol, Fisher chemical; 2% v/v glycerol, 2% w/v

bactopeptone,1% w/v yeast extract). To make solid YPD, YPG or YPEG media 2% w/v agar (Sigma) was added.

To isolate mitochondria cells were grown in lactate medium (LM): 0.3% w/v yeast extract (Difco), 0.05% w/v glucose (Fisher scientific), 0.1% w/v KH_2PO4, 0.1 w/v NH_4Cl, 0.05 w/v $CaCl_2 \cdot 2H_2O$, 0.05 w/v NaCl, 0.06 % w/v $MgCl_2 \cdot 6H_2O$, 0.1% w/v NH_4Cl, 0.8% w/v NaOH pellets, 2.2% v/v DL-Lactic acid (Fluka) in milli-Q H_2O. The final pH was adjusted to 5.5 with concentrated KOH.

2.1.3 Determination of the growth characteristics of the yeast strains

2.1.3.1 Growth curves

To monitor the growth of each strain, cells were first grown in YPD to stationary phase (48h) at 30°C. Cells were then inoculated to the same initial starting density A_{600} of 0.2, grown in YPD or YPEG fur further 30h at 30°C and their growth monitored by A_{600}.

To monitor the sensitivity to higher temperatures, cultures of BY4742 WT or *tom5*Δ were streaked onto fresh YPD or YPG plates from glycerol stocks and grown under aerobic conditions either at 30°C or at 37°C.

2.1.3.2 Spot tests

Cultures of all isogenic derivatives of CY4 were first grown to stationary phase (48h) in YPD media at 30°C, and then adjusted to A_{600} of 1, 0.1, 0.01 and 0.001 before spotting onto fresh YPD or YPEG plates. Cells were grown under aerobic conditions for 48-60h at 30°C.

2.1.3.3 Growth condition for preparing whole cell extracts

Cultures of all isogenic derivatives of CY4 were first grown to stationary phase (48h) in YPD media at 30°C, and then adjusted to A_{600} of 0.2. Cells were then grown in YPD or YPEG at 30°C until A_{600} of 0.7, collected by centrifugation, and then used for preparing whole cell extracts.

2.1.3.4 Growth condition for the shift from YPD to YPEG media

Cultures of all isogenic derivatives of CY4 were grown to stationary phase (48h) in YPD at 30°C, and then adjusted to A_{600} of 0.2. Cells were grown to mid-exponential phase in YPD until A_{600} of 10. Cells were harvested and the pellets washed twice with milli-Q H_2O before switching to YPEG medium. The growth in YPEG was stopped after 6h, and the cells collected by centrifugation and used for mitochondrial isolation. The shift form YPD to YPEG will be indicated as YPD➔YPEG in the text.

2.1.4 Determination of protein levels in whole cell extracts

The cell extracts were prepared from yeast cells grown as described in 2.1.3.3: cells were harvested by centrifugation and washed with 20 mM phosphate buffer (pH 7.4; 0.1M Na_2HPO_4; 0.1 M NaH_2PO_4) containing 0.5 mM PMSF (Phenylmethylsulfonyl fluoride, Roche Diagnostic, Germany). Cells were broken at 4°C with glass beads using a minibead beater (Biospec Products) for 2 x 30 sec within 1 min in between. Cell debris and proteins were pelleted in a refrigerated bench-top centrifuge for 15 min at 4°C and at 13,000 rpm, and the supernatants were used for the determination of mitochondrial protein levels by western blot.

2.1.5 Procedure for the isolation of mitochondria

Mitochondria were purified according to the procedures described by Daum *et al.* (1982a) and Glick and Pon (1995) (Daum *et al*, 1982a, Glick and Pon, 1995). Yeast strains used to isolate mitochondria were: BY4742 WT, BY4742 *tom5*, CY4 WT, CY117 *grx1 grx2* and CY303 *trx1 trx2*.

For BY4742 WT and BY4742 *tom5*, several colonies from the respective YPD plates were used to inoculate 200 ml of LM, and cells were grown to the late exponential phase either for 24h at 30°C or for 43h at 24°C, respectively. For all isogenic derivatives of CY4, cells were grown in LM to the stationary phase, and then cells corresponding to an approximate value of A_{600} of 0.2 were used to inoculate 200 ml of LM at 30°C. Cells were then grown to the late exponential phase at 30°C. The 200 mL pre-cultures were used to inoculate 4 x 1 L flasks of fresh LM. Cells were then grown to the late-exponential phase at the agitation speed of 200 rpm under aerobic conditions. Subsequently, cells were harvested by centrifugation for 10 min at 6,000 g in a JLA8.1000 rotor in a J2-HS centrifuge. Each pellet was washed once with distilled water and the cells were re-isolated by centrifugation at 3.000 g for 5 min. The wet cell pellets were weighed and resuspended in 25 ml of TRIS-DTT buffer (100 mM Tris-SO_4 pH 9.4; 10 mM DTT, Sigma) and incubated for 20 min at 30°C with gentle shaking (60 rpm). Cells were then collected by centrifugation, washed once with 1.2 M Sorbitol buffer (2.4 M Sorbitol, Sigma; 20 mM K_2HPO_4 , Fisher Scientific) and centrifuged again for 5 min. In the meantime 3 mg of Zymolase 20 T (Seikagaku Corporation, Japan) per gram of yeast cells (wet weight) was weighed and dissolved in 1.2 M sorbitol buffer (2 ml per gram of cells) to obtain the zymolase buffer.

The pellet was resuspended in the zymolase buffer and incubated for 35-40 min at 30°C with gentle shaking (80 rpm) to convert the cells into spheroblasts.

To test the efficiency of the spheroblasting process, the value of the A_{600} was monitored until it has reached the 10% of its starting value. The A_{600} was measured every 10 min by diluting 2 ul cell suspension in 998 ul Milli-Q H_2O. From this point all the operations were carried out on ice. Spheroblasts were then harvested by centrifugation for 5 min at 3000 rpm at 4°C and washed twice with 1.2 M sorbitol buffer. Meanwhile, 200 mM PMSF was added drop by drop to 100 ml of ice-cold BB7.4 buffer (0.6 M Sorbitol; 20 mM HEPES-KOH pH 7.4). This solution was filtered through paper (Whatman) before use and used to resuspend the spheroplasts. Spheroblasts were then homogenized with 15-20 strokes of a glass-teflon dounce homogenizer (Sigma-Aldrich). The rupture of spheroblasts was checked under microscope before and after the strokes. The homogenate was then centrifuged for 5 min at 1,500 g, and the supernatant was saved and kept on ice. The pellet was resuspended in homogenization buffer (BB7.4 buffer; 1 mM PMSF) and homogenized again as before. The second homogenate was centrifuged for 5 min at 5,000 g. The supernatant was recovered and combined with the previous supernatant. The combined supernatants were centrifuged at 4,000g for 5 min at 4°C, and the supernatant was recovered and centrifuged in a J25.50 rotor at 10,000 rpm at 4°C for 10 min. The cytosol was poured off and the mitochondrial pellet was resuspended in 2 ml of BB7.4. The protein concentration was determined by measuring the absorbance at 280 nm on the assumption that an A_{280}=0.21 equals a crude mitochondrial concentration of 10 mg/ml. The concentration of mitochondria was adjusted to 10 mg/ml, after addition of 10 mg/ml fatty acid free BSA (bovine

serum albumin, Sigma, ST. Louis, USA) and the samples were then snap frozen in liquid N_2 and stored at -80°C until use.

2.2 Protein purification and molecular biology techniques

2.2.1 Expression and purification of Mia40$_{core}$ from *Escherichia coli*

The pGEX 4T-1 plasmid (GE Healthcare) containing Mia40$_{core}$ gene (expressing the amino acids 284-403 of yeast full length Mia40) was transformed in *E. coli* BL21 (DE3) cells (Stratagene, La Jolla, USA). Cells were grown overnight at 37°C in 100 ml of fresh Luria Broth medium containing 100 mg ml^{-1} of ampicillin (Sigma). 50 ml of the overnight culture was used to inoculate 1 L of fresh LB medium containing ampicillin. The cell culture was grown at 30°C at 200 rpm until the A_{600}=0.6-0.8. Expression of Mia40$_{core}$ was induced overnight at 16°C by addition of IPTG (isopropyl-β-thiogalacto-pyranoside, Roche) to a final concentration of 1 mM at 200 rpm. The day after, cells were harvested by centrifugation at 4°C at 5,000 rpm and then resuspended in 20 ml of buffer AE (50 mM Tris-(hydroxymethyl) aminonethane-HCl pH 7.4; 150 mM NaCl, Fisher Scientific; 1 mM EDTA, Roche). Cell lysis was performed by a 10 x 10 sec, 1 min interval, 35% amplitude sonication in the presence of one EDTA-free protease inhibitor cocktail tablet (Roche, Germany). The cell lysate was centrifuged at 4°C at 18,000 rpm. The supernatant was incubated overnight with 2 ml of Glutathione Sepharose TM 4B beads (Amersham Bioscience) pre-equilibrated with BAE buffer. The beads were then washed with 20X BAE. 100 units of Thrombin (Sigma) were incubated for 4 h with Mia40$_{core}$-bound beads to free the protein in 8-10 ml of BAE. All steps were performed at 4°C.

2.2.2 Gel filtration chromatography

Prior any protein assays, $Mia40_{core}$ was further purified by gel filtration (size exclusion) chromatography using a Superdex 200 (Amersham Pharmacia, Uppsala, Sweden) connected to the AKTA Purifier FPLC system (Amersham Pharmacia, Uppsala, Sweden) operated by Unicorn software. The column was first equilibrated with BAE buffer, and the samples were centrifuged at maximum speed for 5 min in a bench-top centrifuge to remove any protein precipitate before injection into the system. The samples were injected in a 500 ul injection loop; the flow rate was set at 0.5 ml min^{-1} and the length of elution was set to one column volume and the size of the elution was 1 ml. The low molecular weight fraction (second peak) was divided into aliquots and kept at -80 °C until use.

2.2.3 Site-directed mutagenesis

The Tim9 and Tim10 cysteine to serine point mutations were introduced by PCR site-directed mutagenesis. The oligonucleotides containing the mutations used for the PCR reactions are listed in Table 2.2. To generate double or triple cysteine mutants, a oligonucleotide containing a single or double cysteine mutation was used as the template for mutagenesis reaction with the primers for the second or for the second and third cysteine mutations.

The PCR was performed using the following 20 ul reaction mix:

- 10 ng of wild-type or mutant construct as template DNA
- 0.3 mM of deoxynucleotide triphosphate mix
- 12.5 pmol of each primer set
- 2.5 units of Pfu DNA polymerase (Fermentas, Hanover, MD, USA)
- 1X working concentration of the reaction buffer system

and using the following PCR program:

- 95°C for 30 seconds
- 18 cycles at 95°C for 30 seconds
- 55°C for 1 minute and 68°C for 13 minutes

Table 2.2: List of the primer sequences used for the site-directed mutagenesis.

DNA template	Oligonucleotides (5' to 3')
Tim9C35S	F CTAATCTGGTAGAAAGATCTTTCACAGACTGTGTC R GACACAGTCTGTGAAAGATCTTTCTACCAGATTAG
Tim9C39S	F GAAAGATGTTTCACAGACAGTGTCAATGACTTCACAAC R GTTGTGAAGTCATTGACACTGTCTGTGAAACATTC
Tim9C55S	F AATAAGAATGAATCTTCGAGACTAGACAGATGTGTCGCC R GGCCACACATCTGTCTAGGCTCGAAGATTCATTCTTATT
Tim9C59S	F CATGCATCATGAAGTCTTCAGAAAAGTTCTTC R CAAGAACTTTTCTGAAGACTTCATGATGCATG
Tim9C35,39S	F GTAGAAAGATCTTTCACAGACTCTGTCAATGAC R GTCATTGACAGAGTCTGTGAAAGATCTTTCTAC
Tim9C55,59S	F AAGGAACAAACAAGCATCATGAAGAGCTCAGAAAAGTTC R GAACTTTTCTGAGCTCTTCATGATGCTTGTTTGTTCCTT
Tim10C40S	F TAAATTGGTTAATAACTCGTATAAAAAATGTATC R GATACATTTTTTATACGAGTTATTAACCAATTTA
Tim10C44S	F CTGTTATAAAAAATCCATCAATACTTCTTATTC R GAATAAGAAGTATTGATGGATTTTTTATAACAG
Tim10C61S	F AATAAGAATGAATCTTCGAGCCTAGACAGATGTGTGGCC R GGCCACACATCTGTCTAGGCTCGAAGATTCATTCTTATT
Tim10C65S	F CTTCGTGCCTAGACAGAAGTGTGGCCAAATATTTTG R CAAAATATTTGGCCACACTTCTGTCTAGGCACGAAG
Tim10C40,44S	F GTATAAATTGGTTAATAACTCTTATAAAAAATCTATC R GATAGATTTTTTATAAGAGTTATTAACCAATTTATAC
Tim10C61,65S	F GGCCACAGATCTGTCTAGGGACGAAGATTCATTCTTATT R AATAAGAATGAATCTTCGTCCCTAGACAGATCTGTGGCC

Small changes were applied to the program depending on the DNA sequences. The PCR products were examined by agarose gel electrophoresis (2.2.4). Subsequently, the parental plasmid DNA was digested with 10 units of Dpn1 (Stratagene, La Jolla, USA) at 37°C for 1h. Transformation was then achieved by incubating 5 ul of the digested products with 50 ul of competent *E. coli* TOP10 cells (Invitrogen Carisbad, CA, USA) for 1 h on ice followed by heat-shock at 42°C for 60 s, and finally placed on ice for 5 min. 500 ul of LB were added to the mix and then incubated for 30 min at 37°C. Cells were collected by

centrifugation at 6,000 rpm for 20 seconds and resuspended into 200 ul of LB. Approximately 50 ul of the culture was then plated on LB agar plates containing 100 ug ml^{-1} of ampicillin, and incubated at 37°C overnight in a shaking incubator. On the following day, colonies were picked up, inoculated in a liquid culture of 5 ml LB plus ampicillin (100 ug ml^{-1}) and grown o/n at 37°C in a shaking incubator. The day after, the DNA was purified using the QIAprep® Spin Miniprep Kit (Qiagen, Hilden, Germany) according to the manufactures guidelines. Sequencing was sent to the GATC BIOTECH Company to check for correct mutagenesis.

2.2.4 Agarose gel electrophoresis for DNA extraction

The PCR products were analysed by 1X Tris-Acetic Acid agarose gel (TAE, 40 mM Tris pH 7.5; 20 mM acetic acid; 1 mM EDTA) electrophoresis. The PCR products were mixed with 5x loading dye (Qiagen) in a 4:1 ratio, loaded on the 0.4% agarose gel, and run in TAE buffer at 100 V. Molecular weight markers (new England BioLabs) were run alongside the samples. The DNA fragments were visualized under UV light and the fragments of interest excised with a clean scalpel. The DNA was then extracted from the gel using the " QIAquick Gel exctraction kit" (Qiagen) according to the manufacturer's guidelines.

2.3 *In organello* biochemistry

2.3.1 Import of radiolabelled precursors into purified mitochondria

2.3.1.1 *In vitro* synthesis of radiolabelled precursor proteins

Mitochondrial precursor proteins used in this study were cloned into pGEM vectors under the control of the *Sp6* promoter. Top10 E.*coli* cells carrying the plasmid of interest were grown overnight at 37°C in LB containing ampicillin (100 ug ul^{-1}). The day after, plasmids were purified using the QUIAGEN Plasmid Maxi kit according to the manufacturer's protocol. The concentration of the purified plasmids was calculated by measuring the absorbance at 260 nm. Radiolabelled precursors were generated with the TNT® SP6 Coupled Reticulocyte Lysate System (Promega, Fitchburg, USA) in the presence of [^{35}S] Methionine (Perkin Elmer) and the plasmid constructs as DNA template (Söllner *et al.,* 1991). Typically, 30 µl of TnT reaction includes 15 µl TnT rabbit reticulocyte lysate, 1.2 µl TnT reaction buffer, 0.6 µl SP6 TnT RNA polymerase, 0.6 µl amino acids mix minus methionine, 0.6 µl RNasin ribonuclease inhibitor (40 units μl^{-1}), 1 ug DNA template and 1.2 µl ^{35}S-methionine (0.08 mCi μl^{-1}). The reaction was carried out at 30°C for 90 min and stopped by centrifugation at 55,000g for 15 min at 4°C using the refrigerated S100-AT3 fixed angle titanium rotor (Thermo Scientific). The supernatant containing the radiolabelled ^{35}S-precursors was used for the import assays immediately.

2.3.1.2 Mitochondria Preparation

Mitochondria were thawed from -80°C on ice for 20 min. They were diluted 10 times in ice-cold BB7.4 buffer and reisolated by centrifugation at 13,000 rpm for 5 min at 4°C in a refrigerated bench-top centrifuge. The pellet was then washed

again in BB7.4 buffer, reisolated, and then resuspended to 10 mg ml^{-1} in ice-cold BB7.4 buffer.

For the trypsin treatment before import, 75/100 ug of mitochondria were incubated with trypsin buffer (typically 20 ug ml^{-1} of trypsin in BB7.4 buffer unless otherwise stated, Sigma-Aldrich) for 20 min on ice. Trypsin was inactivated by the addition of SBTI buffer (soya bean trypsin inhibitor, Sigma-Aldrich; 0.6 mg ml^{-1} SBTI; BB7.4;) and the samples were further incubated on ice for 10 min. Mitochondria that were pre-treated with trypsin before import (shaved mitochondria) were then reisolated by centrifugation at 13,000 rpm for 5 min at 4°C and washed twice before the import assays. To generate mitoplasts, mitochondria were incubated in hypotonic buffer (10 mM HEPES-KOH pH 7.4) for 30 min, and then re-isolated by centrifugation.

2.3.1.3 Import of radiolabelled precursors into isolated mitochondria

The schematic representation of a typical mitochondrial import assay according to is depicted in Figure 2.1 (Dario Leister and Johannes M. Herrmann, 2007. *Mitochondria: practical protocols*, Humana Press). Import assays were carried out in 150 ul of import buffer **(**0.6 M sorbitol; 50 mM Hepes-KOH pH 7.4, Fisher Scientific; 50 mM KCl, VWR International; 1.5 mg ml^{-1} methionine, Sigma-Aldrich; 2 mg ml^{-1} fatty acid free BSA; 2 mM EDTA) with 75 ug of mitochondria. Where mitochondria were pre-treated with trypsin, a final concentration of SBTI was added in the import buffer in order to prevent any further digestion by trypsin of the added precursor proteins. For import of radiolabelled Su9-DHFR (subunit 9-dihydrofolate reductase), F1-β (F1-ATPase subunit β) and AAC (ATP/ADP carrier) precursors, 2 mM ATP (Fluka) and 2.5 mM NADH (reduced

Nicotinamide adenine dinucleotide, Sigma-Aldrich) were added in the import buffer.

The import mixtures were usually incubated at 25°C for 5 min before adding 3.3% (v/v) of the radiolabelled precursors. The imports of precursor small Tim proteins were always performed at 25°C unless otherwise stated. The imports of Su9-DHFR and F1-β, AAC and porin precursors were performed at 30°C.

For imports in the presence of GSH (Sigma-Aldrich), GSH was included in the import mixtures. For import of precursors in the presence of the Trx1 system, the recombinant Trx1 (1.5 uM) and Trr1 (0.5 uM) proteins with NADPH (0.6 mM, Sigma) were added to the import mixtures and incubated at 25°C for 20 min before adding the radiolabelled precursors.

2.3.1.4 Post-import treatments of mitochondria

To quench import and to remove the unimported precursors from the OM, samples were diluted five fold in ice-cold trypsin buffer (BB7.4 buffer; 50 ug ml^{-1} Trypsin, Sigma) and incubated on ice for 30 min. The protease was inactivated by the addition of SBTI buffer **(**BB7.4; 1 mg ml^{-1} SBTI, Sigma-Aldrich) for 10 min on ice. To analyse the binding of the precursors to the OM, the trypsin treatment was omitted and the import mixtures were diluted five fold in ice-cold BB7.4 buffer for 30 min. To solubilise mitochondria after import, an aliquot of the import reaction was treated with digitonin (1 µg ml^{-1}) for three min before the post-import trypsin treatment. To trap the intermediates between Mia40 and the radiolabelled precursors, mitochondria were incubated with 75 mM of the alkylating agent IAA (2-iodoacamide, Sigma) for 1 h on ice.

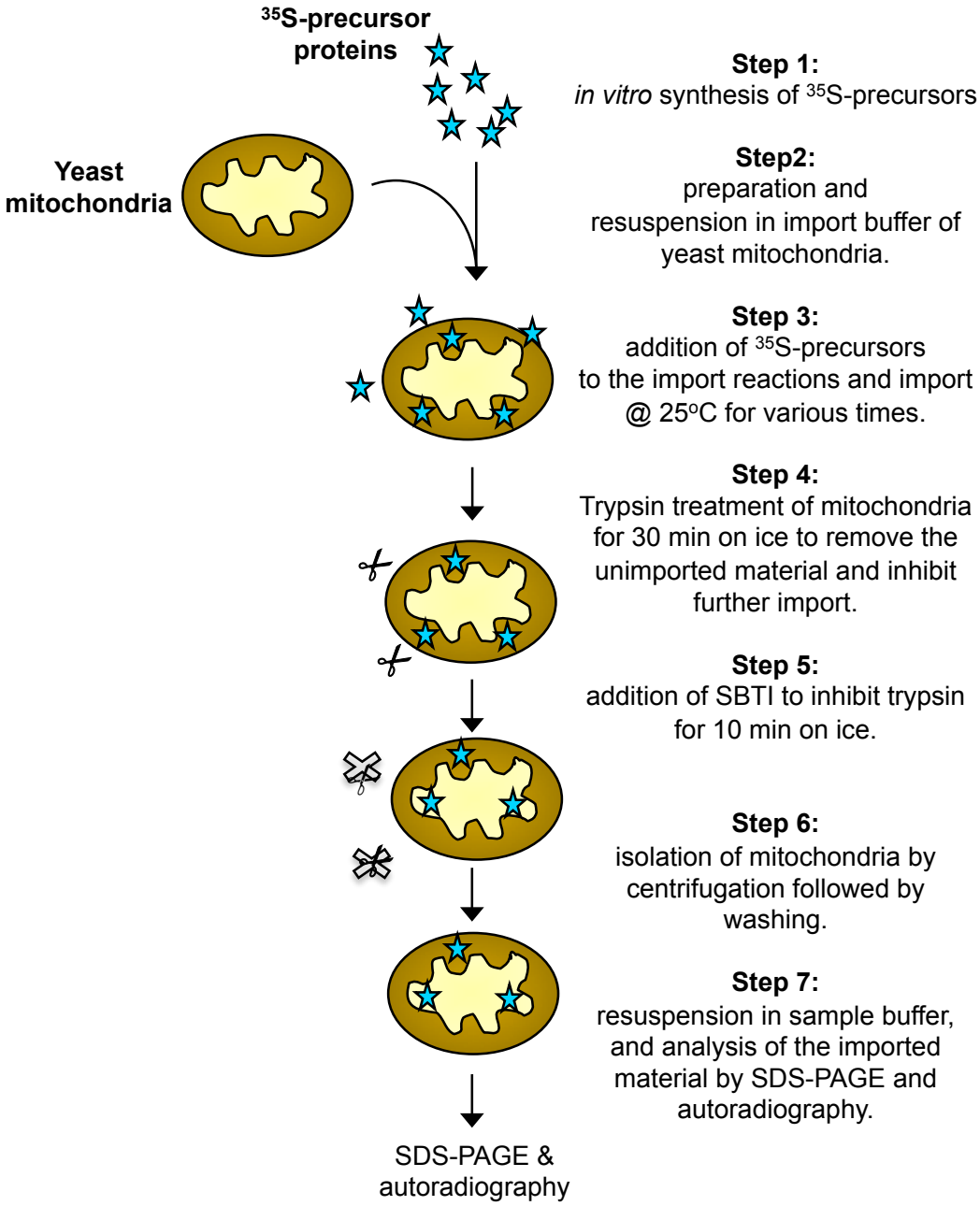

Figure 2.1 Mitochondrial import assay.

The mitochondrial import assay used in this study starts with the generation *in vitro* of radioactive ^{35}S-precursor proteins (step1). At the same time mitochondria are thawed and incubated in import buffer (step 2). The radioactive precursors are added to the import reactions and imported into mitochondria for various time at 25^{o}C (step 3). Following import, the import reactions are diluted with 5-fold ice cold trypsin buffer (step 4) to inhibit further import and digest the unimported material. The reactions are then incubated with the trypsin inhibitor SBTI (step 5). After 10 min, mitochondria are isolated by centrifugation, washed twice, resuspended with sample buffer (step 6), and lastly, analysed by SDS-Page and autoradiography (step 7).

In all cases, mitochondrial samples were then reisolated by centrifugation at 13,000 rpm for 5 min at 4°C and the pellets washed twice with BB7.4 buffer before resuspension in reducing or non-reducing sample buffer. The samples were heated to 95°C for 5 min followed by centrifugation at maximum speed for 5 min, and then applied to a 16% Tris-Tricine SDS-PAGE gel at 25 mA for gel. The gels were transferred to nitrocellulose membrane (Bio-Rad, 0.2 µm) for 1 h and 20 min at 300 V. The membranes were exposed for 24-48 h to either KodaK Biomax MR Film or a Fuji phosphor imaging plate. Plates were read using a Fujifilm, FLA-3000 Image Analyzer and the Typhoon.

2.3.1.5 AMS gel-based shift assay on the unimported precursors

Typically a 15 µl aliquot was removed from the import reaction and subjected to centrifugation to remove mitochondria at 13,000 rpm and 4°C for 5 min in a refrigerated bench-top centrifuge. The supernatant was carefully removed and added to 10 µl AMS buffer (6X sample buffer minus DTT, Apollo Scientific; 12.5 mM AMS, Invitrogen). AMS is a ~500 Da reagent that covalently modifies reduced thiol groups in a 1:1 stoichiometry, thus increasing the protein molecular mass and decreasing its electrophoretic mobility. Samples were then incubated in the dark for 30-60 min, heated to 95°C for 5 min, centrifuged at maximum speed for 5 min and analysed as above.

2.3.2 Determination of protein levels in purified mitochondria

25, 50 and 100 ug of the isolated mitochondria were resuspended in reducing sample buffer and applied to 10%-12% Tris or 16% Tris-Tricine SDS-PAGE gels. The gels were transferred to nitrocellulose membrane for 1h and 20 min

at 300 mV. The membranes were analysed by western blotting with different antibodies against mitochondrial proteins (Table 2.3).

In the case of mitochondria purified from the YPD➔YPEG shifted CY WT and CY *trx1 trx2* cells, the western blot signals for each protein marker were quantified by densitometry using the AIDA 3.28 software and expressed in comparison to the WT. All data are expressed as means ± standard deviations from three independent experiments. The statistical analysis was performed using the t-test, and differences were considered significant at $P < 0.05$.

2.3.3 Determination of the redox state of Tom40 in mitochondria

~ 75 ug of mitochondria were incubated with AMS buffer (50 mM AMS; 0.5 M Tris pH 8) for 30 min at RT. Mitochondria were pelleted for 5 min (at 4°C and 13,000 rpm), and either washed twice or left untreated before resuspension with non-reducing sample buffer. Proteins were separated by 10% Tris SDS-PAGE gel, and analysed as before except that Tom40 antibody was used.

2.3.4 Determination of the redox state of Mia40 in mitochondria

For the analysis of the redox state of mitochondrial Mia40, ~35 ug of mitochondria were incubated with either AMS buffer (12.5 mM AMS; 0.125 M Tris pH8) or with 20 mM NEM (N-ethylmaleimide, Sigma) for 1h on ice.

Similar to AMS, NEM (125 Da) is an alkylating agent that covalently modifies reduced thiols groups in a 1:1 stoichiometry, thus increasing a protein's molecular mass and decreasing its electrophoretic mobility. Mitochondria were pelleted for 5 min (at 4°C and 13,000 rpm), and washed twice before resuspension with non-reducing sample buffer. Proteins were separated by

10% Tris SDS-PAGE analysis, and the gel was transferred onto nitrocellulose membrane as before for western blotting analysis with Mia40 antibody.

For the analysis of Mia40 redox state in mitochondria that were pre-incubated with or without the purified components of the Trx1 system, mitochondria were isolated, washed twice with BB7.4 buffer and then resuspended with non-reducing sample buffer containing 25 mM AMS. As a control for the reduced state of mitochondrial Mia40, mitochondria were pre-treated with 2 mM TCEP (Tris(2-carboxyethyl)phosphine hydrochloride, Sigma) at RT for 30 min, then isolated and washed twice before resuspension with non-reducing sample buffer containing 25 mM AMS. Proteins were then separated as described in the previous paragraph.

2.4 *In vitro* biochemistry

2.4.1 *In vitro* reconstitution experiments

2.4.1.1 Ammonium sulphate precipitation of lysate

After synthesis of radiolabelled precursor small Tims as described in 2.3.1.1, ammonium sulphate precipitation was performed on the lysates because the heme in the lysate presented a significant non-specific labelling and an electrophoretic mobility overlapping with that of oxidised small Tims. Heme does not precipitate well with ammonium sulphate and thus can be removed.

After ultracentrifugation of the lysate to remove ribosomes, the supernatants were diluted with two volumes of ice-cold saturated ammonium sulphate (50 mM Hepes; 150 mM NaCl) and incubated on ice for 30 min. Subsequently,

samples were centrifuged for 30 min at 25,000 g and 4°C. The supernatants were removed and the precipitated pellet was resuspended with BAE buffer and used immediately for *in vitro* reconstituted assays, as described in the following section.

2.4.1.2 Reconstitution experiments and analysis of trapped thiols

Chemical amounts of radioactive ^{35}S-Tim9 WT or ^{35}S-Tim10 WT or variants were diluted 10-fold with buffer BAE containing either an excess (1 μM) or stoichiometric amounts (5-10 nM) of recombinant Mia40$_{core}$ on ice. At various time points, aliquots were removed and incubated with AMS buffer for 1h at RT. Proteins were then resuspended with 6X non-reducing SDS sample buffer, heated for 5 min at 95°C followed by centrifugation at maximum speed for 5 min.

When GSH was included in the reconstituted experiments, radioactive proteins were added as soon as GSH was mixed with recombinant Mia40$_{core}$. Prior the start of each experiment, the redox state of the radiolabelled proteins was verified by AMS alkylation assay: a small aliquot of radioactive material (typically 1/25 of the total volume) was mixed either with BAE buffer or AMS buffer (50 mM AMS; 0.5 M Tris pH 8) for 1 h at RT. Samples were then run on 16% Tris-Tricine SDS-PAGE gels, transferred onto nitrocellulose membrane and analysed by autoradiography or by western blot against Mia40.

2.5 Electrophoresis techniques

2.5.1 Tris SDS-PAGE (sodium dodecyl sulphate polyacrylamide gel electrophoresis)

The electrophoretic run was performed at 100 V. For one 10% or 12% SDS-PAGE gel:

Separating gel: 3.33 ml or 4.17 ml 30% (w/v) acrylamide/ 0.8% (w/v) bis-acrylamide (National Diagnostic), 2.5 ml v/v anode buffer, 4.17 ml- 3.33 ml milli-Q H_20, 50 ul APS (ammonium persulfate, Sigma), 5 ul TEMED (Sigma-Aldrich).

Stacking gel: 0.6 ml 30% (w/v) acrylamide/ 0.8% (w/v) bis-acrylamide, 1.25 ml cathode buffer, 3.15 ml milli-Q H_20, 50 ul APS, 5 ul TEMED.

Running buffer: 0.190 M glycine (Sigma), 25 mM Tris (Melford), 1 mM EDTA and 0.5% SDS (sodium dodecyl sulfate, Formedium).

2.5.2 Tris-Tricine SDS-PAGE

To polymerise separating and stacking gels a final concentration of 0.01% TEMED and 0.1% APS were added. For 1, 16% Tris-Tricine mini-gel:

16% Separating: 2.4 ml 30% (w/v) acrylamide/ 0.8% (w/v) bis-acrylamide, 0.15 ml 2.2% w/v bis-acrylamide (Serva), 1.5 ml 1.5M Tris/ 0.3% SDS (pH 8.45).

Stacking gel: 0.23 ml 30% (w/v) acrylamide/ 0.8% (w/v) bis-acrylamide, 10 ul 2.2% w/v bis-acrylamide, 0.460 ml 1.5M Tris/ 0.3% SDS (pH 8.45), 1.2 ml milli-Q H20.

Cathode Buffer: 0.1 M Tris pH 8.25, 0.1 M Tricine, 0.05% w/v SDS (Fisher Scientific).

Anode buffer: 0.2 M Tris pH 8.9

All gels were run using the Biorad mini-protean III system. For non-reducing conditions, samples were resuspended either in equal volume of 2X SDS-PAGE sample buffer without DTT, or in 1/5 volume of 6X SDS-PAGE sample buffer without DTT. For reducing conditions, 2X or 6X sample buffer with DTT was used. All the samples were heated at 95°C for 3-5 min and centrifuged for 5 min at maximum speed before loading.

2XSDS sample buffer ± DTT: 50 mM Tris-HCl pH 6.8, 20% v/v glycerol, 4% w/v SDS, ± 3% w/v DTT, 0.001% w/v bromophenol blue (Sigma).

6XSDS sample buffer ± DTT: 140 mM Tris-HCl pH 6.8, 30% v/v glycerol, 10% w/v SDS, ± 9.3% w/v DTT, 0.005% w/v bromophenol blue.

2.5.3 Gel transfer and western blotting

SDS-PAGE gels were transferred onto nitrocellulose membranes using a Hoefer TE 22 mini tank transfer gel electrophoresis unit in blotting buffer. The electro transfer was stacked as follows: anode, 3 trans blot transfer papers (Bio-Rad), membrane, gel, 3 trans blot transfer papers and cathode. Everything was pre-soaked for at least 10 min in blotting buffer and the transfer was carried out at 300 mA for 1h and 20 min or at 30 mA for 10 h in the cold room. The membranes were then blocked for 1 hour at RT with blocking buffer. Membranes were then washed with 1X PBS buffer (phosphate buffered saline) three times before incubation with the primary antibodies. Membranes were incubated with the primary antibodies either overnight at 4°C or for 4 h at RT (see Table 8.1 in Appendix). Consequently, membranes were washed as before and incubated with the secondary antibody for 1 h and 20 min at RT.

Membranes were thus washed up to three times with 1X PBS before and analysed. When using the HRP-conjugated secondary antibody (Polyclonal Goat anti-rabbit HRP, Dako, Denmark), the protein signals were revealed by enhanced chemiluminiscence (ECL, GE Healthcare) and exposed on Kodak Biomax MR Film. When using the infrared secondary antibody (IRDye® Secondary antibody, Ly-cor UK), the membranes were scanned in a Odyssey SA Scanner (LICOR Biosciences, UK).

Blotting buffer: 39 mM Tris, 30 mM glycine (Fisher Scientific) and 20% (v/v) methanol (Fisher Scientific).

Blocking buffer: 5% w/v milk in 1X PBS.

Primary antibody incubation buffer: 5% w/v milk, 0.1% Tween20 (Riedel-de Hoein) in 1X PBS.

Secondary antibody incubation buffer: 2% w/v milk, 0.1% Tween20 in 1X PBS.

3. RESULTS and DISCUSSION I: INVESTIGATION OF THE ROLE OF THE TOM COMPLEX ONTO TIM9 BIOGENESIS

3.1 Introduction

Mitochondrial import of small Tim proteins depends on the redox-sensitive MIA pathway. In contrast to the wealth of knowledge in existence about the import and oxidation process into the IMS mediated by the MIA machinery, it is still unknown how they are targeted to and bind to the mitochondrial OM. When this study started, it was known that the import of small Tim precursors into the mitochondria is not mediated by the receptors of the TOM complex, but requires the small subunit Tom5 of the TOM complex (Kurz e*t al.,* 1999).

In addition, differently from the matrix and the IM proteins, the import route of small Tim proteins does not need ATP or membrane potential for their insertion into the IMS (Koehler *et al.,* 1998; Kurz *et al.,* 1999). Therefore, it is not possible to arrest or accumulate the precursors at different stages of import, as can be routinely done by manipulating the in vitro mitochondrial import conditions for the matrix- or IM-targeted precursors (Pfaller *et al.,* 1989; Haucke *et al.,* 1995). As a consequence, no physical interaction between the TOM complex and the translocating small Tims has yet been detected. Thus, it is a common belief that the small Tims may interact only loosely with the TOM complex (Lutz *et al.,* 2003). However, when radiolabelled Tim13 was co-imported with chemical amounts of a matrix protein, the import efficiency of Tim13 was significantly reduced, suggesting that Tim13 and the matrix protein share in part their import routes, most likely while translocating the OM (*Lutz et al*., 2003). More recently,

it has been shown that small Tims cross the OM in a reduced and unfolded form (Lutz *et al.,* 2003; Lu *et al.,* 2004b; Muller *et al.,* 2008).

In order to identify potential proteins of the TOM complex contributing to the Tim9 binding to and translocation into the OM, different approaches were used. Firstly, the effects of different concentrations of salts on mitochondrial binding and import of Tim9 were analysed. Secondly, mitochondria from wild-type (WT) and *tom5Δ* yeast cells were isolated and analysed for their ability to import radiolabelled Tim9. Thirdly, to gain a deeper insight into the role of Tom40 on Tim9 biogenesis, the analysis of the sensitivity to trypsin and of the redox state of the cysteine residues of Tom40 were conducted both in WT and *tom5Δ* mitochondria. Radiolabelled Tim9 was then imported into mitochondria that were either pre-treated with trypsin or with an alkylating agent. Lastly, in order to test if Tim9, as shown for Tim13, shares in part its import route with the matrix-targeted proteins, the effects of purified oxidised Tim9 on import of radiolabelled Tim9 or Su9-DHFR were studied.

3.2 Influence of salts on mitochondrial binding and import of Tim9

For matrix- and IM- targeted precursor proteins binding and/or translocation to or across the OM depend on electrostatic interactions (Pfaller *et al.,* 1989; Haucke *et al,* 1995). In vitro their binding and import can be inhibited or stimulated by varying the ionic strength of the import conditions (Pfaller *et al.,* 1989). To study the influence of salts (KCl and $MgCl_2$) on Tim9 binding and import, Tim9 imports were performed with different concentrations of salt (Figure 3.1 and Figure 3.2). In a first experiment, radiolabelled ^{35}S-Tim9 was imported into mitochondria in the presence of the various amounts of KCl. After import, each import reaction was divided into two halves. One half was treated with trypsin to remove the unimported material and used for the analysis of the imported material. The second half was left untreated and used for the analysis of both bound and imported material. Mitochondria were then isolated by centrifugation and resuspended with reducing sample buffer. Proteins were resolved by SDS-PAGE, transferred onto nitrocellulose membrane and analysed by digital autoradiography (Figure 3.1 A). As a control, ^{35}S-matrix-targeted fusion protein between the presequence of Fo-ATPase subunit 9 and the entire dihydrofolate reductase (Su9-DHFR) was imported in parallel, as both its import and binding are inhibited at high KCl concentrations (Figure 3.1 B).

The results showed that both Tim9 import and binding to the OM were unaffected by the increasing amounts of KCl (Figure 3.1 A, lanes 2-4 and 6-8), in contrast to Su9-DHFR (Figure 3.1 B, lanes 1-8).

In a second experiment, the effects of various $MgCl_2$ concentrations on ^{35}S-Tim9 and ^{35}S-Su9-DHFR imports were analysed (Figure 3.2). As the import

reactions contain an endogenous concentration of $Mg2^{+}$ of about 1 mM, an additional 0-10 mM $MgCl_2$ was added. The results showed that Tim9 import and binding to the OM were not affected by the presence of the divalent cation (Figure 3.2 A, lanes 2-7), whereas, as expected, Su9-DHFR import but not binding to the OM was inhibited only in the absence of the salt (Figure 3.2 B, lanes 2 and 5).

Thus, high salts concentrations appeared not to affect binding and import of Tim9.

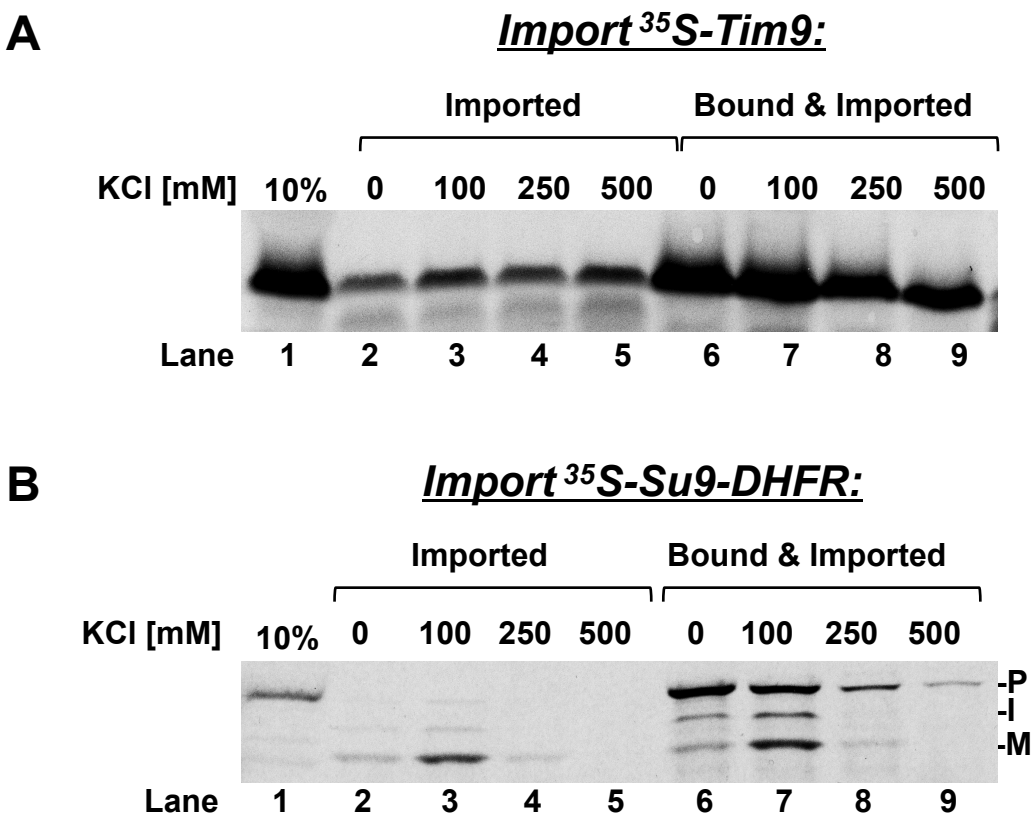

Figure 3.1 Effect of different amounts of KCl on Tim9 binding and import to/into mitochondria.

(A) ^{35}S-Tim9 was imported into mitochondria in the presence of the indicated concentrations of KCl. After import, mitochondria were either treated with trypsin to remove the unimported material for the analysis of the imported material (lanes 2-5), or left untreated for the analysis of the bound and imported material (lanes 6-9). 10% indicates 10% of the total amount of ^{35}S-Tim9 used for each import reaction (lane 1).
(B) As in **(A)** except that ^{35}S-Su9-DHFR was imported into mitochondria in the presence of the indicated amounts of KCl. The premature (*P*), the intermediate (I) and the mature (*M*) forms of ^{35}S-Su9-DHFR are indicated on the right. 10% indicates 10% of the total amount of ^{35}S-Su9-DHFR used for each import reaction (lane 1).

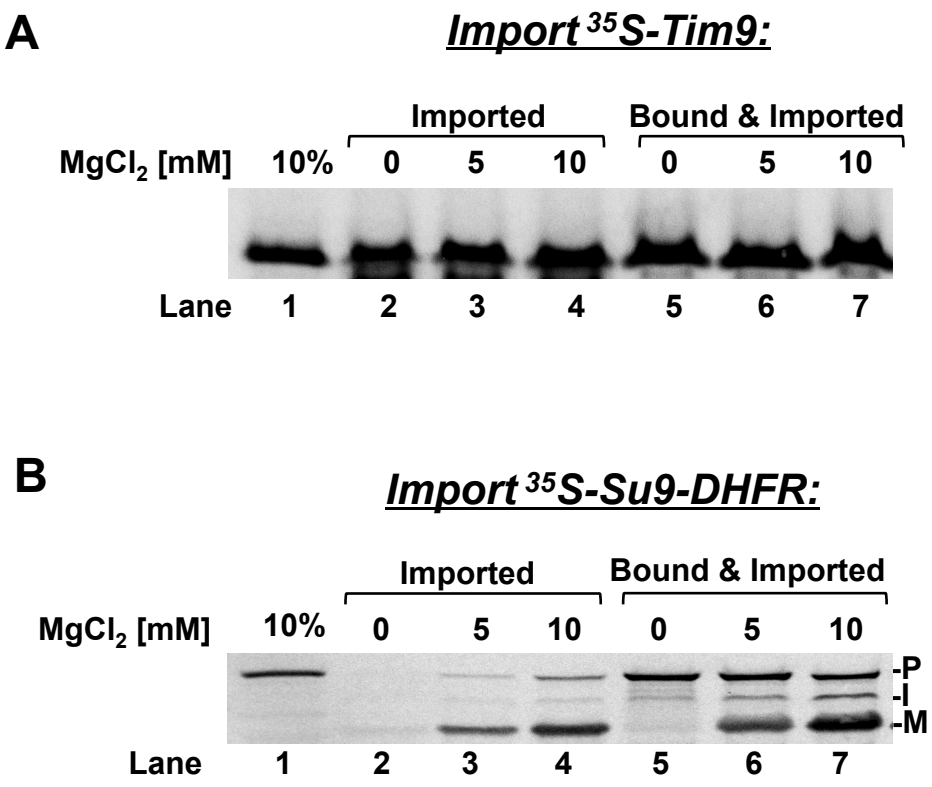

Figure 3.2 Effect of different amounts of $MgCl_2$ in Tim9 binding and import to/into mitochondria.

(A) As in Figure 3.1 A, except that ^{35}S-Tim9 was imported into mitochondria in the presence of the indicated amounts of $MgCl_2$. 10% indicates 10% of the total amount of ^{35}S-Tim9 used for each import reaction (lane 1).
(B) As in Figure 3.1 B, except that ^{35}S-Su9-DHFR was imported into mitochondria in the presence of the indicated amounts of $MgCl_2$. The premature (*P*), the intermediate (I) and the mature (*M*) forms of Su9-DHFR are indicated on the right. 10% indicates 10% of the total amount of ^{35}S-Su9-DHFR used for each import reaction (lane 1).

3.3 The role of the receptors of the TOM complex in Tim9 import

Mild trypsin treatment (5-7.5 ug ml^{-1}) of mitochondria removes the cytosolic-exposed domains of the receptors of the TOM complex (Tom20, Tom22 and Tom70), whereas Tom40 and Tom5 remain intact (Dietmeier *et al*., 1997). It is known that import of the matrix and IM preproteins into isolated mitochondria is inhibited by protease treatment of mitochondria, indicating that the mitochondrial surface receptors play an important role for their translocation across the OM (Riezman *et al.,* 1983; Zwizinski *et al.,* 1984, Pfaller *et al.,* 1989).

In contrast, it has been demonstrated that the pretreatment of mitochondria with up to 20 ug ml^{-1} trypsin did not inhibit Tim9 import into mitochondria (Kurz *et al.,* 1999). However, whether the rate of Tim9 import is affected by the trypsin pre-treatment of mitochondria is unknown. Thus, a time course import of Tim9 was performed in mitochondria that were either trypsin-treated (shaved) or left untreated (unshaved) before import. The experimental scheme is depicted in Figure 3.3. ^{35}S-Tim9 was incubated with shaved or unshaved mitochondria and imported for various time points. At the indicated time points, aliquots were removed from the import reactions and trypsin-treated to remove the unimported material. The effective tryptic digestion of the cytosolic domains of the main receptors of the TOM complex was measured by omitting the trypsin treatment after import and by western blot against Tom22 (Figure 3.4 A, lanes 6 and 13).

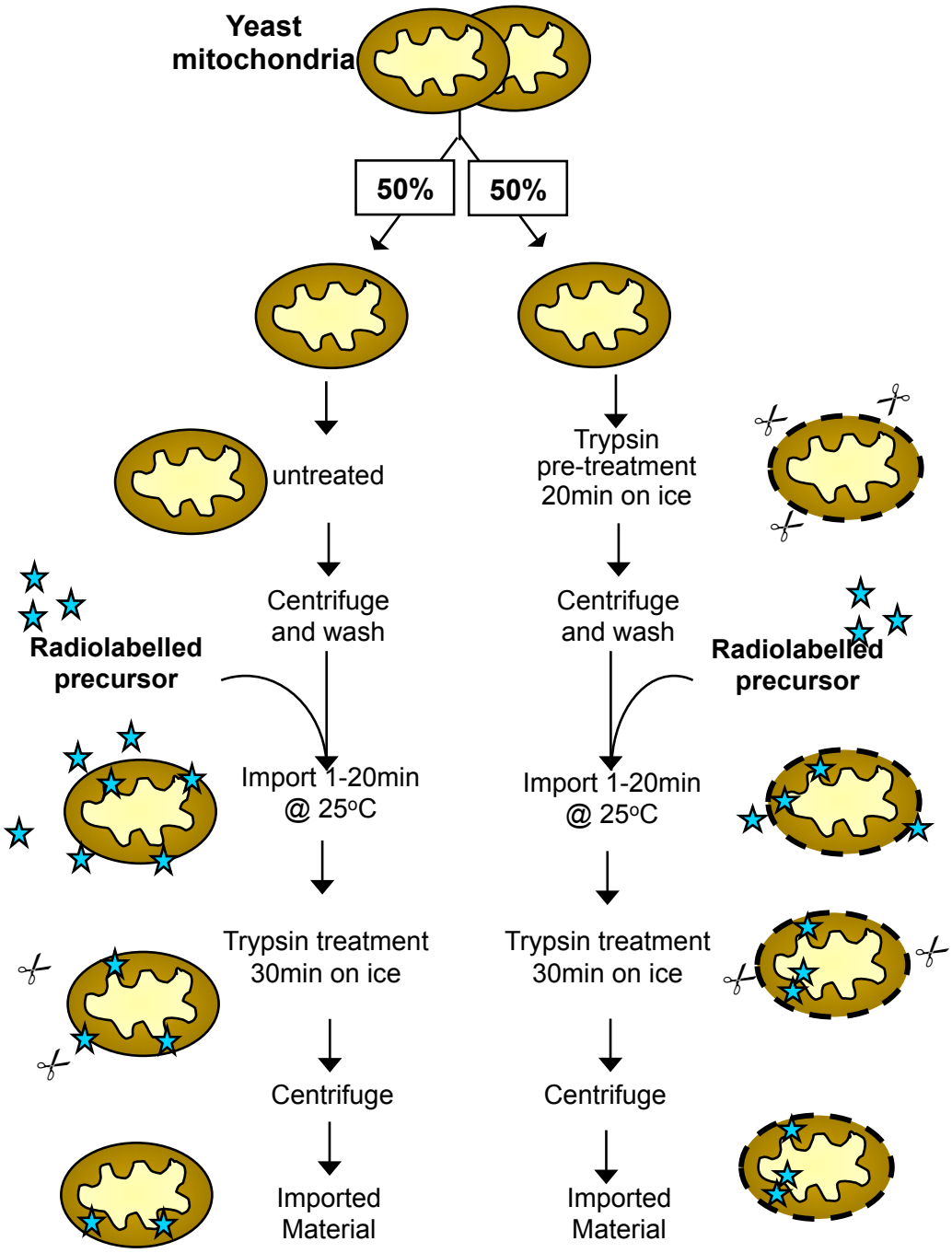

Figure 3.3 Import assay into trypsin pre-treated mitochondria.

Mitochondria were left untreated (unshaved) or treated (shaved) with 20 ug ml^{-1} trypsin for 20 min to remove the cytosolic domains of the TOM complex receptors. Proteolysis was stopped by the addition of excess amount of SBTI. To eliminate any trace of SBTI, shaved and unshaved mitochondria were reisolated by centrifugation and washed twice with BB7.4. Subsequently, ^{35}S-Tim9 was imported into both mitochondria at 25°C for various times. At the indicated time points, aliquots were removed and diluted five-fold in ice-cold trypsin buffer to inhibit further import. Mitochondria were then isolated and resuspended with reducing sample buffer.

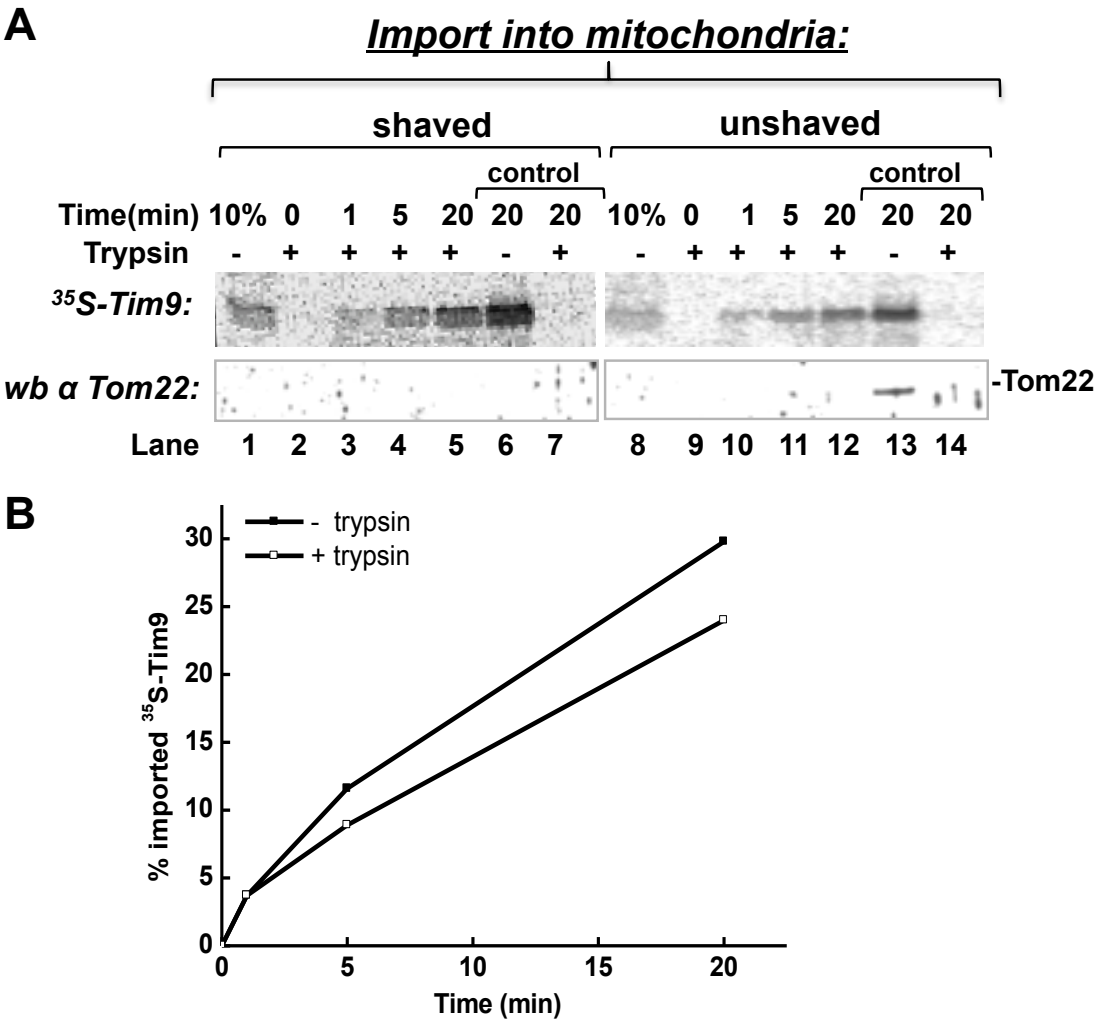

Figure 3.4 Time course import of Tim9 into shaved and unshaved mitochondria.

(A) Before import mitochondria were either treated with 20 ug ml^{-1} trypsin or left untreated as described in figure 3.2. Subsequently, ^{35}S-Tim9 was imported into shaved (lanes 2-7) or unshaved (lanes 8-13) mitochondria for the time periods indicated. Following import, mitochondria were trypsin treated to remove the unimported material. Two controls were included to test the efficiency of the tryptic proteolysis: after import mitochondria were either left untreated (lanes 6 and 13) or treated for 3 min with digitonin buffer before the trypsin treatment (lanes 7 and 14). Proteins were separated by reducing SDS-PAGE and analyzed by autoradiography. 10% indicates 10% of the total ^{35}S-Tim9 added to each import reaction (lanes 1 and 8). The western blot signal for Tom22 on the same membranes of the import experiments shows the successful tryptic digestion of the cytosolic domains of the receptors of the TOM complex.
(B) The levels of imported Tim9 during the time course import of (A) into shaved (open square) and unshaved (solid square) mitochondria were quantified by densitometry and expressed against the 10%.

As a control for the analysis of the imported material, following import mitochondria were incubated shortly with digitonin buffer to permeabilise the OM before the trypsin treatment. By digitonin treatment, trypsin has free access to the IMS digesting the imported material (Figure 3.4 A, lanes 7 and 14). The results showed that the rate of Tim9 import into shaved mitochondria is only slightly reduced in comparison to that one into unshaved mitochondria (Figure 3.4 A, lanes 2-6 and 8-12, respectively). Furthermore, the western blot with Tom22 on the same membranes confirmed the efficiency of the first trypsin digestion, whilst the digitonin controls confirmed that the imported material has been efficiently digested by trypsin (Figure 3.4 A, lanes 7 and 14).

Thus, in contrast to the matrix and IM precursor proteins the rate of Tim9 import is not affected by the absence of the cytosolic domains of the three mayor receptors of the TOM complex.

3.4 The role of Tom5 in Tim9 import

It has been shown that yeast mitochondria lacking Tom5 are generally deficient in the import of precursor proteins of all mitochondrial sub-compartments including the small Tims (Dietmeier *et al.,* 1997; Kurz *et al.,* 1999). It has been proposed that Tom5 can function as a linker between the major receptors of the TOM complex and Tom40 (Kurz *et al.,* 1999). However, it has also been shown that Tom5 is required to maintain the stability of the yeast TOM complex (Schmitt *et al.,* 2005). Thus, it is not clear whether the general mitochondrial import defect observed into *tom5Δ* mitochondria is due to a structural defect of the TOM complex or to the role of Tom5 as linker between the receptors of the

TOM complex and Tom40. To investigate the role of Tom5 in the import of Tim9, a yeast strain lacking the TOM5 gene (*tom5*Δ) was used.

3.4.1 Effects of the TOM5 deletion on cell growth under fermentative and respiratory conditions

To confirm the previous characterization of the *tom5*Δ yeast strain (Dietmeier *et al.,* 1997) and to set up the right growth conditions for the isolation of mitochondria, the growth of *tom5*Δ cells on fermentable (YPD) or non-fermentable (YPG, lactate) carbon sources was compared to that of WT cells. Firstly, WT and *tom5*Δ cells were streaked onto fresh YPD or YPG plates and grown under aerobic conditions both at 30°C and 37°C (Figure 3.5 A and B, respectively).

The results showed that at 30°C *tom5*Δ cells grew as the WT on both YPD and YPG media (Figure 3.5 A), whereas at 37°C growth of *tom5*Δ strain was completely inhibited on YPG terrain, and reduced on YPD terrain compared to the WT (Figure 3.5 B). Thus, the *tom5*Δ strain is a temperature sensitive strain whose growth is inhibited at 37°C under respiratory conditions, consistent with the results published by Dietmeier *et al.* (1997).

Secondly, cultures of WT and *tom*Δ*5* strains were inoculated to the same initial cell density A_{600} of 0.2 in lactate medium (LM) and grown both at 24°C and 30°C. Their growth was monitored by A_{600} and the data obtained plotted against time. The data showed that both strains grew similarly at 24°C (Figure 3.6 A), whereas at 30°C *tom5*Δ cells displayed a slower growth than the WT reaching the stationary phase 24 hours later than the WT cells (Figure 3.6 B). Thus, the best growth conditions for the isolation of mitochondria is at 24°C.

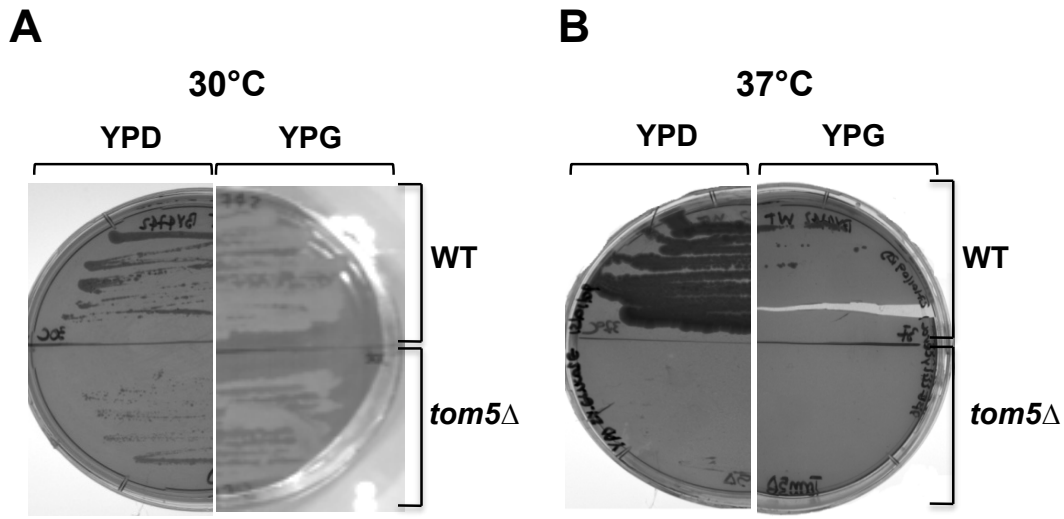

Figure 3.5 Growth of WT and *tom5*Δ yeast cells onto fermentable (YPD) and non-fermentable (YPG) terrain.

WT and *tom5*Δ cells were streaked onto fresh YPD and YPG plates from glycerol stocks and grown under aerobic conditions at 30°C **(A)** or at 37°C (**B)** for 72 hours.

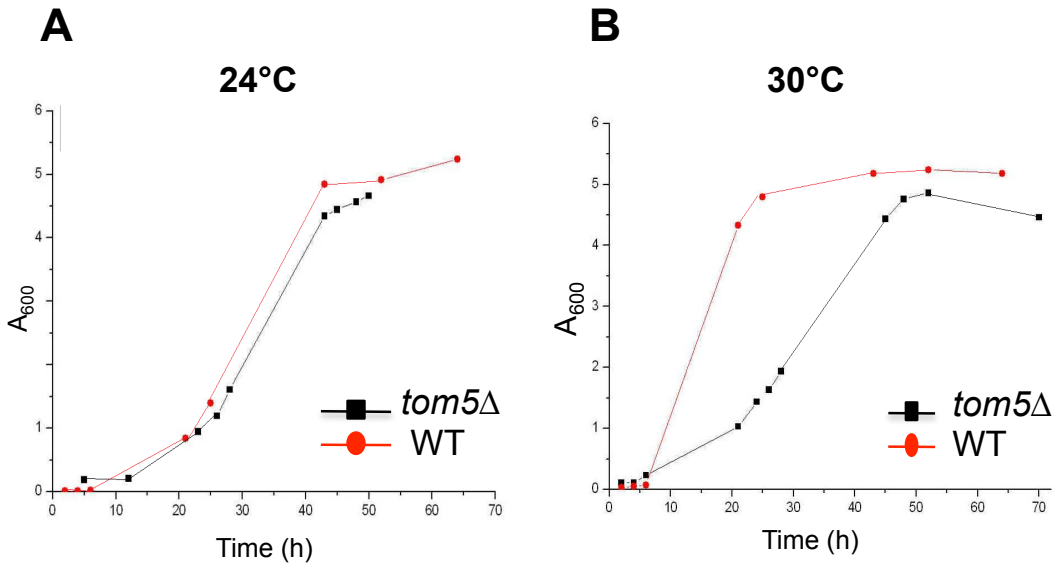

Figure 3.6 Growth of WT and *tom5*Δ cells on lactate medium.

WT and *tom5*Δ cells were inoculated to the same initial cell density A_{600} of 0.2 in lactate medium and grown at 24°C **(A)** or at 30°C **(B)** to the stationary phase. The fitness was monitored by measuring the A_{600}.

3.4.2 Analysis of mitochondrial protein levels in *tom5*Δ mitochondria

WT and *tom5*Δ mitochondria, isolated by gradient centrifugation from the respective strains grown in LM at 24°C, were compared for their mitochondrial protein content. For each type of mitochondria three different amounts of proteins (10, 30 and 60 ug) were loaded, separated by SDS-PAGE and analysed by western blot (Figure 3.7). The analysis shows that, except for the lack of Tom5 in the respective mitochondria, the levels of the OM (Tom40), the IM (Mia40 and ADP/ATP carrier or AAC) and the matrix (mtHsp70) mitochondrial marker proteins were similar between the *tom5*Δ and the WT mitochondria, whereas the levels of the IMS proteins (Tim9 and Cytochrome b2 or Cyt. b2) were slightly decreased in *tom5*Δ than in WT mitochondria. However, this demonstrates that, even in the absence of Tom5, mitochondrial proteins are still imported into the organelle.

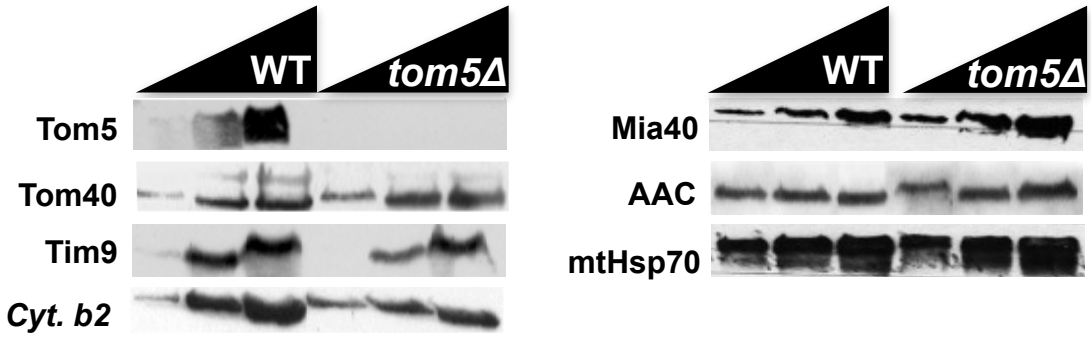

Figure 3.7 Protein content in WT and *tom5Δ* mitochondria.

(A) WT and *tom5*Δ mitochondria were isolated from lactate-grown cells at 24°C to the late exponential phase. 10 ug, 30 ug and 60 ug of mitochondria of each strain were separated by reducing SDS-PAGE and analyzed by western blot. The endogenous levels of the OM (Tom5 and Tom40), the IMS (Tim9 and Cytb2), the IM (Mia40 and AAC), and the matrix (mtHsp70) proteins were analysed. The immunoblotting with the Tom5 antibody confirms the deletion of Tom5 in the respective strain. (Cyt. b2, Cytochrome b2; AAC, ADP/ATP carrier).

3.4.3 Effects of the TOM5 deletion on *in vitro* Tim9 import

Import of radioactive small Tim precursors into an excess amount of mitochondria is typically approximately 10-20%. It has been previously showed that oxidative folding of the precursors is the significant factor limiting the mitochondrial import of small Tim proteins (Morgan and Lu, 2008). To test the efficiency of Tim9 import into *tom5*Δ mitochondria, the same preparations of WT and *tom5*Δ mitochondria were used. Thus, ^{35}S-labelled Tim9 was incubated with WT and *tom5*Δ mitochondria and imported for 1-30 min. At the time point indicated, import was stopped and further import was inhibited by trypsin treatment as described in Figure 3.4 (Figure 3.8). As controls, after 30 min of import an aliquot of mitochondria were either left untreated or shortly incubated with digitonin prior the trypsin treatment (Figure 3.8 A, lanes 7 and 13). As expected, Tim9 import into WT mitochondria increased with time and reached a plateau after approximately 20 minutes, whereas Tim9 import was strongly inhibited in *tom5*Δ mitochondria (Figure 3.8, A lanes 8-11 vs 2-5). Furthermore, the levels of Tim9 imported into *tom5*Δ mitochondria did not exceed the import levels of approximately 2% during the time course, whilst, as expected, approximately 12% of Tim9 was efficiently imported into WT mitochondria (Figure 3.8, B). The controls for the trypsin treatment confirmed that the bound material has been efficiently digested by trypsin (Figure 3.8 A, lanes 7 and 13), and the western blot against the IMS marker protein Cyt.b2 on the same membranes confirmed the same loading (Figure 3.8, lower panel). Thus, the results indicate that in the absence of Tom5, Tim9 is not efficiently imported into the IMS.

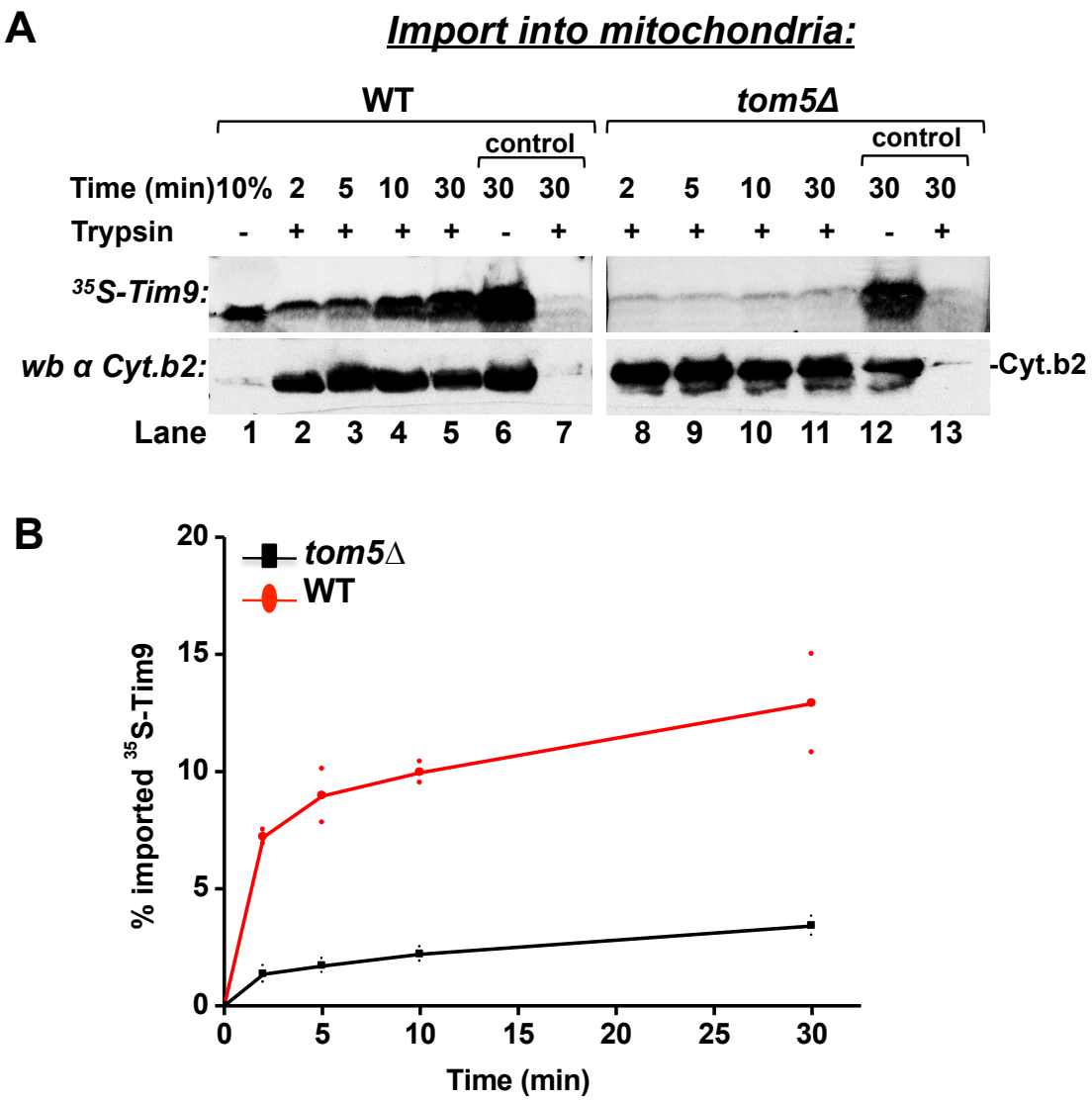

Figure 3.8 Import of Tim9 into WT and *tom5Δ* mitochondria.

(A) ^{35}S-Tim9 was imported into WT (lanes 2-7) and *tom5Δ* (lanes 8-13) mitochondria at 25°C for the time points as indicated. After import, mitochondria were either trypsin treated to remove the unimported material as described before (lanes 2-5 and 8-11), or left untreated (lanes 6 and 12), or treated with the digitonin buffer before the trypsin digestion (lanes 7 and 13). Proteins were separated by reducing SDS-PAGE and analyzed by autoradiography. 10% indicates 10% of the total ^{35}S-Tim9 added to each import reaction (lane 1). The western blot signal for the IMS protein Cyt.b2 on the same membranes of the import experiments showed that the OM is intact and that the same amount of protein was loaded.
(B) The amounts of imported Tim9 were quantified by densitometry and expressed against the 10%. The averages of the Tim9 imported levels into WT (red line) or *tom5Δ* mitochondria (black line) were obtained from two independent time course import experiments. The levels of imported Tim9 into WT (red circles) or *tom5Δ* mitochondria (black squares) at each time point of the two time course import experiments are also shown.

3.4.4 Effects of the TOM5 deletion on Tom40's sensitivity to trypsin digestion

It has been reported that, in the absence of Tom5, the cytosolic domain of Tom40 becomes fully accessible to trypsin digestion, suggesting a close relationship between the two subunits of the TOM complex (Dietmeier *et al.,* 1997). To establish whether the cytosolic domain of Tom40, which Tom5 protects against the trypsin digestion, plays a role in the Tim9 mitochondrial import, the sensitivity of Tom40 to the protease was analysed in WT and *tom5*Δ mitochondria. Thus, WT and *tom5*Δ mitochondria were left untreated or treated with various amounts of trypsin for 20 minutes on ice. After the inactivation of trypsin, mitochondria were reisolated and resuspended in reducing SDS-PAGE. Proteins were resolved by 10% SDS-PAGE and analysed by western blot with Tom40 antibody (Figure 3.9). The results showed that in WT mitochondria a small fraction of Tom40 has been digested from trypsin, whereas the majority appeared to be resistant (Figure 3.9, lanes 3-6). In contrast, in *tom5*Δ mitochondria a small fraction of Tom40 is sensitive to trypsin at the lowest concentration of 0.2 ug ml^{-1} (Figure 3.9, lane 9), whilst the majority of Tom40 was digested by 10 ug ml^{-1} of trypsin (Figure 3.9, lanes 12). These experiments showed that in *tom5*Δ mitochondria Tom40 is more sensitive to trypsin, probably because in the absence of Tom5 a larger domain of Tom40 may be exposed to the cytosol and thus become easily accessible to the protease.

Does the larger domain that Tom40 exposes to the cytosol in *tom5*Δ mitochondria play a role in the biogenesis of small Tims? To address this question, ^{35}S-Tim9 was imported into both WT and *tom5*Δ mitochondria that were pre-treated with 10 ug ml^{-1} of trypsin (Figure 3.10).

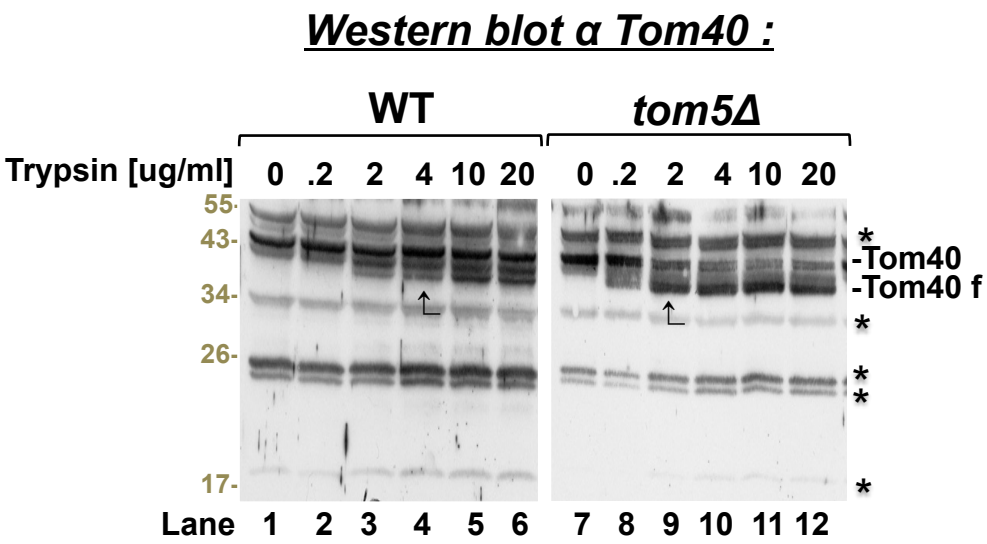

Figure 3.9 Trypsin concentration-dependent sensitivity of Tom40 in WT and *tom5Δ* mitochondria.

WT (lanes 1-6) and *tom5Δ* (lanes 7-12) mitochondria were treated with the indicated different amounts of trypsin for 20 min on ice. Proteolysis was then inhibited with 30-times concentration of SBTI. Mitochondria were reisolated by centrifugation and washed twice before resuspension in reducing sample buffer. Proteins were resolved by 10% TRIS SDS-PAGE and analysed by western blot with Tom40 antibody. The black arrows indicate the tryptic concentrations at which Tom40 showed sensitivity to trypsin. The position of the undigested Tom40 (Tom40) and digested fraction of Tom40 (Tom40 f) are indicated on the right. The asterisks indicate unspecific reactions of the Tom40 antibody.

The trypsin concentration of 10 ug ml^{-1} was chosen based on the results in Figure 3.9. As expected, the pre-treatment of trypsin did not inhibit Tim9 import into WT mitochondria (Figure 3.10 A, lanes 2-5). Similarly, Tim9 import was not completely abolished into shaved *tom5*Δ mitochondria (Figure 3.10 A, lanes 8-11). Furthermore, the results showed that Tim9 binding to the OM was not affected by the trypsin pre-treatment in both WT and *tom5*Δ mitochondria (Figure 3.10 A, lanes 6 and 12).

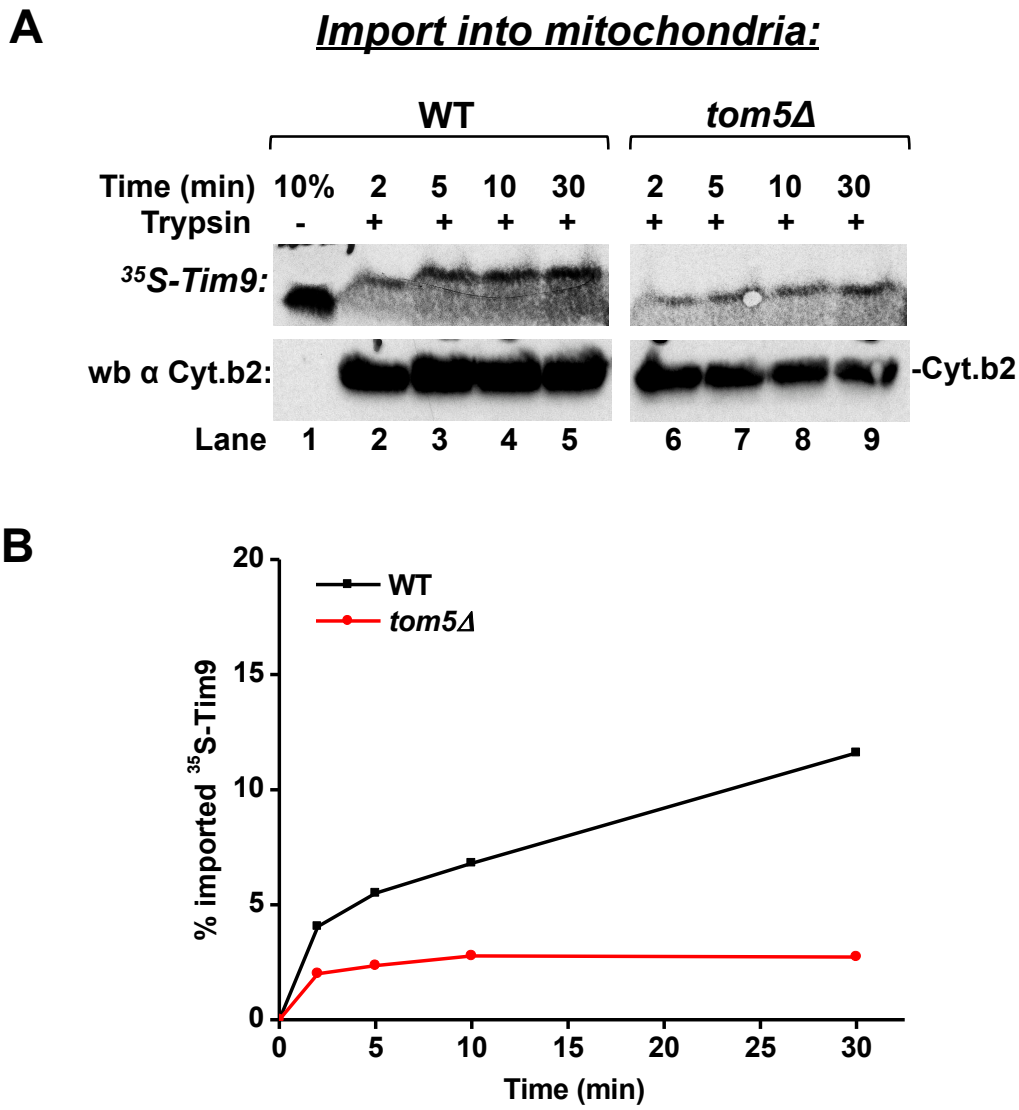

Figure 3.10 Tim9 time course import into shaved WT and *tom5Δ* mitochondria.

(A) WT (lanes 2-5) and *tom5Δ* (lanes 6-9) mitochondria were pre-treated with 10 ug ml^{-1} of trypsin. Following inactivation of trypsin as described in figure 3.3, mitochondria were reisolated and incubated with ^{35}S-Tim9 and imports carried out for the indicated time points. After import, mitochondria were treated with trypsin buffer to remove the unimported material. Proteins were separated by reducing SDS-PAGE and analyzed by autoradiography. 10% indicates 10% of the total ^{35}S-Tim9 added to each import reaction (lane 1). The western blot signal for the IMS protein Cyt. b2 on the same membranes of the import experiments showed that the OM is intact and that the same amount of protein was loaded.
(B) The levels of imported Tim9 into WT (red circle) and *tom5Δ* (black square) mitochondria of the time course import experiment in (A) were quantified by densitometry, expressed against the 10%, and plotted against time (n=1). The same time course import experiment was performed three times and the results were confirmed.

3.5 Redox state of the cysteine residues of Tom40

In the yeast S. cerevisiae, Tom40 is the only subunit of the TOM complex containing cysteine residues in its sequence. In particular, yeast Tom40 contains three cysteines, of which only the most C-terminal is conserved among human, Xenopus tropicalis and Salmo salar (Figure 3.11). Since to cross the OM small Tims need to be in a reduced and unfolded state (Lu *et al.,* 2004; Muller *et al.,* 2008), interactions between the cysteines of small Tims and Tom40 might occur.

To address this hypothesis, the redox state of Tom40's cysteines was analysed by gel shift assay using the alkylating agent 4-Acetoamido-4'-maleimidylstilbene-2,2'-disulphonic acid (AMS) (Figure 3.12). If AMS reacts with any free thiol group of Tom40, the molecular weight of Tom40 shall increase by 0.5 kDa per AMS bound to Tom40. Thus, WT mitochondria were incubated in the absence or in the presence of 50 mM of AMS. Mitochondria were then isolated by centrifugation, and either directly resuspended in non-reducing sample buffer or washed twice before resuspension with non-reducing sample buffer (Figure 3.12, lanes 1-2 and 3, respectively). The results showed that in the presence of AMS, a single shifted band was observed, indicating that at least one of the three cysteines within Tom40 is a free thiol. In addition, Tom40 shifted to a different extent depending whether, following the incubation with AMS, mitochondria were either immediately resuspended with sample buffer or reisolated and washed prior resuspension with sample buffer (Figure 3.12, lanes 2 and 3). The same gel-based shift assays were repeated using the alkylating agents iodoacetamide (IAA) or N-Ethylmaleimide (NEM) and the results confirmed (data not shown).

Figure 3.11 Sequence alignment of Tom40 protein.

The primary sequences of Human (H), Xenopus tropicalis (Xt), Salmo salar (Ss) and S. cerevisiae (Sc) Tom40 are aligned. The yeast Sc and Xt Tom40 contain three cysteine residues, whereas H and S.s four. Only the most C-terminal cysteine is conserved among these species. Identical residues are indicated by *asterisks*, and residues shared by three or two out four species are indicated by two or one *points*, respectively . The cysteine residues are highlighted in blue.

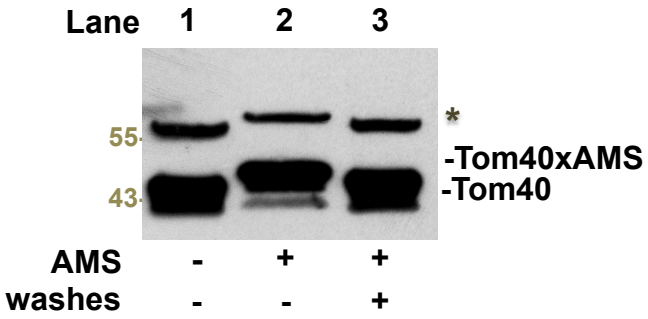

Figure 3.12 Redox state of Tom40 in mitochondria.

WT mitochondria were incubated in buffer in the absence (lane 1) or in the presence of 50 mM AMS (lanes 2 and 3) for 30 minutes at RT. Mitochondria were then isolated by centrifugation and either dissolved directly in non-reducing sample buffer (lanes 1 and 2) or washed twice before dissolution in non-reducing sample buffer (lane 3). Proteins were resolved by SDS-PAGE and analyzed by immunodecoration with Tom40 antibody. The position of unmodified Tom40 and AMS-modified Tom40 (Tom40xAMS) are indicated on the right. The asterisk indicates an unspecific reaction of the antibody.

3.5.1 Investigation of the role of the cysteine residues of Tom40 in Tim9 import

To analyse whether the free cysteine residue/s of Tom40 play/s a role on Tim9 import, WT mitochondria were pre-treated with NEM to block any free thiol groups and assayed for their ability to import Tim9. The scheme of the experiment is depicted in Figure 3.13. After the NEM treatment, mitochondria were reisolated by centrifugation and washed twice to make sure to rid off any free NEM. Subsequently, mitochondria were incubated with ^{35}S-Tim9 and imports carried out for 20 min. Both imported and bound materials were analysed (Figure 3.14, A and B, respectively). The results showed that Tim9 import was less efficient into the NEM pre-treated mitochondria than the controls (Figure 3.14, A lanes 3-4 vs 1-2). Similarly, Tim9 binding to the OM of the NEM pre-treated mitochondria was lower than the controls (Figure 3.14 B, lane 3 vs 1-2). However, in the presence of GSH Tim9 binding to the OM of the NEM pre-treated mitochondria was partially recovered (Figure 3.14 B, lane 3 vs 4).

The import reactions containing GSH were used as control, as mitochondrial import of the MIA substrates is stimulated by physiological concentrations of GSH (Mesecke *et al.,* 2005; Bien *et al.,* 2010). The same experiment was repeated and the results confirmed, suggesting that binding to mitochondria may be dependent on free thiol groups present on the OM (those of Tom40 for example).

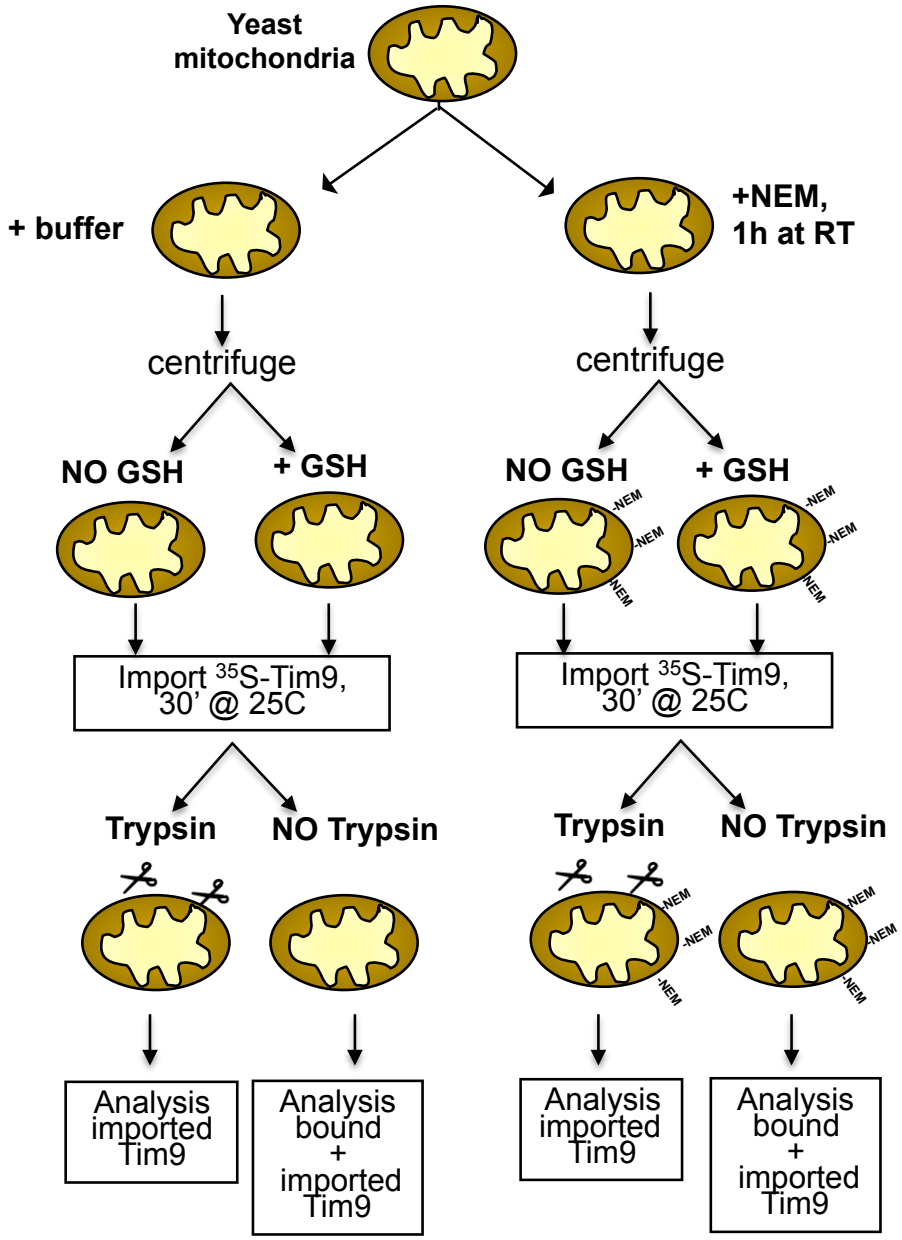

Figure 3.13 Tim9 import into NEM pre-treated mitochondria.

Before import, WT mitochondria were incubated with buffer in the absence or in the presence of 50 mM NEM for 1h at RT. Subsequently, mitochondria were reisolated by centrifugation and washed twice to rid of any free NEM. Mitochondria were then divided into 2 halves, one being incubated with import buffer, and the second one with import buffer containing 5 mM GSH for 5 min. ^{35}S-Tim9 was then added to each import reaction and imports carried out for 20 min. After import, each sample was split into two halves, one being subjected to the trypsin digestion to remove the unimported material, and one being mock-treated for the analysis of the bound and imported material. Samples were analysed by reducing SDS-PAGE and autoradiography.

A

Import ^{35}S-Tim9

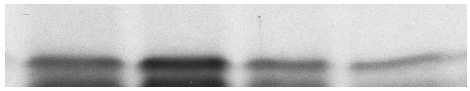

NEM	-	-	+	+
GSH	-	+	-	+
Lane	1	2	3	4
% imported Tim9	100	131±4	78±3	44±4

B

Binding and import ^{35}S-Tim9

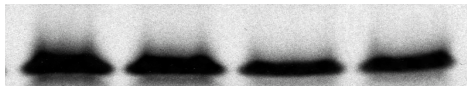

NEM	-	-	+	+
GSH	-	+	-	+
Lane	1	2	3	4
% bound and imported Tim9	100	107±3	64±9	82±9

Figure 3.14 Effects of the NEM pre-treatment of mitochondria in Tim9 import.

^{35}S-Tim9 was imported into mitochondria that were left untreated (lanes 1 and 2) or pre-treated with NEM (lanes 3 and 4) as describe in Figure 3.13. After import, samples were either treated with trypsin for the analysis of the imported material (**A**), or left untreated for the analysis of the bound and imported material (**B**). Proteins were separated by reducing SDS-PAGE and analyzed by autoradiography. The levels of imported (**A**, lower panel) or imported and bound Tim9 (**B**, lower panel) were quantified by densitometry setting as 100% the amount of imported or imported and bound material in untreated mitochondria, respectively. The averages and the random errors were calculated from two independent experiments.

3.6 The effects of oxidised Tim9 on the import of ^{35}S-Tim9

It is known that only the reduced form and not oxidised form of Tim9 is import competent. In this section the investigation whether oxidised (oxTim9) and reduced Tim9 bind to the same binding site on the OM was addressed. For this purpose recombinant Tim10 was used as it has been shown to be best purified in an oxidised state with all the four cysteine residues forming two disulphide bonds (Lu *et al.,* 2004b) In a first experiment mitochondria were pre-incubated with different amounts of purified oxTim9 to allow its binding to the OM. ^{35}S-Tim9 was then added to the import reactions and imported for 30 min. After import, mitochondria were treated with trypsin as usual for the import analysis (Figure 3.15 A, lanes 1-5), or left untreated for the binding analysis (Figure 3.15 A, lanes 6 and 7). Mitochondria were then separated by reducing SDS-PAGE and analysed by autoradiography. The results indicated that import of ^{35}S-Tim9 was not inhibited by the presence of increasing amounts of oxTim9 (Figure 3.15 A, lanes 2-5), whilst binding of ^{35}S-Tim9 to the OM was less efficient in the presence of the highest amounts of oxTim9 (Figure 3.15 A, lane 6 vs 7). The immunodecoration with the Tim9 antibody on the same membrane confirmed that increasing amounts of purified oxTim9 were present (Figure 3.15 A, lower panel).

In a second experiment, oxTim9 was first mixed with ^{35}S-Tim9, and then both were added together to mitochondria (Figure 3.15 B). The results showed that even when co-imported, binding but not import of reduced Tim9 was slightly affected by the presence of oxTim9 (Figure 3.15 B, lanes 1-6).

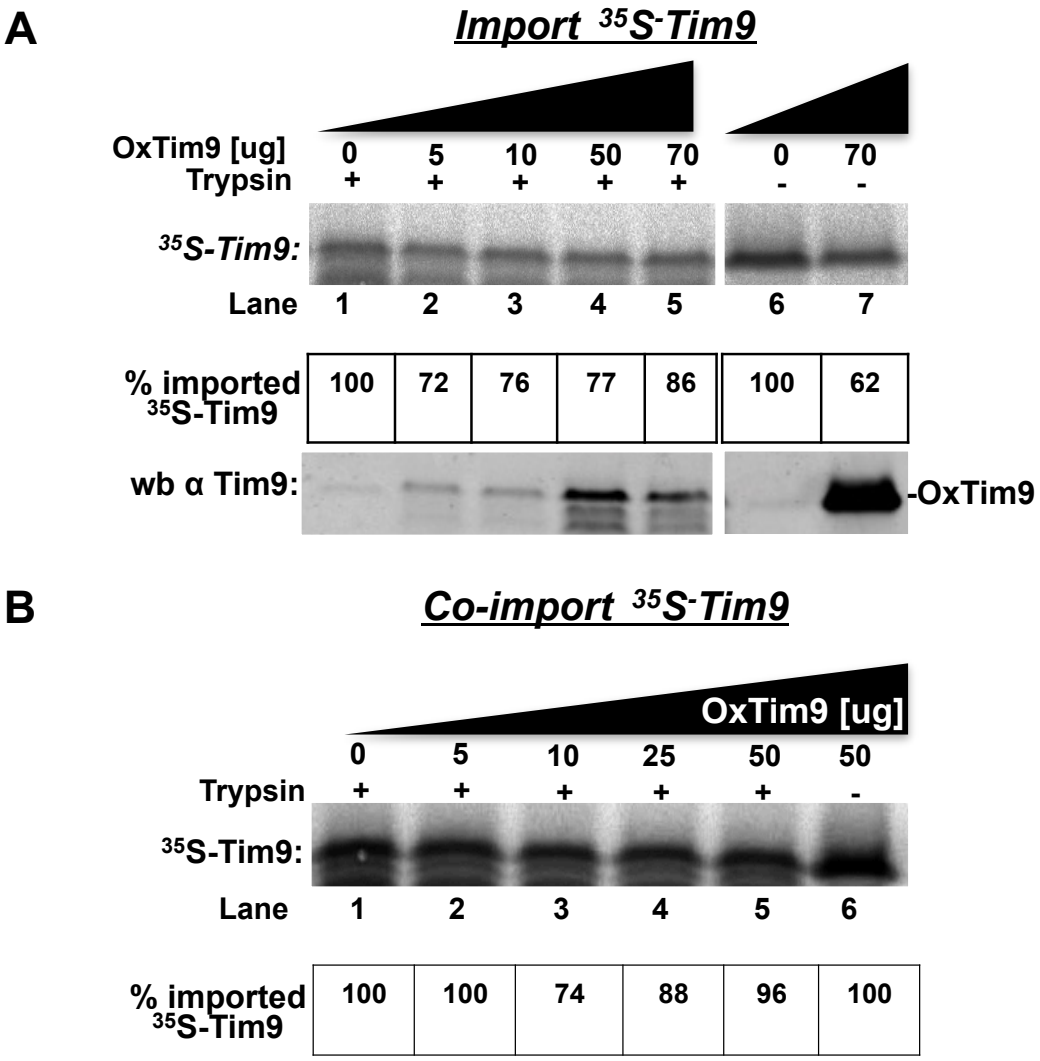

Figure 3.15 Effects of oxidised Tim9 in import of reduced Tim9.

(A) 50 ug mitochondria were pre-incubated with the indicated amounts of purified oxidised Tim9 (oxTim9) for 2 min. ^{35}S-Tim9 was then added to each import solution and imported for 20 min. After import, mitochondria were either treated with trypsin for the analysis of the imported material (lanes 1-5) or left untreated for the analysis of the bound material (lanes 6-7). Proteins were separated by reducing SDS-PAGE and analyzed by autoradiography. The amounts of imported and bound ^{35}S-Tim9 were quantified by densitometry setting respectively as 100% the level of imported or bound Tim9 in the absence of oxTim9. The lower panel shows the immunodecoration with Tim9 antibody on the same membrane of the import experiment.

(B) As in **(A)** except that ^{35}S-Tim9 and the indicated different amounts of OxTim9 were added simultaneously and co-imported into mitochondria. After import, mitochondria were either treated with trypsin for the analysis of the imported material (lanes 1-5) or left untreated for the analysis of the bound material (lane 6). Proteins were separated by reducing SDS-PAGE and analyzed by autoradiography. The amounts of imported and bound ^{35}S-Tim9 were quantified by densitometry setting respectively as 100% the level of imported Tim9 in the absence of oxTim9.

3.7 The effects of oxidised Tim9 on the import of ^{35}S-Su9-DHFR

It has been shown that Tim13 and Su9-DHFR share in part their import routes, most likely while translocating through the TOM complex (Lutz et al., 2003). Thus, the effects of oxTim9 on binding and import of the matrix-targeted ^{35}S-Su-9DHFR were studied. ^{35}S-Su9-DHFR was co-imported in the presence of increasing amounts of purified oxTim9 (Figure 3.16). After import, mitochondria were left untreated and resuspended with reducing sample buffer. The samples were separated by SDS-PAGE and analysed by autoradiography. The results showed that both binding and import of Su9-DHFR are efficient at all tested conditions (Figure 3.16, lanes 2-6), indicating that oxTim9 and matrix-targeted precursor proteins do not share the same binding site on the OM.

Thus, these results indicates that oxidised Tim9 may share the same binding sites with reduced Tim9 on the OM, but it did not compete for binding of matrix targeted precursor proteins.

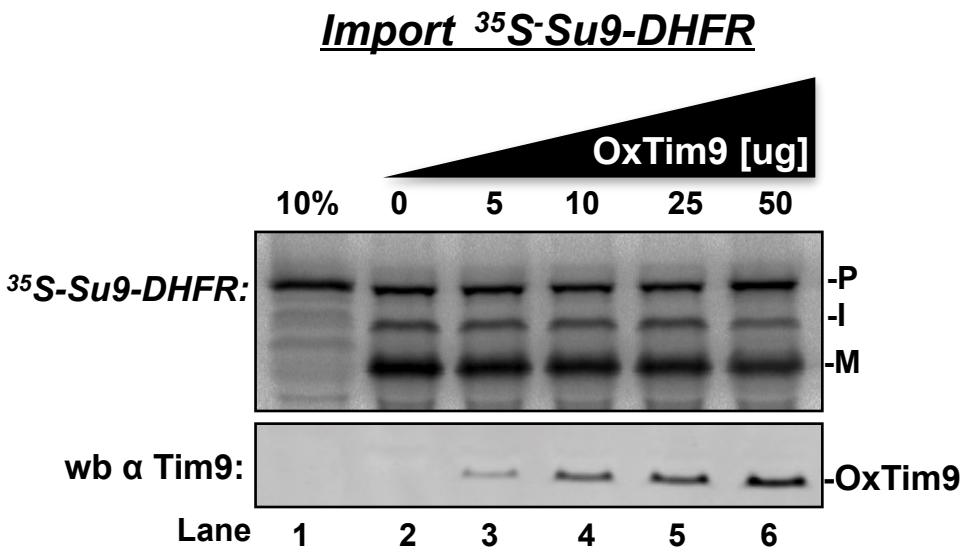

Figure 3.16 Effect of oxTim9 in the import of ^{35}S-Su9-DHFR.

As in Figure 3.15 A, except that ^{35}S-Su9-DHFR was imported into mitochondria that were pre-incubated with the indicated amounts of oxTim9. Proteins were separated by reducing SDS-PAGE and analyzed by autoradiography. 10% indicates 10% of the total ^{35}S-Su9-DHFR added to each import reaction (lane 1). *P*, *I* and *M* indicate the precursor, the intermediate and the mature forms of Su9-DHFR, respectively. The lower panel shows the western blot signal for oxTim9 on the same membrane of the import experiment.

3.8 Discussion

3.8.1 Tim9 import does not require the receptors of the TOM complex

The molecular mechanisms that allow the small Tim proteins to be targeted to the OM and cross the OM are yet poorly defined. The works described in this chapter were aimed to gain insight into how Tim9 binds to the OM and translocates into the IMS. Here, the results confirmed the evidences that the receptors of the TOM complex do not assist Tim9 binding to the OM and translocation into the IMS, at least in vitro. This conclusion is based on the following observations: (1) the rate of Tim9 import was only slightly affected by the trypsin digestion of the TOM complex receptors; and (2) different ionic strengths of the import conditions did not inhibit Tim9 binding to the OM and translocation into the IMS, conversely to the matrix precursor Su9-DHFR.

Lutz et al. (2003) suggested that Tim13 and matrix-targeted preproteins might share part of their import routes, most likely the translocation step. Here, the results showed that binding and import of Tim9 were not affected by the KCl concentrations, whereas import and binding of Su9-DHFR clearly was (Figures 3.1 and 3.2). This may suggest Su9-DHFR interacts ionically with OM factors that may not be used by Tim9. In addition, oxTim9 did not bind to a proteinaceous factor involved in the import route for the matrix-targeted Su9-DHFR, as both binding and import of Su9-DHFR were not inhibited by the presence of oxTim9.

In contrast, the presence of oxTim9 impaired Tim9 binding to the OM, whereas its import was not. This may indicate that oxidised and reduced Tim9 share the same OM binding site, though this is not relevant for the translocation across the OM, as reduced Tim9 was still imported into mitochondria. Thus, the results indicated that Tim9 targeting to the mitochondria occurs without regarding the redox state of the precursors, and that unfolding is a crucial step for the efficient translocation into the IMS.

It has been shown that the MISS/ITS mitochondrial targeting signal identified recently in the primary sequence of small Tims is both necessary and sufficient for targeting small Tims into the IMS (Milenkovic *et al.,* 2009; Sideris *et al.,* 2009). Both groups showed that deleting it results in a complete loss of import, whereas fusing it to a mitochondrial matrix protein or to a non-mitochondrial protein targets the fused proteins to the IMS. Thus, it has been hypothesised that, similarly to the presequence of matrix-precursors, the MISS/ITS signal may direct the precursors to mitochondria and orchestrate the translocation step across the OM (Milenkovic, *et al.,* 2009; Sideris *et al.,* 2009).

3.8.2 Tim9 import requires Tom5

In order to investigate the role of Tom5 in the import of small Tims, both *in vivo* and *in vitro* studies were conducted. Results of *in vivo* studies are consistent with the first work published on Tom5 in 1997 by the German group (Dietmeier *et al.,* 1997): *tom5Δ* cells were unable to grow under respiratory conditions at 37°C, while they can grow at 30°C.

This indicates that Tom5 is essential for cell viability at high temperatures. The observed growth defects were caused only by the lack of TOM5, as transformation of the *tom5Δ* mutant with a plasmid carrying TOM5 restored growth (Dietmeier *et al.,* 1997).

In addition, here it is also shown that mitochondrial protein levels in *tom5Δ* mitochondria is similar to that of the WT mitochondria, indicating that *in vivo* mitochondrial import is not generally inhibited in the absence of Tom5 (Figure 3.7, Dietmeier *et al.,* 1997). However, the levels of the IMS proteins in *tom5Δ* mitochondria, such as Tim9 and Cyt.b2, were found to be slightly lower than in WT mitochondria. In addition, previous and my *in vitro* studies showed that mitochondria isolated from *tom5Δ* cells were strongly impaired in the import of Tim9, indicating that Tom5 plays a direct role for the import of Tim9 (Figure 3.10; Kurz *et al.,* 1999).

Furthermore, the results in this chapter showed that: (1) in *tom5Δ* mitochondria Tom40 is more accessible to the trypsin digestion; and (2) Tim9 import into shaved *tom5Δ* mitochondria was not completely inhibited in comparison to that into unshaved *tom5Δ* mitochondria. This suggests that this larger trypsin-cleavable domain of Tom40 is not involved in Tim9 import. Unfortunately, it is not possible to establish from these *in vitro* studies the precise role of Tom5 in the import of small Tims.

3.8.3 Tom40 contains at least one free thiol group

In yeast Tom40 is the only subunit of the TOM complex to contain cysteine residues, of which the most C-terminal one is conserved among yeast, human, salmon and X. tropicalis.

Although the Tom40 topology is still unknown (Hill, Model *et al.,* 1998), an increasing amount of studies is demonstrating that Tom40 is not a passive channel that all preproteins use to transverse the OM, instead it is a "…sophisticated sorting station…" that distinguishes substrates and ensures the final targeting via distinct interactions (Gabriel *et al.,* 2003; Sherman *et al.,* 2006). Thus, it is possible that Tom40 may play an active role as receptor for small Tims too.

In this study, I showed that the alkylating agent AMS can modify Tom40 (Figure 3.12). This indicates that Tom40 contains at least one free thiol group available for potential cysteine-cysteine interactions. To test this hypothesis an *in vitro* Tim9 import assay was performed in mitochondria that were pre-treated with NEM to allow the blockage of free thiol groups (Figure 3.14). The results indicated that Tim9 binding to the OM might be facilitated by cysteine-cysteine interactions based on the observation that both import and binding were less efficient into NEM pre-treated mitochondria than in the control.

Lutz *et al.* (1999) showed that already imported Tim13 can be released from the IMS upon NEM-treatment, because NEM impedes the assembly of newly imported Tim13 in the IMS (Lutz *et al.,* 1999). Thus, we cannot exclude that NEM was not effectively removed from mitochondria causing the release of the

newly imported Tim9 from the IMS. If this is the case, this will explain the results obtained for imported Tim9 but not the results obtained for bound Tim9. In fact, the presence of NEM in the IMS should not affect Tim9 binding to the OM. Here, I showed that Tim9 binding to the OM was less efficient into NEM pre-treated mitochondria, indicating that binding to the OM may depend on cysteine-cysteine interactions between Tim9 and the OM.

It has been demonstrated that mitochondrial import for MIA substrates is considerably stimulated by physiological GSH concentrations (Mesecke *et al.,* 2005; Bien *et al*., 2010). It was suggested that GSH may prevent and/or remove the long-lived trapped intermediates than can be formed between Mia40 and its substrates, resulting in an increase of free functional Mia40 (Bien *et al.,* 2010). Here, I showed that GSH recovered Tim9 binding, but did not enhance Tim9 import into NEM pre-treated mitochondria. Although the majority of Mia40 and Erv1 is oxidised and thus, unable to react with NEM, it cannot be excluded that NEM in the IMS might have modified Mia40 during import. This would result in less free functional Mia40 during import, and thus in reduced levels of imported Tim9. This explanation would justify why GSH did not recover Tim9 import in the NEM pre-treated mitochondria. On the other hand, the reason why GSH did not recover Tim9 binding is unknown.

Thus, based on these observations, I have concluded that Tim9 binding may be facilitated by cysteine-cysteine interactions occurring in the OM, whether these are between Tom40 or another protein of the OM is unknown and future studies needed to be done to address this question.

3.9 Conclusions

In summary, this study confirmed that in vitro Tim9 import does not require the major receptors of the TOM complex; instead it is strongly inhibited in the absence of Tom5. On the other hand, the protein levels of WT and *tom5Δ* mitochondria are similar, indicating that Tom5 is not essential for Tim9 import, and other factors may be involved.

Tom40 may represent a possible candidate that interacts directly with the translocating Tim9, as it contains at least one free thiol group.

It will be interesting in the future addressing whether Tom40 or another OM proteinaceous factor can interact directly with the small Tims during their translocation across the OM. This could be shown, for example, by attaching tightly folded domains to the C-extremity of Tim9, such as DHFR. The ligand methotrexate stabilises DHFR and prevents its translocation through the TOM complex. Thus, a DHFR-Tim9 construct can be arrested across the OM in the presence of methotrexate, such that DHFR stays exposed on the mitochondrial surface whilst Tim9 is crossing the OM. At the same time, the existence of interactions between Tom40 and Tim9 can be tested by chemically cross-linking.

4. RESULTS AND DISCUSSION II: OXIDATIVE FOLDING OF TIM9 *IN VITRO* AND *IN ORGANELLO*

4.1 INTRODUCTION

Several IMS cysteine-containing proteins are imported into the IMS via the redox-sensitive MIA pathway (Chacinska *et al.,* 2004; Koehler 2004; Mesecke *et al.,* 2005; Tokatlidis 2005). Substrates of the MIA pathway include proteins containing the twin CX_3C motif (e.g. Tim9 and Tim10) and the twin CX_9C motif (e.g. Cox17 and Cox19). The major protein catalysts of the MIA pathway are the oxidoreductase Mia40 and the FAD-linked sulfhydryl oxidase Erv1. Mia40 functions as a receptor interacting with the incoming reduced substrates via formation of an intermolecular disulphide bonded intermediate (Chacinska *et al.,* 2004; Naoé *et al.,* 2004). During this interaction, the substrates undergo oxidative folding and are released from Mia40 in an oxidised state, whereas the CPC motif of Mia40 becomes reduced. The sulphydryl oxidase Erv1 is then necessary to re-oxidise Mia40 (Chacinska *et al.,* 2004; Naoé *et al.,* 2004; Mesecke *et al.,* 2005; Terziyska *et al.,* 2005, 2007; Grumbt *et al.,* 2007; Milenkovic *et al.,* 2007; Müller *et al*., 2008).

However, the events leading to the fully oxidation driven by Mia40 and to the release of the substrates from Mia40 are not fully mechanistically understood. Based on *in vitro* reconstitution assays, a recent study reported that an excess of Mia40 is sufficient to generate the fully oxidised form of Cox19 (Bien *et al.,* 2010).

Furthermore, this study suggested that Mia40 may first introduce the intra-molecular disulphide bond C2-C3 (the **inner disulphide** bond) and, subsequently, the intra-molecular disulphide bond C1-C4 (the **outer disulphide** bond). Bien *et al.* (2010) also demonstrated that the Mia40-mediated oxidative folding of Cox19 is further enhanced upon addition of GSH. They suggested that GSH may have a "proofreading' role in preventing and/or removing mis-formed complexes between Mia40 and its substrates.

The **aims** of this chapter were (**1**) to understand the molecular mechanisms of oxidative folding of small Tim proteins mediated by $Mia40_{core}$, and (**2**) to investigate the effects of GSH during the $Mia40_{core}$-mediated oxidative folding of small Tim proteins. To achieve these, firstly, the interactions between small Tims and Mia40 were studied using purified $Mia40_{core}$ and radiolabelled Tim9 or Tim10. Secondly, to understand how $Mia40_{core}$ introduces both disulphide bonds in small Tims, different combinations of double and triple cysteine-to-serine mutants of Tim9 and Tim10 were generated, and their oxidative folding was investigated.

Thirdly, to obtain more physiologically relevant results, the ability of both WT and mutants of Tim9 to form a complex with Mia40 was tested *in organello*. Finally, the effects of GSH on the Mia40-mediated oxidative reactions were investigated using both purified $Mia40_{core}$ and mitochondria.

4.2 PART I: INVESTIGATION OF THE INTERACTION BETWEEN MIA40$_{core}$ AND TIM9

4.2.1 Purification of Mia40$_{core}$ protein

To analyse the oxidative folding of small Tims catalysed by Mia40, the C-terminal domain of yeast Mia40 consisting amino acid residues from 284 to 403, named Mia40$_{core}$, was used. It has been extensively shown that Mia40$_{core}$ represents the functional domain of the yeast full-length Mia40 (Rissler *et al.,* 2005; Chacinska *et al.,* 2008; Grumbt *et al.,* 2007). Mia40 $_{core}$ contains both the CPC redox motif and the twin CX_9C motifs (Figure 4.1 A). Mia40$_{core}$ has been successfully purified as C-terminally 6x His-tagged recombinant protein from E. coli.

The size exclusion chromatography profile showed two peaks (P_1 and P_2) corresponding to the dimer (30 kDa) and monomer of Mia40$_{core}$ (15 kDa) (lab unpublished results; Figure 4.1 B). The analysis of a sample from P_2 by SDS-PAGE on reducing and non-reducing conditions confirmed the purity of the sample and the absence of disulphide-linked forms of Mia40$_{core}$ (Figure 4.1 C). The same fractions of P_2 were then used for subsequent *in vitro* reconstitution assays.

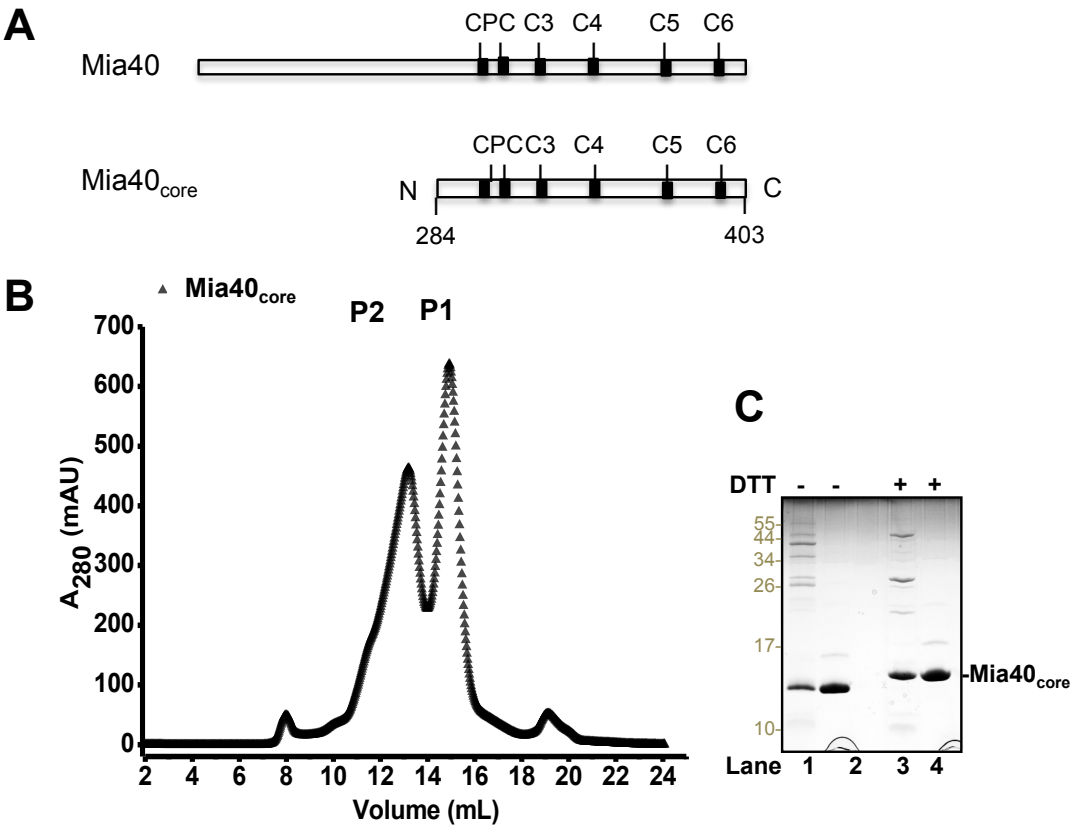

Figure 4.1 Characterization of purified Mia40$_{core}$.

(A) Schematic representation of the catalytic core of yeast Mia40, named Mia40$_{core}$. The CPC redox motif and the twin CX_9C motifs are indicated.
(B) Size exclusion chromatography profile of Mia40$_{core}$:the protein was separated using a Superdex 200 gel filtration column using BAE buffer.
(C) 16% Tricine SDS-PAGE of a sample of Mia40$_{core}$ from P_2 under non reducing (lanes 1-2) or reducing (lanes 3-4) conditions, followed by Coomassie-blue staining.

4.2.2 Effects of Mia40$_{core}$ on oxidation of small Tim proteins

An excess amount of purified Mia40$_{core}$ (1 µM) was incubated with radiolabelled ^{35}S-Tim9 or ^{35}S-Tim10 (pM) in a time course assay. At indicated time points, the reactions were stopped by addition of an excess amount of the alkylating agent AMS. Proteins were then resolved by non-reducing SDS-PAGE, transferred onto nitrocellulose membrane and visualised by autoradiography (Figure 4.2). The results showed that in the absence of Mia40$_{core}$, Tim9 did not oxidise spontaneously, albeit a fraction underwent partially oxidation (Figure 4.2 A, lanes 3-7). In contrast, in the presence of Mia40$_{core}$, a complex between Mia40$_{core}$ and Tim9 was generated within 10 s and persisted throughout the time course (Figure 4.2 A, lanes 8-12). This complex consisted of mixed disulphides between Mia40$_{core}$ and Tim9 as it dissociated after the addition of DTT (Figure 4.2 A, lane 13). The complete oxidation of Tim9 within the first minute of the incubation time with Mia40$_{core}$ demonstrates that Mia40$_{core}$ alone is able to introduce both disulphide bonds in the substrate. With 1 µM of Mia40$_{core}$, the generation of a fully oxidised substrate was rapid and single disulphide-bonded Tim9 intermediates dissociating from Mia40$_{core}$ were not observed. In addition, two species of Mia40$_{core}$ -Tim9 intermediates with slightly different molecular weight were observed. They may represent intermediates having Tim9 at different oxidation states. The upper band, named **Complex I**, may be an intermediate where Mia40$_{core}$ is bound via an inter-disulphide bond to Tim9 having the other three cysteines reduced (3 AMS modifications), and the lower band, named **Complex II**, may be an intermediate in which Mia40$_{core}$ is bound to a semi-oxidised Tim9 leaving only one cysteine for AMS modification.

The same results were obtained when analysing the oxidative folding of ^{35}S-Tim10 in the presence of 1 µM of Mia40$_{core}$ (Figure 4.2 B), indicating that Tim9 and Tim10 may be oxidised by Mia40$_{core}$ in a similar manner.

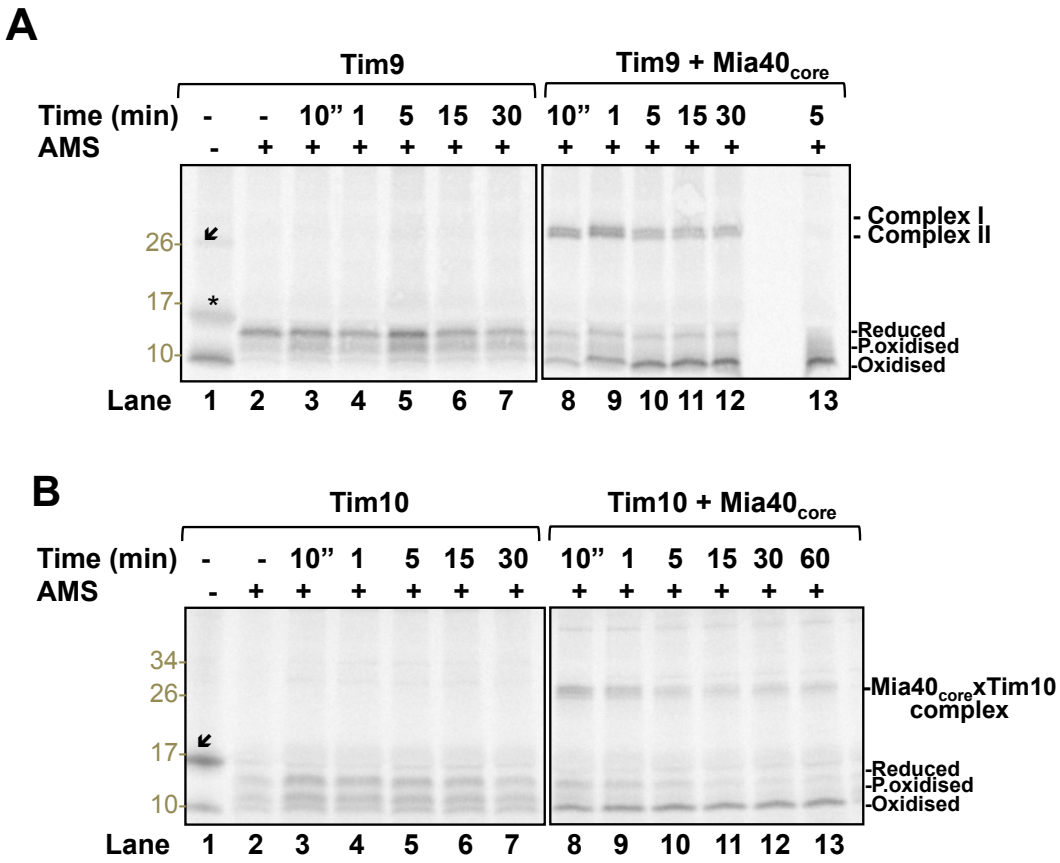

Figure 4.2 Time course of the interactions between Mia40$_{core}$ and small Tim proteins.

(A) ^{35}S-Tim9 was incubated with buffer (lanes 3-7) or buffer containing 1 µM Mia40$_{core}$ (lanes 8-13) for the indicated times. Subsequently, samples were treated with 12.5 mM AMS for 1h at RT, then subjected to non-reducing (lanes 1-12) or reducing (lane 13) SDS-PAGE and analyzed by autoradiography. Lane 1 and 2 are controls showing the redox state of the starting material. The Mia40$_{core}$-Tim9 Complex I and II, the *Reduced*, *P. oxidized* (partially oxidized) and *Oxidized* forms of Tim9 are indicated. The asterisk indicates the heme protein coming from the lysate used to synthesize radiolabelled ^{35}S-proteins, which usually disappears upon AMS treatment of the sample (lane 2). The arrowhead indicates an unidentified band.
(B) As in **(A)** except that ^{35}S-Tim10 was used.

4.2.3 Identification of the mixed-disulphide intermediates between Mia40$_{core}$ and Tim9

In order to know whether the Mia40$_{core}$-Tim9wt Complex I and Complex II were modified with three or one AMS molecules respectively, the double cys-mutants of Tim9 in which either the outer or the inner cysteine pair was mutated to serine (Tim9^{C1,4S} or Tim9^{C2,3S}) were generated. Both mutants were then incubated with 1 µM of Mia40$_{core}$ for various time points, and the effects of Mia40$_{core}$ on the oxidation of these mutants were analysed as described in Figure 4.2 (Figure 4.3). The results showed the presence of the two intermediate complexes in the Tim9wt samples and of only one complex for both mutants (Figure 4.3 B, lanes 7-8 vs 9-12). More importantly, the bands corresponding to Mia40$_{core}$-Tim9^{C1,4S} and Mia40$_{core}$-Tim9^{C2,3S} complexes migrated at the same size of the Complex II band of Mia40$_{core}$-Tim9wt. Hence this confirmed that in Complex II Tim9wt has one of the four cysteines modified by AMS, whilst in Complex I Tim9wt may be modified by 3 AMS. This result also showed that both mutants form a more stable and long-lasting complex with Mia40$_{core}$ than Tim9wt.

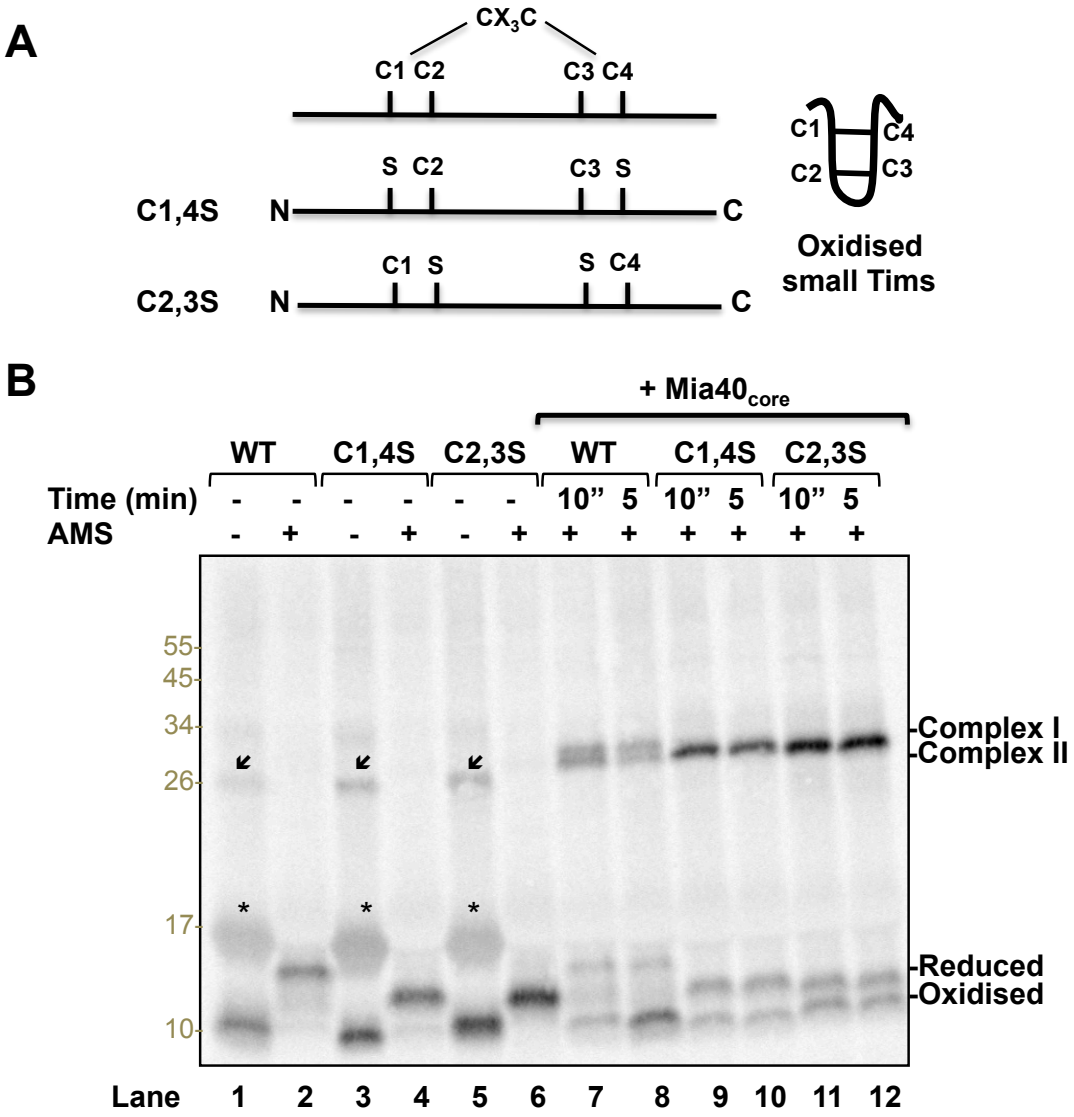

Figure 4.3 Identification of the mixed-disulphide bonds between Mia40$_{core}$ and Tim9.

(A) Schematic representation of Tim9wt and of the double Cys-mutants of Tim9 carrying the conversion of the outer or inner pair of cysteines to serine residues, C1,4S and C2,3S, respectively. The oxidized form of small Tims in which the outer and the inner pair of cysteines form respectively the outer and inner disulfide bonds is also shown.
(B) ^{35}S-Tim9wt (lanes 7-8), ^{35}S-Tim9^{C1,4S} (lanes 9-10), and ^{35}S-Tim9^{C2,3S} (lanes 11-12) were incubated with buffer containing 1 µM Mia40$_{core}$ for the indicated time points. Subsequently, samples were treated with 12.5 mM AMS and analysed as in figure 4.2. Lanes 1-6 are the controls showing the redox state of the starting material. *Complex I* and *Complex II*, the *Reduced* and *Oxidized* monomeric forms of Tim9 are indicated. The asterisks and the arrowheads in lanes 1,3 and 5 indicate respectively the heme protein coming from the lysate and unidentified bands which both disappear upon AMS treatment of the samples (e.g. lanes 2, 4 and 6).

4.2.4 Mia40$_{core}$ concentration-dependent Tim9 oxidative folding

The previous results showed that an excess amount of Mia40$_{core}$ (1 μM) rapidly oxidises both Tim9wt and Tim10wt. To pinpoint the dosage effect of Mia40$_{core}$ on Tim9 oxidative folding, the oxidative folding of ^{35}S-Tim9wt was carried out in the presence of different concentrations of Mia40$_{core}$ for 5 min on ice. The reactions were analysed using non-reducing and reducing SDS-PAGE (Figure 4.4). The results showed that Tim9wt formed a disulphide linked complex with Mia40$_{core}$ at all concentrations of Mia40$_{core}$ tested, and that the intensity of the Mia40$_{core}$-Tim9 complex reduced with the decreasing of the concentrations of Mia40$_{core}$ (Figure 4.4, lanes 3-9). In all cases, under reducing conditions the Mia40$_{core}$-Tim9wt intermediate disappeared, confirming the existence of intermolecular disulphide bridges (Figure 4.4, lanes 10-16). Furthermore, it should be noted that when Mia40$_{core}$ was present in excess, the majority of Tim9 was fully oxidised, whilst in the presence of nanomolar amounts of Mia40$_{core}$, free partially oxidised forms of Tim9wt were generated (indicated by arrows in Figure 4.4.).

Thus, these results showed that: (1) Tim9wt is fully oxidised in the presence of an excess amount of Mia40$_{core}$, and (2) single disulphide-bonded intermediates of Tim9wt can be released from Mia40$_{core}$ (Figure 4.4, lanes 1-6 vs 7-9).

Next, to test whether these single disulphide-bonded intermediates of Tim9 are productive intermediates of the Mia40$_{core}$-mediated oxidation of Tim9, the time course of the Tim9 oxidative folding was analysed in the presence of 50 nM or 5 nM of Mia40$_{core}$ (Figure 4.5).

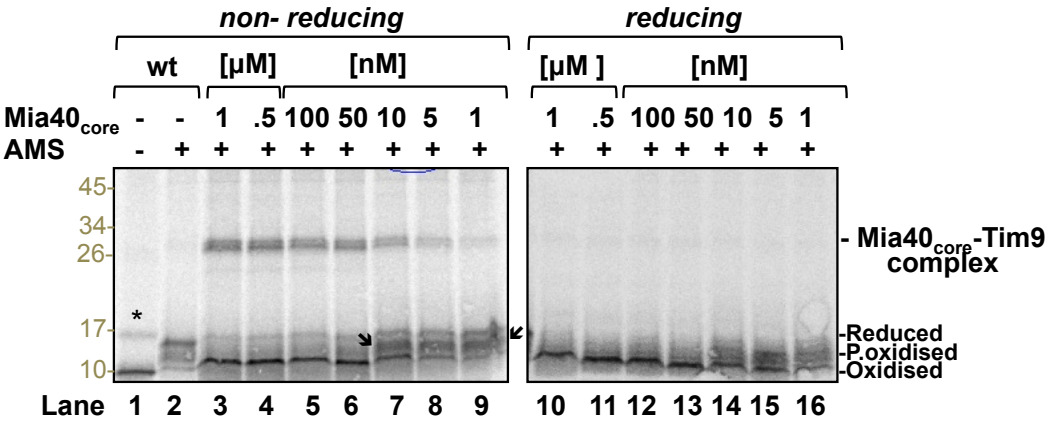

Figure 4.4 Mia40$_{core}$-concentration dependent oxidative folding of Tim9.

^{35}S-Tim9wt was incubated with the indicated different concentrations of Mia40$_{core}$ for 5 minutes on ice. Subsequently, samples were treated with 12.5 mM AMS as described in figure 4.2, subjected to non-reducing (lanes 3-9) or reducing (lanes 10-16) SDS-PAGE and analyzed by autoradiography. Lanes 1 and 2 are the controls showing the redox state of the starting material.
The Mia40$_{core}$-Tim9 complex, the *Reduced*, *P.oxidized* and *Oxidized* forms of Tim9 are indicated. The arrowheads indicate the presence in lanes 6-9 of single disulphide-bonded monomeric Tim9, whereas the asterisk in lane 1 indicates the heme protein.

In the presence of 50 nM Mia40$_{core}$, after 10 s the majority of Tim9wt is bound to Mia40$_{core}$ in Complex I and only a small amount of Tim9wt is in Complex II, whereas all free oxidised, partially oxidised and reduced Tim9 were observed at the bottom of the gel (Figure 4.5 A, lane 3). After 1 min the Complex II intensity became as strong as that of Complex I, and concomitantly more fully oxidised Tim9 appeared at the bottom of the gel (Figure 4.5 A, lane 4). After 5 min the majority of Tim9 was released from the complexes, and both the reduced and partially oxidised Tim9 have become fully oxidised (Figure 4.5 A, lanes 5-7).

In the presence of 5 nM Mia40$_{core}$, the oxidative folding of Tim9wt followed the same pattern except that it was slower. The results showed that Complex I

and Complex II have the same intensity after 5 min, and that the Tim9 oxidative folding completed after 15 min (Figure 4.5 A, lanes 9-13 and Figure 4.5 B).

Thus, the time course of the Tim9 oxidative folding in the presence of nM amounts of $Mia40_{core}$ confirmed that Tim9 undergoes complete oxidation. In addition, the results revealed that the free partially oxidised forms of Tim9 are products of the oxidative reaction mediated by $Mia40_{core}$, as they appeared at the beginning of the oxidative reaction and disappeared after Complexes I and II have reached the same intensity. Thus, semi-oxidised forms of Tim9 can be released from $Mia40_{core}$ after the transfer from $Mia40_{core}$ to the substrate of the first disulphide, and undergo complete oxidative folding shortly after. This seems to be due to the presence of $Mia40_{core}$, as the opposite was observed for Tim9 alone, which did not undergo complete oxidative folding in the absence of $Mia40_{core}$ (Figure 4.2, lanes 3-7).

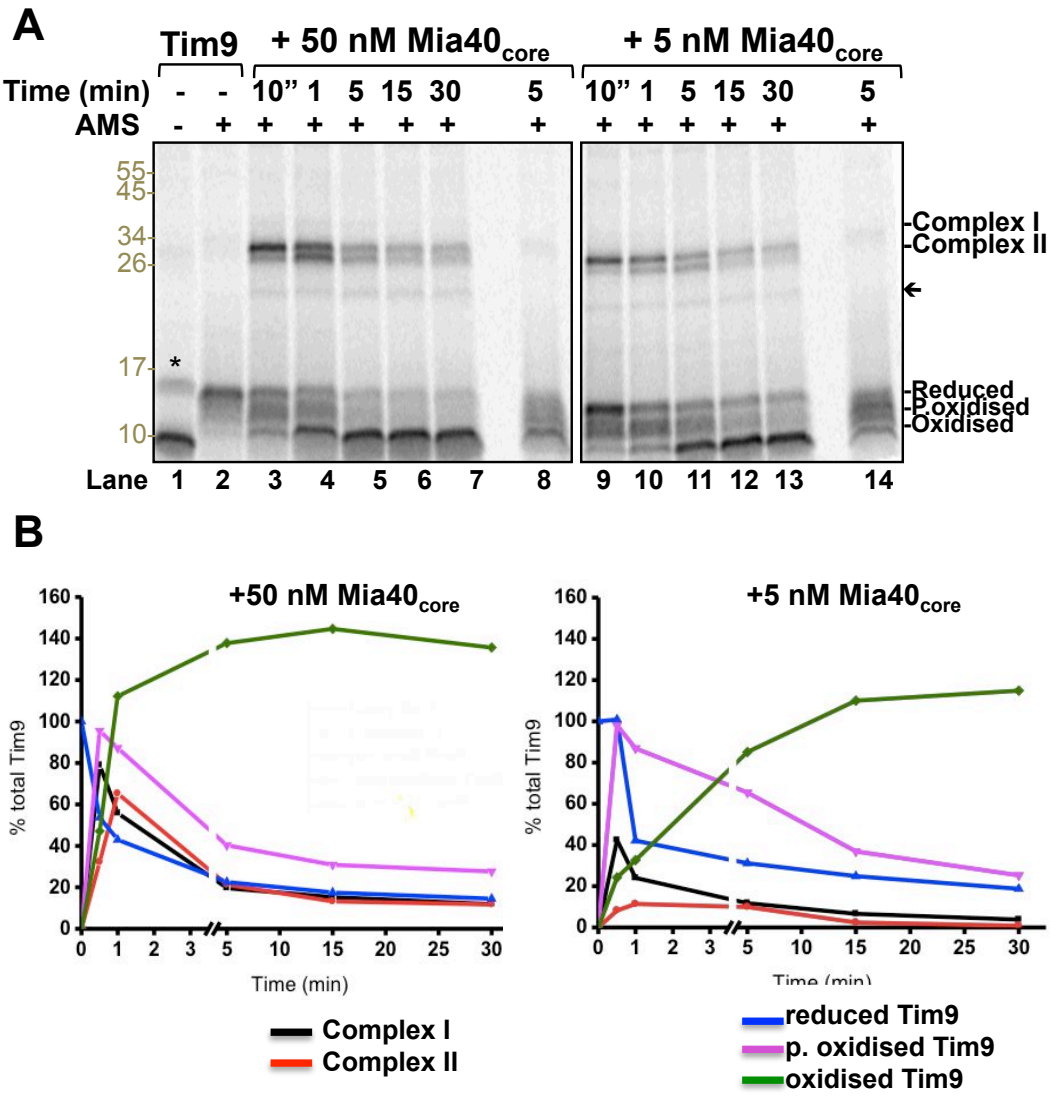

Figure 4.5 Time course of the oxidative folding of Tim9wt in the presence of 50 or 5 nM of Mia40$_{core}$.

(A) ^{35}S-Tim9wt was incubated with buffer containing 50 nM Mia40$_{core}$ (lanes 3-8) or containing 5 nM Mia40$_{core}$ (lanes 9-14) for the times as indicated. Subsequently, samples were treated with 12.5 mM AMS as described in figure 4.2, subjected to non reducing (lanes 3-7 and 9-13) or reducing (lanes 8 and 14) SDS-PAGE and analyzed by autoradiography. Lanes 1 and 2 are the controls showing the redox state of the starting material. The Mia40$_{core}$-Tim9 *Complex I* and *II,* the *Reduced*, *P.oxidised* and *Oxidised* forms of Tim9 are indicated. The asterisk in lane 1 indicates the heme protein, whereas the arrowhead indicates unidentified bands of approximately 20kDa in lanes 3-7 and 8-13 .
(B) The amounts of Tim9 in Complex I or Complex II, or the amounts of reduced, partially oxidised or oxidised Tim9 of the experiments in (A) were quantified by densitometry, expressed in comparison to the total Tim9, and plotted against time.

4.2.5 Effects of $Mia40_{core}$ on the oxidation of the double cysteine mutants of Tim9 and Tim10

It was shown for Cox19 that upon the interaction with $Mia40_{core}$, the formation of the intramolecular disulphide bonds occurs between the two outer (C1-C4) and the inner (C2-C3) cysteines of the twin CX_9C motif of yeast Cox19 (Bien *et al.,* 2010). However, whether the same principle is true for Tim9, a CX_3C motif-containing protein, is unknown.

In order to address this, the effects of $Mia40_{core}$ on the oxidative folding of the double-Cys mutants $Tim9^{C1,4S}$ and $Tim9^{C2,3S}$ were analysed (Figure 4.6 A and B). Both an excess (1 µM) and smaller concentrations (5 nM and 2.5 nM) of $Mia40_{core}$ were used. The experiments were performed and analysed as described for Figure 4.2. The results showed that in the absence of $Mia40_{core}$, both mutants did not spontaneously oxidise throughout the time course, although a small fraction of $Tim9^{C1,4S}$ underwent air oxidation (Figure 4.6 A and B, lanes 3-7). In the presence of an excess of $Mia40_{core}$, both mutants formed a stable intermediate complex with $Mia40_{core}$ within 10 s that lasted throughout the time course. These intermediates represented a mixed disulphide between Tim9 mutants and $Mia40_{core}$ as it dissociated after the addition of DTT (Figure 4.6 A and B, lane 23). Moreover, only a small fraction of both mutants were oxidised at the beginning of the time course, and the amount of oxidised substrates stayed the same during the time course (Figure 4.6 A and B, lanes 8-12). Thus, it cannot be excluded that their oxidation may be result of air oxidation.

In contrast, when incubated with 5 nM or 2.5 nM of $Mia40_{core}$, only a small fraction of both mutants formed a complex with $Mia40_{core}$. However, the majority of $Tim9^{C1,4S}$ was released from $Mia40_{core}$ within the first minutes of the time course, indicating that the complex $Mia40_{core}$-$Tim9^{C1,4S}$ was less stable than the complex $Mia40_{core}$-$Tim9^{C2,3S}$ (Figure 4.6, A vs B, lanes 13-22).

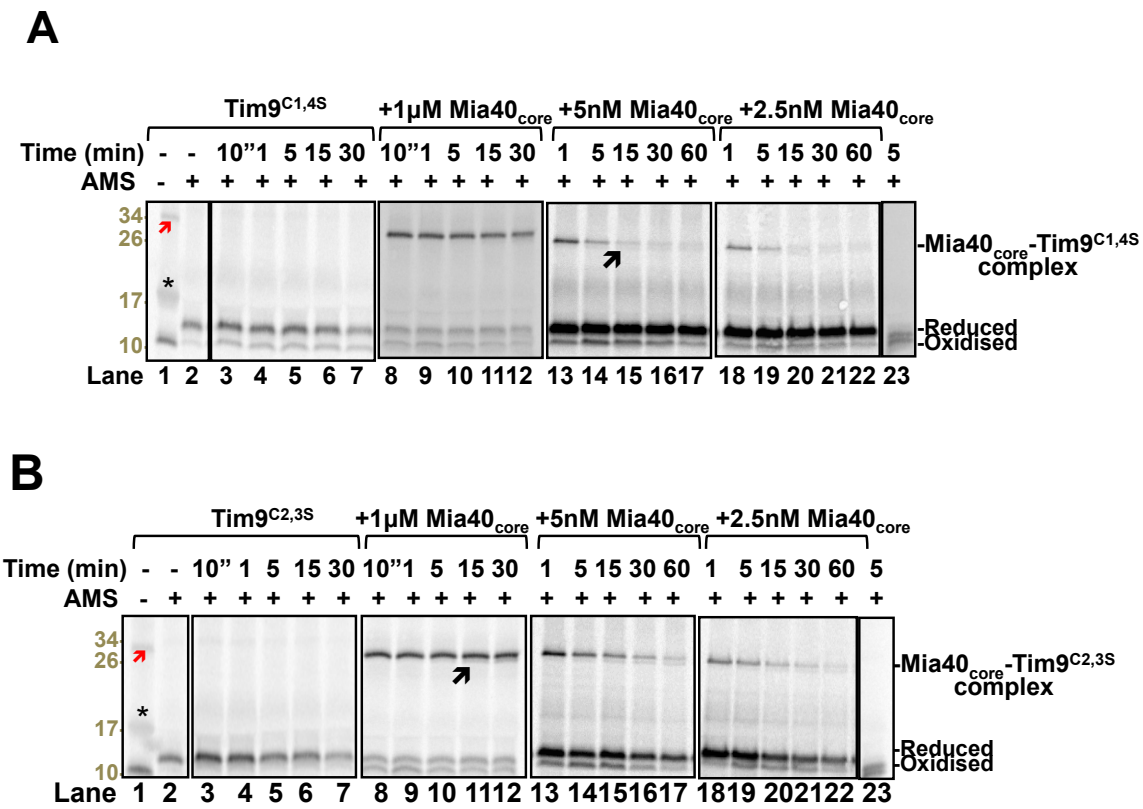

Figure 4.6 Time course of the interactions between $Mia40_{core}$ and the double Cys-mutants of Tim9.

(A) ^{35}S-$Tim9^{C1,4S}$ was incubated with buffer in the absence (lanes 3-7), or in the presence of 1 µM $Mia40_{core}$ (lanes 8-12 and 23), or 5 nM $Mia40_{core}$ (lanes 13-17), or 2.5 nM $Mia40_{core}$ (lanes 18-22) for the indicated times. Subsequently, samples were treated with 12.5 mM AMS as described in figure 4.2, subjected to non-reducing (lanes 1-22) or reducing (lane 23) SDS-PAGE. Lanes 1 and 2 are the controls showing the redox state of the starting material. The $Mia40_{core}$-$Tim9^{C1,4S}$ complex, the reduced and oxidised forms of $Tim9^{C1,4S}$ are indicated. The asterisk and the red arrowhead in lane 1 indicate respectively the heme protein and an unidentified band of approximately 34 kDa, whereas the black arrowhead may indicate a presumptive $Mia40_{core}$-substrate complex in which both cysteines of the substrate are linked to the CPC motif of $Mia40_{core}$.
(B) as in **(A)** except that ^{35}S-$Tim9^{C2,3S}$ was used.

Similar results were obtained when 1 µM $Mia40_{core}$ was incubated with the double cysteine mutants $Tim10^{C1,4S}$ and $Tim10^{C2,3S}$ of Tim10, suggesting again that both Tim9 and Tim10 interact with $Mia40_{core}$ in the same manner (Figure 4.7).

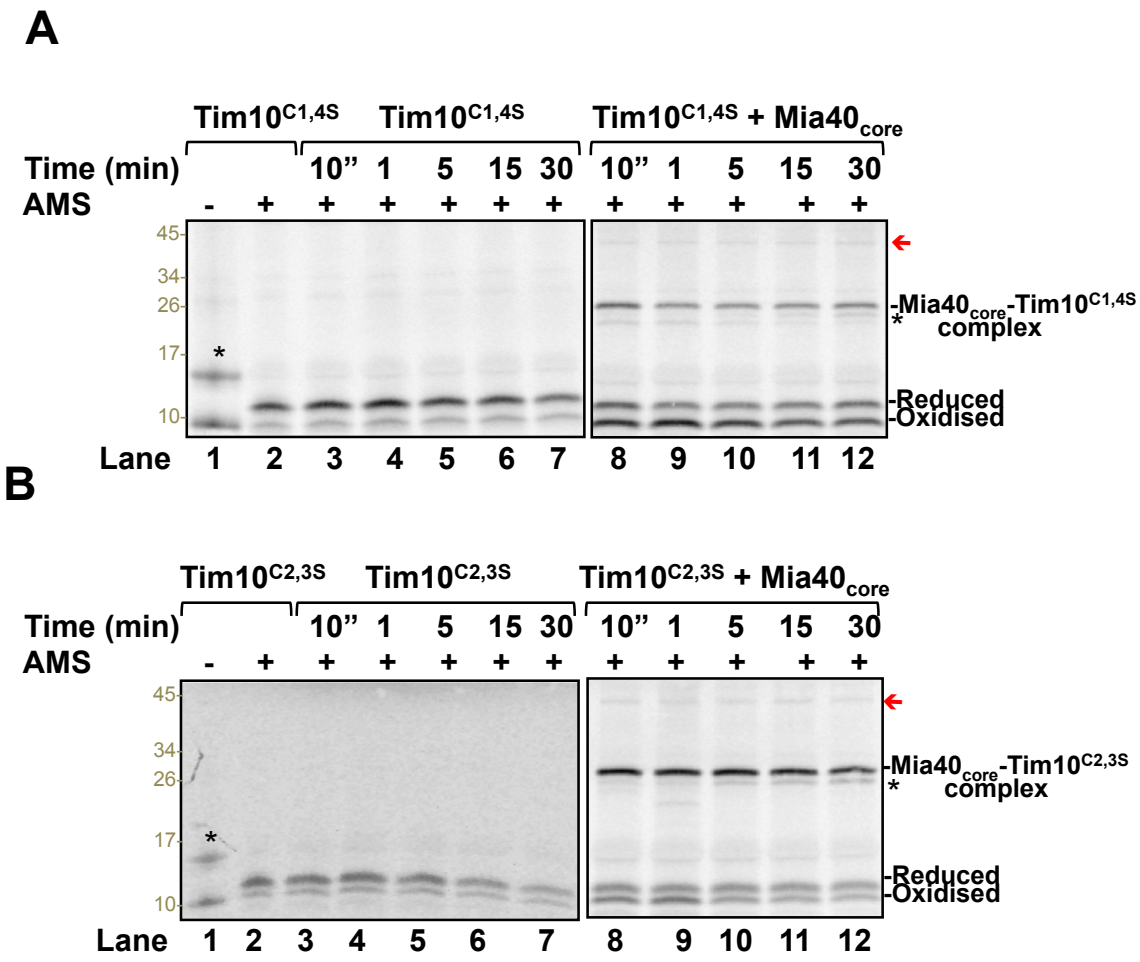

Figure 4.7 Time course of the interactions between the double Cys-mutants $Tim10^{C1,4S}$ or $Tim10^{C2,3S}$ and $Mia40_{core}$.

(A) and **(B)** as in figure 4.2 except that ^{35}S-$Tim10^{C1,4S}$ or ^{35}S-$Tim10^{C2,3S}$ were used respectively. The asterisk may indicate a presumptive $Mia40_{core}$-substrate complex in which both cysteines of the substrate are linked to the CPC motif of $Mia40_{core}$. The asterisk and the red arrowhead indicate respectively the heme protein in lane 1 and an unidentified band of approximately 40 kDa in lanes 8-12.

4.2.6 Formation of a mixed disulphide intermediate between $Mia40_{core}$ and the triple cysteine mutants of Tim9

The previous section showed that *in vitro* $Mia40_{core}$ binds with both double cysteine mutants of Tim9 and forms a stable complex whose stability depended on the concentration of $Mia40_{core}$. Thus, the next step was to explore the relevance of each cysteine present in Tim9 for the interaction with $Mia40_{core}$. In order to address this point, the Tim9 triple cysteine mutants $Tim9^{C2,3,4S}$, $Tim9^{C1,3,4S}$, $Tim9^{C1,2,4S}$ and $Tim9^{C1,2,3S}$ were created, and incubated with $Mia40_{core}$ for various time points. Both an excess of (1 uM) and nM concentrations (5 nM) of $Mia40_{core}$ were used (Figure 4.8).

When incubated with 1uM $Mia40_{core}$, $Mia40_{core}$ interacted and formed a stable complex with all the triple cys-mutants of Tim9 although to less extent with the third cysteine (Figure 4.8 middle column). The same results were obtained when 5 nM $Mia40_{core}$ was used (Figure 4.8 right column). Under reducing conditions all complexes disappeared, confirming that they are disulphides linked complexes (Figure 4.8 A and B-D, lanes 12 and 13). Thus, these results showed that all the four cysteines of Tim9 within the twin CX_3C motif can bind to $Mia40_{core}$, and it seems in the order of C1>C4>C2>C3 in terms of intensity.

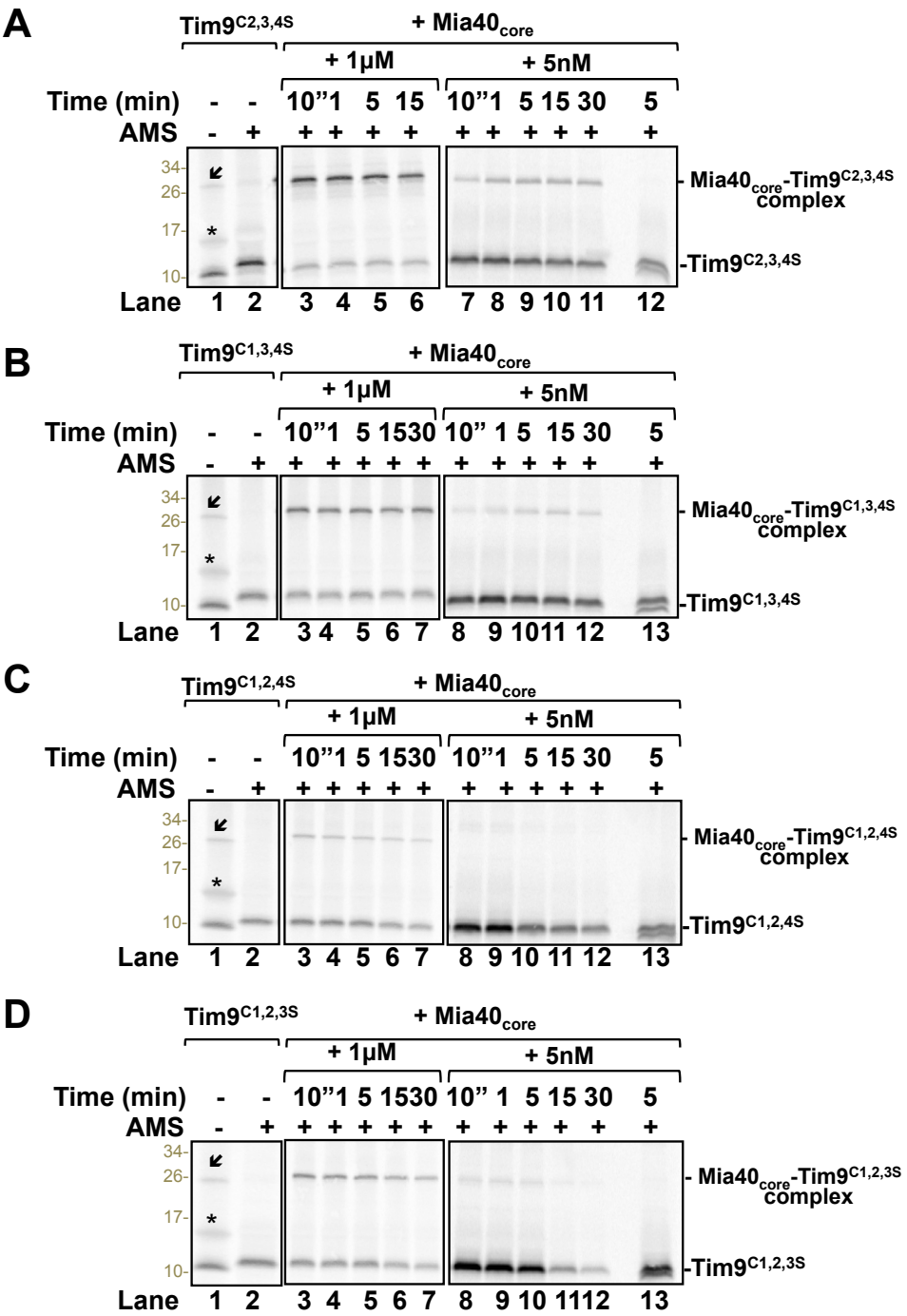

Figure 4.8 Mia40$_{core}$ interacts with all the triple cys-mutants of Tim9.

(A) ^{35}S-Tim9^{C2,3,4S} was incubated with with 1 µM Mia40$_{core}$ (lanes 3-7), or with 5 nM Mia40$_{core}$ (lanes 8-13) for the indicated time points. Subsequently, samples were treated with 12.5 mM AMS as described in figure 4.2, subjected to non-reducing (lanes 3-11) or reducing (lane 12) SDS-PAGE and analyzed by autoradiography. Lanes 1 and 2 are the controls showing the redox state of the starting material. The Mia40$_{core}$-Tim9^{C2,3,4S}complex and reduced Tim9^{C2,3,4S} are indicated. The asterisk and the arrowhead in lane 1 indicate respectively the heme protein coming from the lysate and an unidentified band.
(B), **(C)**, and **(D)** as in **(A)** except that ^{35}S-Tim9^{C1,3,4S}, ^{35}S-Tim9^{C1,2,4S}, or ^{35}S-Tim9^{C1,2,3S} were used, respectively.

4.3 PART II: IMPORT OF THE CYSTEINE MUTANTS OF TIM9 INTO MITOCHONDRIA

The results showed in the previous section indicated that $Mia40_{core}$ interacts and forms a disulphide linked complex possibly with all the cysteines of Tim9 *in vitro*. Previous studies reported that during mitochondrial import the first cysteine residue in Tim9 (C1) has a critical role for binding of Tim9 to mitochondria-located Mia40 (Milenkovic *et al.,* 2007). Thus, in order to obtain more biologically relevant data, the ability of the mutants of Tim9 to interact with Mia40 in the native environment of mitochondria were tested by *in organello* import assays.

4.3.1 Import of the double cys-mutants of Tim9

^{35}S-Tim9wt, ^{35}S-Tim9^{C1,4S} and ^{35}S-Tim9^{C2,3S} were incubated with WT mitochondria, and imports carried out for various time points. Following import, mitochondria were either treated with trypsin to remove the unimported material or left untreated for the analysis of the bound material. The proteins were then separated by SDS-PAGE under reducing conditions, and visualised by autoradiography (Figure 4.9). The results showed that both Tim9^{C1,4S} and Tim9^{C2,3S} bound efficiently to the OM (lanes 2-5), and were imported into a protease-protected location (lanes 6-9) although less efficiently than Tim9wt.

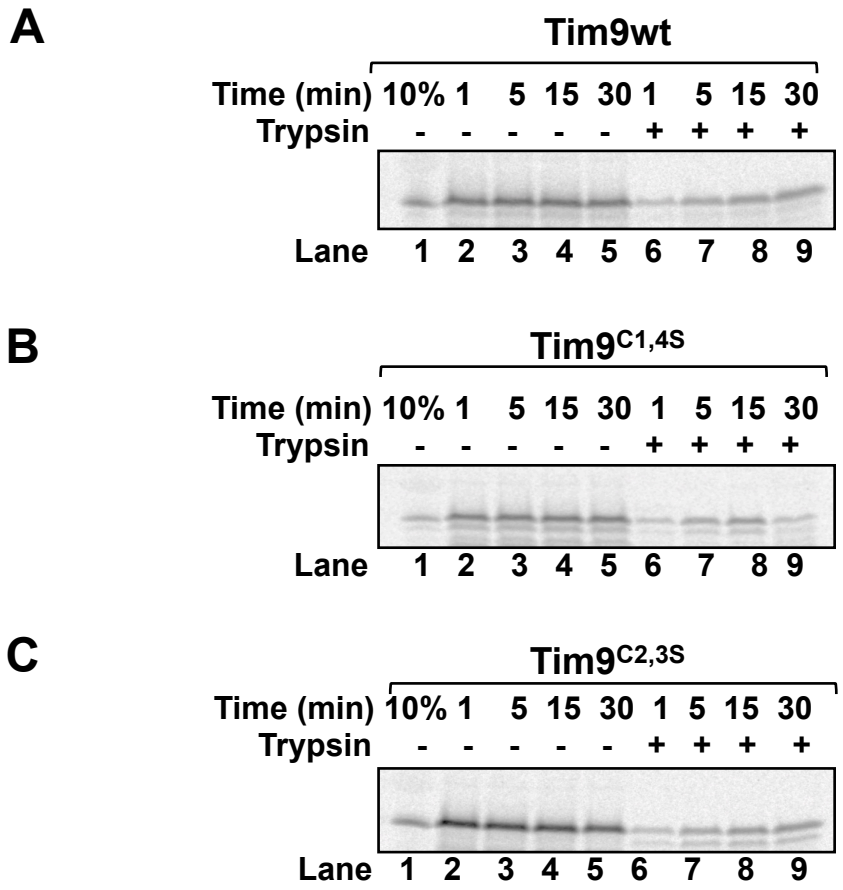

Figure 4.9 Import of the double cys-mutants of Tim9.

(A) WT mitochondria were incubated with ^{35}S-Tim9wt for the indicated times at 25°C. Following import half of the reactions were left untreated (lanes 2-5) or trypsin-treated (lanes 6-9) for the analysis of the bound or imported material, respectively. All samples were analyzed by reducing SDS-PAGE and autoradiography. 10% represents the amount of ^{35}S-Tim9 added to ach import of reaction.
(B) and **(C)** as in **(A)** except that Tim9^{C1,4S} and Tim9^{C2,3S} were used, respectively.

Next, to investigate whether the Tim9 double-cysteine mutants form a complex with Mia40 during import, ^{35}S-Tim9^{C1,4S} and ^{35}S-Tim9^{C2,3S} were imported into mitochondria and their interaction with Mia40 was trapped by the addition of 75 mM IAA at various time points (IAA is a small molecule that irreversibly alkylates free thiol groups and therefore traps the mixed disulphide intermediates). Mitochondria were then re-isolated and washed twice before the resuspension with either non-reducing or reducing sample buffer. Proteins were then resolved by SDS-PAGE and analysed by autoradiography (Figure 4.10 A). The results showed that Tim9^{C1,4S} interacted less efficiently with Mia40 than Tim9wt (Figure 4.10 A, lanes 4-6 vs 1-3), whilst Tim9^{C2,3S} formed a more stable complex with Mia40 in comparison to both Tim9wt and Tim9^{C1,4S} (Figure 4.10 A, lanes 7-9 vs 1-6). These intermediates consisted of mixed disulphide linked complexes, as they disintegrated upon addition of DTT (Figure 4.10 A, lanes 10-18).

To further confirm the result above, the two double cysteine mutants of Tim9 were imported into mitoplasts (Figure 4.10 B). Mitoplasts represent an alternative *in organello* suitable system to analyse the binding to Mia40, as in mitoplasts the OM is ruptured, Mia40 is exposed to the external solution and the amount of Erv1 is reduced by 50% (Wiedemann et al., 2004; Chacinska et al., 2004; Stojanovski et al., 2008). Thus, mitoplasts, generated by hypo-osmotic swelling, were incubated with ^{35}S-Tim9wt, ^{35}S-Tim9^{C1,4S} or ^{35}S-Tim9^{C2,3S} for different time points. Following import, mitoplasts were analysed as in Figure 4.10 A (Figure 4.10 B). The results confirmed that the mutant Tim9^{C2,3S} formed a longer lasting complex with Mia40 than Tim9wt or Tim9^{C1,4S} (Figure 4.10 B, lanes 7-9 vs lanes 1-6).

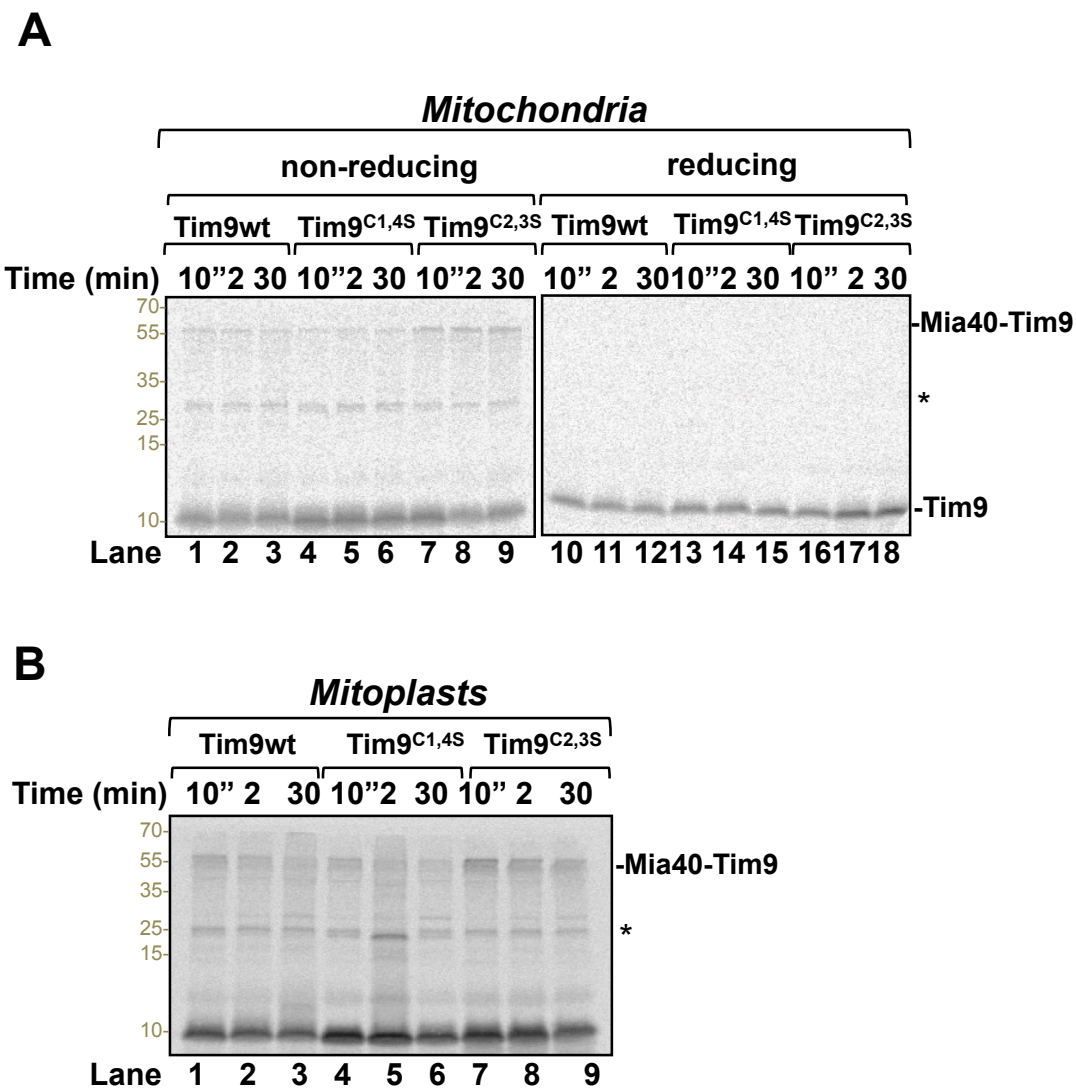

Figure 4.10 Import of Tim9wt, Tim9^{C1,4S} and Tim9^{C2,3S} and their interaction with Mia40.

(A) Mitochondria were incubated with ^{35}S-Tim9wt or ^{35}S-Tim9^{C1,4S} or ^{35}S-Tim9^{C2,3S} for the indicated times at 25°C. Then, mitochondria were treated with 75 mM IAA for 1 h on ice. Subsequently, mitochondria were washed twice, resuspended with non reducing (lanes 1-9) or reducing (lanes 10-18) sample buffer, analysed by SDS-PAGE and autoradiography. The asterisk indicates the presence of a putative trimeric Tim9 complex in the IMS.
(B) as in **(A)** except that ^{35}S-Tim9wt, ^{35}S-Tim9^{C1,4S} or ^{35}S-Tim9^{C2,3S} were imported in mitoplasts instead of mitochondria.

Together the mitochondria and mitoplasts import assays suggested that Mia40 does not release or releases very slowly the variant Tim9^{C2,3S} that lacks the cysteine residues involved in the formation of the inner intramolecular disulphide.

4.3.2 Import of the triple cys-mutants of Tim9

Next, the ability of the triple cysteine mutants of Tim9 to be imported into mitochondria was analysed using the same method as above (Figure 4.11 A). The results showed that all of the triple variants bound to the OM but only Tim9^{C2,3,4S} could efficiently translocate to a protease-protected location as the WT. To confirm further that the triple mutant Tim9^{C2,3,4S} can form a complex with mitochondria-located Mia40, a time course import experiment for Tim9wt and Tim9^{C2,3,4S} was performed and analysed under non-reducing conditions (Figure 4.11 B). The results showed that both Tim9^{C2,3,4S} and Tim9wt formed a disulphide linked intermediate with Mia40, as it disintegrated under reducing conditions (Figure 4.11 B, lanes 1-4 and 5-8, respectively).

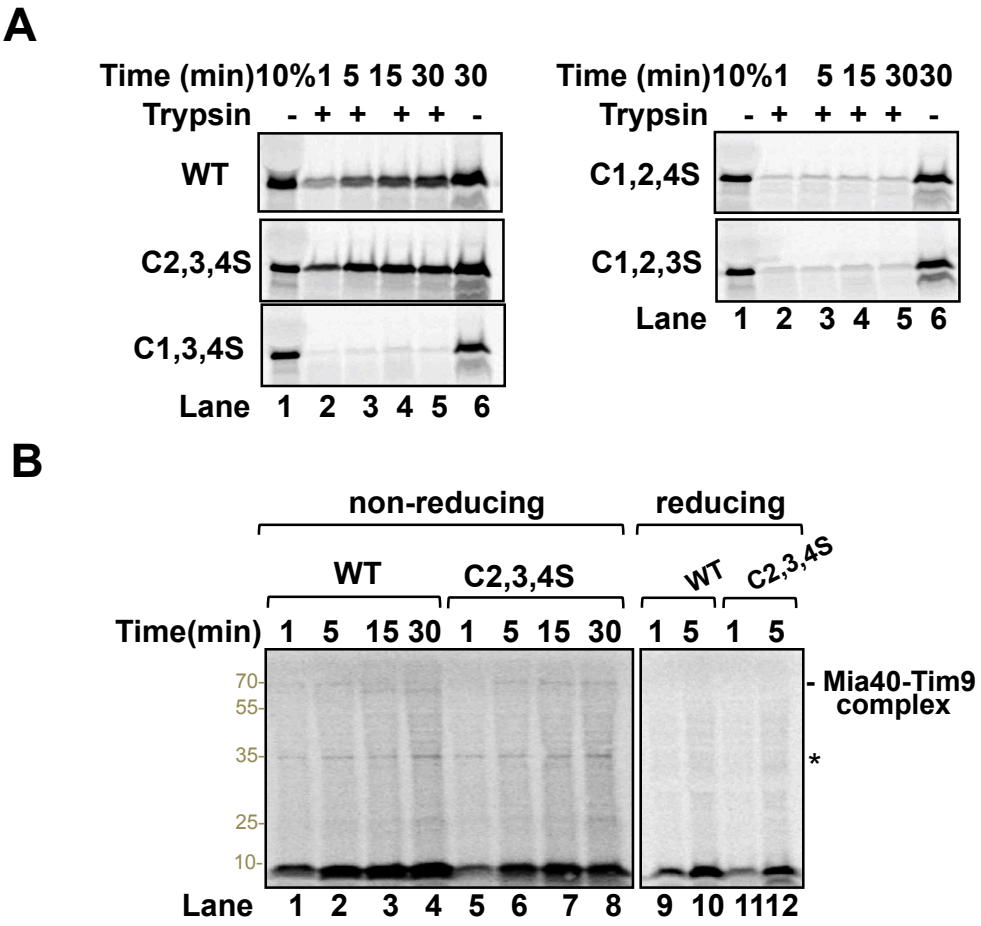

Figure 4.11 Import of the triple cys-mutants of Tim9.

(A) ^{35}S-Tim9wt, ^{35}S-Tim9^{C2,3,4S}, ^{35}S-Tim9^{C1,3,4S}, ^{35}S-Tim9^{C1,2,4S}, or ^{35}S-Tim9^{C1,2,3S} were incubated with mitochondria and imported for the indicated times. Following import, mitochondria were trypsin treated to remove the unimported precursors (lanes 2-5) or left untreated (lanes 6), separated by reducing SDS-PAGE, and analyzed by autoradiography. 10% indicates the 10% of total Tim9 added to the import reaction prior trypsin treatment.
(B) ^{35}S-Tim9wt (lanes 1-4) and ^{35}S-Tim9^{C2,3,4S} (lanes 5-8) were incubated with mitochondria and imported for the indicated time points. Following import, mitochondria were trypsin treated, re-isolated by centrifugation, washed twice and resuspended in non-reducing (lanes 1-8) or reducing (lanes 9 -12) sample buffer. Proteins were then separated by SDS-PAGE, and analyzed by autoradiography. The Mia40-Tim9 complexes are shown. The asterisk indicates an unidentified band.

4.4 PART III: THE EFFECTS OF GSH ON THE INTERACTION BETWEEN MIA40 AND TIM9

One recent study demonstrated that import of Cox19 was enhanced by physiological concentrations of GSH, as GSH may counteract and/or remove the kinetically trapped intermediates formed between Mia40 and Cox19 (Bien *et al.,* 2010). The aims of this part of the study were to investigate the effects of GSH on the Mia40-mediated oxidative folding of Tim9 both *in vitro* and *in organello*. In some experiments Cox19 was used as a control to compare the results with those published by Bien *et al.* (2010). All the experiments were performed in an aerobic environment.

4.4.1 Effects of GSH on mitochondrial import of Tim9

In order to assess the effect of GSH in mitochondrial import of Tim9, mitochondria were incubated with import buffer in the absence or presence of increasing amounts of GSH for 5 min. ^{35}S-Tim9 was then added to mitochondria and imported for 20 min. After import, mitochondria were trypsin-treated as usual, and analysed by reducing SDS-PAGE (Figure 4.12 A). The results showed that even the lowest concentrations of GSH (2.5 and 5 mM) increased the levels of mitochondrial import of Tim9 in comparison the control (Figure 4.12 A, lanes 2-7). Such a positive effect was not observed when using DTT as a reductant: Tim9 import into mitochondria was more efficient when 2.5 mM DTT were used, whereas increased DTT concentrations either decreased or completely inhibited the import of Tim9 (Figure 4.12 B, lane 4-6 vs 7). This could be explained by the fact that high concentrations of DTT may reduce Mia40 and/or prevent oxidation of the substrates (Mesecke *et al.,* 2005).

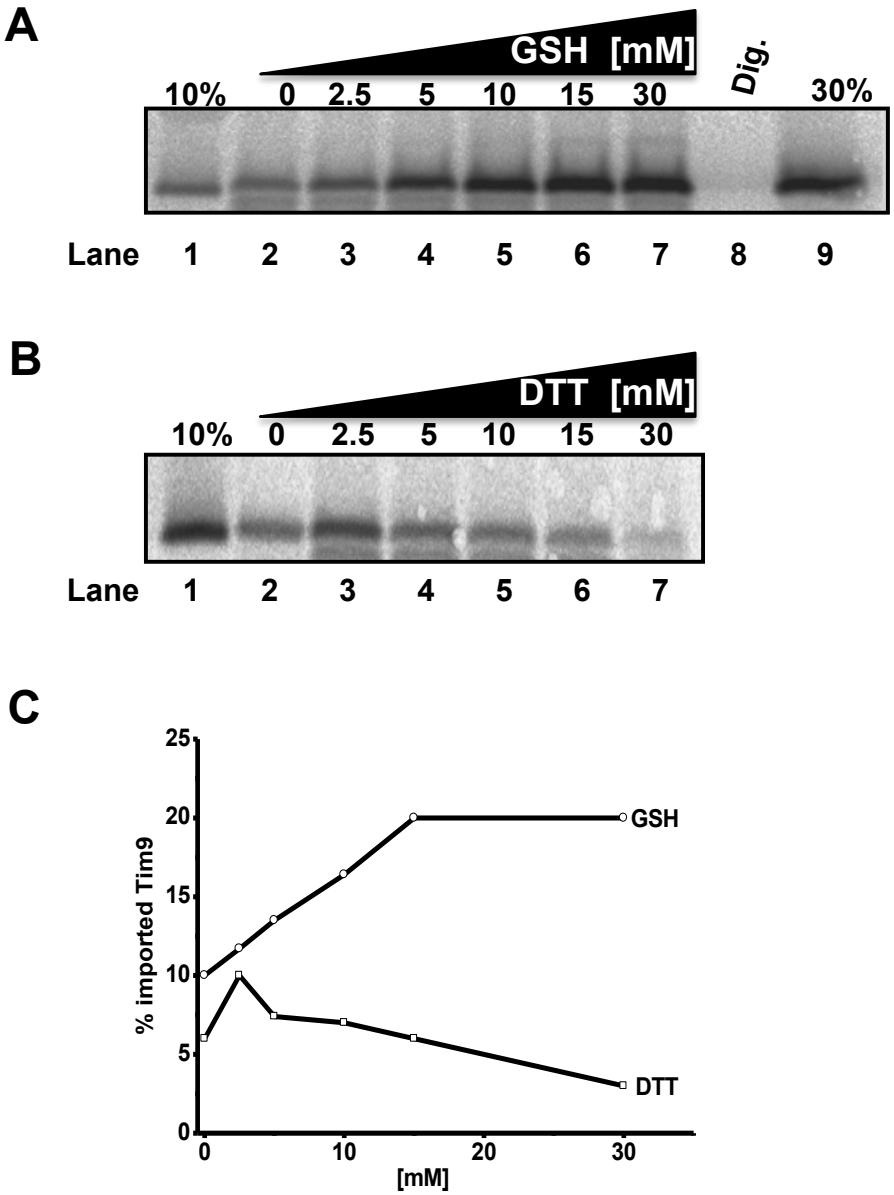

Figure 4.12 Effects of GSH in import of Tim9.

(A) ^{35}S-Tim9 was imported into mitochondria in the absence of GSH (lane 2) or in the presence of the indicated amounts of GSH (lanes 3- 7) for 20 min. Following import samples were trypsin treated, analyzed by reducing SDS-PAGE and autoradiography. Lanes 1 and 9 indicate the 10% and the 30% respectively of ^{35}S-Tim9 added to ach import of reaction. As control for the import assay, one sample was treated with digitonin buffer (Dig.) before the trypsin treatment (lane 8).
(B) As in **(A)** except that DTT was used as a reducing agent.
(C) Quantification of the imported levels of Tim9 in (A) and (B). The amount of Tim9 imported in each condition was quantified by densitometry and expressed in comparison to the 10%, and plotted against the amount of the reductant used.

Next, the effects of different amounts of GSH on the complex formation between Tim9 and mitochondrial-Mia40 were also investigated (Figure 4.13). The import was performed as described for Figure 4.12 with the exception that after import the samples were subjected to non-reducing SDS-PAGE. The results showed that as the concentration of GSH increased, the amount of Mia40-Tim9 intermediate increased together with imported levels of Tim9 (Figure 4.13, upper panel, lanes 1-5 vs 6-7). However, the western blot signal against Mia40 on the same membrane did not show the amount of Mia40 that is in the complex with Tim9 or as monomeric Mia40 (Figure 4.13, lower panel), probably because samples were separated by a non-reducing 16% tricine SDS-PAGE.

To analyse the effects of GSH on the kinetics of Tim9 import, time course of Tim9 import into mitochondria that were pre-incubated with 5 or 10 mM GSH was carried out (Figure 4.14). At the time points indicated, aliquots were removed and treated as usual for the analysis of the imported material. Proteins were analysed by reducing SDS-PAGE and autoradiography. The results showed that in the presence of both 5 mM and 10 mM GSH Tim9 import increased 2 folds in comparison to that without GSH.

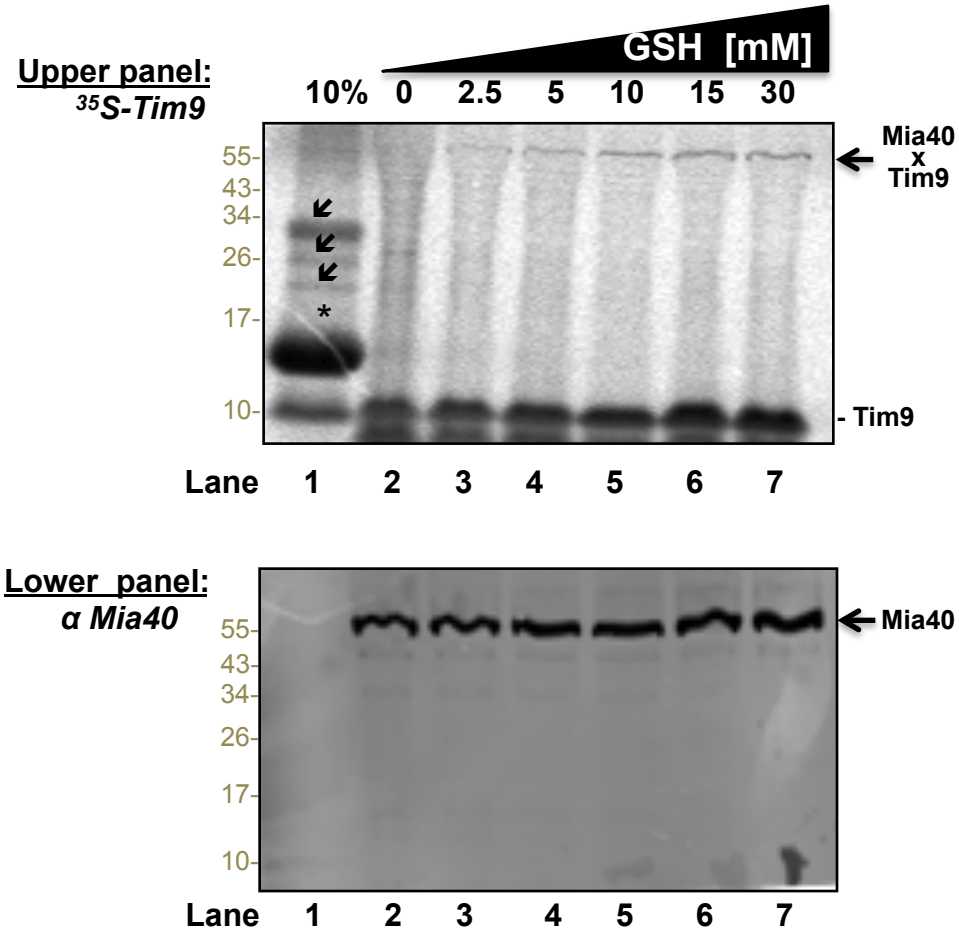

Figure 4.13 Effects of GSH in Tim9 import.

Upper panel: as in figure 4.12 **(A)** except that after import, samples were separated by non reducing 16% tricine SDS-PAGE. The complex Mia40xTim9 is indicated. The asterisk and the arrowheads in lane 1 indicate respectively the heme protein coming from the lysate and unidentified bands. **Lower panel:** western blot signal for Mia40 of the membrane in the upper panel showing both of monomeric Mia40 and Mia40 in the complex with Tim9.

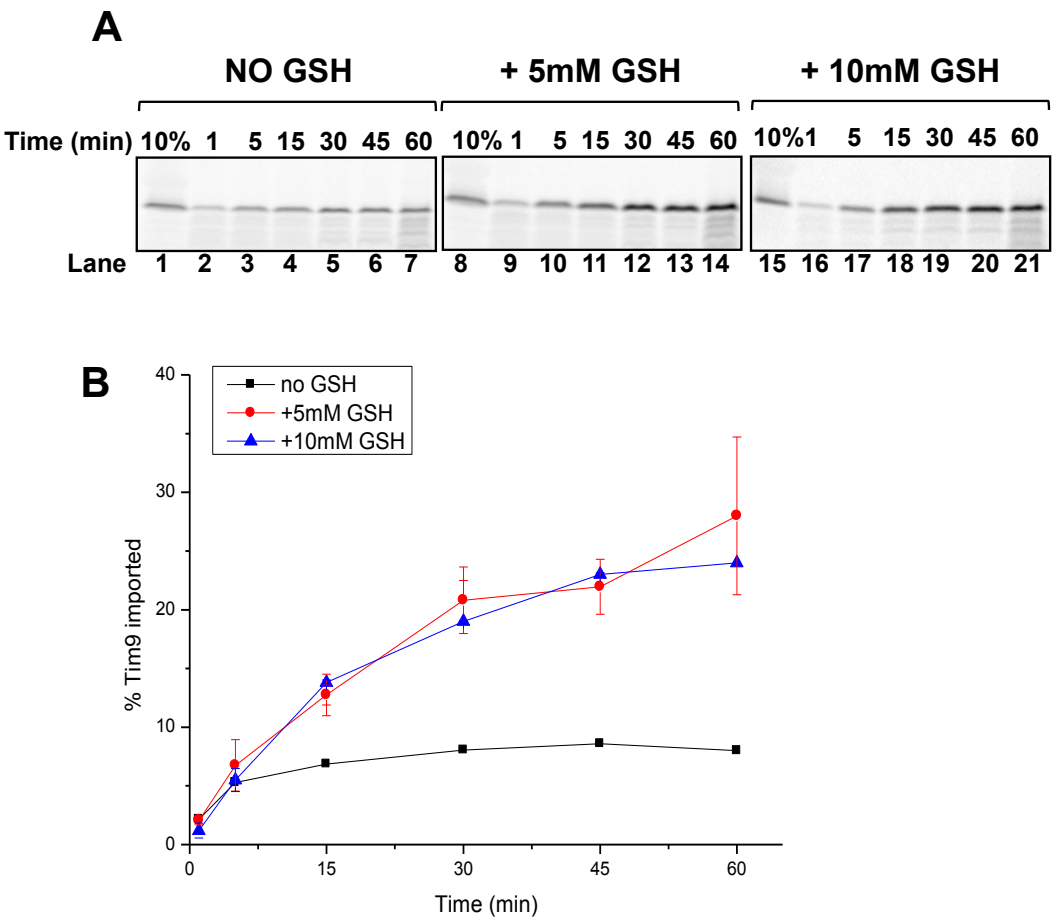

Figure 4.14 The time course of import of Tim9 in the presence of different amounts of GSH.

(A) Before import mitochondria were incubated for 5' with import buffer (lanes 2-7), or with import buffers containing 5 mM GSH (lanes 9-14), or 10 mM GSH (lanes 16-21). ^{35}S-Tim9 was then added to each import reaction and imports were carried out for the indicated time points. Following import, mitochondria were treated as usual for the analysis of the imported material. All samples were analyzed by SDS-PAGE and autoradiography. 10% indicates 10% of the total ^{35}S-Tim9 added to each import reaction.

(B) Quantification of the imported Tim9 as in (A). The amount of Tim9 imported in each condition was quantified by densitometry using the AIDA2.31 software, expressed in comparison to the 10%. Errors bars represent the deviation standard from two independent experiments.

4.4.2 Effects of GSH on the *in vitro* Mia40$_{core}$-mediated oxidative folding of Tim9

It is unknown how GSH affects positively the mitochondrial import of Tim9. A possible hypothesis is that that GSH might remove the kinetically trapped intermediates formed between Mia40 and Tim9, as suggested for Cox19 by Bien et al. (2010). To test this, the oxidative folding of ^{35}S-Tim9 in buffer either containing 1 µM Mia40$_{core}$ or 1 µM Mia40$_{core}$ and 5 mM GSH for various times was investigated (Figure 4.15). At the indicated times, the reactions were stopped by addition of an excess amount of the alkylating agent AMS, and the redox state of Tim9 was analysed as for Figure 4.2. The results showed that upon mixing reduced ^{35}S-Tim9 with Mia40$_{core}$, a mixed disulphide bond complex between Mia40$_{core}$ and Tim9 appeared rapidly and persisted throughout the time course (Figure 4.15 A, lanes 3-7). This complex dissolved to monomeric Tim9 upon addition of DTT (Figure 4.15 A, lane 9). The Mia40$_{core}$-Tim9 complex generated fully oxidised monomeric species of Tim9, since an increased amount of oxidised Tim9 appeared at the bottom of the gel (Figure 4.15 A, lanes 3-4 vs 5-7). In contrast, upon mixing ^{35}S-Tim9 with buffer containing Mia40$_{core}$ and 5 mM GSH, no Mia40$_{core}$-Tim9 complex was detected, whilst oxidised Tim9 formed rapidly (Figure 4.15 A, lanes 10-15). Thus, in the presence of GSH, the Mia40$_{core}$-Tim9 complex disassembled very fast. The immunodecoration with Mia40 antibody on the same membranes showed that Mia40$_{core}$ became gradually reduced in the absence of GSH, whilst in the presence of GSH the majority of Mia40$_{core}$ is reduced at the beginning of the time course (Figure 4.15 B, lanes 3-7 vs 9-13).

However, technical problems arose when performing the AMS assay in the samples containing GSH. It seemed that the AMS thiol-modification assays did not work properly in the presence of high amounts of GSH, as the monomeric species of Tim9 appeared to be unmodified at all time points (Figure 4.15 A, lanes 10-15). Therefore, it was not possible to determine the redox state of the monomeric forms of Tim9 in the sample reactions containing both Mia40 and GSH. For this reason the attention on this and the next 2 figures will be focused on the upper part of the gel (highlighted with a box in the figures 4.15, 4.16 and 4.17).

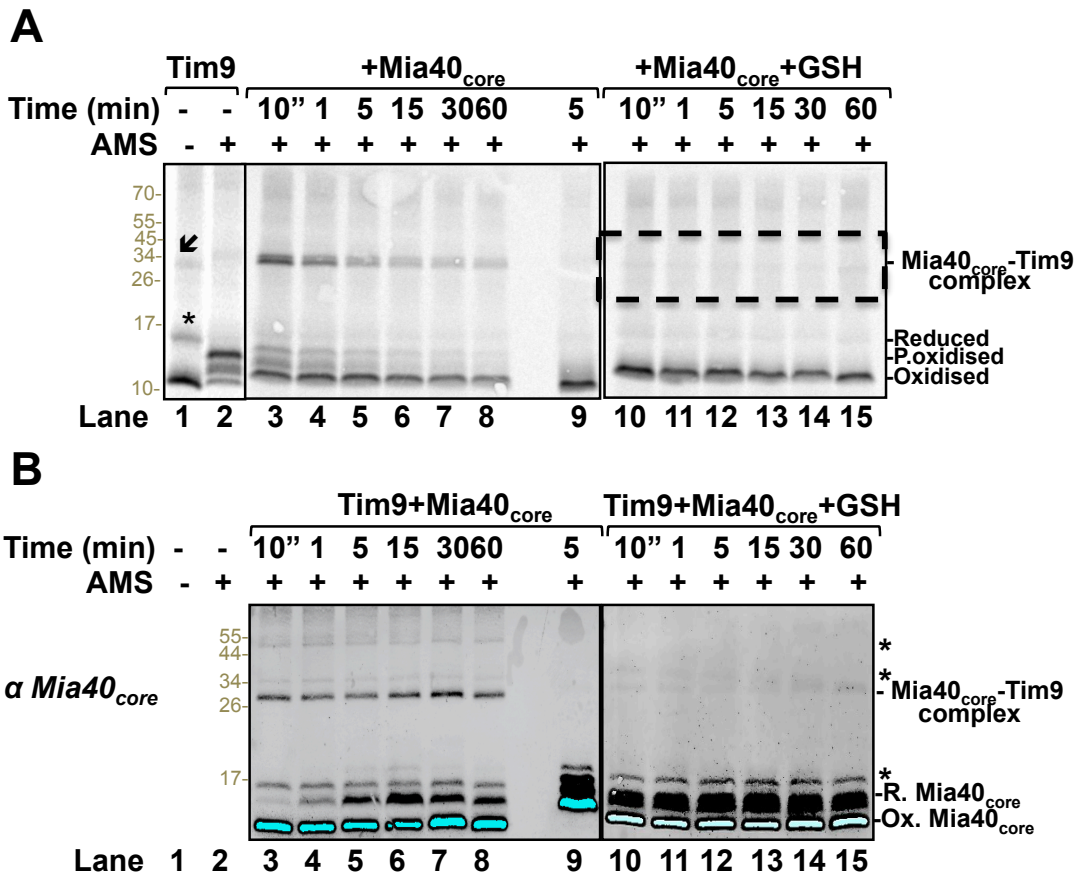

Figure 4.15 Effects of GSH on the Mia40$_{core}$-mediated oxidative folding of Tim9.

(A) ^{35}S-Tim9 was incubated in buffer in the presence of 1 µM Mia40$_{core}$ (lanes 3-9) or in the presence of 1 µM Mia40$_{core}$ and 5 mM GSH (lanes 10-16) for the times as indicated. Subsequently, samples were treated with 12.5 mM AMS for 20 min, and then subjected to non reducing (lanes 3-8 and 10-15) or reducing (lanes 9 and 16) SDS-PAGE and analyzed by autoradiography. Lanes 1 and 2 are the controls showing the redox state of the starting material. The *Reduced*, *P.oxidized* and *Oxidized* forms of Tim9, and the Mia40$_{core}$-Tim9 *Complex* are indicated. The asterisk and the arrowhead in lane 1 indicate respectively the heme protein coming from the lysate and an unidentified band.

(B) Western blot of Mia40 in the membranes in (A). Both Mia40$_{core}$ in the complex with Tim9, and monomeric Mia40$_{core}$ in a reduced (*R. Mia40$_{core}$*) and oxidised (*Ox.Mia40$_{core}$*) form are indicated. The membrane was overexposed. The asterisks indicate unspecific reactions of the antibody.

4.4.3 Effects of GSH on the *in vitro* Mia40$_{core}$-mediated oxidative folding of Cox19

Similar results were also obtained using ^{35}S-Cox19 as substrate of Mia40$_{core}$ (Figure 4.16). When Cox19 was incubated with Mia40$_{core}$ alone, the Mia40$_{core}$-Cox19 complex formed lasting throughout the time course, whereas when incubated with Mia40$_{core}$ and GSH the Mia40$_{core}$-Cox19 complex was not observed (Figure 4.16 B, lanes 9-13). Interestingly, a band of about 55 kDa appeared during the Mia40$_{core}$-mediated oxidation of Cox19 (Figure 4.16 A, lanes 3-7 indicated by an asterisk). This 55 kDa band may represent a high oligomer disulphide-linked complex formed between Mia40$_{core}$ and Cox19, as its intensity weakened along the time course, and it disintegrated upon addition of DTT (Figure 4.16 A, lane 8). Moreover, the immunodecoration with Mia40 antibody on the same membrane confirmed the presence of Mia40$_{core}$ in both 35 kDa and 55 kDa bands (Figure 4.16 B, lanes 3-7). Therefore, the 55kDa complex may represent a Mia40$_{core}$-Cox19 complex with stoichiometry of 2:1. These results show that the Mia40$_{core}$-Cox19 complex almost disappeared as soon as GSH was added to the sample, whereas in the study by Bien et al. (2010), the dissociation of the Mia40$_{core}$-Cox19 complex was not so fast in the presence of GSH.

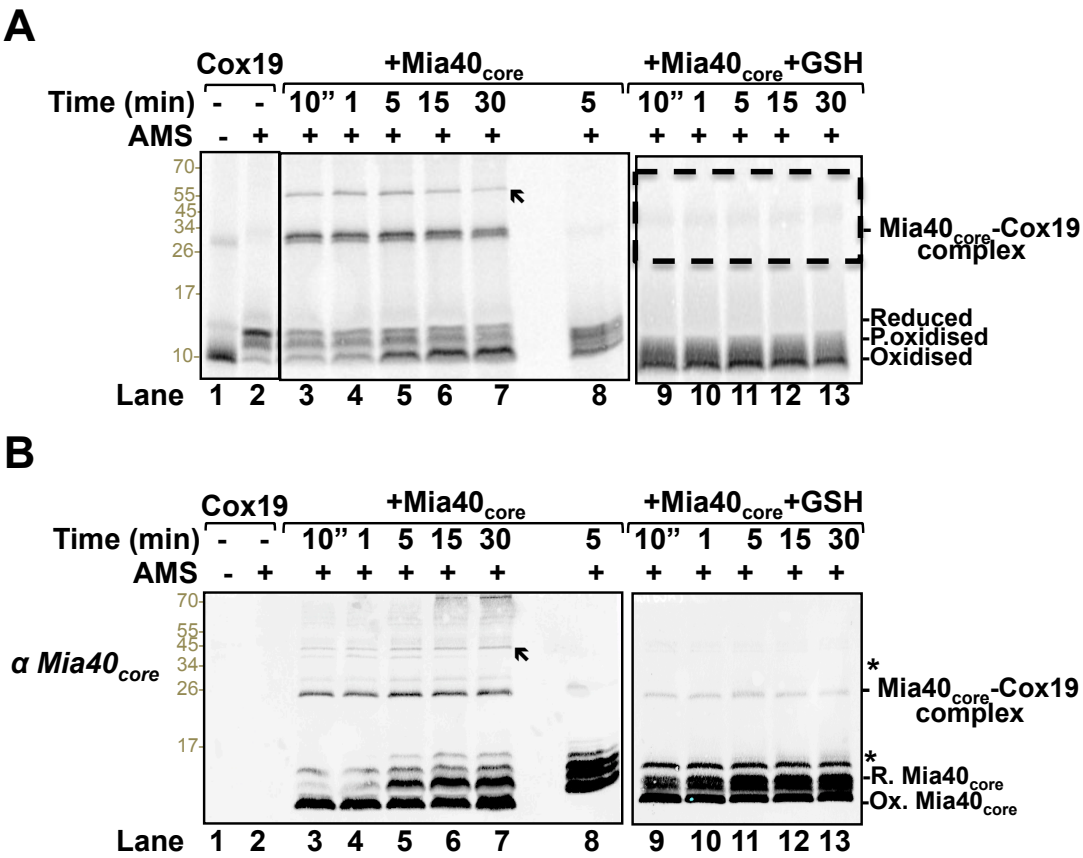

Figure 4.16 Effects of GSH on the Mia40$_{core}$-mediated oxidative folding of Cox19.

(A) As in Figure 4.15 except that ^{35}S-Cox19 was used. Lanes 1 and 2 are the controls showing the redox state of the starting material. Reduced, Intermediate and Oxidized represent the different redox states of Cox19; Mia40$_{core}$-Cox19 indicates the mixed disulfide bond between Mia40$_{core}$ and Cox19. The arrowhead indicates a possible complex Mia40$_{core}$-Cox19 with stoichiometry 2:1.
(B) Western blot of Mia40$_{core}$ in the membranes in **(A)** showing both Mia40$_{core}$ in the complex with Cox19, and monomeric Mia40$_{core}$ in a reduced (*R. Mia40$_{core}$*) and oxidised (*Ox.Mia40$_{core}$*). The arrowhead indicates the presence of Mia40$_{core}$ in the complex Mia40$_{core}$-Cox19 2:1, whereas the asterisks indicate unspecific reactions of the antibody.

4.4.4 Effects of GSH on the interaction between Mia40$_{core}$ and the double cysteine mutants of Tim9

One reason to explain the effect of GSH on the formation of the Mia40$_{core}$-Tim9 or Mia40$_{core}$-Cox19 intermediate could be that GSH disassociates the complex as soon as it forms. To verify this, the chase-experiment as described in Figure 4.17 A was performed: ^{35}S-Tim9wt, Tim9^{C1,4S} or Tim9^{C2,3S} were pre-incubated with an excess amount (1 µM) of Mia40$_{core}$ on ice for 5 min to allow the formation of the Mia40$_{core}$-Substrate complex. The samples were then divided into two halves, with one of them incubated with 5 mM of GSH. At various time points, aliquots from each sample were removed and the reactions quenched by an excess amount of AMS, followed by resuspension withnon-reducing SDS-PAGE. In this experiment, both Tim9wt and Tim9^{C1,4S} showed the same results: after 5 min, without the addition GSH, the substrate was still linked to Mia40$_{core}$ in the complex Mia40$_{core}$-Tim9, and the amount of monomeric oxidised forms of Tim9 increased while the intensity of the complex Mia40$_{core}$-Tim9 decreased (Figure 4.17 B-C, lanes 3-8). In contrast, upon the addition of GSH, majority of the complex Mia40$_{core}$-Tim9 again disappeared within the first 10 s (Figure 4.17 B-C, lanes 9-14).

In contrast to Tim9wt and Tim9^{C1,4S}, Tim9^{C2,3S} seemed to be more resistant to GSH: in the absence of GSH, Tim9^{C2,3S} formed a long-lasting complex with Mia40$_{core}$ with little oxidation occurring (Figure 4.17 D, lanes 6-8), and this complex is more resistant to GSH throughout the time course (Figure 4.17 D, lanes 9-14).

It is worth to note the appearance upon the addition of GSH of a distinct third band representing the monomeric species of $Tim9^{C1,4S}$ modified by 1 molecule of AMS persisting throughout the time course (Figure 4.17 C, lanes 9-14). This band may represent the fraction of $Tim9^{C1,4S}$ that was originally bound to $Mia40_{core}$ and released from $Mia40_{core}$ by GSH.

Since a similar band was not observed in the samples containing $Tim9^{C2,3S}$, this may suggest that GSH acts on specific cysteines of the complex between Mia40 and the substrate (i.e. C2 and/or C3), or at specific times of the oxidative folding of Mia40 substrates (i.e. after the generation of the first disulphide bond in the substrate; Figure 4.17 C, lanes 9-14 vs Figure 4.17 D, lanes 9-14).

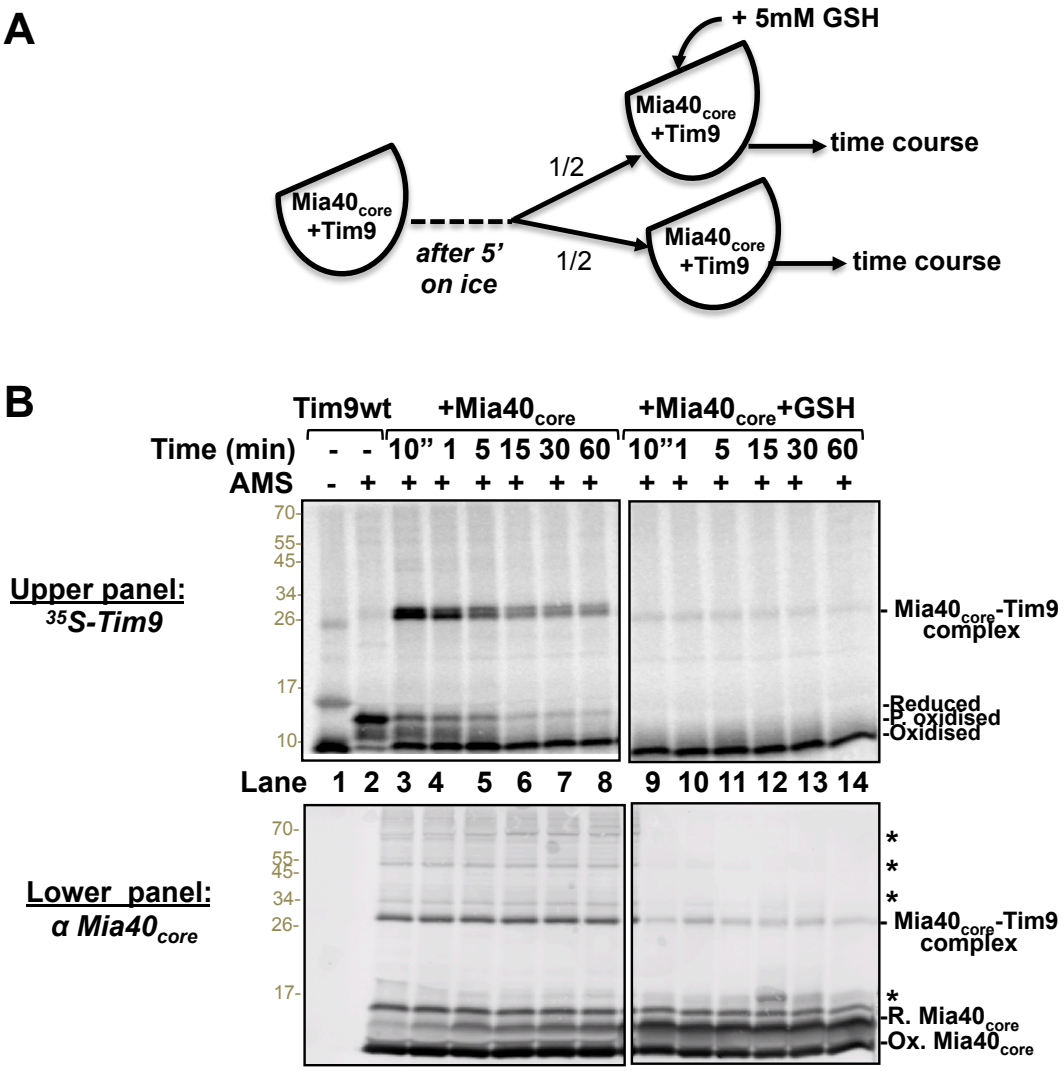

Figure 4.17 Effects of GSH on the formation of Mia40$_{core}$-Tim9 complex.

(A) The scheme depicts the design of the experiment: Tim9 was first incubated with 1 µM Mia40$_{core}$ for 5 min on ice. Subsequently, the sample was divided into two halves, one half being and the other half not being incubated with 5 mM GSH for various times. At the indicated times, the reactions were stopped with an excess of AMS, and analyzed by SDS-PAGE and autoradiography.

(B) **Upper panel:** Tim9wt oxidative folding was performed by incubating ^{35}S-Tim9 with Mia40 for 5 min before following the reaction in the absence of 5 mM GSH (lanes 3-8) or in the presence of 5 mM GSH (lanes 9-14) for the indicated time points. At each time point samples were treated with 12.5 mM AMS for 20 min, and then subjected to non reducing SDS-PAGE and analyzed by autoradiography. Lanes 1 and 2 are the controls showing the redox state of the starting material. The *Reduced*, *P.oxidized* and *Oxidized* forms of Tim9, and the Mia40$_{core}$-Tim9 *Complex* are indicated.

Lower panel: western blot signal for Mia40$_{core}$ on the same membranes showing Mia40$_{core}$ in the complex with Tim9wt and the monomeric reduced (R.Mia40$_{core}$) or oxidised forms of Mia40$_{core}$ (Ox.Mia40$_{core}$). The asterisk indicate unspecific reactions of the antibody.

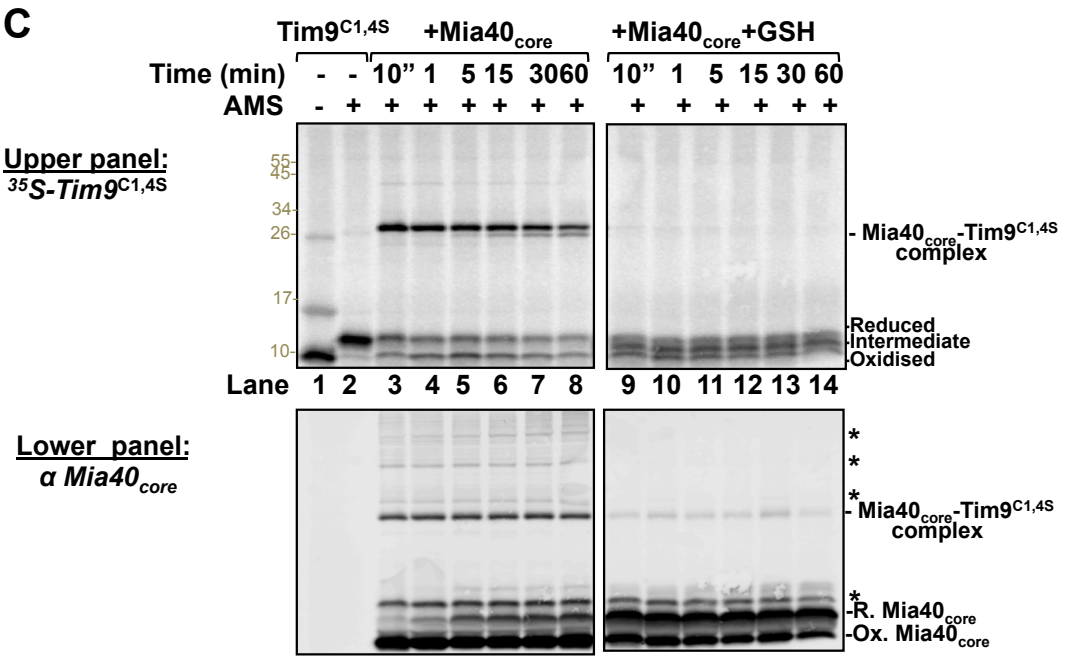

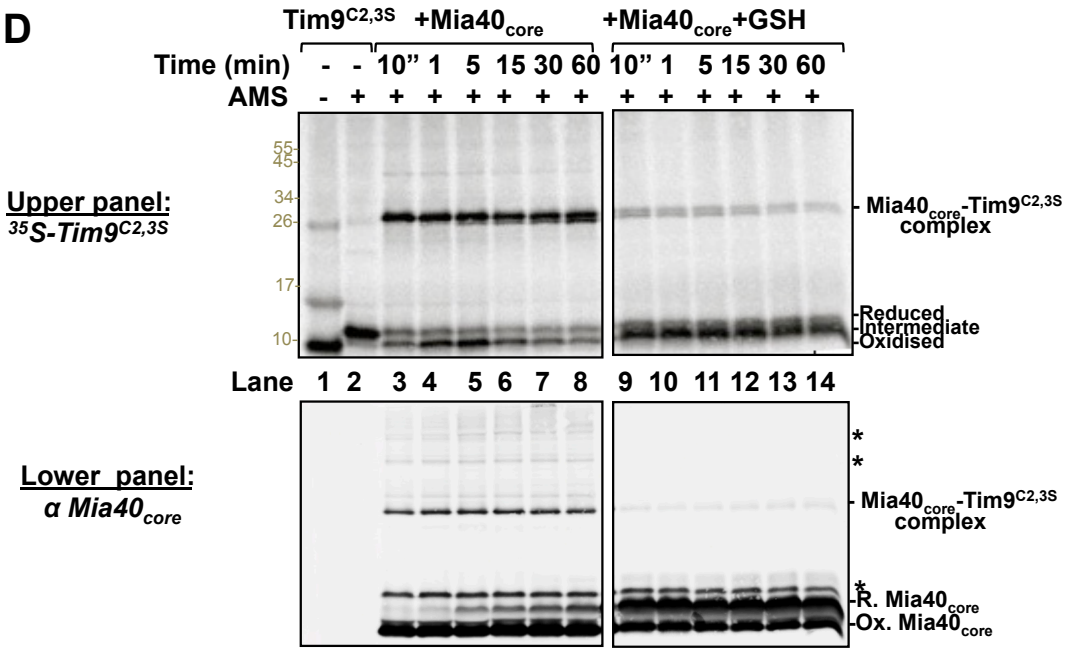

(C) and **(D)** as in **(B)** except that ^{35}S-Tim9^{C1,4S} and ^{35}S-Tim9^{C2,3S} were used, respectively.

4.4.5 Effects of GSH on the Mia40-Tim9 interaction during import

The above result showed that GSH might have a preference to break the disulphide between Mia40 and the 2nd or the 3rd cysteine of Tim9 rather than the disulphide between Mia40 and the 1st or the 4th cysteine of Tim9. To determine whether the same phenomenon occurs in mitochondria, a time course import of ^{35}S-Tim9wt or double cys-mutants of Tim9 into mitochondria that were pre-incubated with import buffer containing or not containing 10 mM GSH for 5 min was performed (Figure 4.18). At various time points, aliquots were removed and imports were stopped by trypsin treatment as described before. Mitochondria were then analysed using both non-reducing and reducing SDS-PAGE. The results showed that in the absence of GSH, Tim9^{C2,3S} formed a more durable complex with Mia40 than Tim9wt and Tim9^{C1,4S} (Figure 4.18, A lanes 7-9 vs 1-6). All these complexes dissociated to monomeric species under reducing conditions, confirming the disulphides-linked nature of the complex (Figure 4.18, A lanes 10-12). In the presence of GSH, the mixed disulphide Mia40-Tim9^{C2,3S} complex did not dissociate in comparison to both Mia40-Tim9^{C1,4S} and Mia40-Tim9wt complexes (Figure 4.18, B lanes 7-9 vs 3-5 and 4-6). This result is in line with the reconstituted systems shown in Figure 4.17, where GSH resolved all the Mia40-Tim9wt and Mia40-Tim9^{C1,4S} complexes, but not all the Mia40-Tim9^{C2,3S} complexes, suggesting that GSH may act either on certain cysteines or at specific times of the oxidative folding of Tim9.

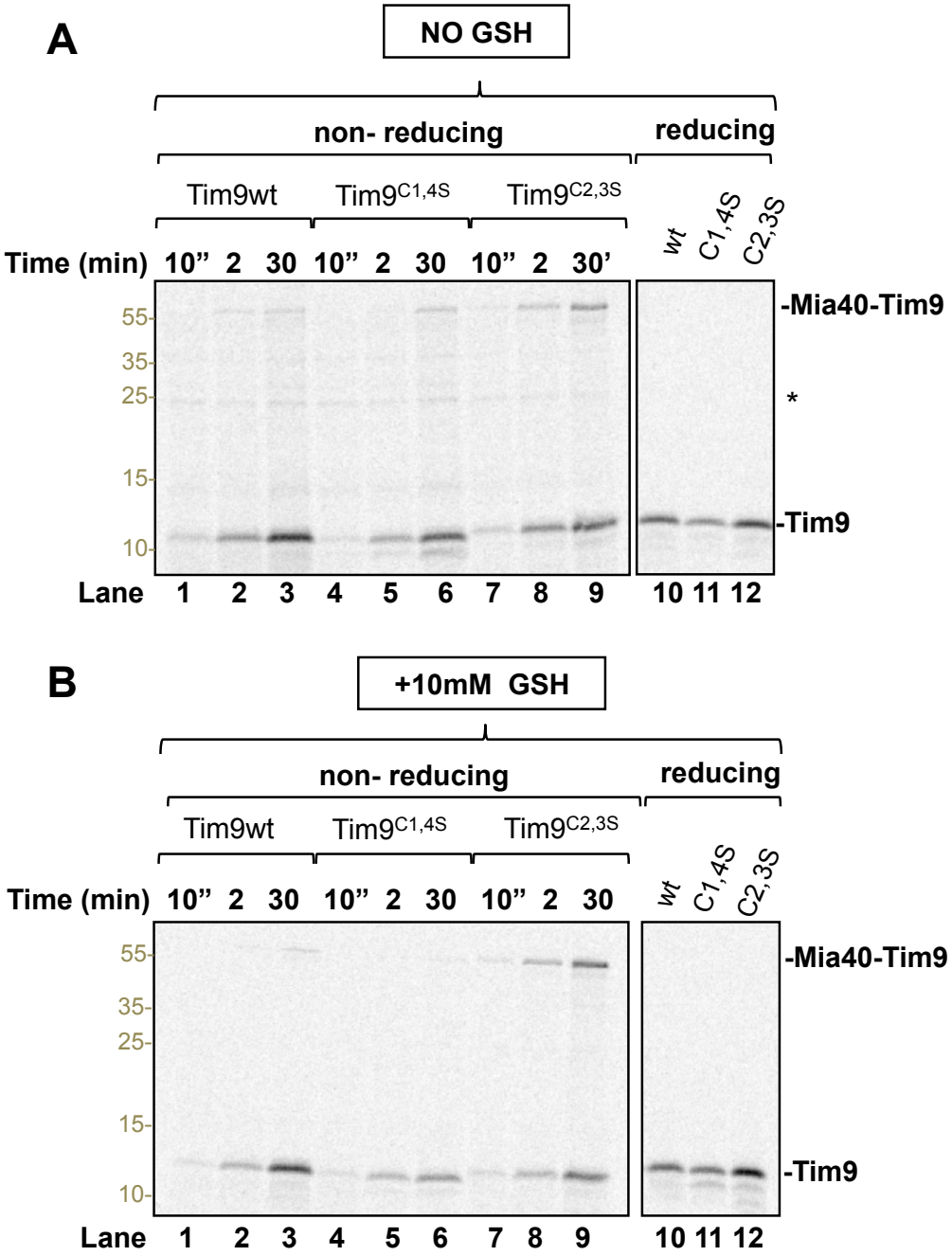

Figure 4.18 Effects of 10 mM GSH on the formation of Mia40-Tim9 complex in mitochondria.

Mitochondria were left untreated **(A)** or pre-incubated with 10 mM GSH **(B)**. After 5’ min, ^{35}S-Tim9wt, or ^{35}S-Tim9^{C1,4S}, or ^{35}S-Tim9^{C2,3S} were added to each import reaction and imports were carried out for various times. At the times indicated, aliquots were removed and treated with trypsin as before. Proteins were analyzed either by non-reducing (lanes 1-9) or reducing (lanes 10-12) SDS-PAGE and autoradiography. The asterisk indicates the presence of a putative trimeric Tim9 complex in the IMS.

4.5 Discussion

4.5.1 Mia40$_{core}$ can introduce both disulphide bonds in Tim9 and Tim10

Currently, it is still unclear how substrates of the MIA pathway undergo oxidative folding when they are imported into the IMS. The aims of this chapter were to investigate the mechanisms of oxidative folding of small Tims mediated by Mia40 both *in vitro* and *in organello*. Works described in this chapter showed *in vitro* that Tim9 and Tim10 can be fully oxidised by Mia40$_{core}$. This conclusion is based on the following observations: **(1)** Mia40$_{core}$ generated fully oxidised forms of both Tim9 and Tim10 (Figure 4.2); **(2)** the Mia40$_{core}$-dependent oxidative reaction of Tim9 is characterised by the formation of two disulphide-linked Mia40$_{core}$-substrate intermediates, named Complex I and Complex II, representing respectively Mia40$_{core}$ bound to a reduced substrate or to a single disulphide-bonded substrate (Figure 4.3); **(3)** the rate of Tim9 oxidation is dependent on the concentration of Mia40$_{core}$, being rapid in the presence of an excess amount of Mia40$_{core}$, or slow in the presence of nM concentrations of Mia40$_{core}$ (Figures 4.4 & 4.5).

In addition, following the oxidative folding of Tim9 driven by nM amounts of Mia40$_{core}$ (Figure 4.5), it was possible to dissect the Tim9 oxidative folding reaction into distinct steps (Figure 4.19):

Steps 1 and 2: Following binding of the MISS/ITS signal of Tim9 to the hydrophobic binding cleft of Mia40 (Banci *et al*, 2010) and formation of a mixed disulphide complex between Mia40 and Tim9 (Complex I), two different events can occur to complete the oxidation of Tim9:

3a step: The first intramolecular disulphide bond is introduced in Tim9 while in the complex with $Mia40_{core}$ either by molecular oxygen or by a currently unknown factor (e.g. Erv1). Based on the results presented in this chapter, the inner disulphide bond is most probably the first intramolecular disulphide bond to be introduced in Tim9. This is based on the observation that the Tim9 mutant lacking the inner cysteine pair was trapped in the complex with $Mia40_{core}$ longer than the mutant of Tim9 lacking the outer cysteine pair (Figure 4.6).

4a step: The second disulphide in Tim9 may be formed by nucleophilically attack of the remaining cysteine to the mixed disulphide releasing Tim9 in the fully oxidised state and reduced Mia40.

3b step: Alternatively, partially oxidised Tim9 is released from Complex I via nucleophilic attack by the reduced Cys of Mia40 to the mixed disulphide.

4b step: The second intramolecular disulphide bond in the partially folded substrate may be then introduced either by molecular oxygen or by the action of a second oxidised molecule of Mia40.

The ability of Mia40 to fully oxidise proteins *in vitro* was shown before for other substrates, such as yeast Cox19, human Cox17, yeast Tim10, and Atp23 (Bien *et al.*, 2010; Banci *et al.*, 2010; Weckbecker *et al.*, 2012). In a recent study, Banci *et al.* (2010) attributed to Mia40 the new function of a "chaperone with a foldase action", meaning that one molecule of Mia40 may be needed for the oxidation of the MIA substrates. By NMR analysis of the covalent human Cox17-Mia40 intermediate complex, Banci *et al.* (2010) showed that upon recognition of the ITS signal by Mia40 and formation of disulphide pairing, Mia40 induces the helical conformation in the ITS signal. This last event triggers

the nucleophilic attack of the second inner cysteine to the inter-molecular disulphide bond, and consequently the release of a half folded and oxidised substrate. Thus, they postulated that only the first intra-disulphide bond is dependent on Mia40, whereas the second may be dependent on the substrate, or on small oxidants (oxygen or metals), and/or on different cellular conditions.

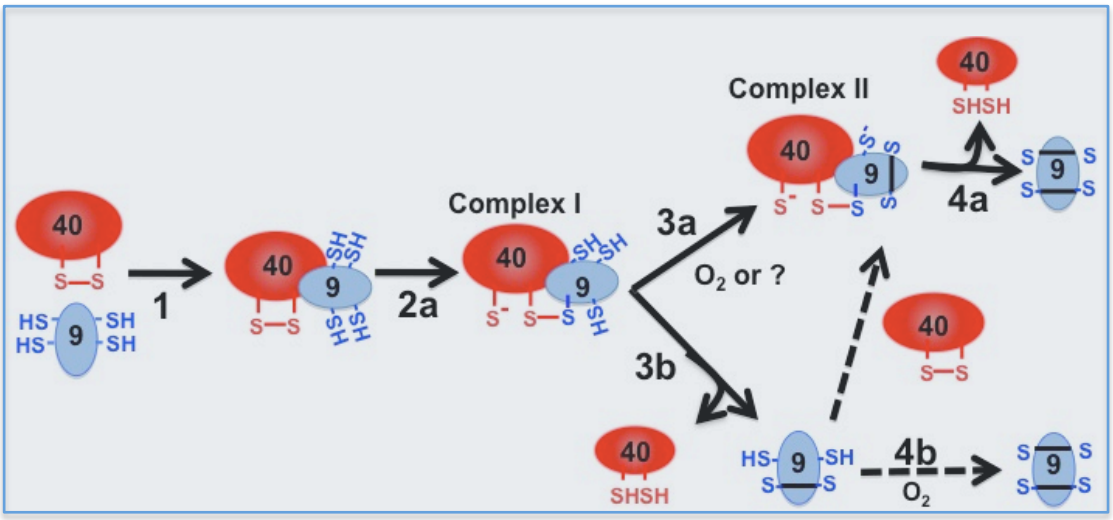

Fig. 4.19. Model for a possible mechanism of Tim9 oxidation in the presence of Mia40$_{core}$.
Binding of the MISS/ITS signal of Tim9 to the hydrophobic cleft of Mia40 (step 1) is followed by formation of a mixed disulphide complex between Mia40$_{core}$ and Tim9 (Complex I, step 2). Then, there are two alternative pathways (a, b) for formation of the fully oxidised Tim9.
a: the first intramolecular disulphide bond is introduced in Tim9 while in complex with Mia40$_{core}$ (Complex II) by molecular oxygen or a currently unknown factor X (step 3a). Then, the second disulphide is formed by nucleophilic attack of the remaining cysteine to the mixed disulphide releasing Tim9 in the fully oxidised state (step 4).
b: Partially oxidised Tim9 is released from the complex I via nucleophilic attack by the reduced Cys of Mia40$_{core}$ to the mixed disulphide. The 2nd intramolecular disulphide in Tim9 may be introduced either by O_2 or by the action of a second molecule of oxidised Mia40.

The *in vitro* reconstitution assays presented in this study have been performed under aerobic conditions. Thus, molecular oxygen is most probably the oxidant for Tim9 both while in the Complex I with Mia40 and after being released from Mia40 as partially folded intermediate. The time course of the oxidative folding of Tim9 in the absence of Mia40$_{core}$ showed that the first disulphide bond in

Tim9 can be result of air oxidation, whereas the formation of the second intramolecular disulphide bonds may depend on a catalyst such as Mia40, as Tim9 underwent complete oxidative folding only in the presence of $Mia40_{core}$ (Figure 4.2).

However, recent studies raised a possibility that Erv1 can also play a role in the Mia40-mediated oxidative folding of Tim9. Analysis of the conditional *erv1* mutant showed that the MIA substrates were trapped at the Mia40-bound stage and failed to complete oxidative folding (Rissler *et al*., 2005; Stojanoski *et al.,* 2008). A first ternary complex involving Mia40, Tim9 and Erv1 has been detected by a combination of *in organello* import assay followed by immunoprecipitation (Stojanoski *et al.,* 2008b). More recently other studies revealed the formation of such a ternary complex during *in vitro* import assay of the novel twin CX_9C-containing MIA substrate Cmc1, Tim10, Cox17, and other MIA substrates such as Pet191 and Mic17 (Bourens *et al.,* 2012, Böttinger *et al.,* 2012). Thus, it cannot exclude that *in vivo* Erv1 may promote disulphide transfer to Mia40-bound Tim9, although how exactly a total of four electrons are transferred in consecutive steps from the substrate to Erv1 is still unknown. Another possibility could be that Erv1 may be the direct donor of the second disulphide bond in the substrate that is linked to Mia40.

4.5.2 $Mia40_{core}$ interacts *in vitro* with all cysteine mutants of Tim9

The *in vitro* results showed that $Mia40_{core}$ was capable of interacting and forming a stable complex with both double Cys-mutants of Tim9 and Tim10 (Figure 4.3 and 4.7). By comparing the rate of oxidative folding, the two cys-

double mutants of Tim9 are oxidised by $Mia40_{core}$ slower than Tim9wt (Figure 4.6 vs Figure 4.2), suggesting that $Mia40_{core}$ prefers to oxidise and release the substrate when all cysteines are present.

In addition, as for the WT, the stability of the complex between $Mia40_{core}$ and the mutants was dependent on the concentration of $Mia40_{core}$; at low concentrations of $Mia40_{core}$, the $Tim9^{C2,3S}$ variant formed a complex with $Mia40_{core}$ which persisted for more than 30 min, whilst $Tim9^{C1,4S}$ was released from $Mia40_{core}$ within 2 min. Similarly, the *in organello* assays showed that the $Tim9^{C2,3S}$ mutant accumulated as intermediate with Mia40, whereas the $Tim9^{C1,4S}$ mutant did not (Figure 4.10). This suggests that Mia40 may be prone to release a substrate that contains at least the inner intra-disulphide bond and that the inner intra-disulphide bond is formed before the generation of the outer one.

Bien *et al.* (2010) obtained similar results by using the $Cox19^{C1,4S}$ and $Cox19^{C2,3S}$ mutants. Their data showed that the $Cox19^{C1,4S}$ mutant was fully oxidised by Mia40 and released from the complex within the 1^{st} min of the time course, whilst $Cox19^{C2,3S}$ showed poor oxidative folding and formed a stable complex with Mia40 that persisted throughout the time course. Therefore, they proposed that the outer disulphide bond of Cox19 may be formed only after the generation of the inner disulphide bond.

The results also revealed that $Mia40_{core}$ formed a disulphide bond with all the triple cys-mutants of Tim9, although to less extent with the mutant having C3 only (Figure 4.8). This suggests that *in vitro* Mia40 can interact with at least C1, C2 and C4 cysteines of the twin CX_3C motif without regarding to their proximity

to the MISS/ITS signal. However, when imported into mitochondria, only the triple cysteine mutant having C1 was able to interact with Mia40 and to be imported into mitochondria, confirming that C1 is required for mitochondrial import and interaction with Mia40 (Figure 4.11). This suggests that for an efficient mitochondrial import, other factors may influence the interaction of Tim9 with Mia40, such as the MISS/ITS signal and/or the orientation with which Tim9 crosses the OM.

4.5.3 GSH resolves the complex between $Mia40_{core}$ and its substrates

GSH is a ubiquitous low-molecular-weight molecule that, due to the presence of its cysteine, plays an important role in the thiol-disulphide redox regulation. GSH and its oxidised counterpart (GSSG) constitute the major redox buffer in the cells. Glutathione is exclusively synthesised in the cytosol and distributed to intracellular organelles, such as nucleus, ER, the mitochondrial matrix and IMS. Mitochondria do not contain the necessary enzymes to synthesise GSH, and the mitochondrial GSH arises from the cytosolic pool. Specifically, porin channels of the mitochondrial OM allow free exchange of GSH and GSSG between the IMS and the cytosol, whilst the matrix GSH pool is maintained by active transport mediated by ATP-dependent carriers located in the IM (Griffith and Meister, 1985; Kaplowitz *et al*., 1996; Chen and Lash, 1998).

The concentration and the redox potentials of mitochondrial GSH have been determined. In isolated yeast mitochondria the concentration of GSH in the IMS is in the range of the cytosolic one (10-13 mM; Østergaard *et al.,* 2004).

The redox potential of GSH in the IMS has been estimated to be E_{GSH}=-255±3mV, more oxidising than the redox potential of the cytosolic and mitochondrial matrix redox potentials (E_{GSH}=-286±5mV and E_{GSH}=-296±5mV, respectively; Hu *et al.,* 2008).

It has been observed that physiological concentrations of GSH stimulated mitochondrial import of the substrates of the MIA machinery (Mesecke *et al.,* 2005; Bien *et al.,* 2010; Weckbecker *et al.,* 2012). It was proposed that GSH prevents the formation of and/or removes long-lived kinetically trapped intermediates formed between Mia40 and its substrates (Bien *et al.,* 2010).

The *in vitro* results presented in this chapter showed that: **(1)** GSH resolved the $Mia40_{core}$-Tim9wt or $Mia40_{core}$-Cox19 complexes rapidly (figures 4.15 and 4.16); **(2)** GSH dissociated efficiently the $Mia40_{core}$-Tim9wt or $Mia40_{core}$-$Tim9^{C1,4S}$ complexes and less efficiently the $Mia40_{core}$-$Tim9^{C2,3S}$ complex (Figures 4.17 and 4.18). The reason of this may be because GSH may prefer to interact with the Mia40-Tim9 intermediate where the inner disulphide bond is going to be introduced by Mia40 rather than with Mia40-$Tim9^{C2,3S}$, where the inner disulphide bond cannot be formed. So one might conclude that GSH might act by improving the release of Tim9 from Mia40, but only after the generation of the first disulphide bond, presumably the inner disulphide bond. This could also explain why GSH increases the Tim9 mitochondrial import: in accelerating the release cascade of the substrate from Mia40, more Mia40 results to be free for being re-oxidised by Erv1, and thus participating to a new interaction with incoming substrate.

5. Results and Discussion III: THE ROLE OF THE CYTOSOLIC THIOREDOXIN SYSTEM IN THE BIOGENESIS OF SMALL TIMS PROTEINS

5.1 Introduction

The aims of this chapter are to investigate whether or not the cytosolic Trx and Grx systems play a role in the biogenesis of small Tim proteins. Small Tim proteins and many other MIA substrates are imported into mitochondria in a cys-reduced form. The oxidised precursors are import-incompetent (Lu and Woodburn, 2005; Mesecke *et al*., 2005; Morgan and Lu, 2008). The oxidised small Tims are thermodynamically stable under the cellular glutathione conditions. These proteins have a redox potential of -0.31 V to -0.33 V, which is more negative than that of the glutathione redox conditions in both the cytosol and IMS (Woodburn and Lu, 2005; Morgan and Lu, 2008; Tienson *et al.,* 2009). The redox stability of small Tims is consistent with their oxidised state in the IMS, but not with their reduced state in the cytosol. Hence, how these redox-sensitive IMS precursors are maintained in an import-competent form in the cytosol is still unknown. It could be that cytosolic factors are required to maintain these precursors in an import-competent form before their import into mitochondria.

The ubiquitous thioredoxin (Trx) and the glutaredoxin (Grx) oxidoreductases may represent possible cytosolic factors for preventing cytosolic oxidation of small Tim proteins. The yeast *S. cerevisiae* contains two cytosolic Trx homologues (Trx1 and Trx2) and the two classical dithiol Grx homologues (Grx1 and Grx2). A main function of these enzymes is to reduce disulphide bonds in

their substrate proteins using electrons donated by NADPH. Oxidised Trx is reduced directly by NADPH and the thioredoxin reductase (Trr), whereas Grx is reduced by GSH, using electrons donated by NADPH via glutathione reductase (Glr1).

Part I of this chapter includes the *in vivo* studies: yeast strains lacking the TRX1 and TRX2 genes (*trx1 trx2*), or GRX1 and GRX2 genes (*grx1 grx2*) were used. Firstly, to determine if the cytosolic Trx and Grx systems were required for mitochondrial function and/or activity, cultures of WT, *trx1 trx2* and *grx1 grx2* strains were grown both under fermentative (YPD), or respiratory (YPEG) conditions. Then, mitochondrial proteins levels were analysed using whole cell extracts and mitochondria isolated from WT, *trx1 trx2* and *grx1 grx2* cells, respectively.

Part II of this chapter includes the *in vitro* studies: the effects of the Trx1 system on mitochondrial import of small Tims were investigated. For this purpose, purified proteins of the Trx1 system, including Trx1 and Trr1, were used in the mitochondrial import analysis of ^{35}S-Tim9 and ^{35}S-Tim10. At the same time, the analysis of the effects of the Trx1 system on the redox state of unimported small Tims was carried out by AMS thiol-group modification assay. In addition, the investigation of the effects of the Trx1 system was extended to the mitochondrial import of Cox19, a twin CX_9C substrate of Mia40. Finally, the effects of the Trx1 system on precursors proteins destined to the other three mitochondrial sub-compartments (OM, IM and matrix) were assayed to confirm that the observed Trx1-mediated positive effects are unique to the import of MIA substrates.

5.2 PART I: *in vivo* analysis

5.2.1 Effects of the Trx and Grx systems on cell growth under fermentative and respiratory conditions

To determine whether the cytosolic Trx systems are required for mitochondrial function, the growth of *trr1*, *trx1 trx2* and *trr1 trx1 trx2* yeast strains were investigated under fermentative (YPD), or respiratory (YPEG) conditions. All yeast strains were inoculated to the same initial starting density A_{600} of 0.2 in YPD, or YPEG liquid media and their growths were monitored by A_{600} (Figure 5.1 A). When grown in YPD all mutant strains displayed relatively similar growth kinetics to the WT, although the *trr1* mutant grew slower. However, when grown in YPEG, all mutants displayed a longer lag phase and a lower final cell yield than the WT (Figure 5.1 B). Thus, the results showed that the cytosolic Trx system might become important during respiratory growth conditions, and that the Grx system may be not sufficient alone for the growth in respiratory medium.

To further support the above result, the effects of the loss of the two cytosolic Trxs (Trx1 and Trx2), or the two cytosolic Grxs (Grx1 and Grx2) on growth in YPD and YPEG conditions were analysed using the spot test. Cultures of WT, *trx1 trx2* and *grx1 grx2* strains were first grown to stationary phase in YPD for 48h at 30°C, and then adjusted to A_{600} of 1, 0.1, 0.01 and 0.001 before spotting onto YPD, or YPEG plates (Figure 5.2 A). The results showed that, although the *trx1 trx2* mutant grows somewhat slower than the WT and *grx1 grx2* mutant under fermentative conditions, it is particularly inhibited for growth under respiratory conditions. In contrast, the *grx1 grx2* mutant grew comparably to the

WT under both growth conditions. Same results were obtained when using the CY302 a-mating type strain deleted for TRX1 and TRX2 (Figure 5.2 B).

Taken together, these results showed that the cytosolic Trx systems are necessary for maintenance of normal growth under respiratory conditions, suggesting that they might be required for preserving functional mitochondria and/or facilitating their biogenesis.

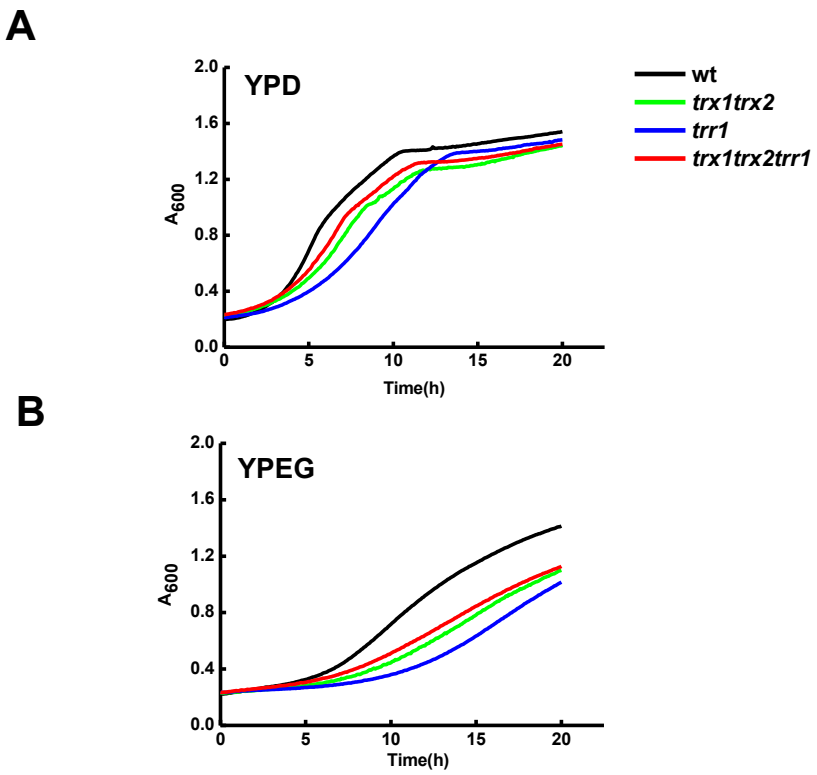

Figure 5.1 Growth of the thioredoxin system mutant cells in fermentative or respiratory media.

WT cells, and *trr1*, *trx1 trx2* and *trr1 trx1 trx2* mutants cells were inoculated to the same initial cell density (A_{600}=0.2) at 30°C in liquid YPD medium **(A)** or YPEG **(B)**, and growth was monitored by measuring the A_{600}.

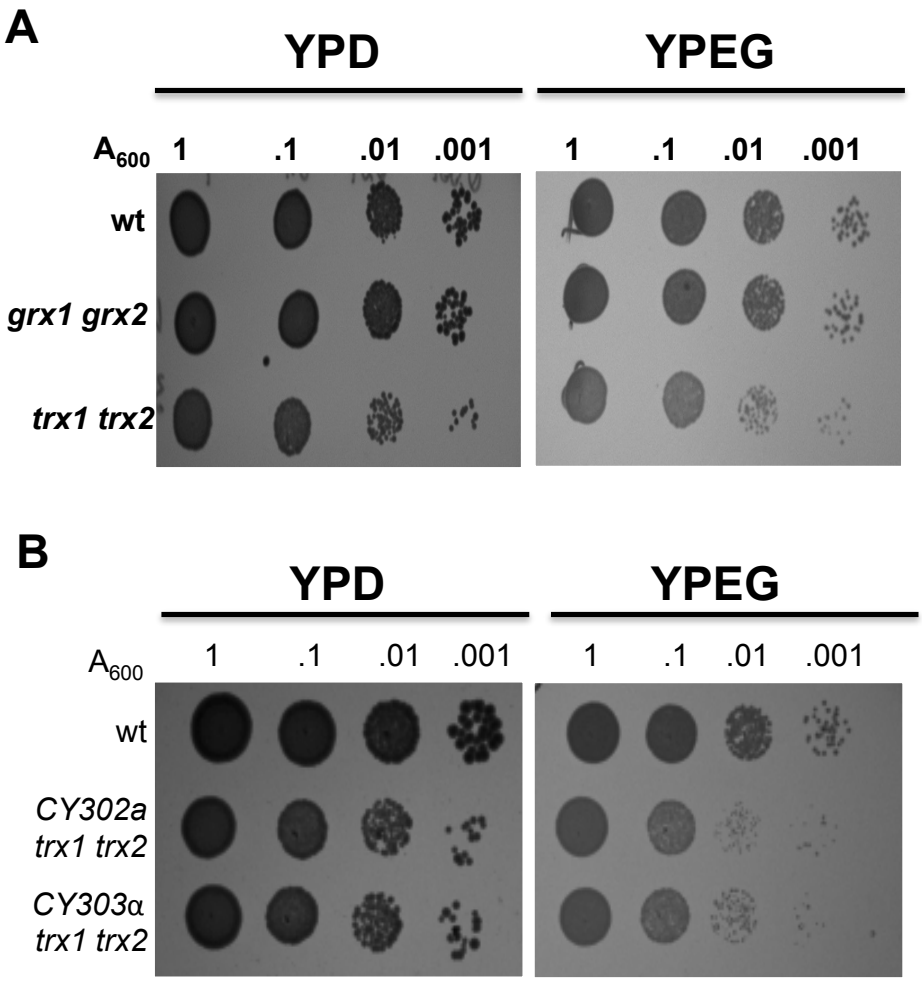

Figure 5.2 The effects of the TRXs and GRXs deletions on yeast growth under fermentative and respiratory conditions.

(A) Cultures of WT, *grx1 grx2*, and *trx1 trx2* cells were grown at 30°C in YPD to stationary phase, and the A_{600} was adjusted to 1, 0.1, 0.01 and 0.001 before strains were spotted onto fermentative (YPD) or respiratory (YPEG) plates. Growth was monitored after 3 days of incubation at 30°C.
(B) As in **(A)** except that CY302 a- and CY303 α-mating type strains carrying the deletions for TRX1 and TRX2 were used.

5.2.2 Effects of the Trx and Grx systems on mitochondrial biogenesis

To assess the function of the Trx systems in the biogenesis of mitochondrial proteins, the level of protein expression was examined. The effects of the deletions of GRX1 and GRX2 on levels of mitochondrial proteins were also assessed for comparison.

Cultures of WT, *grx1 grx2* and *trx1 trx2* mutants were grown to early exponential phase at 30°C in YPD, or YPEG. Subsequently, cells were harvested and lysed. The cellular extracts from each strain were separated on SDS-PAGE and analysed by western blotting. For each strain, three different amounts of protein (2.5 ug, 5 ug and 12.5 ug) were used (Figure 5.3). Whilst the antibodies against Trx and Grx confirmed the deletion of these proteins in the *trx1 trx2* and *grx1 grx2* mutants, respectively, the western blot against the cytosolic marker glucose-6-phosphate dehydrogenase (6-GPD) confirmed that the same total amount of protein was loaded. The results from the cellular extracts prepared from cells grown in YPD showed that there were no obvious difference in the levels of the mitochondrial proteins (Tom20 for the OM, Mia40 for the IM, Tim9, Tim10 and Cytb2 for the IMS, and mtHsp70 for the matrix) (Figure 5.3 A), whereas Tim9 and Tim10 levels seemed to be slightly decreased in the *trx1 trx2* mutants grown in YPEG in comparison to the WT and *grx1 grx2* cells (Figure 5.3 B).

Similar results were obtained, when analysing by western blot the mitochondrial protein levels in mitochondria purified from lactate-grown WT, *grx1 grx2* and *trx1 trx2* cells (Figure 5.4).

Thus, all together these results showed that there was no obvious difference in mitochondrial protein levels in cells grown either in fermentative (YPD), or respiratory (YPEG and LM) media, therefore the same analysis was performed under more stressed growth conditions, as detailed in the following section.

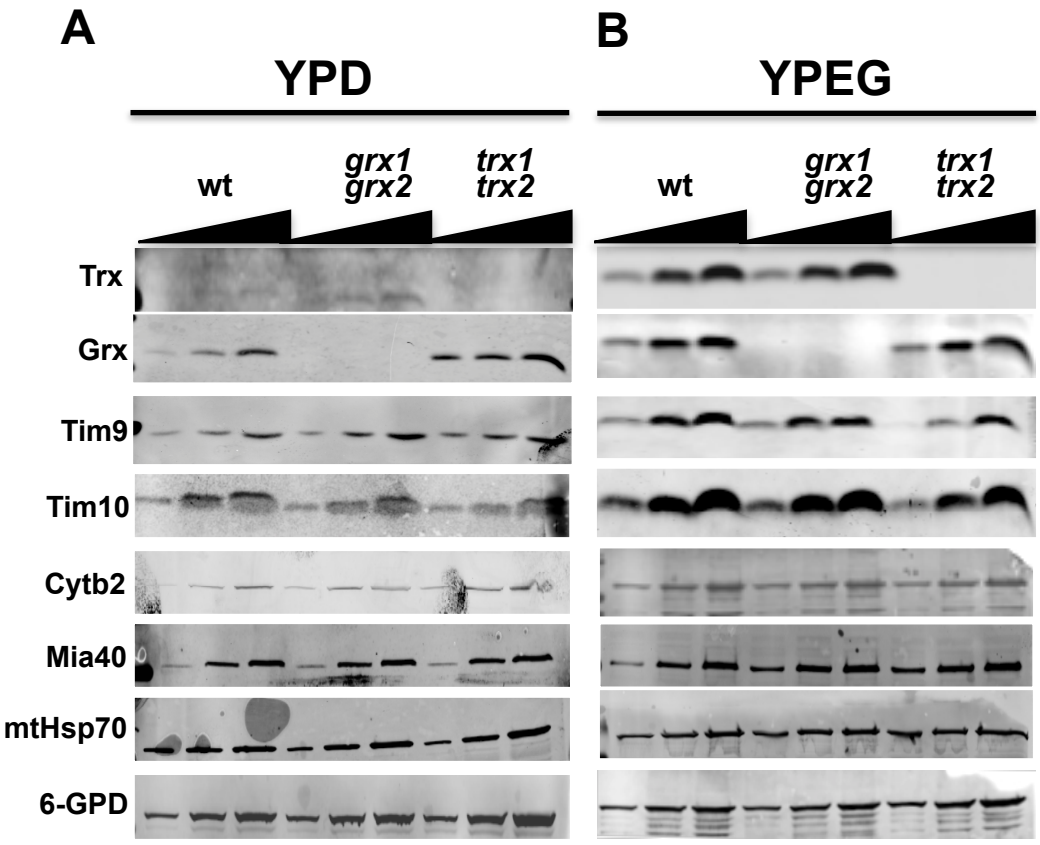

Figure 5.3 Effects of the TRXs and GRX deletions on protein expression in whole cell extracts.

Cellular extracts were prepared from cultures of WT, *grx1 grx2*, and *trx1 trx2* cells grown in YPD **(A)** or YPEG **(B)**. For each strain, 2.5 ug, 5 ug and 12.5 ug of protein were resolved by reducing SDS-PAGE and analysed by western blotting. The immunoblotting with the Trx and Grx antibodies confirmed the deletion of the Trxs and Grxs proteins in the respective strains, whereas the western blot against the cytosolic marker 6-GPD showed that the same amount of protein was loaded. The endogenous levels of the OM (Tom20), the IMS (Tim9, Tim10 and Cytb2), the IM (Mia40), and the matrix (mtHsp70) proteins were analysed.

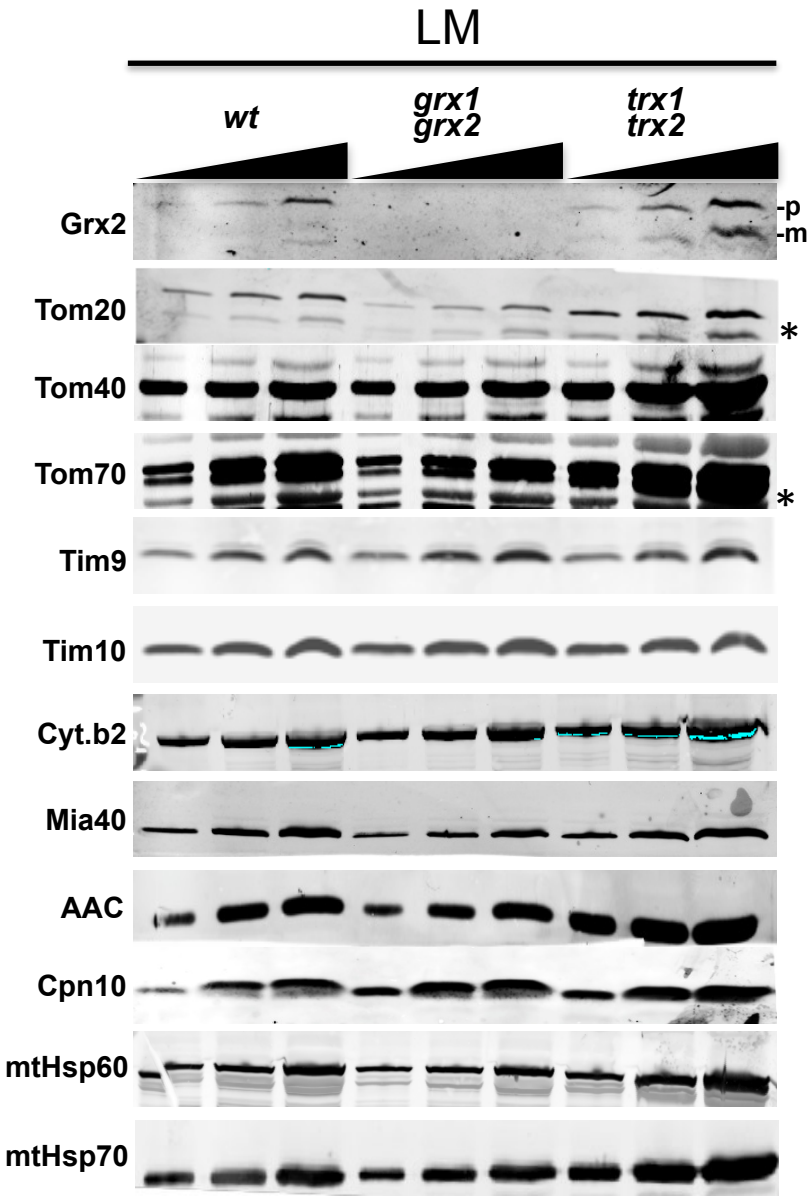

Figure 5.4 Expression levels of mitochondrial proteins in mitochondria isolated from lactate-grown cells.

Mitochondria were isolated from WT, *grx1 grx2* and *trx1 trx2* cells grown in LM. For each strain, 25 ug, 50 ug and 100 ug of proteins were analysed by reducing SDS-PAGE and western blot. The endogenous levels of the OM (Tom20, Tom40 and Tom70), the IMS (Tim9, Tim10 and Cytb2), the IM (Mia40 and AAC), and the matrix (mtHsp70, mtHsp60 and Cpn10) proteins were analysed. The OM- (p) and matrix- (m) located Grx2 isoforms are indicated. The asterisks indicate unspecific reaction of the Tom20 and Tom70 antibodies.

5.2.3 Effects of the Trx systems on mitochondrial protein levels under more stressed conditions

To test the hypothesis that the cytosolic Trx systems play a role in the biogenesis of small Tim proteins, the levels of mitochondrial proteins under more stressed growth conditions were analysed. To induce stress, WT and *trx1 trx2* cells were grown in YPD medium to exponential phase followed by a medium shift to respiratory YPEG for six hours, and then mitochondria were isolated (the shift will be indicated as "YPD➔YPEG" in the text). The decision to isolate mitochondria from cells grown first in YPD, and then shifted to YPEG is based on the fact that the growth on fermentable carbon source (YPD) suppresses mitochondrial function, whereas the subsequent switch to non-fermentable carbon source (YPEG) strongly boosts respiration, increases the mitochondrial mass and generally enhances the mitochondrial function (Madeo et al., 2009). Therefore, if the cytosolic Trx systems are involved in small Tim biogenesis, small Tim levels in the *trx1 trx2* mutant should be decreased in comparison to the WT.

For each type of mitochondria, three different amounts of proteins (25 ug, 50 ug, and 75 ug) were analysed (Figure 5.5 A). The results showed clearly that the steady-state levels of small Tim proteins (Tim9, Tim10 and Tim13) were decreased in the *trx1 trx2* mitochondria, whereas those of the IMS protein but not MIA substrate cyt.b2, the OM protein Tom40, the IM protein ACC and the matrix enzyme malate-dehydrogenase (MDH) were not affected. The same mitochondrial isolation and western blotting experiment were performed three times, and the levels of small Tim proteins of the mutant strain were statistically lower than that of the WT strain ($p<0.05$, Figure 5.5 B).

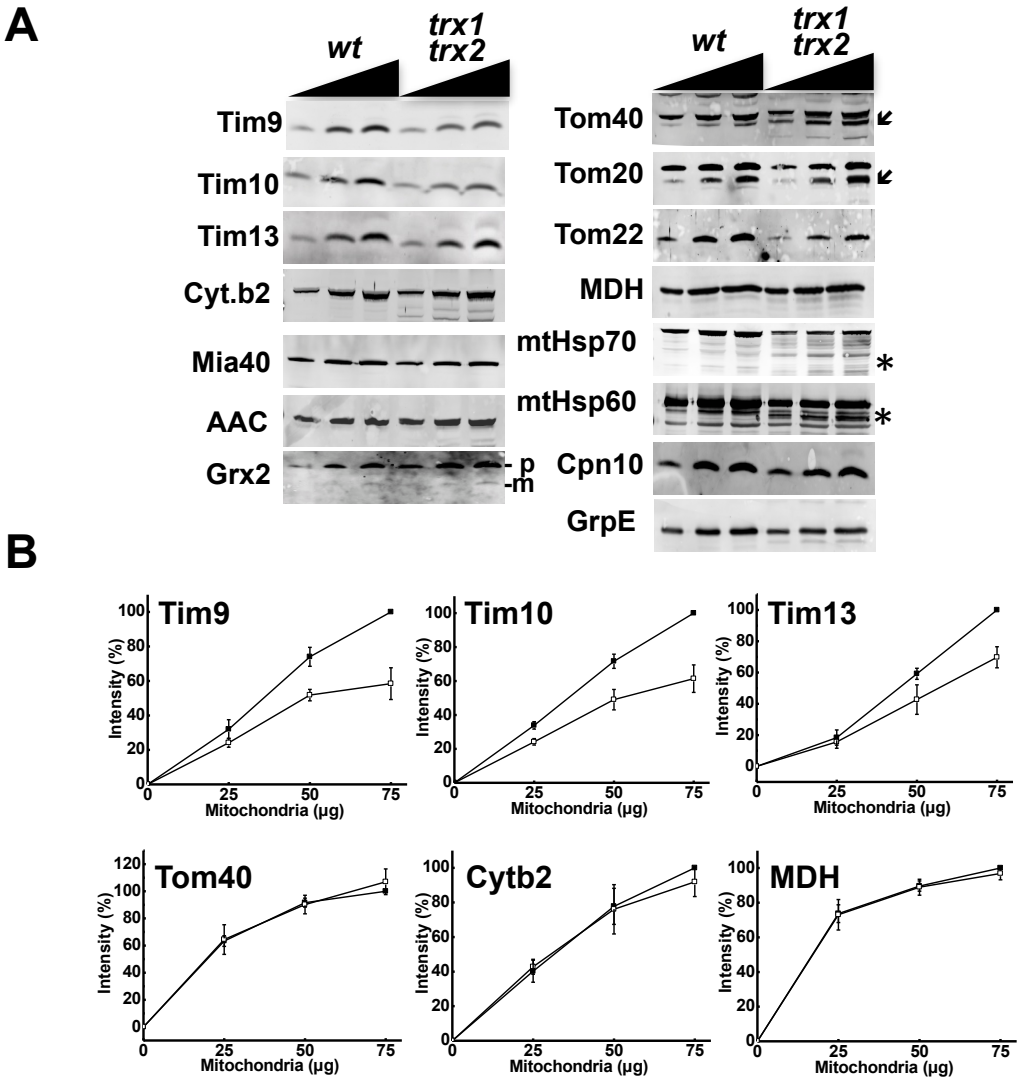

Figure 5.5 Expression levels of proteins in mitochondria isolated from YPD➔YPEG WT and *trx1 trx2* cells.

(A) WT and *trx1 trx2* mutant cells were grown in YPD to A_{600} of 10 and then shifted to YPEG for 6 h. Then, mitochondria were purified and analysed using antibodies against the IMS (Tim9, Tim10, Tim13 and Cytb2), the IM (Mia40 and AAC), Grx2 and OM (Tom40, Tom22 and Tom20), and matrix (MDH, mtHsp70, mtHsp60, Cpn10, GrpE) proteins. The asterisks indicate presumptive degraded fractions of proteins, whereas the arrowheads indicates unspecific reactions of the Tom22 and Tom40 antibodies. The OM-(p) and matrix- (m) located Grx2 isoforms are indicated.
(B) Quantification of protein levels in mitochondria isolated from WT (solid squares) and *trx1 trx2* (open squares) cells as described in **A**. The levels of small Tim proteins were significantly different (by Student t-test: Tim10 $p<0.05$ at all points, Tim9 and Tim13 $p< 0.05$ at 50 and 75 ug), and not significant for the marker proteins Tom40, Cytb2 and MDH. Error bar represent S.E. (n=3).

Interestingly, the levels of Mia40, the OM proteins Tom20 and Tom22 and the matrix chaperones mtHsp60, mtHsp70, Cpn10 and GrpE seem to be reduced as well. The reason for this decrease is unclear.

In contrast, the levels of the matrix enzyme MDH were similar both in WT and *trx1 trx2* mitochondria. This is in agreement with a study published by Steinmetz et al. (2002), which showed that MDH is one of the enzymes of the Kreb's cycle not to be affected by respiratory growth (Steinmetz et al., 2002). Particularly interesting is the fact that Grx2 levels are slightly increased in *trx1 trx2* mitochondria, although the majority of Grx2 seems to be OM-located (compare to the distribution of Grx2 between the OM and matrix in Figure 5.4 and Figure 5.5 B).

Overall, this analysis provides the *in vivo* evidence that the cytosolic Trx systems are involved in facilitating the biogenesis of small Tim proteins.

5.2.4 Redox state of Mia40 in the WT and *trx1 trx2* mutant strains

The results above showed that following the YPD➔YPEG shift, the mitochondrial steady-state levels of the small Tims were decreased in *trx1 trx2* mitochondria. To exclude that such defect is due to a variation of the IMS redox conditions (i.e. the redox state of the Mia40/Erv1 machinery), the redox state of Mia40 both of WT and *trx1 trx2* mitochondria was analysed using gel shift assays (Figure 5.6). The same preparations of mitochondria purified from the YPD➔YPEG shifted cells were either untreated, or treated with 20 mM of NEM. Samples were then resolved by non-reducing SDS-PAGE and analysed by western blotting with Mia40 antibody (Figure 5.6 A). The results showed that

Mia40 existed as a mixture of partially reduced and oxidised forms both in WT and *trx1 trx2* mitochondria (Figure 5.6 A, lane 3-6).

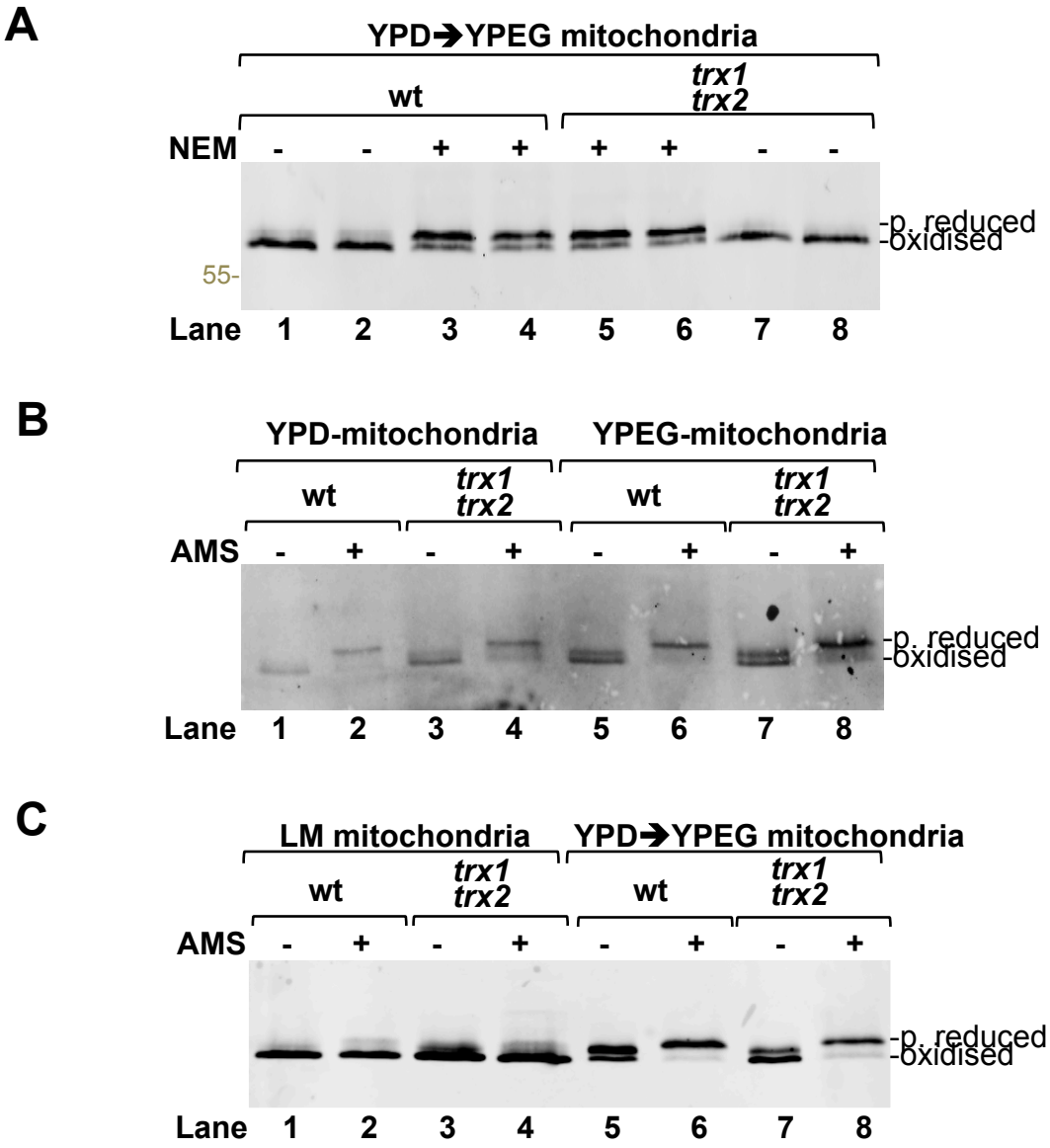

Figure 5.6 Mia40 redox state in WT and *trx1 trx2* mitochondria.

(A) Redox state of Mia40 in WT (lanes 1-4) and t*rx1 trx2* (lanes 5-8) mitochondria isolated from cells grown under YPD➔YPEG conditions. The partially reduced (p. reduced) and oxidised forms of Mia40 are indicated.
(B) The redox state of Mia40 of WT and *trx1 trx2* mitochondria isolated from cells grown in YPD (lanes 1-4) or YPEG (lanes 5-8) was analysed.
(C) The redox state of Mia40 of WT and *trx1 trx2* mitochondria isolated from cells grown in LM (lanes 1-4) or in YPD➔YPEG conditions (lanes 5-8) was analysed on the same gel.

The same results were obtained when using WT and *trx1 trx2* mitochondria isolated from either YPD-, or YPEG-grown cells (Figure 5.6 B), confirming that the Mia40 redox state in the mutant is similar to that of the WT at least at these tested growth conditions.

Hence, the lack of both Trx enzymes and the YPD➔YPEG shift did not influence the Mia40 redox state.

Previous studies reported that Mia40 existed mainly as oxidised form, at least in mitochondria isolated from lactate medium cells (Mesecke et al., 2005; Terziyska, et al., 2008). Thus, as a control of the above results, the Mia40 redox state of the same preparations of WT and *trx1 trx2* mitochondria was analysed on the same gel with the Mia40 redox state of WT and *trx1 trx2* mitochondria purified from cells grown in LM (Figure 5.6 C).

The results confirmed that Mia40 is almost reduced in both WT and *trx1 trx2* mitochondria isolated from YPD➔YPEG-grown cells, whereas it is mainly oxidised in both WT and *trx1 trx2* mitochondria isolated from LM-grown cells (Figure 5.6 C, lanes 1-4 vs 5-8).

Thus, it seems that under the YPD➔YPEG growth conditions the majority of Mia40 existed as partially reduced molecules. In addition, this result suggests that the fraction of oxidised Mia40 may be enough to import small Tims, as both WT and *trx1 trx2* mitochondria contain endogenous levels of small Tims. Thus, the decreased levels of small Tim levels observed in the *trx1 trx2* mitochondria are not due to a change towards a more reduced form of Mia40, but possibly to the lack of the cytosolic Trx systems.

5.3 PART II: *in vitro* analysis

5.3.1 Effects of the Trx1 system on the mitochondrial import of small Tim proteins

The *in vivo* studies shown in the previous sections demonstrated that the cytosolic Trx systems are important for the biogenesis of small Tim proteins. To verify whether the Trx1 system has an affect on the mitochondrial import of small Tims, mitochondrial import of ^{35}S-Tim9 in the presence or in the absence of the purified components of the Trx1 system were performed. Prior import WT mitochondria were incubated in import buffer in the absence, or in the presence of the Trx1 system components for 20 minutes at 25°C. Subsequently, ^{35}S-Tim9 was added to each import reaction and imports were carried out for 30 minutes. Following import, reactions were treated with trypsin to remove the unimported material, and mitochondrial import was analysed by reducing SDS-PAGE (Figure 5.7).

The results revealed that in the presence of the Trx1 system (Figure 5.7 A, lane 2) Tim9 import level was at least triple in comparison to the control (Figure 5.7 A, lane 1). A partial Trx1 system (without Trx1, or Trr1) slightly enhanced the import level in comparison to the control, but not as efficiently as the full system (Figure 5.7 A, lanes 3 and 4). It should be noted that small amounts of the redoxin components might be present in the rabbit reticulocyte lysate; however, the addition of the purified yeast system clearly increased import (Figure 5.7 A, lane 2 vs 1). The partial system lacking only NADPH did not increase the import levels at all in comparison to the control (Figure 5.7 A, lane 5), suggesting that NADPH is essential for the activity of the Trx1 system.

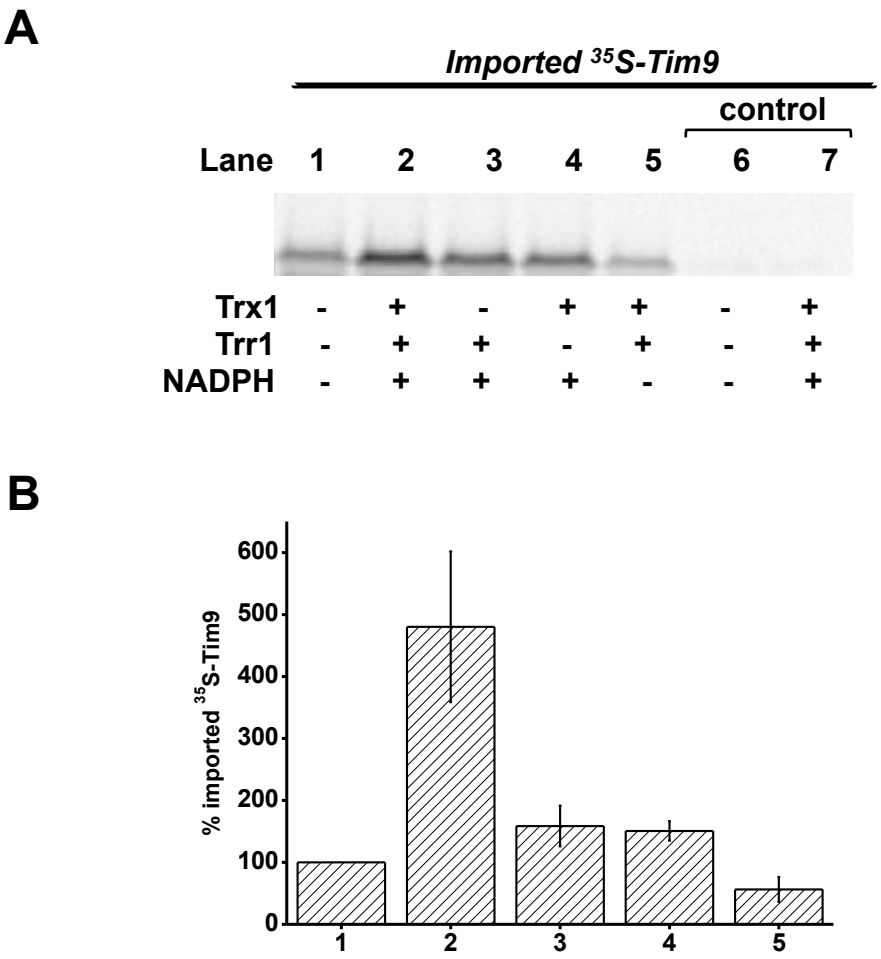

Figure 5.7 Effects of the Trx1 system on Tim9 import.

(A) Prior import mitochondria were incubated with import buffer in the absence or in the presence of the purified Trx system as indicated at 25°C for 20 min. Subsequently, ^{35}S-Tim9 was imported for 30 min. Following import, samples were trypsin treated as usual for the analysis of imported Tim9. As a control for the tryptic proteolysis: after import mitochondria were solubilized with digitonin buffer before the tryptic digestion (lanes 6 and 7). Samples were separated by reducing SDS-PAGE and analyzed by autoradiography.
(B) The amount of Tim9 imported as described in **A** was quantified by densitometry. The level of imported Tim9 in the absence of the Trx1 system was set as 100%. The average and the deviation standard were obtained from three independent experiments.

Lanes 6 and 7 are the controls where the mitochondria were solubilised with digitonin before trypsin treatment, and show that all bound and imported material were digested. This indicates that complete import has occurred in the other lanes. This finding thus provides *in organello* evidence that the Trx1 system facilitates Tim9 import into mitochondria. To confirm the above conclusion, a Tim9 time course import experiment was performed in the presence, or absence of the full Trx1 system. Thus, radiolabelled ^{35}S-Tim9 was incubated with mitochondria in the absence, or in the presence of the Trx1, and imports carried out at 25°C for various time. At the indicated times, aliquots were removed and trypsin treated to remove the unimported material and imports analysed by SDS-PAGE (Figure 5.8). The results showed that in the presence of the Trx1 system the levels of Tim9 import were higher, being at least twice those of the control throughout the time course (Figure 5.8 A, lanes 2-8 vs 10-16). Furthermore, in contrast to the control, Tim9 import increased throughout the time course without reaching a stationary level, which in contrast was reached in the control reaction within the first 10 minutes of the time course (Figure 5.8, B).

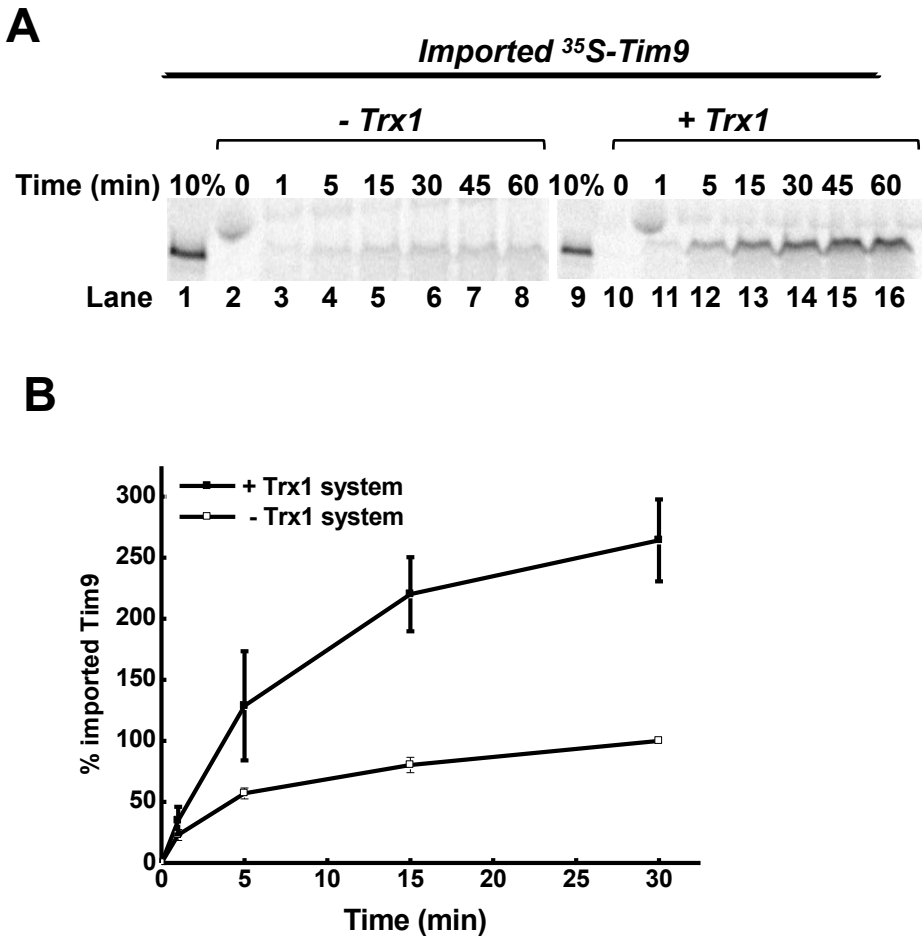

Figure 5.8 Tim9 time course import in the presence of the Trx1 system.

(A) Before import mitochondria were incubated in the absence (lanes 2-8), or in the presence of the Trx1 system (lanes 9-15) at 25°C for 20 minutes. ^{35}S-Tim9 was then imported at 25°C for various time points. At the indicated time points, samples were trypsin treated for the analysis of the imported material. Proteins were separated by reducing SDS-PAGE and analyzed by autoradiography. 10% indicates 10% of the total amount of ^{35}S-Tim9 used for each import reaction (lane 1).
(B) The amount of imported Tim9 import as described in A was quantified by densitometry. The amount of imported Tim9 in the absence of the Trx1 system was set as 100%. The average and the deviation standard were obtained from four independent experiments.

In order to test whether the Trx1 system affects the mitochondrial import of small Tims positively in general, the import assays described above for Tim9 were repeated for ^{35}S-Tim10 (Figure 5.9). The results showed that in the presence of the Trx1 system (Figure 5.9 A, lane 2), the Tim10 imported level was more than doubled compared to the control (Figure 5.9 A, lane 1). The partial Trx1 system (without Trr1) enhanced the import level slightly in comparison to the control, but not as much as the full Trx1 system (Figure 5.9 A, lane 4 vs lanes 1-3). These results thus demonstrated that the full Trx1 system enhances the imported levels of Tim10, consistent with what was observed for Tim9.

Similarly to Tim9, the Tim10 time course import experiment showed that the levels of imported Tim10 were higher than those of the control, being as the rate of Tim10 import increased along the time course (Figure 5.10).

All together the results for both Tim9 and Tim10 indicated that the Trx1 system increases the import levels of small Tims into mitochondria.

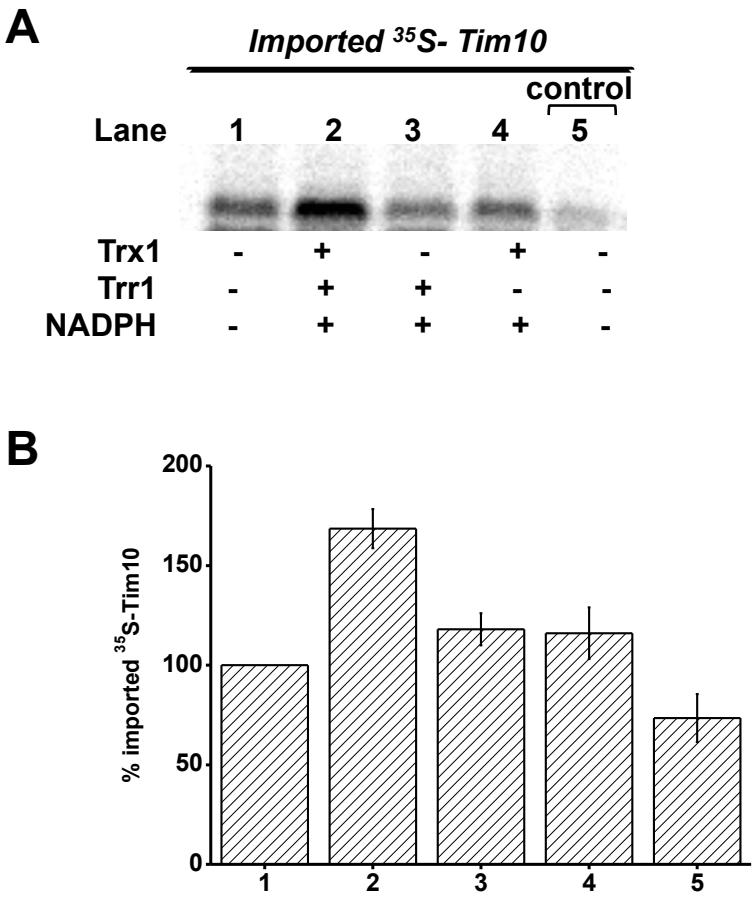

Figure 5.9 Effects of the Trx1 system on Tim10 import.

(A) As in figure 5.7 A except that ^{35}S-Tim10 was imported into mitochondria. **(B)** The amount of Tim10 imported as described in A was quantified by densitometry. The level of imported Tim10 in the absence of the Trx1 system was set as 100%. The average and the deviation standard were obtained from three independent experiments.

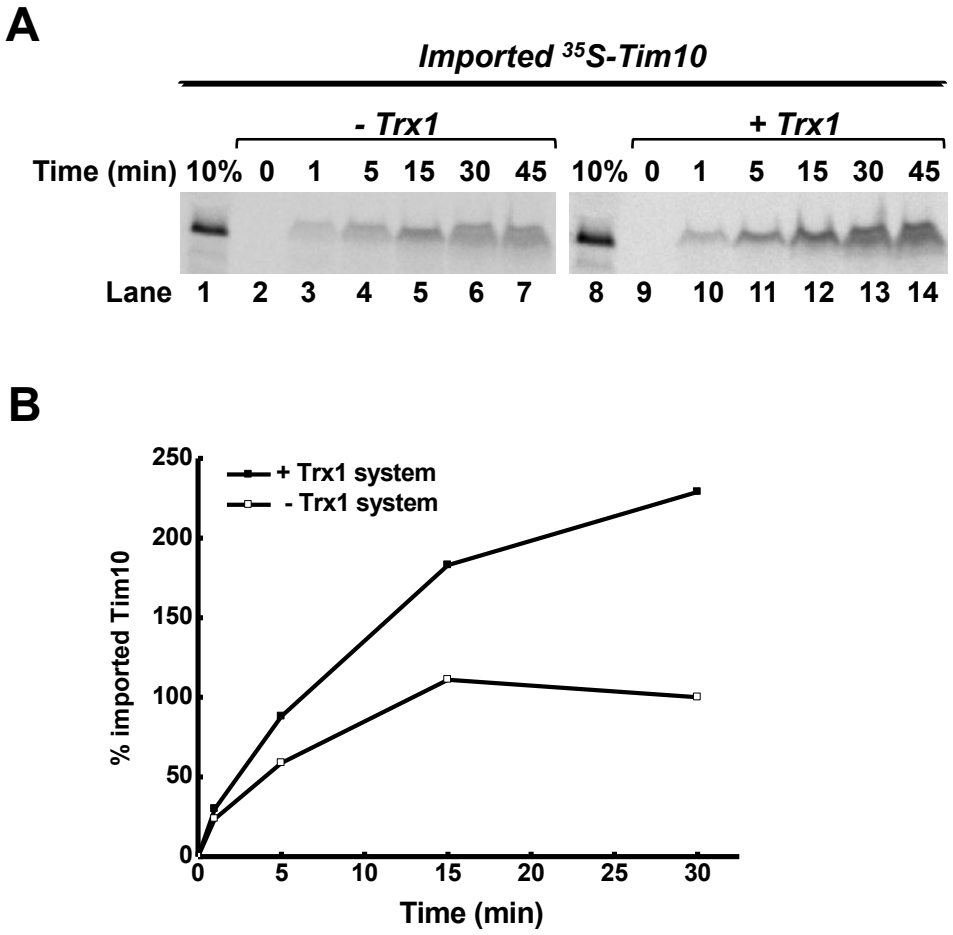

Figure 5.10 Tim10 time course import in the presence of the Trx1 system.

(A) As in figure 5.8 except that ^{35}S-Tim10 was used. 10% represents the 10% of the total amount of ^{35}S-Tim10 used for each import reaction (lane 1).
(B) The levels of imported Tim10 during the time course in (A) were quantified by densitometry, and expressed in comparison to the 10%.

5.3.2 The Trx1 system maintains the small Tim proteins in reduced form

Only the reduced forms of small Tims are import-competent, whilst the oxidised forms cannot be imported into mitochondria. So, we anticipated that the Trx1 system enhances the mitochondrial import of small Tims because it can maintain the precursors in a reduced form. To test this hypothesis, following the import assays described above, the redox state of the remaining unimported Tim9 was analysed by AMS-thiol-modification assay (Figure 5.11, A). The results revealed that whereas all the unimported Tim9 was oxidised in the control (Figure 5.11 B, lane 3), the Trx1 system maintained a large fraction of Tim9 in a reduced form (Figure 5.11 B, lane 4). A small fraction of reduced unimported Tim9 also existed in the reaction containing the partial Trx1 system (Trx1 and NADPH) (Figure 5.11 B, lane 6), but not in the reactions containing Trr1 and NADPH, or Trx1 and Trr1 (Figure 5.11 B, lanes 5 and 7, respectively). Thus, this indicates that the complete Trx1 system maintains the majority of Tim9 precursors in a reduced form.

This result was confirmed by the analysis of the redox state of Tim9 during the time course import described above (Figure 5.11 B). The results revealed that in the presence of the Trx1 system the majority of Tim9 is reduced, being as only a small fraction oxidised and kept constant throughout the time course (Figure 5.11B, lanes 9-14), whereas in the control, the rate of oxidative folding of Tim9 is fast, being as the majority of Tim9 is oxidised within the first 5 minutes of the time course (Figure 5.11, B lanes 3-8). This weak, or strong oxidative folding of unimported Tim9 correlates perfectly with the stronger, or weaker import occurring in the presence, or absence of the Trx1 system, respectively.

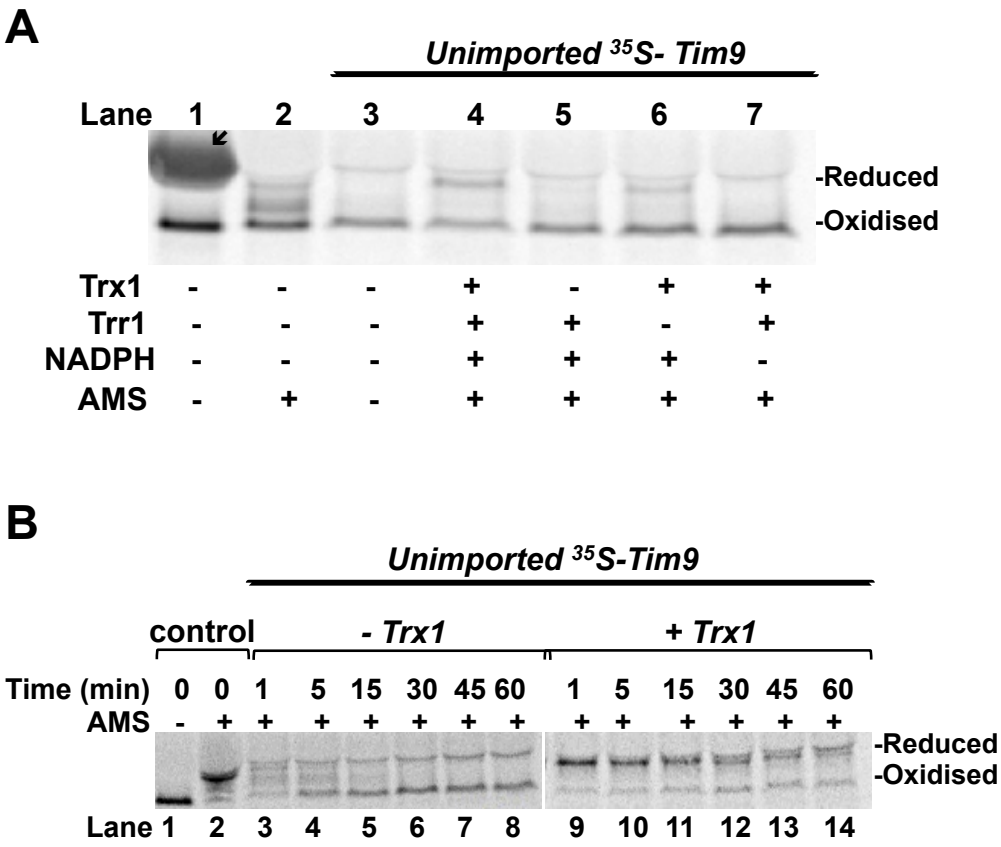

Figure 5.11 Effects of the Trx1 system on the redox state of unimported Tim9.

(A) AMS thiol-modification assay of the unimported material from the import reactions in Figure 5.7A: after import in the presence or absence of the purified components of the Trx1 system, an aliquot from each import reaction was centrifuged and the supernatants treated with AMS buffer. All samples were separated by non-reducing SDS-PAGE and analyzed by autoradiography. Lanes 1 and 2 showed the redox state of the precursors before imports started. The reduced and oxidised forms of unimported Tim9 are indicated. The arrowhead in lane 1 indicates the band corresponding to the heme protein coming form the lysate.
(B) As in A, except that the the redox state of the unimported material during the Tim9 time course import in Figure 5.8A was analysed at various time points. Lanes 1 and 2 showed the redox state of the precursors before imports started.

The same results were obtained when analysing the redox state of unimported Tim10, as in the presence of the full Trx1 system no oxidised Tim10 is present in the reaction (Figure 5.12 B, lane 2). However, oxidised Tim10 was found in the control and in the reactions containing partial Trx systems (Figure 5.12 B, lanes 1, 3 and 4).

Taken together, the results of this section showed that the **Trx1 system maintains** small Tims in a **reduced** and **import-competent form** in the cytosol, and **so facilitates** their import into mitochondria.

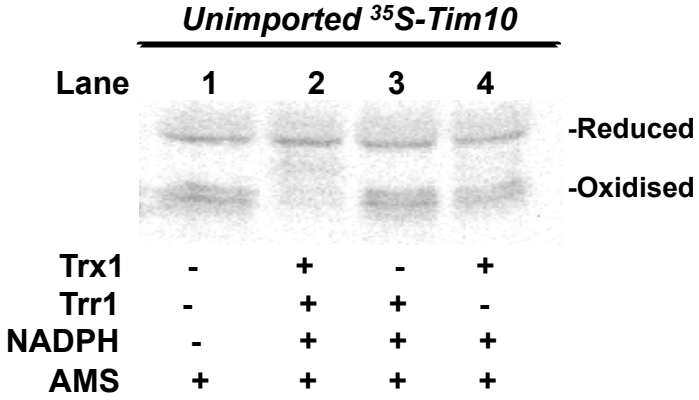

Figure 5.12 Effects of the Trx1 system on the redox state of unimported Tim10.

As in figure 5.11 A, except that the AMS thiol-modification assay of the unimported Tim10 was analysed. Lanes 1 and 2 show the redox state of Tim10 precursors before starting import experiments. All samples were separated by non-reducing SDS-PAGE, and analyzed by autoradiography. The reduced and the oxidised forms of Tim10 are indicated.

5.3.3 Effects of the Trx1 system on the mitochondrial import of Cox19, a twin CX_9C motif-containing substrate of the MIA machinery

To examine whether the same effects can be observed for other substrate of the MIA pathway, the same analysis was performed for the CX_9C motif-containing protein Cox19. Thus, radiolabelled ^{35}S-Cox19 was imported into wt mitochondria in the presence, or absence of the Trx1 system. After import, the analysis of both total imported Cox19 and the redox state of unimported Cox19 were carried out as described before (Figure 5.13). The results for the imported material showed that in the presence of the Trx1 system Cox19 import was strongly increased in comparison to the control (Figure 5.13 A, lane 2 vs 1). A partial Trx1 system (without Trx1, or Trr1) slightly enhanced the import level, but not as much as the full system (Figure 5.13 A, lanes 3 and 4). This finding thus provides the *in organello* evidence that the Trx1 system facilitates Cox19 import as well.

The results for the redox state of unimported Cox19 showed that, whilst in the presence of the Trx1 system, all the unimported material is reduced (Figure 5.13 B, lane 4), Cox19 is oxidised, or partially reduced in the control (Figure 5.13, lane 3). A small fraction of reduced Cox19 was also observed in the reactions containing either Trx1 and NADPH, or Trr1 and NADPH (Figure 5.13 B, lanes 5 and 6, respectively), whereas most of the unimported material was oxidised in the reaction lacking NADPH (Figure 5.13 B, lane 7). Thus, the results demonstrated that the Trx1 system is efficient at maintaining the "cytosolic pool" of Cox19 in a fully reduced form.

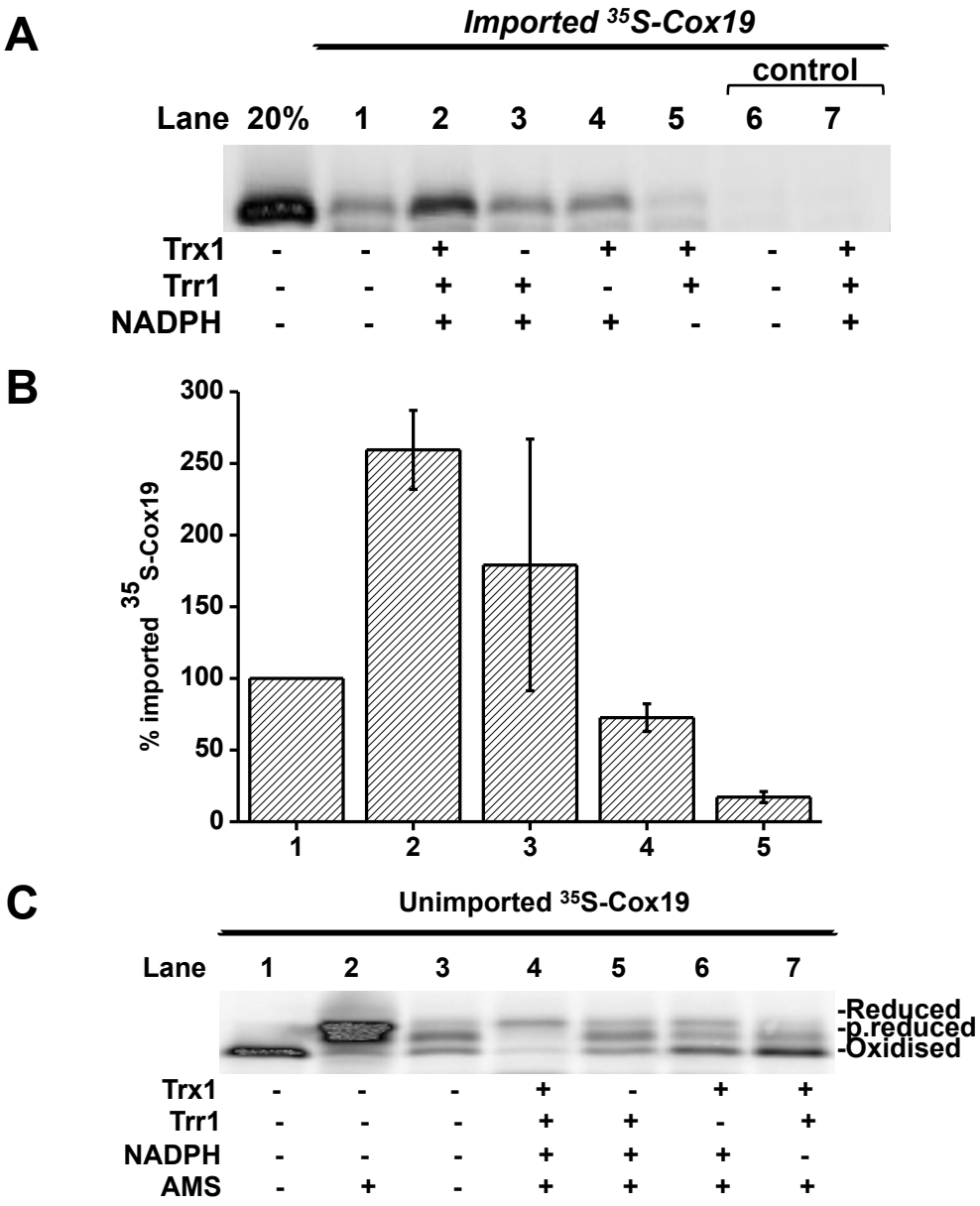

Figure 5.13 Effects of the Trx1 system on Cox19 import.

(A) As in figure 5.7 A except that ^{35}S-Cox19 was imported into mitochondria. Proteins were separated by reducing SDS-PAGE, and analyzed by autoradiography. 20% represents the 20% of the total amount of ^{35}S-Cox19 used for each import reaction (lane 1).
(B) The levels of imported ^{35}S-Cox19 as described in (A) were quantified by densitometry setting as 100% the level of imported Cox19 in the absence of the Trx1 system. The average and the random errors were calculated from two independent experiments.
(C) AMS thiol-modification assay of redox state of unimported Cox19 from the import reaction in A. Lanes 1 and 2 indicated the redox state of Cox19 before imports started. The reduced, partially reduced (p.reduced) and oxidised forms are indicated.

The above results were confirmed by the Cox19 time course import in the presence, or absence of the full Trx1 system, since the analysis showed that in the presence of the Trx1 system the levels of imported Cox19 were higher than those of the control (Figure 5.14).

Taken together, these findings provide *in organello* evidence that the Trx1 system facilitates the import of IMS cysteine-rich proteins because of its capability at maintaining their cytosolic pools in a reduced and import-competent form.

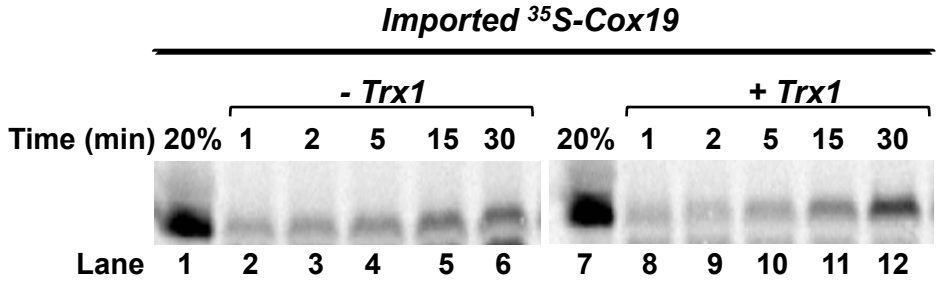

Figure 5.14 Cox19 time course import in the presence of the Trx1 system.

^{35}S-Cox19 was imported into mitochondria in the absence (lanes 2-6) or in the presence of theTrx1 system (lanes 8-12) for various times. At the indicated time points, mitochondria were treated with trypsin to remove the unimported material, and analysed by reducing SDS-PAGE and autoradiography. 20% represents the 20% of the total amount of ^{35}S-Cox19 used for each import reaction (lanes 1 and 7).

5.3.4 Effects of the purified Trx1 system on the redox state of mitochondrial Mia40

To confirm that the positive effects that the Trx1 system has on the import of MIA substrates “occurred” at the *cis*- and not at the *trans*-side of the OM (i.e. Mia40/Erv1 machinery), the redox state of endogenous mitochondrial Mia40 was analysed in the absence, or presence of the purified components of the Trx1 system by AMS shift-based gel assay. Thus, wt mitochondria were incubated with, or without the Trx1 system for 20 minutes at 25°C, then isolated by centrifugation and resuspended in non-reducing sample buffer containing an excess of AMS (Figure 5.15). All samples were left 1 hour in the dark at RT to let the thiol-modifications occur, and then heated at 95°C for 5 min. Proteins were resolved by a 10% SDS-PAGE gel, transferred onto a nitrocellulose membrane and analysed by immnunoblotting with Mia40 antibody. Two samples were set up as controls for the oxidised and partially reduced states of Mia40. As a control of the partially reduced state of Mia40, the sample was pre-treated with the reducing agent TCEP before the addition of non-reducing sample buffer containing AMS (Figure 5.15, lane 7). As a control of the oxidised state of Mia40 another sample was mock-treated and resuspended with non-reducing sample buffer without AMS (Figure 5.15, lane 6). The results showed that the redox state of endogenous Mia40 was not affected by the addition of the Trx1 system components, as Mia40 was mainly in its oxidised state, as previously shown (Terziyska et al., 2009) (Figure 5.15, lane 2 vs 1 and 6). Thus, this data indicated that the Trx1 components do not affect the Mia40 redox state.

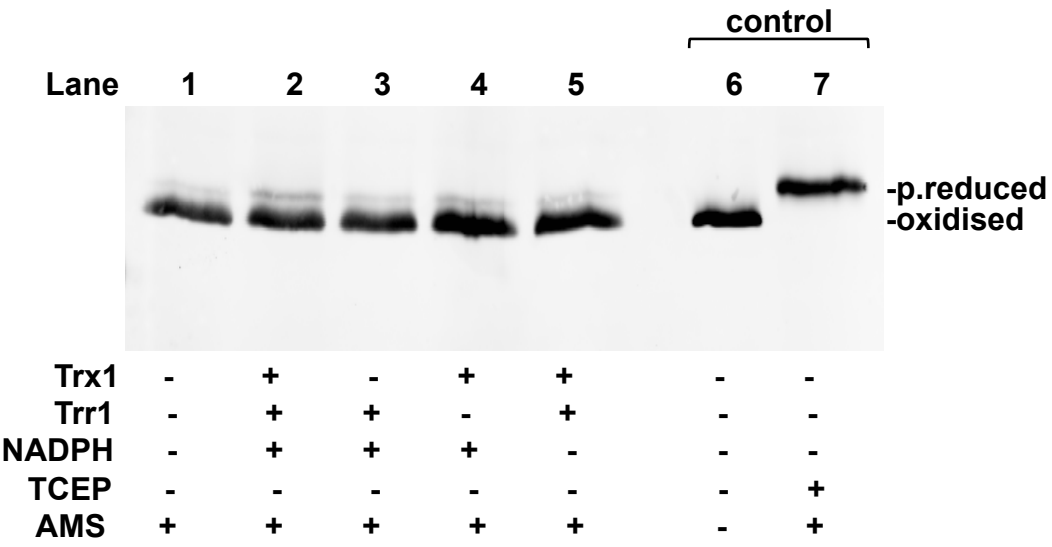

Figure 5.15 Effects of the Trx1 system on Mia40 redox state.

60 ug of mitochondria were incubated at 25°C for 20 min in the absence (lane 1) or presence of the purified components of the Trx1 system as indicated. Mitochondria were then isolated by centrifugation and resuspended in non-reducing sample buffer containing 25 mM of AMS. As a control respectively for the oxidised and partially reduced forms of Mia40, mitochondria were left untreated (lane 6) or pre-treated with 2 mM of TCEP at RT for 30 min before resuspension with non-reducing sample buffer containing 25 mM AMS (lane 7). Samples were loaded an a 10% SDS-PAGE analyzed by immunoblotting with Mia40 antibody. The partially reduced (p.reduced) and oxidised forms of Mia40 are indicated.

5.3.5 The Trx1 system does not affect the import of non-MIA substrates

To test whether the effects of the Trx1 system are unique to the redox-sensitive precursors of the MIA pathway, imports of precursors destinated to the OM, IM and matrix were examined in the presence, or absence of the Trx1 components. The matrix precursor Su9-DHFR, commonly used as model for the TIM23 pathway, could not be used for this analysis, as NADPH arrests its translocation through the OM. Thus, the matrix precursors mtHsp60 and the F_1-ATPase subunit β were used as models for the TIM23 pathway, porin was used as model for the OM β-barrel proteins and AAC was used as model for and TIM22 import pathway (Figure 5.15 A).

Radiolabelled ^{35}S-precursors were imported into mitochondria in the absence, or in the presence of the components of the Trx1 system as described before, with the exceptions that imports were carried out at 30°C and in the presence of both ATP and NADH. The successful import of the matrix precursors into the matrix can be visualized on the membrane *via* the formation of the mature forms (Figure 5.15 A, indicated by the letters “p” for precursor and “m” for mature). The results showed that the presence of a full, or partial Trx1 system did not affect the import of these proteins.

To further confirm this result, a time course import experiment was performed for ^{35}S-AAC in wt mitochondria in the absence (Figure 5.15 B, lanes 1-4), or in the presence of the Trx1 system (Figure 5.15 B, lanes 5-8) for 30 minutes at 25°C. The results showed that the presence of the Trx1 system did not increase the levels of AAC imported in comparison to the control. Thus, this confirmed that the Trx1 system does not interfere with the TIM22 pathway even though AAC uses the IMS small TIM complex to be targeted to the IM.

In summary, these results confirmed that Trx1 system does not interfere with the molecular mechanisms of the other mitochondrial import routes, but it selectively facilitates the import of Mia40 substrates.

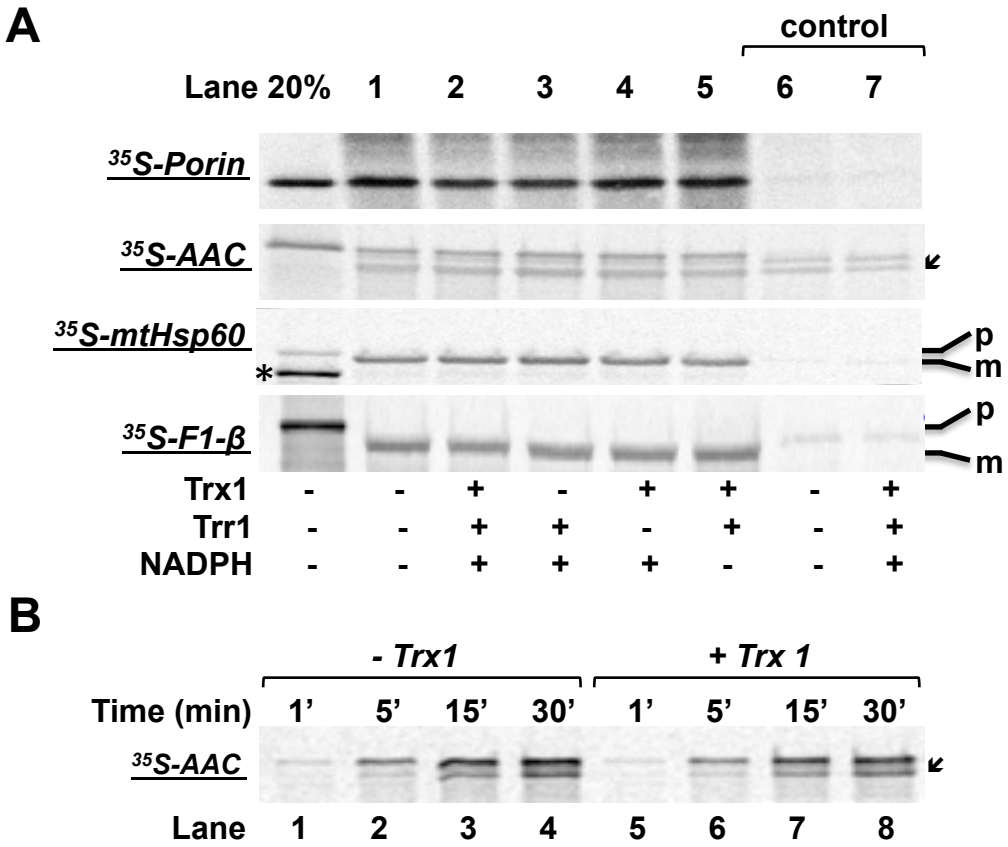

Figure 5.16 The Trx1 system has no effect on mitochondrial import of non MIA substrate.

(A) Precursors of the OM ^{35}S-Porin, or of the IM ^{35}S-AAC, or of the matrix ^{35}S-F1-β and ^{35}S-mtHsp60 were imported into mitochondria in the absence of in the presence of the Trx1 system as indicated. Following import, mitochondria were treated with trypsin to remove the unimported material, analysed by reducing SDS-PAGE and autoradiography. 20% represents the 20% of the total amount of each radiolabelled ^{35}S-precursor used for each import reaction. The arrowhead at the right of the import panel for ^{35}S-AAC may represent the fraction of ^{35}S-AAC that is translocating through the OM and not yet fully inserted into the IM, and therefore accessible to proteolysis. The precursor (p) and the mature (m) forms of the matrix proteins are indicated at the right of the import panels. The asterisk in the first lane of the ^{35}S-mtHsp60 import panel probably represents the fraction of the precursor proteins that were not fully translated during the *in vitro* transcription-translation reaction.
(B) Time course of import of ^{35}S-AAC into mitochondria in the absence (lanes 1-4) or in the presence (lanes 5-8) of the Trx1 system. The arrowhead at the right of import panel for ^{35}S-AAC may probably indicate the AAC precursors that are translocating through the OM and not yet inserted into the IM.

5.4 Discussion

5.4.1 The cytosolic Trx systems are required for mitochondrial biogenesis under respiratory conditions

Currently, little is known about how the redox sensitive substrates of the MIA pathway are maintained in a reduced and import-competent form in the cytosol. Here, the investigation whether the major cytosolic oxidoreductases, the Trxs and Grxs, play a role in the biogenesis of small Tim proteins has been undertaken. The Trx and Grx enzymes, together with GSH/GSSG are responsible for maintaining cytosolic proteins in their reduced state and preventing oxidative stress (Holmgren, 1985; Gilbert, 1990; Aslund and Beckwith, 1999). In particular, thioredoxin enzymes mainly reduce intra-, or inter-molecular disulfides (Jung and Thomas, 1996), whilst the glutaredoxin enzymes most likely reduce the GSH-mixed proteins disulphides bonds (Holmgren 1989; Collison *et al.,* 2002). Yeast cytosolic Trx and Grx enzymes are similar, as both are small proteins (around 10-15 kDa), have the typical Trx fold and contain the catalytic site Cys-X-X-Cys motif, and appear to be functional redundant.

Here, I reported the first *in vivo* evidence that the cytosolic Trx enzymes play an important role during mitochondrial protein biogenesis. This is shown by the fact that the *trx1 trx2* mutant grew more slowly under respiratory conditions than the *grx1 grx2* mutant and the WT (Figure 5.2). On the other hand, the single *trx1,* or *trx2* mutants do not display a similar growth defect under respiratory conditions (Durigon *et al.,* 2012), probably because of the overlapping role of the two Trx proteins. This indicates that the respiratory growth defect is not simply due to

respiratory ROS production, as *trx2* mutant is hypersensitive to ROS, in contrast to *trx1* mutant having WT resistance (Garrido and Grant, 2002). However, since the cytosolic Trx proteins participate in various processes and have many client proteins, other effects may also contribute to the respiratory growth defects seen in *trx1 trx2* mutant.

5.4.2 The cytosolic Trx systems facilitates *in vivo* the biogenesis of small Tim proteins

The link between the cytosolic Trx systems and the biogenesis of small Tim proteins was established by analysing the levels of small Tims in WT and *trx1 trx2* mitochondria isolated from cells grown under YPD➔YPEG stress conditions (Figure 5.5). Moreover, the protein expression of mitochondria purified from the *trx1 trx2* cells grown in YEPG was undistinguishable from that of the WT (Figure 5.3). This can be explained by the fact that the mutant *trx1 trx2* is not unviable, but grows slowly in YPEG, and a small intensity difference in protein content will not be detectable by western blot (Figure 5.2). On the other hand, under YPD➔YPEG stress conditions, the levels of small Tim proteins were found to be remarkably lower in *trx1 trx2* mitochondria than in WT, indicating that *in vivo* the cytosolic Trx systems play a role in the biogenesis of small Tim proteins (Figure 5.5). Mitochondrial import of small Tims is regulated by the redox state of their cysteines and by the MIA machinery. Thus, the most likely explanation for the decreased endogenous levels of small Tims is that, in the absence of the cytosolic Trx enzymes, one of the major cellular oxidoreductase systems, oxidative folding of small Tims

occurs in the cytosol preventing their import into mitochondria. This hypothesis may be supported by the study showing that in the *trx1 trx2* mutant the cytosolic redox ratio GSH/GSSG is towards a more oxidised state, environmental condition favouring oxidative stress (Muller 1996; Luikenhuis *et al.,* 1998; Garrido and Grant, 2002; Dardalhon *et al.,* 2012).

The results from the analysis of the expression of various mitochondrial markers in the *trx1 trx2* mutant also showed that other mitochondrial proteins were negatively affected by the deletion of TRX1 and TRX2. Particularly for the IM protein Mia40 and the OM proteins Tom20 and Tom22 (Figure 5.5). Whilst the fact that yMia40 can be imported into mitochondria via both the stop-transfer or the MIA pathways can explain this result to a certain extent, the reasons of the decreased Tom20 and Tom22 endogenous levels observed in *trx1 trx2* cells are unknown.

Conversely, the IMS Cytb2, the OM Tom40, the IM AAC and the matrix MDH were not affected in the *trx1 trrx2* mutant. The fact that the mitochondrial endogenous levels of Cytb2 did not decrease in the mutant confirmed that the Trx enzymes are specifically required for the biogenesis of MIA substrates. Cytb2 precursor, in fact, does not possess conserved cysteine residues and is not a MIA substrate, but contains a bipartite targeting sequence that directs the precursor to the TIM23 translocase (Daum *et al.,* 1982b; Mossmann *et al,* 2012).

On the other hand, both Tom40 and AAC are substrates of the soluble IMS Tim9-Tim10 complex to be chaperoned to the OM, or IM, respectively (Luciano *et al,* 2001; Zara *et al.,* 2001; Truscott *et al,* 2002; Wiedemann *et al.,* 2004). Thus, as a consequence of the decreased endogenous levels of small Tims in the *trx1 trx2* mitochondria, one could argue that the endogenous levels of Tom40 and AAC should be decreased as well. One possible explanation of this may be that the remaining amount of small Tims in the IMS is enough to chaperone the coming precursors to their final mitochondrial sub-compartments.

5.4.3 The cytosolic Trx1 system is unique to MIA import route substrates

The importance of the cytosolic Trx systems in the biogenesis of small Tim proteins is supported by both *in vitro* studies obtained in our lab and *in organello* import assays presented here (Durigon *et al.,* 2012). By both *in vitro* reconstitution assays and NADPH consumption assays using purified proteins, our lab demonstrated that the Trx1 system preferentially catalyses the reduction of folding intermediates of Tim10 rather than fully oxidised Tim10 with a substrate efficiency similar to that of well characterized substrates of Trx (i.e. ribonucleotide reductase, arsenate reductase and insulin; Durigon *et al.,* 2012; Holmgren, 1979; Messens *et al.,* 2004; Zahedi Avval and Holmgren, 2009). This finding indicates that the Trx1 system reduces disulphide bonds at an early stage of the oxidative folding of small Tims, thus preventing premature oxidation in the cytosol and therefore facilitating their import into mitochondria.

The in vitro findings using purified proteins are further supported by the *in organello* import assays shown in this chapter, where it is shown that the Trx1 system enhances mitochondrial import of both Tim9 and Tim10. This positive effect is due to the capability of the full Trx1 system of maintaining the cytosolic pool of small Tims in a reduced and, therefore, import-competent form. Furthermore, incubation of mitochondria with purified components of the Trx1 system does not affect the redox state of Mia40, consistent with the fact that the purified components of the Trx1 system and mitochondrial Mia40 are located in different cellular compartments, respectively at the *trans*- and *cis*- side of mitochondria.

In addition, as for the small Tims, the Trx1 system facilitates mitochondrial import of Cox19, a member of the twin CX_9CX family and substrate of the MIA pathway, but does not affect import of the OM, IM and matrix precursors, demonstrating that the Trx1 system is unique to the MIA pathway substrates.

5.4.4 Cytosolic factors and biogenesis of small Tim proteins

Previous published studies from our lab have shown *in vitro* that Zn^{2+}-binding can inhibit the oxidative folding of small Tims and maintain small Tims in a reduced state (Lu and Woodburn, 2005; Morgan et al., 2009). A similar role for Zn^{2+}-binding was suggested for Cox17 (Voronova *et al.,* 2007). In fact, the above studies showed *in vitro* that, by preventing cytosolic oxidation, Zn^{2+}-binding enhances import of small Tim proteins into mitochondria. However, the zinc-bound proteins cannot be imported effectively into the IMS. In addition, zinc has an inhibitory effect on the oxidase activity of Erv1, and hence on the activity

of Mia40/Erv1 machinery (Morgan *et al.,* 2009). Thus, it is necessary to limit and/or control the availability of free zinc in the IMS. It has been suggested that Hot13 can promote oxidation of Mia40 by removing zinc from Mia40 (Mesecke *et al.,* 2008).

Although the cellular concentration of Zn^{2+} is estimated to be high (~ 0.5 mM), the vast majority of Zn^{2+} in the cell is tightly bound to cellular macromolecules. Consequently, there is very little free ionic zinc in the cytoplasm. In addition, the relative low binding affinities (sub-micromolar to nanomolar) between zinc and small Tims suggests that the molecular basis for the chaperone-like function of zinc may require specific physiological conditions and/or pathways, as it has been shown for the heat shock protein Hsp33, metallothionein (MT) and the copper/zinc-superoxide dismutase SOD1 (Maret and Vallee, 1998; Jakob *et al.,* 1999; Field *et al.,* 2003; Lu *et al.,* 2004b; Woodburn and Lu, 2005; Ivanova *et al.,* 2008; Morgan *et al.,* 2009). In the case of Hsp33, zinc-binding maintains the protein in a reduced inactive and monomeric state. Exposure to reactive oxygen species induces the loss of the Zn^{2+} from Hsp33 and the formation of two intramolecular disulphide bonds leading to the dimerization and activation of the protein (Graumann *et al.,* 2001).

In this study, to reduce the amount of free ionic zinc present in the lysate 2 mM of EDTA was added to each import reaction. Thus, the above-mentioned studies about zinc, as well as the study presented in this chapter, propose two different mechanisms that are both able to maintain reduced the cytosolic pool of the IMS cysteine-rich proteins and facilitate import into mitochondria. It may

be that a combination of both mechanisms in protein biogenesis and function may occur, depending for example on the redox potential of the environment and/or the cellular physiological conditions. For example, during stress conditions, when the cytosolic Trx system is working to protect cells against oxidative stress and more free ionic zinc can be available, Zn-binding to small Tims may prevent oxidative folding in the cytosol allowing import into the IMS.

On the other hand, the *in vivo* results presented here indicate that in the absence of Trx1 and Trx2 and under more stressed conditions mitochondrial small Tim levels were decreased. Hence, it will be interesting to investigate in the future whether this is due to oxidative folding followed either by accumulation in the cytosol of oxidised precursors, or by degradation of the precursors. Thus, these are the first *in vivo* and *in vitro* evidences that cytosolic factors (Trx1 and Trx2) and physiological conditions (YPD➔YPEG) regulate the import into mitochondria of small Tim proteins.

5.5 Conclusions

In summary, the *in vivo* and *in organello* data presented here and the *in vitro* data obtained in our lab showed clearly that the Trx1 system can directly reduce unfolded, or partially folded Tim10 and facilitates mitochondrial import of MIA substrates. Thus, this study provides the first evidence that the cytosolic Trx system play an important role in the initial steps of mitochondrial biogenesis of small Tim proteins and presumably of other redox sensitive MIA precursors.

6. CONCLUSIONS AND FUTURE DIRECTIONS

6.1 Conclusions

In summary, the overall aims of this study were to investigate the initial steps of mitochondrial import of small Tim proteins (Chapters 3 and 5) and the mechanisms of oxidative folding of small Tim proteins in the presence of the IMS oxidoreductase Mia40 (Chapter 4).

Whereas it is known that the small Tim proteins use the MIA pathway for import and oxidative folding into the IMS, this present study investigated on the unknown molecular mechanisms mediating the oxidative folding of Tim9 in the presence of Mia40. Using Tim9 and Tim10 as a model, both *in vitro* and *in organello* studies provided the evidence that Tim9 and Tim10 are fully oxidised by Mia40 (Figure 4.2), and that the rate of Tim9 oxidation is dependent on the concentration of Mia40 (Figure 4.4). Furthermore, in the presence of an excess of Mia40 Tim9 is fully oxidised immediately and very efficiently, whilst in the presence of nM amounts of Mia40 the Tim9 oxidative folding process is slower and produces partially oxidised Tim9 as intermediates. These monomeric half-oxidised intermediates can be further oxidised by an unknown mechanism. Since the experiments were performed under aerobic conditions, these free single disulphide-bonded intermediated may be most likely oxidised by molecular oxygen.

An investigation of the interactions between Mia40 and the mutants lacking either the outermost or the innermost cysteine pairs of Tim9 revealed that Mia40 may first introduce the inner disulphide bond (C2-C3) and then the outer disulphide bond (C1-C4) in Tim9.

Lastly, this study expanded on earlier observations that GSH enhances import of MIA substrates into the IMS. Using small Tims as model and *in vitro* assays, the results showed that GSH resolved the complex between Mia40 and its substrates very rapidly, and that GSH may prefer to interact with the complex after the formation of the first intramolecular bond in the substrate, presumably the inner disulphide bond. This will result in the acceleration of the release cascade of the substrate from Mia40, and thus in more free subunits of reduced Mia40, which needs to be re-oxidised by Erv1 before interacting with newly imported reduced substrates.

In the other two chapters I investigated on the earlier steps of the biogenesis of small Tim proteins. In particular on the mechanisms of binding to and translocation across the OM (Chapter 3), and on the cytosolic factors responsible in maintaining in an import-competent form the cytosolic small Tim precursors (Chapter 5). Using Tim9 as a model, the work presented here confirmed the previous observations that Tim9 import into the IMS occurs in the absence of the trypsin accessible receptor domains of the TOM complex. In addition, this study showed that Tim9 binding to the OM does not also require the receptors of the TOM complex. Tim9 binding to the OM is independent of the redox state of the precursors, as both oxidised and reduced forms of Tim9 bind to the same binding site at the OM. However, this common binding site resulted not be important for the full translocation process across the OM, as reduced Tim9 was still efficiently imported into mitochondria in the presence of oxidised Tim9.

This is consistent with the observation that only Tim9 precursors in a reduced and unfolded conformation cross the OM (Lutz *et al.,* 2003; Lu *et al.,* 2004). My results also showed that NEM pre-treatment of mitochondria inhibits binding of Tim9 to the OM, suggesting that Tim9 binding to and/or translocation across the OM may depend on cysteine-cysteine interactions. Thus, it will be interesting to investigate in the future whether Tom40 (which the studies here showed to contain free thiol group/s) or other OM proteinaceous factors (such as Grx2) are involved during binding and/or translocation across the OM of small Tim precursor proteins.

In chapter 5, *in organello* import assays provided the first evidence that the cytosolic Trx system facilitates the import of redox-sensitive IMS proteins, without affecting matrix and membrane proteins. In addition, we showed that single disulphide folding intermediates of Tim10 are excellent substrates of the Trx1 system, as the Trx1 system specifically catalyses the reduction of partially folded or unfolded proteins more efficiently than that of the folded proteins (Durigon *et al.,* 2012). This finding provides important insight into the **initial steps** of small Tim proteins biogenesis, specifically how these precursors can be maintained in a reduced and therefore import-competent form in the cytosol (Figure 6.1). This study is particularly important, since it has been shown that small Tim proteins are oxidised by GSSG under normal cellular glutathione redox conditions (Lu and Woodburn, 2005). Here, it is also showed that at least *in vitro* the cytosolic Trx1 system does not affect either the biogenesis of precursors proteins destined to the mitochondrial matrix or membrane, or the redox state of Mia40, one of the two key players of the MIA pathway.

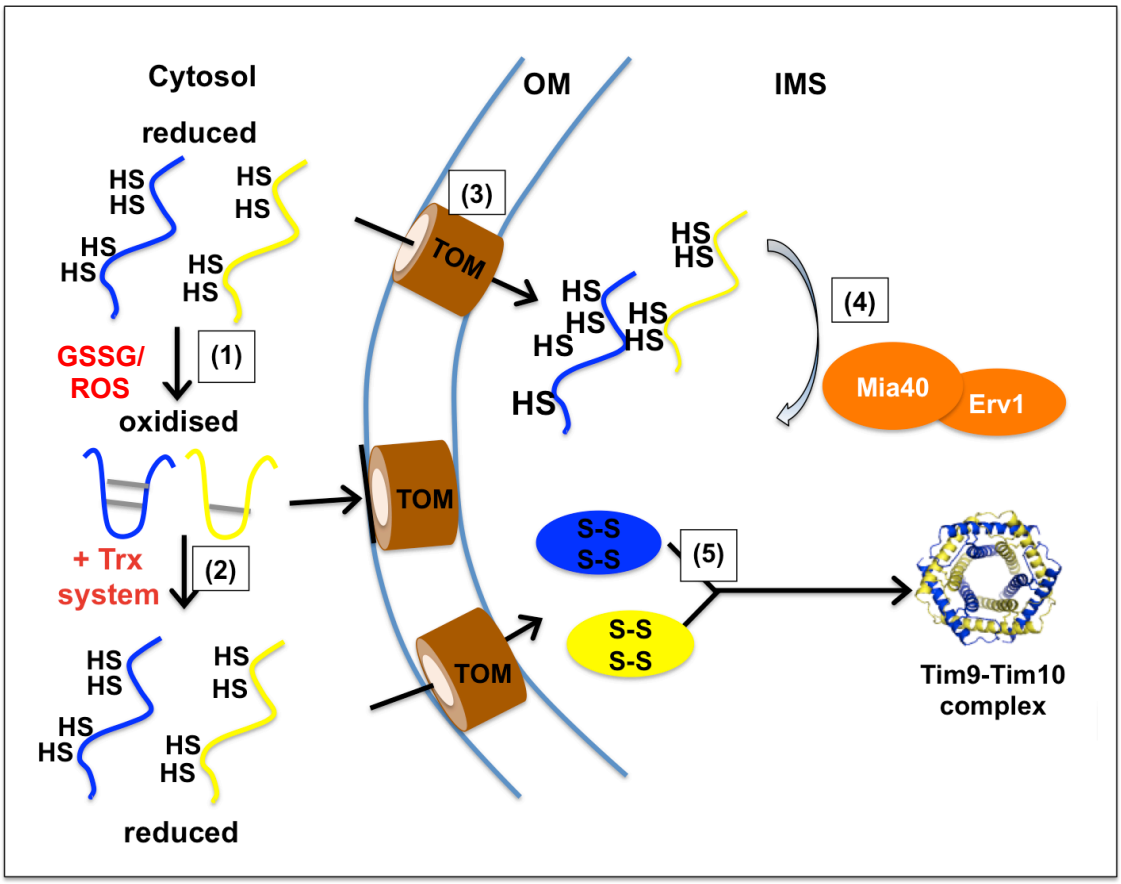

Figure 6.1 A Model of the role of the cytosolic Trx systems on the biogenesis of small Tim proteins.

Mitochondrial import of small Tim proteins is regulated by their thiol-disulphide redox state, as only unfolded and reduced small Tim precursor proteins are import-competent and can translocate through the OM (step 1), whereas oxidised proteins cannot. Once in the IMS, small Tim proteins undergo oxidative folding via the MIA machinery (step 2), and then assemble into the Tim9-Tim10 complex (step 3**).** Under stressed conditions small Tim proteins can be oxidised (e.g. by GSSG, ROS) losing their mitochondrial import-competence (step a). This study and Durigon *et al.* (2012) showed that the cytosolic Trx systems can facilitate import of small Tim proteins by reducing the oxidized small Tim proteins, especially the single-disulphide intermediates efficiently (**b**). Thus, the cytosolic Trx systems can prevent the formation of early folding intermediates of small Tims and maintain small Tim precursors in an import-competent form.

Mitochondria harbour many metabolic and redox pathways. It is, therefore, clear that mitochondrial function and activity is regulated by or adapt to different cellular conditions. Here, it is shown for the first time a connection between the mitochondrial import of the MIA redox-sensitive substrates and the cytosolic thioredoxin system. Previous studies showed that Erv1 of the IMS disulphide relay system donates its electrons either to O_2 or to Cytc of the respiratory chain generating H_2O_2 or H_20, respectively. H_2O_2 is known to function as a signal that, crossing the OM, triggers responses to protect cells against oxidative stress, such as the activation of the transcription factor Yap1 (Kuge, Jones et al., 1997; Okazaki, Tachibana et al., 2007; Collins *et al.*, 2012).

Although the potential of the IMS disulphide relay system for redox signalling is unclear, the MIA pathway may be regulated by the redox state of the cell. Thus, it will be exciting in the future to investigate the mechanisms and/or the different physiological cellular conditions that regulate the MIA pathway, and thus the import of its substrates.

6.2 Future directions:

Questions raised from this thesis include:

1) Have the Trx systems the same effect on the biogenesis of the small Tim proteins?

It will be interesting in the future to investigate the role of the two cytosolic Trx1 and Trx2 systems in the biogenesis of small Tim proteins. The two Trxs are functional redundant, with Trx2 having a predominant role against oxidative stress. In this study I showed that expression levels of small Tims is decreased in the *trx1 trx2* mitochondria. Spot testing study suggested that both Trxs play a role in biogenesis of mitochondrial (Durigon *et a*l., 2012). However, whether both Trxs are equally active or function at different cellular conditions are unknown.

Firstly, in order to assess whether the cytosolic Trx2 has the same effect of Trx1 on the biogenesis of the small Tims, the same *in organello* experiments presented here with the Trx1 system need to be done using the Trx2 system. In addition, *in vitro* assays using purified components of the Trx2 system and fully and partially oxidised small Tim proteins are needed (as shown in Durigon *et al.*, 2012).

Secondly, the analysis of the expression levels of small Tims in the *trx1* or *trx2* purified mitochondria from cells under YPD➔YPEG conditions may be the experiments to start with. Subsequently, the [^{35}S]-methionine pulse-labelling technique using the *trx1, trx2*, or *trr1* mutant cells followed by purification of both mitochondrial and cytosolic fractions.

Analysis by western blot of the mitochondrial fractions and by immunoprecipitation of the cytosolic fractions may help identify the role of each Trx homolog in the biogenesis of the small Tim proteins, for example, under different cellular conditions.

2) Is the biogenesis of the small Tim proteins regulated by the cellular redox conditions?

One of the principal functions of the Trx and Grx systems is to protect cells from oxidative stress. Mitochondria are one of the major cellular sources of ROS, and also take part to various biological processes, such as apoptosis, calcium homeostasis, and oxygen sensing (Duchem, 2004, Murphy, 2009a, Murphy, 2009b). Consequently, mitochondrial function is integrated with that of the cell and vice versa. Thus, based on the results presented here, we can hypothesise that the biogenesis of small Tims may be regulated by the redox state of the cell. One way to address this *in vivo* consists in performing [^{35}S]-methionine pulse-labelling studies using WT, *trx1 trx2* and *grx1 grx2* yeast cells, followed by purification of both mitochondrial and cytosolic fractions. In this case it is possible to measure both cytosolic and mitochondrial levels of small Tim proteins under different cellular conditions, for example under oxidative stress conditions (i.e. in the presence of H_20_2) or different concentrations of oxygen. One limitation to this experiment could be that the amount of cytosolic precursors is relatively low and difficult to detect. Thus, the *tx1 trx2* yeast mutant strain harbouring a gene for the TIM9, for example, under the control of a strong and inducible promoter can be used to overexpress Tim9.

Alternatively, the *tx1 trx2* yeast mutant strain expressing one of the genes for the redoxins under the control of a strong and inducible promoter can be used. Thus, the expression of either the TRX or GRX can be induced during the growth, and the levels of cytosolic and imported small Tims can be detected after various induction times as explained before.

3) Does the Grx system play a role in biogenesis of mitochondrial proteins?

It will be interesting in the future to analyse whether the cytosolic Grx systems, may play the same role of the Trx system in the biogenesis of the small Tims and/or other MIA substrates. In order to answer this question, mitochondrial import of ^{35}S-Tim9 may be performed in the presence of the Grx1/2 systems followed by analysis of the redox state of the unimported material by AMS gel-based shift assay. Secondly, based on the fact that Grx2 localises both to the cytosol, the mitochondrial matrix, and the mitochondrial OM, it will be interesting to study the effects of its deletion in the mitochondrial import of ^{35}S-Tim9 using *grx2Δ* mitochondria.

3) Does GSH play a role in the release step of the substrate from Mia40?

The mechanisms leading to oxidative folding in the IMS are controversial. The *in vitro* studies presented here showed that Mia40-Tim9 mixed disulphides formed in all possible cysteine combinations of Tim9.

In addition, this study showed that both double cysteine mutants of Tim9 formed stable intermediates with purified Mia40. The *in organello* assays showed that the double cysteine mutant lacking C2 and C3 was trapped in the complex with Mia40, suggesting that Mia40 is less prone to release a substrate without the formation of the inner disulphide bond in the substrate. In addition, this study showed that GSH prefers to resolve the complex between Mia40 and Tim9wt or between Mia40 and the double cys mutant containing the innermost cysteines C2 and C3. To confirm these results, the well-characterised *mia40-4* mitochondria can be used (Muller et al., 2008 Stojanovski et al., 2008b). Mia40-4 binds the substrates but is defective in the step of release of fully oxidised precursors. Thus, import of recombinant $Tim9_{His}$ WT or double cysteine mutants of Tim9 into *mia40-4* mitochondria in the presence or absence of GSH followed by affinity purification may clarify the role of GSH in the complex Mia40-substrate.

7. REFERENCES

Adam, A., Endres, M., Sirrenberg, C, Lottspeich, F., Neupert, W., and Brunner, M. (1999) Tim9, a new component of the TIM22.54 translocase in mitochondria. EMBO J. 18:313-319.

Alconada, A., Kübrich, M., Moczko, M., Hönlinger, A. and Pfanner, N. (1995) The mitochondrial receptor complex: the small subunit Mom8b/Isp6 supports association of receptors with the general insertion pore and transfer of preproteins. Mol Cell Biol. 15(11): 6196-6205.

Ang, S.K. and Lu, H. (2009) Deciphering structural and functional roles of individual disulfide bonds of the mitochondiral sulfhydryl oxidase Erv1p. J Biol Chem. 284(42): 28754-28761

Akiyama, Y., Kamitani, S., Kusukawa, N. and Ito, K. (1992) In vitro catalysis of oxidative folding of disulfided-bonded proteins by the Escherichia coli dsbA (ppfA) gene product. J. Biol. Chem. 267(31): 22440-22445.

Allen, S., Lu, H., Thomton, D., and Tokatlidis, K. (2003) Juxtaposition of two distal CX3C motifs via intrachain disulfide bonding is essential for the folding of Tim10. J Biol Chem. 278: 38505-38513.

Allen, S., Balabanidou, V., Sideris, D.P., Lisowsky, T and Tokatlidis, K. (2005) Erv1 mediates the Mia40-dependent protein import pathway and provides a functional link to the respiratory chain by shuttling electrons to cytochrome c. J. Mol. Biol. 353: 937-944.

Arner, E.S. and Holmgren, A. (2006) The thioredoxin system in cancer. Semin. Cancer Biol. 16: 420–426

Arnesano, F., Balatri, E., Banci, Bertini, I. and Winge, D.R. (2005) Folding studies of Cox17 reveal an important interplay of cysteine oxidation and copper binding. Structure 13(5): 713-722.

Aslund, F. and Beckwith, J. (1999) Bridge over troubled waters: sensing stress by disulfide bond formation. Cell 96(6): 751-753.

Banci, L., Bertini, I., Cefaro, C., Ciofi-baffoni, S., Gallo, A., Martinelli, M., Sideris, D.P., Katrakili, N. and Tokatlidis, K. (2009) Mia40 is an oxidoreductase that catalyzes oxidative protein folding in mitochondria. Nat Struct Mol Biol 16: 198-206.

Banci, L Bertini, I., Cefaro, C., Cenacchi, L., Ciofi-baffoni, S., Felli, I.C., Gallo, A., Gonelli, L., Luchinat, E., Sideris, D.P. and Tokatlidis, K. (2010) Molecular chaperone function of Mia40 triggers consecutive induced folding steps of the substrate in mitochondrial protein import. Proc Natl Acad Sci USA 107(47): 20190-20195.

Baker, K.P., Schaniel, A., Vestweber, D. and Schatz G. (1990) A yeast mitochondrial outer membrane protein essential for protein import and cell viability. Nature 348(6302): 605-609.

Baker, M.J., Webb, C.T., Stroud, D.A., Palmer, C.S., Frazier, A.E., Guiard, B, Chacinska, A, Gulbis, J.M. and Ryan, M.T. (2009) MIA40 is an oxidoreductase that catalyzes oxidative protein folding in mitochondria. Nat Struct Mol Biol. 16:198-206.

Bao, R., Zhang, Y., Lou, X., Zhou, C.Z. and Chen, Y. (2009) Structural and kinetic analysis of Saccharomyces cerevisiae thioredoxin Trx1: implications for the catalytic mechanism of GSSG reduced by the thioredoxin system. Biochim Biophys Acta. 8:1218-23.

Bardwell, J.C., McGovern, C.K. and Beckwith, J. (1991) Identification of a protein required for disulfide bond formation in vivo. Cell 67(3): 581-589.

Bauer, M.F., Rothbauer, U., Muhlenbein, N., Smith, R.J., Gerbitz, K., Neupert, W. Brunner, M. and Hofmann, S. (1999) The mitochondrial TIM22 preprotein translocase is highly conserved throughout the eukaryotic kingdom. FEBS Lett. 464: 41-47.

Becker, T., Vögtle, F.N., Stojanovski, D. and Meisinger C. (2008) Sorting and assembly of mitochondrial outer membrane proteins. Biochim Biophys Acta.1777(7-8): 557-563.

Becker, T., Gebert, M., Pfanner, N. and van der Laan, M. (2009) Biogenesis of mitochondrial proteins. Current Opinion in cell Biology 21:484-493.

Beverly, K.N., Sawaya, M.R., Schmid, E. and Koehler, C.M. (2008) the Tim8-Tim13 complex has multiple substrate binding sites and binds cooperatively to Tim23. J. Mol. Biol. 382: 1144-1156.

Bien, M., Longen, S., Wagener, N., Chwalla, I., Herrmann, J. and Riemer, J. (2010) Mitochondrial disulfide bond formation is driven by intersubunit electron transfer in Erv1 and proofread by glutathione. Mol Cell 37: 516-528.

Bihlmaier, K., Mesecke, N., Terziyska, N., Bien, M., Hell, K., and Herrmann, J.M. (2007) The disulfide relay system of mitochondria is connected to the respiratory chain. J. Cell. Biol. 179: 389-395.

Boisnard, S., Lagniel, G., Garmendia-Torres, C., Molin, M., Boy-Marcotte, E., Jacquet, M., Toledano, M.B., Labarre, J. and Chédin, S. (2009) H_2O_2 activates the nuclear localization of Msn2 and Maf1 through thioredoxins in Saccharomyces cerevisiae. Eukaryot Cell. 9: 1429-1438.

Böttinger, L., Gornicka, A., Czerwik, T., Bragoszewski, P., Loniewska-Lwowska, A., Schulze-Specking, A., Truscott, K.N., Guiard, B., Milenkovic, D. and Chacinska, A. (2012) In vivo evidence for cooperation of Mia40 and Erv1 in the oxidation of mitochondrial proteins. Mol Biol Cell. *In press*

Bouress, M., Dabir, D.V., Tienson, H.L., Sorokina, I., Koehler, C.M. and Barrientos, A. (2012) Role of the twin–CysX_9Cys motif cysteines in mitochondrial import of the cytochrome c oxidase biogenesis factor Cmc1. J Biol Chem 287(37): 31258-31269.

Brandes, H.K., Larimer, F.W., Geck, M.K., Stringer, C.D., Schürmann, P. and Hartman, F.C. (1993) Direct identification of the primary nucleophile of thioredoxin f. J Biol chem 268(25): 18411-18414. J Biol Chem 268(25): 18411-18414.

Braun, H.P. and Schmitz, U.K. (1997) The mitochondrial processing peptidase. Int J Biochem Cell Biol. 29(8-9): 1043-5. Review.

Burger, G, Gray M.W., Lang, B.F. (2003) Mitochondrial genomes: anything goes. Trends Genet. Dec. 19(12): 709-716.

Chacinska, A., Pfannschmidt, S., Wiedemann, N., Kozjak, V., Sanjuán Szklarz, L.K., Schulze-Specking, A., Truscott, K.N., Guiard, B., Meisinger, C. and Pfanner, N. (2004) Essential role of Mia40 in import and assembly of mitochondrial intermembrane space proteins. The EMBO Journal 23: 3735:3746.

Chacinska, A., Lind, M., Frazier, A.E., Dudek, J., Meisinger, C., Geissler, A., Sickmann, A., Meyer, H.E., Truscott, K.N., Guiard, B., Pfanner, N. and Rehling, P. (2005) Mitochondrial presequence translocase: switching between TOM tethering and motor recruitment involves Tim21 and Tim17. Cell 120(6): 817-829.

Chacinska, A., Guiard, B., Müller, J.M., Schulze-Specking, A., Gabriel, K., Kutik, S. and Pfanner, N. (2008a) Mitochondrial biogenesis, switching the sorting pathway of the intermembrane space receptor Mia40. J Biol Chem. 283(44): 29723-29729.

Chacinska, A. (2008b) Mitochondrial protein import: precursor oxidation in a ternary complex with disulfide carrier and sulfhydryl oxidase. J Cell Biol, 183: 195-202.

Chacinska, A., Koehler, C.M., Milenkovic, D., Lithgow, T. and Pfanner, N. (2009) Importing mitochondrial proteins: machineries and mechanisms.Cell 138(4): 628-644.

Changping, L., Thompson, M.A., Tamayo, A.T., Zuo, Z., Lee, J., Vega, F., Ford, R.J. and Pham, L.V. (2012) Over-expression of Thioredoxin-1 mediates growth, survival, and chemoresistance and is a druggable target in diffuse large B-cell lymphoma. Oncotarget 3: 314-326.

Chen, Z. and Lash, L.H. (1998) Evidence for mitochondrial uptake of glutathione by dicarboxylate and 2-oxoglutarate carriers. J Pharmacol Exp Ther. 285(2): 608-618.

Collins, Y., Chouchani, E.T., James, A.M., Menger, K. E., Cochemé, H.M. and Murphy, M.P. (2012) Mitochondrial redox signalling at a glance. J. Cell Sci. 125: 801-806.

Collinson, E.J., Wheeler, G.L., Garrido, E.O., Avery, A.M., Avery, S.V. and Grant, C.M. (2002) The yeast glutaredoxins are active as glutathione peroxidases. J Biol Chem. 277(19): 16712-16717.

Collinson, E.J. and Grant C.M. (2003) Role of yeast glutaredoxins as glutathione S-transferases. J Biol Chem. 278(25): 22492-22497.

Coppock, D.L. and Thorpe, C. (2006) Multidomain flavin-dependent sulfhydryl oxidases. Antioxid Redox Signal. 8(3-4): 300-311.

Corral-Debrinski, M., Blugeon, C. and Jacq, C. (2000) In yeast, the 3' untraslated region or the presequence of ATM1 is required for the exclusive localization of its mRNA to the vicinity of mitochondria. Mol. Cell. Biol. 358: 396-405.

Curran, S.P., Leuenberger, D., Opplinger, W. and Koehler C.M. (2002a) The Tim9p-Tim10p complex binds to the transmembrane domains of the ADP/ATP carrier. EMBO J. 21: 942-953.

Curran, S.P. Leuenberger, D., Leverich, E.P., Hwang, D.K., Beverly, K.N. and Koehler C.M. (2004) The role of Hot13p and redox chemistry in the mitochondrial TIM22 import pathway. J Biol Chem. 279(42): 43744-43751.

Curran, S.P., Leuenberger, D., Schmidt, E. and Koehler C.M. (2002b) The role of the Tim8p-Tim13p complex in a conserved import pathway for mitochondrial polytopic inner membrane proteins. J. Cell. Biol. 158: 1017-1027.

Dabir, D.V., Leverich, E.P., Kim, S.K., Tsai, F.D., Hirasawa, M., Knaff, D.B. and Koehler, C.M. (2007) A role for cytochrome c and cytochrome c reductase in electron shuttling from Erv1. Embo J. 26: 4801-4811.

Daithankar, V., Farrell, S.R., and Thorpe, C. (2009) Augmenter of liver regeneration: Substrate specificity of a flavin-dependent oxidoreductase from the mitochondrial intermembrane space. Biochemistry, 48: 4828-4837.

Dardalhon, M., Kumar, C., Iraqui, I., Vernis, L., Kienda, G., Banach-Latapy, A., He, T., Chanet, R., Faye, G., Outten, C.E. and Huang ME (2012) Redox-sensitive YFP sensors monitor dynamic nuclear and cytosolic glutathione redox changes. Free Radic Biol Med. 52(11-12): 2254-65.

Day, A.M., Brown, J.B., Taylor, S.R., Rand, J.D., Morgan, B.A. and Veal, E. Inactivation of a peroxiredoxin by hydrogen peroxide is critical for thioredoxin-mediated repair of oxidized proteins and cell survival. Molecular Cell 45: 398-408.

Davis, A.J., Sepuri, N.B., Holder, J., Johnson, A.E., Jensen, R.E. (2000) Two intermembrane space TIM complexes interact with different domains of Tim23p during its import into mitochondria. J Cell Biol. 150(6): 1271-1282.

Daum, G., Böhni, P.C. and Schatz, G. (1982a) Import of proteins into mitochondria. Cytochrome b2 and cytochrome c peroxidase are located in the intermembrane space of yeast mitochondria. J Biol Chem. 257(21): 13028-13033.

Daum, S.M., Gasser, G. and Schatz, G. (1982b) Import of proteins into mitochondria. Energy-dependent, two-step processing of the intermembrane space enzyme cytochrome b2 by isolated yeast mitochondria. J. Biol. Chem. 257: 13075-13080.

Dekker, P.J., Ryan, M.T., Brix, J., Müller, H., Hönlinger, A. and Pfanner, N. (1998) Preprotein translocase of the outer mitochondrial membrane: molecular dissection and assembly of the general import pore complex. Mol Cell Biol. 11: 6515-6524.

Derman, A.I. and Beckwith, J. (1991) Escherichia coli alkaline phosphatase fails to acquire disulfide bonds when retained in the cytoplasm. J Bacteriol. 173(23): 7719-7722.

Diekert, K., de Kroon, AI., Ahting, U., Niggemeyer, B., Neupert, W., de Kruijff, B. and Lill R. (2001) Apocytochrome c requires the TOM complex for translocation across the mitochondrial outer membrane. EMBO J. 20(20): 5626-5635.

Dietmeier, K., Hönlinger, A., Bömer, U., Dekker, P.J., Eckerskorn, C., Lottspeich, F., Kübrich, M, and Pfanner, N. (1997) Tom5 functionally links mitochondrial preprotein receptors to the general import pore. Nature 388(6638): 195-200.

Dimmer, K.S., Papic, D., Schumann, B., Sperl, D., Krumpe, K., Walther, D.M. and Rapaport D. (2012) A crucial role for Mim2 in the biogenesis of mitochondrial outer membrane proteins. J Cell Sci. 125(Pt14): 3464-3473.

Draculic, T., Dawes, I.W. and Grant, C.M. (2000) A single glutaredoxin or thioredoxin gene is essential for viability in the yeast Saccharomyces cerevisiae. Mol Microbiol. 36(5): 1167-1174.

D'Silva, P., Liu, Q., Walter, W. and Craig, E.A. (2004) Regulated interactions of mtHsp70 with Tim44 at the translocon in the mitochondrial inner membrane. Nat Struct Mol Biol. 11(11): 1084-1091.

Duhl, D.M., Powell, T. and Poyton, R.O. (1990) Mitochondrial import of cytochrome c oxidase subunit VIIa in Saccharomyces cerevisiae. Identification of sequences required for mitochondrial localization in vivo. J Biol Chem. 265(13): 7273-7.

Durigon, R., Wang, Q., Ceh Pavia, E., Grant, C.M. and Lu, H. (2012) Cytosolic thioredoxin system facilitates the import of mitochondrial small Tim proteins. EMBO *reports* 13: 916-922.

Dutton, R.J., Boyd, D., Berkmen, M. and Beckwith, J. (2008) Bacterial species exhibit diversity in their mechanisms and capacity for protein disulfide bond formation. Proc Natl Acad Sci USA 105(33): 11933-11938.

Dutton, R.J., Wayman, A., Wei, J.R., Rubin, E.J., Beckwith, J. and Boyd, D. (2010) Inhibition of bacterial disulfide bond formation by the anticoagulant warfarin. Proc Natl Acad Sci USA 107(1): 297-301.

Eckers, E., Bien, M, Stroobant, V., Herrmann, J.M. and Deponte, M. (2009). Biochemical characterization of dithiol glutaredoxin 8 from Saccharomyces cerevisiae: the catalytic redox mechanism redux. Biochemistry 48: 1410-1423.

Endres, M., Neupert, W. and Brunner, M. (1999) Transport of the ADP/ATP carrier of mitochondria from the TOM complex to the TIM22.54 complex. EMBO J. 18(12): 3214-21.
Esaki, M., Kanamori, T., Nishikawa, S., Shin, I., Schultz, P.G. and Endo T. (2003) Tom40 protein import channel binds to non-native proteins and prevents their aggregation. Nat Struct Biol. 10(12): 988-994.

Esaki, M., Shimizu, H., Ono, T., Yamamoto, H., Kanamori, T., Nishikawa, S. and Endo, T. (2004) Mitochondrial protein import. Requirement of presequence elements and tom components for precursor binding to the TOM complex. J Biol Chem. 279(44):45701-7

Fass, D. (2008) The Erv family of sulphydryl oxidases. Biochim Biophys Acta. 1783(4): 557-566.

Feng, Y., Zhong, N., Rouhier, N., Hase, T., Kusunoki, M., Jacquot, J.P., Jin, C. and Xia B. (2006) Structural insight into poplar glutaredoxin C1 with a bridging iron-sulfur cluster at the active site. Biochemistry 26: 7998-8008.

Field, L.S., Furukawa, Y., O'Halloran, T.V. and Culotta, V.C. (2003) Factors controlling the uptake of yeast copper/zinc superoxide dismutase into mitochondria. J Biol Chem. 278(30): 28052-28059.

Frazier, A.E., Dudek, J., Guiard, B., Voos, W., Li, Y., Lind, M., Meisinger, C., Geissler, A., Sickmann, A., Meyer, H.E,, Bilanchone, V., Cumsky, M.G., Truscott, K.N., Pfanner, N. and Rehling P. (2004) Pam16 has an essential role in the mitochondrial protein import motor. Nat Struct Mol Biol. 11(3): 226-33.

Gabriel, K., Egan, B. and Lithgow, T. (2003) Tom40, the import channel of the mitochondrial outer membrane, plays an active role in sorting imported proteins. EMBO J. 22(10): 2380-2386.

Gabriel, K., Milenkovic, D., Chacinska, A., Müller, J., Guiard, B., Pfanner, N. and Meisinger, C. (2007) Novel mitochondrial intermembrane space proteins as substrates of the MIA import pathway. J. Mol. Biol. 365: 612-620.

Gakh, O., Cavadini, P. and Isaya, G. (2002) Mitochondrial processing peptidases. Biochim Biophys 1592(1): 63-77. Review.

Garrido, E.O. and Grant, C.M. (2002) Role of thioredioxins in the response of saccharomyces cerevisiae to oxidative stress induced by hydroperoxides. Mol Microbiol. 43(4): 993-1003.

Gärtner, F., Voos, W., Querol, A., Miller, B.R., Craig, E.A., Cumsky, M.G. and Pfanner N. (1995) Mitochondrial import of subunit Va of cytochrome c oxidase characterized with yeast mutants. J Biol Chem. 270(8): 3788-95.

Gentle, I.E., Perry, A.J., Alcock, F.H., Likić, V.A., Dolezal, P., Ting Ng, E., Purcell, A.W., McConnville, M., Naderer, T., Chanez, A., Charrière, F., Aschinger, C., Schneider, A., Tokatlidis, K. and Lithgow, T. (2007) Conserved motifs reveal details of ancestry and structure in the small TIM chaperones of the mitochondrial intermembrane space. Mol. Biol. Evol. 24(5): 1149-1160.

Gevorkyan-Airapetov, L., Zohary, K., Popov-Celeketic, D., Mapa, K., Hell, K., Neupert, W., Azem, A. and Mokranjac, D. (2009) Interaction of Tim23 with Tim50 Is essential for protein translocation by the mitochondrial TIM23 complex. J Biol Chem. 284(8): 4865-4672.

Gilbert, H.F. (1990) Molecular and cellular aspects of thiol-disulfide exchange. Adv Enzymol Relat Areas Mol Biol. 63: 69-172.

Glick, B.S., Brandt, A., Cunningham, K., Müller, S., Hallberg, R.L. and Schatz G. (1992) Cytochromes c1 and b2 are sorted to the intermembrane space of yeast mitochondria by a stop-transfer mechanism. Cell. 69(5): 809-22.

Glick, B.S. and Pon, L.A. (1995) Isolation of highly purified mitochondria from Saccharomyces cerevisiae. Methods Enzymol. 260: 213-223.

Goldberger, R.F., Epstein, C.J., and Anfinsen, C.B. (1963) Acceleration of reactivation of reduced bovin pancreatic ribonuclease by a microsomal system from rat liver. J. Bio. Vhem. 238: 628-635.

Grant, C.M., MacIver, F.H. and Dawes, I.W. (1997) Glutathione synthetase is dispensable for growth under both normal and oxidative stress conditions in the yeast Saccharomyces cerevisiae due to an accumulation of the dipeptide gamma-glutamylcysteine. Mol Biol Cell. 8(9): 1699-1707.

Grant, C.M., Perrone, G. and Dawes, I.W. (1998) Glutathione and catalase provide overlapping defenses for protection against hydrogen peroxide in the yeast Saccharomyces cerevisiae. Biochem Biophys Res Commun. 3: 893-898.

Grant, C.M., Luikenhuis, S., Beckhouse, A,, Soderbergh, M., Dawes, I.W. (2000) Differential regulation of glutaredoxin gene expression in response to stress conditions in the yeast Saccharomyces cerevisiae. Biochim Biophys Acta 1490 (1-2): 33-42.

Graumann, J., Lilie, H., Tang, X., Tucker, K.A., Hoffmann, J.H., Vijayalakshmi, J., Saper, M., Bardwell, J.C. and Jakob, U. (2001) Activation of the redox-regulated molecular chaperone Hsp33-a two-step mechanism. Structure 9(5): 377-387.

Gray, M.W., Burger, G and Lang, F. (1999) Mitochondrial evolution. Science 283: 1476-1481.

Griffith, O.W. and Meister, A. (1985) Origin and turnover of mitochondrial glutathione. Proc Natl Acad Sci U S A. 82(14): 4668-4672.

Gromer, S., Urig, S. and Becker, K. (2004) The thioredoxin system—from science to clinic. Med. Res. Rev. 24: 40–89.

Grumbt, B., Stroobant, V., Terziyska, N., Israel, L. and Hell, K. (2007) Functional characterization of Mia40p, the central component of the disulfide relay system of the mitochondrial intermembrane space. J Biol Chem. 282(52): 37461-37470.

Hachiya, N., Alam, R., Sakasegawa, Y., Sakaguchi, M., Mihara, K. and Omura, T. (1993) A mitochondrial import factor purified from rat liver cytosol is an ATP-dependent conformational modulator for precursor proteins. EMBO J. 12(4): 1579-1586.

Hadj Amor, I.Y., Smaoui, K., Chaabène, I., Mabrouk, I., Djemal, L., Elleuch, H., Allouche, M., Mokdad-Gargouri, R. and Gargouri, A. (2008) Human p53 induces cell death and downregulates thioredoxin expression in Saccharomyces cerevisiae.FEMS Yeast Res. 8: 1254-1262.

Hagiya, M., Francavilla, A., Polimeno, L., Ihara, I., Sakai, H., Seki, T., Shimonishi, M., Porter, K.A. and Starzi, T.E. (1994) Cloning and sequence analysis of the rat augmenter of liver regeneration (ALR) gene: expression of biologically active recombinant ALR and demonstration of tissue distribution. Proc Natl Acad Sci USA. 91(17): 8142-8146.

Hansen, R.E., Roth, D. and Winther, J.R. (2009) Quantifying the global cellular thiol-disulfide status. Proc Natl Acad Sci USA. 106(2): 422-427.

Haucke, V., Lithgow, T., Rospert, S., Hahne, K. and Schatz, G. (1995) The yeast mitochondrial protein import receptor Mas20p binds precursor proteins through electrostatic interaction with the positively charged presequence. J Biol Chem. 270(10): 5565-5570.

Hell, K., Herrmann, J.M., Pratje, E., Neupert, W. and Stuart, R.A. (1998) Oxa1p, an essential component of the N-tail protein export machinery in mitochondria. Proc Natl Acad Sci U S A. 95(5): 2250-5.

Hell, K., Neupert, W. and Stuart, R.A. (2001) Oxa1p acts as a general membrane insertion machinery for proteins encoded by mitochondrial DNA. EMBO J. 20(6): 1281-8.

Herrmann, J.M. and Neupert, W. (2003) Protein insertion into the inner membrane of mitochondria. IUBMB Life. 55(4-5): 219-225.

Hill. K., Model, K., Ryan, M.T., Dietmeier, K., Martin, F., Wagner, R. and Pfanner, N. (1998) Tom40 forms the hydrophilic channel of the mitochondrial import pore for preproteins. Nature 395(6701): 516-521.

Ho, Y.S., Xiong, Y., Ho, D.S., Gao, J., Chua, B.H.L., *et al.* (2007) Targeted disruption of the glutaredoxin 1 gene does not sensitize adult mice to tissue injury induced by ischemia/reperfusion and hyperoxia. Free Radic. Biol. Med. 43: 1299–312

Holmgren, A. (1976) Hydrogen donor system for Escherichia coli ribonucleoside-diphosphate reductase dependent upon glutathione. Proc Natl Acad Sci USA 73(7): 2275-2279.

Holmgren, A. (1979) Thioredoxin catalyzes the reduction of insulin disulfide by dithiothreitol and dihydrolipoamide. J Biol Chem. 254(19): 9627-9632.

Holmgren, A. (1985) Thioredoxin. Annu Rev Biochem. 54: 237-271.

Holmgren, A. (1989) Thioredoxin and glutaredoxin systems. J Biol Chem. 264(24): 13963-13966.

Holst, B., Tachibana, C. and Winther, J.R. (1997) Active site mutations in yeast protein disulfide isomerase cause dithiothreitol sensitivity and a reduced rate of protein folding in the endoplasmic reticulum. J Cell Biol 138(6): 1229-1238.

Hoongeraad, N.J. and Ryan, M.T. (2001) Translocation of proteins into mitochondria. IUBMB Life. 51(6): 345-350.

Horn, D., Zhou, W., Trevisson, E., Al-Ali, H., Harris, T.K., Salviati, L. and Barrientos, A. (2010) The conserved mitochondrial twin Cx9C protein Cmc2 is a Cmc1 homologue essential for cytochrome c oxidase biogenesis. J Biol Chem. 285(20): 15088-15099.

Hu, J., Ding, L. and Outten, C.E. (2008) The redox environment in the mitochondrial intermembrane space is maintained separately from the cytosol and the matrix. J Biol Chem. 283(43): 29126-29134.

Hutu, D.P., Guiard, B., Chacinska, A., Becker, D., Pfanner, N., Rehling, P. and van der Laan, M. (2008) Mitochondrial protein import motor: differential role of Tim44 in the recruitment of Pam17 and J-complex to the presequence translocase. Mol Biol Cell 19(6): 2642-2649.

Hwang, D.K., Claypool, S.M., Leuenberger, D., Tienson, H.L. and Koehler C.M. (2007) Tim54p connects inner membrane assembly and proteolytic pathways in the mitochondrion. J Cell Biol. 178(7): 1161-75.

Ivanova, E., Jowitt, T.A. and Lu, H. (2008) Assembly of the mitochondrial Tim9-Tim10 complex: a multi-step reaction with novel intermediates. J Mol Biol. 375(1): 229-239.

Izawa, S., Maeda, K., Sugiyama, K., Mano, J., Inoue, Y., Kimura, A. (1999) Thioredoxin deficiency causes the constitutive activation of Yap1, an AP-1-like

transcription factor in Saccharomyces cerevisiae. J Biol Chem. 274(40): 28459-28465.

Izquierdo, A., Casas, C. and Herrero, E. (2010) Selenite-induced cell death in Saccharomyces cerevisiae: protective role of glutaredoxins. Microbiology 156(Pt 9): 2608-2620.

Jan, P.S., Esser, K., Pratje, E. and Michaelis G. (2000) Som1, a third component of the yeast mitochondrial inner membrane peptidase complex that contains Imp1 and Imp2. Mol Gen Genet. 263(3): 483-91.

Jakob, U., Muse, W, Eser, M. and Bardwell, J.C.A., Chaperone activity with a redox switch. Cell 96:341-352.

Jarosch, E., Tuller, G., Daum, G., Waldherr, M., Voskova, A. and Schweyen, R.J. (1996) Mrs5p, an essential protein of the mitochondrial intermembrane space, affects protein import into yeast mitochondria. J. Biol. Chem. 271:17219-17225.

Jin, H., May, M., Tranebjaerg, L., Kendall, E., Fontán, G., Jackson, J., Subramony, S.H., Arena, F., Lubs, H, Smith, S, Stevenson, R., Schwartz, C and

Jin, H., Kendall, E., Freeman, T.C, Roberts, R.G. and Vetrie, D.L.P. (1999) The human family of deafness/Dystonia peptide (DDP) related mitochondrial import proteins. Genomics 61:259-267.

Jung, C.H. and Thomas, J.A. (1996) S-glutathiolated hepatocyte proteins and insulin disulfides as substrates for reduction by glutaredoxin, thioredoxin, protein disulfide isomerase, and glutathione. Arch Biochem Biophys. 335(1): 61-72.

Kanamori, T., Nishikawa, S., Nakai, M., Shin, I., Schultz, P.G. and Endo T. (1999) Uncoupling of transfer of the presequence and unfolding of the mature domain in precursor translocation across the mitochondrial outer membrane. Proc Natl Acad Sci U S A. 96(7):3634-9.

Kaplowitz, N., Fernández-Checa, J.C., Kannan, R., Garcia-Ruiz, C., Ookhtens, M. and Yi, J.R. (1996) GSH transporters: molecular characterization and role in GSH homeostasis. Biol Chem Hoppe Seyler. 377(5): 267-273.

Káldi, K., Bauer, M.F., Sirrenberg, C., Neupert, W. and Brunner M. (1998) Biogenesis of Tim23 and Tim17, integral components of the TIM machinery for matrix-targeted preproteins. EMBO J. 17(6): 1569-76.

Kawano, S., Yamano, K., Naoe, M., Momose, T., Terao. K., Nishikawa, S., Watanabe, N., and Endo, T. (2009) structural basis of yeast Tim40/Mia40 as an oxidative translocator in the mitochondrial intermembrane space. Proc Natl Acad Sci USA 106:14403-14407.

Kawamata, H and Manfredi, G. (2008) Different regulation of wild-type and mutant Cu,Zn superoxide dismutase localization in mammalian mitochondria. Hum Mol Genet. 17(21): 3303-3317.

Kiebler, M., Keil, P., Schneider, H., van der Klei, I.J., Pfanner, N. and Neupert W. (1993) The mitochondrial receptor complex: a central role of MOM22 in mediating preprotein transfer from receptors to the general insertion pore. Cell. 74(3): 483-492.

Koehler, C.M., Merchant, S., Oppliger, W., Schmid, K., Jarosch, E., Dolfini, L., Junne, T., Schatz, G. and Tokatlidis, K. (1998) Tim9p, an essential partner subunit of Tim10p for the import of mitochondrial carrier proteins. Embo J. 17: 6477-6486.

Koehler, C.M., Leuenberger, D., Merchant, S., Renold, A., Junne, T., Schatz, G. (1999). Human deafness dystonia syndrome is a mitochondrial disease. Proc Natl Acad Sci USA. 96: 2141-2146.

Koehler, C.M. (2000) Protein translocation pathways of the mitochondrion. *FEBS Lett.* 476, 27-31.

Koehler, C.M. (2004) The small Tim proteins and the twin Cx3C motif. TRENDS in Biochemical Science 29 (1): 1-4.

Komiya, T., Rospert, S., Koehler, C., Looser, R., Schatz, G. and Mihara, K. (1998) Interaction of mitochondrial targeting signals with acidic receptor domains along the protein import pathway: evidence for the 'acid chain' hypothesis. EMBO J. 17(14): 3886-3898.

Kovermann, P., Truscott, K.N., Guiard, B., Rehling, P., Sepuri, N.B., Müller, H., Jensen, R.E., Wagner, R. and Pfanner, N. (2002) Tim22, the essential core of the mitochondrial protein insertion complex, forms a voltage-activated and signal-gated channel. Mol Cell. 9(2): 363-73

Kozany, C., Mokranjac, D., Sichting, M., Neupert, W. and Hell, K. (2004) The J domain-related cochaperone Tim16 is a constituent of the mitochondrial TIM23 preprotein translocase. Nat Struct Mol Biol. 11(3): 234-41.

Kuge, S. and Jones, N. (1994) YAP1 dependent activation of TRX2 is essential for the response of Saccharomyces cerevisiae to oxidative stress by hydroperoxides. EMBO J. 13(3): 655-64.

Künkele, K.P, Heins, S., Dembowski, M. Nargang, F.E., Benz, R., Thieffry, M., Walz, J., Lill, R., Nussberger, S. and Neupert, W. (1998) The preprotein translocation channel of the outer membrane of mitochondria. Cell 93(6): 1009-1019.

Kurz, M., Martin, H., Rassow, J., Pfanner, N. and Ryan M.T. (1999) Biogenesis of Tim proteins of the mitochondrial carrier import pathway: differential targeting mechanisms and crossing over with the main import pathway. Mol Biol Cell. 10(7): 2461-2474

Lee, J., Hofhaus, G. and Lisowsky, T. (2000) Erv1p from Saccatomyces cerevisiae is a FAD-linked sulfhydryl oxidase. FEBS Lett. 477: 62-66.

Dario Leister and Johannes M. Herrmann, 2007. *Mitochondria: practical protocols*, Humana Press.

Leuenberger, D., Bally, N.A., Schatz, G. and Koehler, C.M. (1999) Different import pathways through the mitochondrial intermembrane space for inner membrane proteins. EMBO J. 18(17): 4816-4822.

Lian, F.M., Yu, J., Ma, X.X., Yu, X.J., Chen, Y. and Zhou, C.Z. (2012) Structural snapshots of yeast alkyl hydroperoxide reducatse Ahp1 peroxiredoxin reveal a novel two-cysteine mechanism of electron transfer to eliminate reactive oxygen species. J Biol Chem. 287(21): 17077-17087.

Lillig, C.H., Prior, A., Schwenn, J.D., Aslund, F, Ritz, D., Vlamis-Gradikas, A., Holmgren, A. (1999) New thioredoxins and glutaredoxins as electron donors of 3'-phosphoadenylylsulfate reductase. J Biol chem 274(12): 7695-7698.

Lillig, C.H., Berndt, C., Vergnolle, O., Lönn, M.E., Hudemann, C., Bill, E. and Holmgren A. (2005) Characterization of human glutaredoxin 2 as iron-sulfur protein: a possible role as redox sensor. Proc Natl Acad Sci U S A. (23): 8168-73.

Lillig, C.H. and Holmgren, A. (2007) Thioredoxin and related molecules—from biology to health and disease. Antioxid. Redox Signal. 9: 25–47

Lionaki, E., de Marcos Lousa, C., Baud, C., Vougioukalaki, M., Panayotou, G. and Tokatlidis, K. (2008) The essential function of Tim12 in vivo is ensured by the assembly interactions of its C-terminal domain. J Biol Chem. 283(23): 15747-53.

Lisowsky, T. (1992) Dual function of a new nuclear gene for oxidative phosphorylation and vegetative growth in yeast. Mol Gen Genet 323: 58-64.

Liu, Q., D'Silva, P., Walter, W., Marszalek, J. and Craig, E.A. (2003) Regulated cycling of mitochondrial Hsp70 at the protein import channel. Science 300(5616): 139-141.

Longen, S., Bien, M. Bihlmaier, K., Kloeppel, C., Kauff, F., Hammermeister, M., Westermann, B., Herrmann, J.M. and Riemer, J. (2009) Systematic analysis of the twin CX_9C protein familiy. J Mol Biol. 393 (2): 356-368.

Lu, H., Golovanov, A.P., Alcock, F., Grossman, J.G., Allen, Lian, L.Y. and Tokatlidis, K. (2004a) The structural basis of the TIM10 chaperone assembly. J. Biol Chem. 279: 18959-966.

Lu, H., Allen, S, Wardleworth, L., Savory, P., and Tokatlidis, K. (2004b) Functional TIM10 chaperone assembly is redox regulated in vivo. J. Biol. Chem. 279: 18952-18958.

Lu, H. and Woodburn, J. (2005) Zinc binding stabilizes mitochondrial Tim10 in a reduced and import-competent state kinetically. J Mol. Biol. 353: 897-910.

Lu, J., Holmgren, A. (2012) Thioredoxin system in cell death progression. Antioxidants and Redox Signaling. 15: 1738-1747.

Luciano, P., Vial, S., Vergnolle, M.A., Dyall, S.D., Robinson, D.R., and Tokatlidis, K. (2005) Functional reconstitution of the import of the yeast ADP/ATP carrier mediated by Tim10 complex. EMBO J. 20: 4099-4106.

Luikenhuis, S., Dawes, I.W. and Grant, C.M. (1998) The yeast Saccharomyces cerevisiae contains two glutaredoxin genes that are required for protection against reactive oxygen species. Mol Biol Cell. 9: 1081-1091.

Lutz, T., Neupert, W. and Herrmann, J.M. (2003) Import of small Tim proteins into the mitochondrial intermembrane space. EMBO J. 22: 4400-4408.

Machado, A.K., Morgan, B.A. and Merrill, G.F. (1997) Thioredoxin reductase-dependent inhibition of MCB cell cycle box activity in Saccharomyces cerevisiae. J Biol Chem. 272(27): 17045-17054.

Marc, P., Margeot, A., Devaux, F., Blugeon, C., Corral-Debrinski, M. and Jacq, C. (2002) Genome-wide analysis of mRNAs targeted to yeast mitochondria. EMBO Rep. 3: 159-164.

Mallick, P., Boutz, D.R., Eisenberg, D. and Yeates, T.O. (2002) Genomic evidence that the intracellular proteins of archaeal microbes contain disulfide bonds. Proc Natl Acad Sci USA 99(15): 9679-9684.

Maret, W. and Vallee, B.L. (1998) Thiolate ligands in metallothionein confer redox activity on zinc clusters. Proc Natl Acad Sci U S A. 95(7): 3478-3482.

Martin, J.L. (1995) Thioredoxin–a fold for all reasons. Structure 3: 245–250.

Mayer, A., Neupert, W. and Lill, R. (1995) Translocation of apocytochrome c across the outer membrane of mitochondria. J Biol Chem. 270(21): 12390-12397.

Margulis, L., 1970 Origin of Eukaryotic Cells, Yale University Press.

Matsui M, Oshima M, Oshima H, Takaku K, Maruyama T, *et al.* (1996) Early embryonic lethality caused by targeted disruption of the mouse thioredoxin gene. Dev. Biol. 178: 179–85.

Mckenzie, M., Liolitsa, D. and Hanna, M.G. (2004) Mitochondrial disease: mutations and mechanisms. Neurochem Res. Mar: 29(3): 589-600.

Meinecke, M., Wagner, R., Kovermann, P., Guiard, B., Mick, D.U, Hutu, D.P., Voos, W., Truscott, K.N,, Chacinska, A., Pfanner, N. and Rehling, P. (2006) Tim50 maintains the permeability barrier of the mitochondrial inner membrane. Science 312(5779): 1523-1526.

Meisinger, C., Rissler, M, Chacinska, A., Sanjuán Szklarz, L.K., Milenkovic, D., Kozjak, V., Schönfisch, B., Lohaus, C., Meyer, H.E., Yaffe, M.P. et al. (2004) The mitochondrial morphology protein Mdm10 functions in assembly of the preprotein translcoate of the outer membrane. Dev Cell 7: 61-71.

Meyer, Y., Buchanan, B.B, Vignols, F. and Reichheld, J.P. (2009) Thioredoxins and glutaredoxins: unifying elememts in redox biology. Annu ev Genet. 43: 335-367.

Mesecke, N., Terziyska, N., Kozany, C., Baumann, F., Neupert, W., Hell, K., and Herrmann, J.M. (2005) A disulfide relay system in the intermembrane space of mitochondria that mediates protein import. Cell 121: 1059:1069.

Mesecke, N., Bihlmaier, K., Grumbt, B, Longen, s, Terziysha, N., Hell, K. and Herrmann, J.M. (2008) The zinc-binding protein Hot13 promotes oxidation of the mitochondrial import receptor Mia40. Embo Rep. 9: 1107-1113.

Messens, J., Van Molle, I., Vanhaesebrouck, P., Limbourg, M., Van Belle, K., Wahni, K., Martins, J.C., Loris, R. and Wyns L. (2004) How thioredoxin can reduce a buried disulphide bond. J Mol Biol. 339(3): 527-537.

Milenkovic, D., K., Guiard, B., Schulze-Specking, A., Pfanner, N., and Chacinska, A. (2007) Biogenesis of the essential Tim9-Tim10 chaperone complex of mitochondria. The Journal of Biological Chemistry 272(31): 22472-22480.

Milenkovic, D., Ramming, T., Müller, J.M., Wenz, L.S., gbert, N., Schulze-Speckig, A., Stojanovski, D., Ropert, S. and Chacinska, A. (2009) Identification of the signal directing Tim9 an Tim01 into the intermembrane space of mitochondria. Mol Biol Cell 20:2530-2539.

Miller, B.R. and Cumsky, M.G. (1993) Intramitochondrial sorting of the precursor to yeast cytochrome c oxidase subunit Va. J Cell Biol. 121(5): 1021-9.

Mokranjac, D., Sichting, M., Neupert, W. and Hell, K. (2003) Tim14, a novel key component of the import motor of the TIM23 protein translocase of mitochondria. EMBO J. 22(19): 4945-4956.

Mokranjac, D. and Neupert, W. (2009). Thirty years of protein translocation into mitochondria: Unexpectedly complex and still puzzling. Biochim Biophys Acta, 1793(1):33-41.

Mokranjac, D. and Neupert, W. (2008) Energetics of protein translocation into mitochondria. Biochim Biophys Acta, 1777(7-8): 758-62.

Mokranjac, D., Sichting, M., Popov-Celeketić, D., Mapa, K., Gevorkyan-Airapetov, L., Zohary, K., Hell, K., Azem, A. and Neupert, W. (2009) Role of Tim50 in the transfer of precursor proteins from the outer to the inner membrane of mitochondria. Mol Biol Cell 20(5): 1400-1407.

Mossmann, D., Meisinger, C., and Vögtle, F.N. (2011) Processing of mitochondrial presequences. Biochim. Biophys. Acta. 1819(9-10): 1098-1106.

Morgan, B. and Lu, H. (2008) Oxidative folding competes with mitochondrial import of the small Tim proteins. Biochem. J. 411:115-122.

Morgan, B., Ang, S.K., Yan, G. and Lu, H (2009) Zinc can play chaperone-like and inhibitor roles during import of mitochondrial small Tim proteins. J. Biol. Chem. 284:6818-6825.

Mühlenbein, N., Hofmann, S., Rothbauer, U. and Bauer, M.F. (2004) Organization and function of the small Tim complexes acting along the import pathway of metabolite carriers into mammalian mitochondria. J Biol Chem. 279(14): 13540-6.

Muller, E.G. (1991) Thioredoxin deficiency in yeast prolongs S phase and shortens the G1 interval of the cell cycle. J Biol Chem. 266(14): 9194-9202.

Muller, E.G. (1995) A redox-dependent function of thioredoxin is necessary to sustain a rapid rate of DNA synthesis in yeast. Arch Biochem Biophys. 318(2): 356-361.

Muller, E.G. (1996) A glutathione reductase mutant of yeast accumulates high levels of oxidized glutathione and requires thioredoxin for growth. Mol Biol Cell. 7(11): 1805-1813.

Müller, J.M., Milenkovic, D., Guiard, B., Pfanner, N. and Chacinska A. (2008) Precursor oxidation by Mia40 and Erv1 promotes vectorial transport of proteins into the mitochondrial intermembrane space. Mol Biol Cell. 19(1): 226-236.

Naoe, M., Ohwa, Y., Ishikawa, D., Ohshima, C., Nishikawa, S., Yamamoto, H., and Endo, T. (2004) Identification of Tim40 that mediates protein sorting to the mitochondrial intermembrane space. J Biol Chem 279(12): 47815-47821.

Nargang, F.E., Drygas, M.E., Kwong, P.L., Nicholson, D.W. and Neupert, W. (1988) A mutant of Neurospora crassa deficient in cytochrome c heme lyase activity cannot import cytochrome c into mitochondria. J Biol Chem. 263(19): 9388-9394.

Neupert, W. (1997) Protein import into mitochondria. Annu Rev Biochem. 66: 863-917.

Neupert, W and Herrmann, J.M. (2007) Translocation of proteins into mitochondria. Annu. Rev. Biochem. 76: 723-749.

Ng, C.H., Tan, S.X., Perrone, G.G., Thorpe, G.W., Higgins, V.J. and Dawes, I.W. (2008) Adaptation to hydrogen peroxide in Saccharomyces cerevisiae: the

role of NADPH-generating systems and the SKN7 transcription factor. Free Radic Biol Med. 44(6): 1131-1145.

Nobrega, M.P., Bandeira, S.C., Beers, J. and Tzagoloff, A. (2002) Characterization of COX19, a widely distributed gene required for expression of mitochondrial cytochrome oxidase. J Biol Chem. 277: 40206-40211.

Nordberg, J. and Arnér, E.S.J. (2001) Reactive oxygen species, antioxidants, and the mammalian thioredoxin system. Free Radic. Biol. Med., 31: 1287–1312

Østergaard, H., Tachibana, C. and Winther, J.R. (2004) Monitoring disulfide bond formation in the eukaryotic cytosol. J Cell Biol 166(3) 337-345.

Paschen, S.A. and Neupert, W. (2001) Protein import into mitochondria. *IUBMB Life* 52, 101-112.

Paschen, S.A., Waizenegger, T., Stan, T., Preuss, M., Cyrklaff, M., Hell, K., Rapaport, D. and Neupert, W. (2003) Evolutionary conservation of biogenesis of beta-barrel membrane proteins. Nature 426(6968): 862-866.

Pearson, G.D. and Merrill, G.F. (1998) Deletion of the Saccharomyces cerevisiae TRR1 gene encoding thioredoxin reductase inhibits p53-dependent reporter gene expression. J Biol Chem. 273(10): 5431-5434.

Perry, A.J., Rimmer, K.A., Mertens, H.D., Mulhern, T.D., Lithgow, T. and Gooley, P.R. (2008) Structure, topology and function of the translocase of the outer membrane of mitochondria. Plant Physiol Biochem. Ma; 47(3): 256-274.

Pe'er, I., Felder, C.E., Man, O., Silman, I., Sussman, J.L, and Beckmann J.S. (2004) Proteomic signatures: amino acid and oligopeptide compositions differentiate among phyla. Proteins 54(1): 20-40.

Pfaller, R., Pfanner, N. and Neupert, W. (1989) Mitochondrial protein import. Bypass of proteinaceous surface receptors can occur with low specificity and efficiency. J Biol Chem. 264(1): 34-39.

Pfanner, N. and Geissler, A. (2001) Versatility of the mitochondrial protein import machinery. Nat rev Mol Cell Biol. 2(5): 339-349.

Pollitt, S. and Zalkin, H. (1983) Role of primary structure and disulfide bond formation in beta-lactamase secretion. J. Bacteriol. 153(1): 27-32.

Popov-Celeketić, J., Waizenegger, T. and Rapaport, D. (2008) Mim1 functions in an oligomeric form to facilitate the integration of Tom20 into the mitochondrial outer membrane. J Mol Biol. 376(3): 671-680.

Porras, P., Padilla, C.A., Krayl, M., Voos, W and Bárcena, J.A. (2006). One single in-frame AUG codon is responsible for a diversity of subcellular localizations of glutaredoxin 2 in *Saccharomices cerevisiae*. J Biol Chem 281: 16551-16562.

Prinz, W.A., Aslund, F., Holmgren, A. and Beckwith, J. (1997) The role of the thioredoxin and glutaredoxin pathways in reducing protein disulfide bonds in the Escherichia coli cytoplasm. J Biol Chem. 272(25): 15661-1567.

Qi, Y. and Grishin, N.V. (2005) Structural classification of thioredoxin-like fold proteins. Proteins 58: 376–388.

Rapaport, D., Neupert, W. and Lill, R. (1997) Mitochondrial protein import. Tom40 plays a major role in targeting and translocation of preproteins by forming a specific binding site for the presequence. J Biol Chem. 272(30): 18725-18731.

Rapaport, D., Künkele, K.P., Dembowski, M., Ahting, U., Nargang, F.E., Neupert, W. and Lill, R. (1998) Dynamics of the TOM complex of mitochondria during binding and translocation of preproteins. Mol Cell Biol 18(9): 5256-5262.

Reddehase, S., Grumbt, B., Neupert, W and Hell, K. (2009) The disulfide relay system of mitochondria is required for the biogenesis of mitochondrial Css1 and Sod1. J Mol Biol. 385(2): 331-338.

Rehling, P., Pfanner, N. and Meisinger, C. (2003) Insertion of hydrophobic membrane proteins into the inner mitochondrial membrane--a guided tour. J Mol Biol. 326(3): 639-57.

Rietsch, A., Beckwith, J. (1998) The genetics of disulfide bond metabolism. Annu Rev Genet. 32: 163-184.

Riezman, H., Hay, R., Witte, C., Nelson, N. and Schatz, G. (1983) Yeast mitochondrial outer membrane specifically binds cytoplasmically-synthesized precursors of mitochondrial proteins. EMBO J. 2(7): 1113-1118.

Rissler, M., Wiedemann, N., Pfannschmidt, S., Gabriel, K., Guiard, B., Pfanner, N. and Chacinska, A. (2005) The essential mitochondrial protein Erv1 cooperates with Mia40 in biogenesis of intermembrane space proteins. J Mol Biol. 353(3): 485-492.

Rothbauer, U., Hofmann, S., Mühlenbein, N., Paschen, S.A., Gerbitz, K.D., Neupert, W., Brunner, M. and Bauer, M.F. (2001) Role of the deafness dystonia peptide 1 (DDP1) in import of human Tim23 into the inner membrane of mitochondria. J Biol Chem. 276(40): 37327-34.

Rouhier, N., Unno, H., Bandyopadhyay, S., Masip, L., Kim, S.K., Hirasawa, M., Gualberto, J.M., Lattard, V., Kusunoki, M., Knaff, D.B., Georgiou, G., Hase, T., Johnson, M.K. and Jacquot, J.P. (2007) Functional, structural, and spectroscopic characterization of a glutathione-ligated [2Fe-2S] cluster in poplar glutaredoxin C1. Proc Natl Acad Sci U S A. 18: 7379-84.

Saitoh, T., Igura, M., Obita, T., Ose, T., Kojima, R., Maenaka, K., Endo, T. and Kohda, D. (2007) Tom20 recognizes mitochondrial presequences through dynamic equilibrium among multiple bound states. EMBO J. 26(22): 4777-4787.

Scherens, B., Dubois, E. and Messenguy, F. (1991) Determination of the sequence of the yeast YCL313 gene localized on chromosome III. Homology with the protein disulfide isomerase (PDI gene product) of other organisms. Yeast 7(2): 185-193.

Schneider, H.C., Westermann, B., Neupert, W. and Brunner, M. (1996) The nucleotide exchange factor MGE exerts a key function in the ATP-dependent cycle of mt-Hsp70-Tim44 interaction driving mitochondrial protein import. EMBO J. 15(21): 5796-5803.

Schmitt, S., Ahting, U., Eichacker, L., Granvogl, B., Go, N.E., Nargang, F.E., Neupert, W. and Nussberger, S. (2005) Role of Tom5 in maintaining the

structural stability of the TOM complex of mitochondria. J Biol Chem 280(15): 14499-14506.

Sherman, E.L., Taylor, R.D., Go, N.E. and Nargang, F.E. (2006) Effect of mutations in Tom40 on stability of the translocase of the outer mitochondrial membrane (TOM) complex, assembly of Tom40, and import of mitochondrial preproteins. J Biol Chem. 281(32): 22554-22565.

Sideris, D.P. and Tokatlidis, K. (2007) Oxidative folding of small Tims is mediated by site-specific docking onto Mia40 in the mitochondrial intermembrane space. Mol Microbiol. 65(5): 1360-1373.

Sideris, D.P., Petrakis, N., Katrakili, N., Mikropoulou, D., Gallo, A., Ciofi-Baffoni, S., Banci, L., Bertini, I, and Tokatlidis, K. (2009) A novel intermembrane space targeting signal primes cysteines for docking onto Mia40 in mitochondrial oxidative folding. J Cell Biol 187: 1007-1022.

Sirrenberg, C., Bauer, M.F., Guiard, B., Neupert, W. and Brunner M. (1996) Import of carrier proteins into the mitochondrial inner membrane mediated by Tim22. Nature 384(6609): 582-5.

Sirrenberg, C., Endres, M., Folsch, H., Stuart, R.A., Neupert, W. and Brunner, M. (1998) Carrier protein import into mitochondria mediated by the intermembrane proteins Tim10/Mrs11 and Tim12/Mrs5. Nature 391: 912-915.

Sherman, F. and Ephrussi, B. (1962) The relationship between respiratory deficiency and suppressiveness in yeast as determined with segregational mutants. Genetics. 47: 695-700.

Söllner, T., Rassow, J., and Pfanner, N. (1991) Methods Cell Biol. 34, 345–358.

Steiner, H., Zollner, A., Haid, A., Neupert, W. and Lill, R. (1995) Biogenesis of mitochondrial heme lyases in yeast. Import and folding in the intermembrane space. J Biol Chem. 270(39): 22842-22849.

Stojanovski, D., Guiard, B., Kozjak-Pavlovic, V., Pfanner, N. and Meisinger, C. (2007) Alternative function for the mitochondrial SAM complex in biogenesis of alpha-helical TOM proteins. J Cell Biol. 179(5): 881-893.

Stojanovski, D., Müller, J.M., Milenkovic, D., Guiard, B., Pfanner, N and Chacinska, A. (2008a) The MIA system for protein import into the mitochondrial intermembrane space. Biochim Biophys Acta 1783: 610-617.

Stojanovski, D., Milenkovic, D., Müller, J. M., Gabriel, K., Schulzespecking, A., Baker, M. J., Ryan, M. T., Guiard, B., Pfanner, N. & Sturtz, L.A., Diekert, K., Jensen, L.T., Lill, R. and Culotta, V.C. A fraction of yeast Cu,Zn-superoxide dismutase and its metallochaperone, CCS, localize to the intermembrane space of mitochondria. A physiological role for SOD1 in guarding against mitochondrial oxidative damage. J Biol Chem. 276(41): 38084-38089.

Tamura, Y., Harada, Y., Shiota, T., Yamano, K., Watanabe, K., Yokota, M., Yamamoto, H., Sesaki, H. and Endo, T. (2009) Tim23-Tim50 pair coordinates functions of translocators and motor proteins in mitochondrial protein import. J Cell Biol. 184(1): 129-41.

Tan, S.X., Greetham, D., Raeth, S., Grant, C.M., Dawes, I.W. and Perrone, G.G. (2009) The thioredoxin-thioredoxin reductase system can function in vivo as an alternative system to reduce oxidized glutathione in Saccharomyces cerevisiae. J Biol Chem. 9: 6118-6126.

Terziyska, N., Lutz, T., Kozany, C., Mokranjac, D., Mesecke, N., Neupert, W, Herrmann, J.M., and Hell, K. (2005) Mia40, a novel factor for protein import into the intermembrane space of mitochondria is able to bind metal ions. FEBS Lett, 579: 179-184.

Terziyska, N., Grumbt, B, Bien, M., Neupert, W., Herrmann, J.M. and Hell, K. (2007) The sulfhydryl oxidase erv1 is a substrate of the Mia40-dependent protein translocation pathway. FEBS Lett. 581: 1098-1102

Terziyska, N.,Grumbt, B., kozany, C. and Hell, K. (2009) Structural and functional roles of the conserved cysteine residues of the redox-regulated import receptor Mia40 in the intermembrane space of mitochondria. J Biol Chem. 284(3): 1353-1363.

Tienson, H.L., Dabir, D.V., Neal, S.E., Loo, R., Hasson, S.A., Boontheung, P., Kim, S.K., Loo, J.A. and Koehler, C.M. (2009) Reconstitution of the Mia40-Erv1 oxidative folding pathway for the small Tim proteins. Mol. Biol. Cell. 20: 3481-3490.

Tokatlidis, K. (2005) A disulfide relay system in mitochondria. Cell 121: 965-967.

Toledano, M.B., Kumar, C., Le Moan, N., Spector, D. and Tacnet, F. (2007) The system biology of thiol redox system in Escherichia coli and yeast: differential functions in oxidative stress, iron metabolism and DNA synthesis. FEBS Lett. 581:3598-3607.

Tranebjaerg, L., Schwartz, C., Eriksen, H., Andreasson, S., Ponjavic, V., Dahl, A., Stevenson, R. E., May, M., Arena, F., Barker, D., et al. (1995) A new X-linked recessive deafness syndrome with blindness, dystonia, fractures and mental deficiency is linked to Xq22. J. Med. Genet. 32: 257–263.

Trotter, E.W. and Grant, C.M. (2003) Non-reciprocal regulation of the redox state of the glutathione-glutaredoxin and thioredoxin systems. EMBO Rep 4(2): 184-188.

Trotter, E.W. and Grant, C.M. (2005) Overlapping roles of the cytoplasmic and mitochondrial redox regulatory systems in the yeast Saccharomyces cerevisiae. Eukaryot Cell. 4(2): 392-400.

Truscott, K.N., Wiedemann, N., Rehling, P., Müller, H., Meisinger, C., Pfanner, N. and Guiard, B. (2002) Mitochondrial import of the ADP/ATP carrier: the essential TIM complex of the intermembrane space is required for precursor release from the TOM complex. Mol Cell Biol. 22: 7780-9.

van Wilpe, S., Ryan, M.T., Hill, K., Maarse, A.C,, Meisinger, C., Brix, J., Dekker, P.J,, Moczko, M., Wagner, R., Meijer, M., Guiard, B., Hönlinger, A. and Pfanner N. (1999) Tom22 is a multifunctional organizer of the mitochondrial preprotein translocase. Nature. 401(6752): 485-489.

Vetrie, D. (1996) A novel X-linked gene, DDP, shows mutations in families with deafness (DFN-1), dystonia, mental deficiency and blindness. Nat. Genet. 14(2): 177-180.

Vignols, F., Bréhélin, C., Surdin;kerjan, Y., Thomas, D. and Meyer, Y. (2005) A yeast two hybrid knockout strain to explore thioredoxin-interacting proteins in vivo. Proc Natl Acad Sci USA 102(46): 16729-16734.

Voronova, A., Meyer-Klaucke, W., Meyer, T., Rompel, A., Krebs, B., Kazantseva, J., Sillard, R. and Palumaa, P. (2007) Oxidative switches in functioning of mammalian copper chaperone Cox17. Biochem J. 408(1): 139-148.

Wallenberg, M., Olm, E., Hebert, C., Björnstedt, M. and Fernandes A.P. (2010) Selenium compounds are substrates for glutaredoxins: a novel pathway for selenium metabolism and a potential mechanism for selenium-mediated cytotoxicity. Biochem J. 429(1): 85-93.

Webb, C.T., Gorman, M.A., Lazarou, M., Ryan, M.T. and Gulbis, J.M. (2006) Crystal structure of the mitochondrial chaperone TIM9.10 reveals a six-bladed alpha-propeller. Mol Cell. 21: 122-123.

Weckbecker, D., Longen, S., Riemer, J. and Herrmann, H. (2012) Atp23 biogenesis reveals a chaperone-like folding activity of Mia40 in the IMS of mitochondria. The EMBO Journal, 1-11.

Wells, W.W, Yang, Y., Deits, T.L.and Gan, Z.R. (1993) Thioltransferases. Adv Enzymol relat Areas Mol Biol. 66: 149-201.

Wheeler, G.L. and Grant, C.M. (2004) Regulation of redox homeostasis in the yeast Saccharomyces cerevisiae. Physiol Plant. 120(1): 12-20.

Wiedemann, N., Kozjak, V., Chacinska, A., Schönfisch, B., Rospert, S., Ryan, M.T., Pfanner, N. and Meisinger, C. (2003) Machinery for protein sorting and assembly in the mitochondrial outer membrane. Nature 424(6948): 565-571.

Yaffe, M.P. (2003) The cutting edge of mitochondrial fusion. Nat cell Biol. 5: 97-499.

Young, J.C., Hoogenraad, N.J. and Hartl, F.U. (2003) Molecular chaperones Hsp90 and Hsp70 deliver preproteins to the mitochondrial import receptor Tom70. Cell 112(1):41-50.

Zahedi Avval, F. and Holmgren, A. (2009) Molecular mechanisms of thioredoxin and glutaredoxin as hydrogen donors for Mammalian s phase ribonucleotide reductase. J Biol Chem. 284(13): 8233-40.

Zapun, A., Bardwell, J.C. and Creighton, T.E. (1993) The reactive and destabilizing disulfide bond of DsbA, a protein required for protein disulfide bond fomation in vivo. Biochemistry 32(19): 5083-5092.

Zara, V., Palmisano, I., Rassow, J. and Palmieri, F. (2001) Biogenesis of the dicarboxylate carrier (DIC): translocation across the mitochondrial outer membrane and subsequent release from the TOM channel are membrane potential-independent. J Mol Biol. 310(5): 965-71.

Zwizinski, C., Schleyer, M. and Neupert, W. (1984) Proteinaceous receptors for the import of mitochondrial precursor proteins. J Biol Chem. 259(12): 7850-7856.

8. APPENDICES

8.1 Appendix 1: List of primary antibodies used in this study.

Table 2.3. List of the primary antibodies used for this study (all obtained from rabbit unless otherwise stated).

Antibody	Dilution	Localisation	Notes
Tom5	1:350	OM	Dr Jan Brix, Germany
Tom40	1:4000	OM	Lab stock
Tom70	1:6000	OM	Lab stock
Tom22	1:6000	OM	Lab stock
Tom20	1:4000	OM	Lab stock
Tim9	1:1000/2000	IMS	R844
Tim10	1:1000/2000	IMS	R843
Tim13	1:1000/2000	IMS	Lab stock
Cytb2	1:5000	IMS	BG-532-T
AAC	1:6000	IM	Lab stock
Mia40	1:2000	IM/IMS	Lab stock
mtHsp60	1:5000	matrix	Lab stock
mtHsp70	1:6000	matrix	KS-3111 (Prof. KostasTokatlidis, Greece)
GrpE	1:2000	Matrix	Lab stock
Cpn10	1:2000	Matrix	Lab stock
Grx1/2	1:500/1000	OM and matrix	Chris Grant (Manchester)
Trx1/2	1:500/1000	cytosol	Chris Grant (Manchester)
KDH	1:2000	matrix	Lab stock
MDH	1:2000	matrix	Lab stock
G-6-PDH	1:1000	cytosol	Sigma

8.2 Appendix 2:

Publication: Durigon *et al.,* EMBO *reports* 2012*(*13): 916-922.

EMBO reports

scientific report

Cytosolic thioredoxin system facilitates the import of mitochondrial small Tim proteins

Romina Durigon[1], Qi Wang[1], Efrain Ceh Pavia[1], Chris M. Grant[2] & Hui Lu[1+]

[1]Manchester Institute of Biotechnology, Faculty of Life Sciences, and [2]Faculty of Life Sciences, University of Manchester, Manchester, UK

Thiol-disulphide redox regulation has a key role during the biogenesis of mitochondrial intermembrane space (IMS) proteins. Only the Cys-reduced form of precursor proteins can be imported into mitochondria, which is followed by disulphide bond formation in the mitochondrial IMS. In contrast to the wealth of knowledge on the oxidation process inside mitochondria, little is known about how precursors are maintained in an import-competent form in the cytosol. Here we provide the first evidence that the cytosolic thioredoxin system is required to maintain the IMS small Tim proteins in reduced forms and facilitate their mitochondrial import during respiratory growth.

Keywords: redox regulation; mitochondrial import; thioredoxin; oxidoreductase; folding

EMBO *reports* advance online publication 10 August 2012; doi:10.1038/embor.2012.116

INTRODUCTION

Mitochondria has important roles in various regulatory processes ranging from ATP generation to cell growth and apoptosis. Not surprisingly, therefore, mitochondrial dysfunction leads to life-threatening diseases, including diabetes, stroke, Alzheimer, and cancer. Protein import is essential for the biogenesis of mitochondria, as the majority (99%) of mitochondrial proteins are synthesized in the cytosol on cytosolic ribosomes, and thus have to be imported into mitochondria for their function. How precursor proteins are imported into mitochondria is a subject of intensive study and at least four main import pathways have now been characterized [1,2]. In contrast, little is known about how mitochondrial precursors are maintained in an import-competent form in the cytosol.

The import of many essential mitochondrial intermembrane space (IMS) proteins is regulated by their thiol-disulphide redox state [3–6]. Although disulphide bond formation is crucial for the function of these proteins inside mitochondria, oxidized precursor proteins cannot be imported into mitochondria and only Cys-reduced forms are import-competent [5,7,8]. Many IMS proteins, such as members of the 'small Tim' (e.g., Tim9, Tim10) and Cox17 (e.g., Cox17, Cox19) families, contain conserved Cys residues. Import of these proteins depends on the redox-sensitive mitochondrial import and assembly (MIA) pathway. Mia40 and Erv1 are the central components of the MIA pathway; they form a disulphide relay system in the IMS mediating the import and oxidative folding of these Cys-containing proteins [2,9].

Using the small Tim proteins as models, it has been shown that the oxidized proteins are thermodynamically stable under cellular glutathione redox conditions [7,10,11]. These proteins have a standard redox potential of -0.31 V to -0.33 V, which is more negative than that of the glutathione redox conditions in both the cytosol and mitochondrial IMS [7,10,12,13]. Such a redox stability of the small Tim proteins is consistent with their oxidized (disulphide bonded) state in the IMS, but not their reduced (thiol) states in the cytosol. Furthermore, studies showed that the precursors become oxidized during mitochondrial import and that this oxidation kinetically competes with their import [7]. Cytosolic factors are required to maintain these redox-sensitive precursors in a Cys-reduced, import-competent form in the cytosol before their import into mitochondria. Although zinc-binding can stabilize the small Tim proteins in their reduced forms *in vitro*, their relatively low-binding affinities (submicromolar to nanomolar) suggest that zinc-binding might not be the only or an important stabilizing factor during normal cell growth conditions [14,15]. How these redox-sensitive IMS precursors are maintained in an import-competent form in the cytosol is unknown.

The thioredoxin (Trx) and glutaredoxin (Grx) systems are ubiquitous oxidoreductases required for cellular thiol regulation and oxidative stress defence [16,17]. In the yeast *Saccharomyces cerevisiae*, there are two cytosolic Trx homologues (Trx1, 2) and two classical dithiol Grx homologues (Grx1, 2) located in the cytosol. A main function of these enzymes is to reduce disulphide bonds in their substrate proteins using electrons donated by nicotinamide adenine dinucleotide phosphate (NADPH). Oxidized Trx is reduced directly by NADPH and thioredoxin reductase (Trr), whereas Grx is reduced by glutathione using electrons donated by

[1]Manchester Institute of Biotechnology, Faculty of Life Sciences, University of Manchester 131 Princess Street, Manchester M1 7DN,
[2]Faculty of Life Sciences, University of Manchester, Oxford Road, Manchester M13 9PT, UK
[+]Corresponding author. Tel: +44 161 2751553; Fax: +44 161 3065201;
E-mail: hui.lu@manchester.ac.uk

Received 28 January 2012; revised 5 July 2012; accepted 13 July 2012; published online 10 August 2012

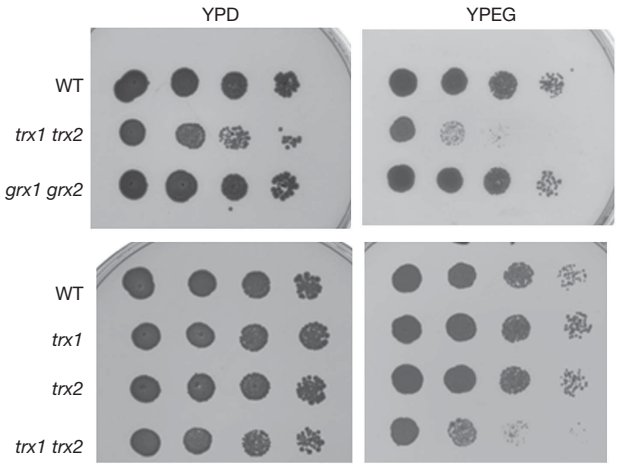

Fig 1 | The cytosolic Trx system is required for mitochondrial function. (**A**) Spot testing of cell growth with the wild-type (WT) and mutant yeast strains. The WT, *trx1 trx2* and *grx1 grx2* double or *trx1* and *trx2* single-deletion strains were spotted on YPD (left column) and YPEG (right column) plates at a series of 10-fold dilutions, followed by incubation at 30 °C for 2 days. grx, glutaredoxin; Trx, thioredoxin.

NADPH through glutathione reductase (Glr). In this present study we show that the cytosolic Trx system is required for yeast growth under respiratory condition and facilitates the import of mitochondrial MIA substrates by maintaining the precursors in a reduced form. An efficient disulphide bond transfer reaction was reconstituted using purified proteins, and we show that the Trx system preferentially catalyses the reduction of folding intermediates, rather than the fully oxidized protein.

RESULTS AND DISCUSSION

The Trx system is required for respiratory growth

To determine whether the cytosolic Trx and Grx systems are required for mitochondrial function, the wild-type (WT), *trx* and *grx* mutant strains were spotted onto fermentative and respiratory growth media (Fig 1). Although a double *TRX* deletion mutant (*trx1 trx2*) grows somewhat slower than the WT strain during fermentative growth (YPD), it is particularly inhibited for growth under respiratory conditions (YPEG). In contrast, the double *GRX* deletion mutant (*grx1 grx2*) grew comparably to the WT under both conditions. These results indicate that the Trx system might have an important role during the biogenesis of mitochondria. Growth of both the *trx1* and *trx2* single mutants was unaffected under respiratory conditions, consistent with an overlapping role for the two Trx proteins. This indicates that the respiratory growth defect of *TRX* deletion mutant (*trx1 trx2*) is not simply because of respiratory reactive oxygen species (ROS) production, as *trx2* mutants are hypersensitive to ROS, in contrast to *trx1* mutants that have WT levels of resistance [18]. Taken together, these results indicate that the cytosolic Trx system is required for maintaining mitochondrial function and probably facilitating the biogenesis of mitochondria. However, we cannot rule out that the defects seen in the *trx1 trx2* mutant strain is also contributed by other effects, as Trx proteins participate in various processes and have many client proteins.

To assess the function of Trx in biogenesis of mitochondrial proteins, protein expression was examined. While antibodies against Trx and Grx confirmed the deletion of these proteins, there were no obvious differences in the levels of the mitochondrial proteins (Mia 40 and MtHsp 70), although Tim9 and Tim10 seem to be slightly decreased in the *trx1 trx2* mutant (Fig 2A). To check this, mitochondria were isolated from the WT and mutant cells grown in YPEG, and protein concentrations determined. The steady-state levels of mitochondrial proteins from all four subcompartments are similar (not shown). This was not surprising, as the mutant was not unviable but grows slowly, and a small intensity difference will not be detectable by western blot. A similar result was shown for a *TOM5* (a non-essential component of the mitochondrial TOM translocase complex) deletion mutant [19]. Thus, the levels of the mitochondrial proteins under more stressful conditions were analysed. Cells were grown in fermentative YPD followed by a medium shift to respiratory YPEG for 6 h before mitochondria were isolated. The results clearly showed that the levels of the small Tim proteins (Tim9, Tim10 and Tim13) were decreased in the mitochondria of the *trx1 trx2* mutant strain, while no obvious decrease was observed for the other control proteins (Fig 2B). The same mitochondrial isolation and western blotting experiment were performed three times, and the levels of the small Tim proteins of the mutant strain were statistically lower than that of the WT strain ($P<0.05$, Fig 2C). These results provide *in vivo* evidence that the cytosolic Trx system is involved in facilitating biogenesis of the mitochondrial small Tim proteins.

The Trx system facilitates the import of IMS proteins *in vitro*

To verify whether the Trx system has an effect on the import of mitochondrial proteins, mitochondrial import was examined using radiolabelled Tim9 and Tim10, synthesized in rabbit reticulocyte lysates, in the presence or absence of purified Trx1, Trr1 and/or NADPH. To eliminate the effect of metal ions such as Zn^{2+}, all import experiments were carried out in the presence of 2 mM EDTA. After import for 30 min, reactions were treated with trypsin to remove un-imported materials, and mitochondrial import was analysed using SDS–PAGE (Fig 3A), revealing that in the presence of the Trx1 system (lane 2) the import level was increased compared with the control (lane 1; Fig 3A). A partial Trx system (without Trx1 or Trr1) slightly enhanced the import level, but not as efficiently as the full system. It should be noted that small amounts of the Trx and/or Grx system components might be present in reticulocyte lysates; however, the addition of the purified yeast system clearly increased import (lane 1 versus lane 2) confirming that the Trx system facilitates import of the small Tim proteins. The same effect was observed when Cox19, a CX_9C motif containing substrate of the MIA pathway (Fig 3A), was used as an import substrate. In contrast, no obvious effect was observed on the import of the matrix marker proteins F_1-ATPase subunit-β ($F_1β$) and mtHsp60, the inner membrane (IM) protein AAC, or the outer membrane porin. A time-course experiment confirmed that the Trx system increases the import of the small Tim proteins (Fig 3B). While the import seems to reach a stationary level after 5 min in the absence of Trx system, it was continuously increased with the presence of the Trx system over the whole time course. Furthermore, an 4-acetamido-4′-maleimidylstilbene-2,2′-disulfonic acid (AMS) assay showed that the redox state of mitochondrial Mia 40 was not

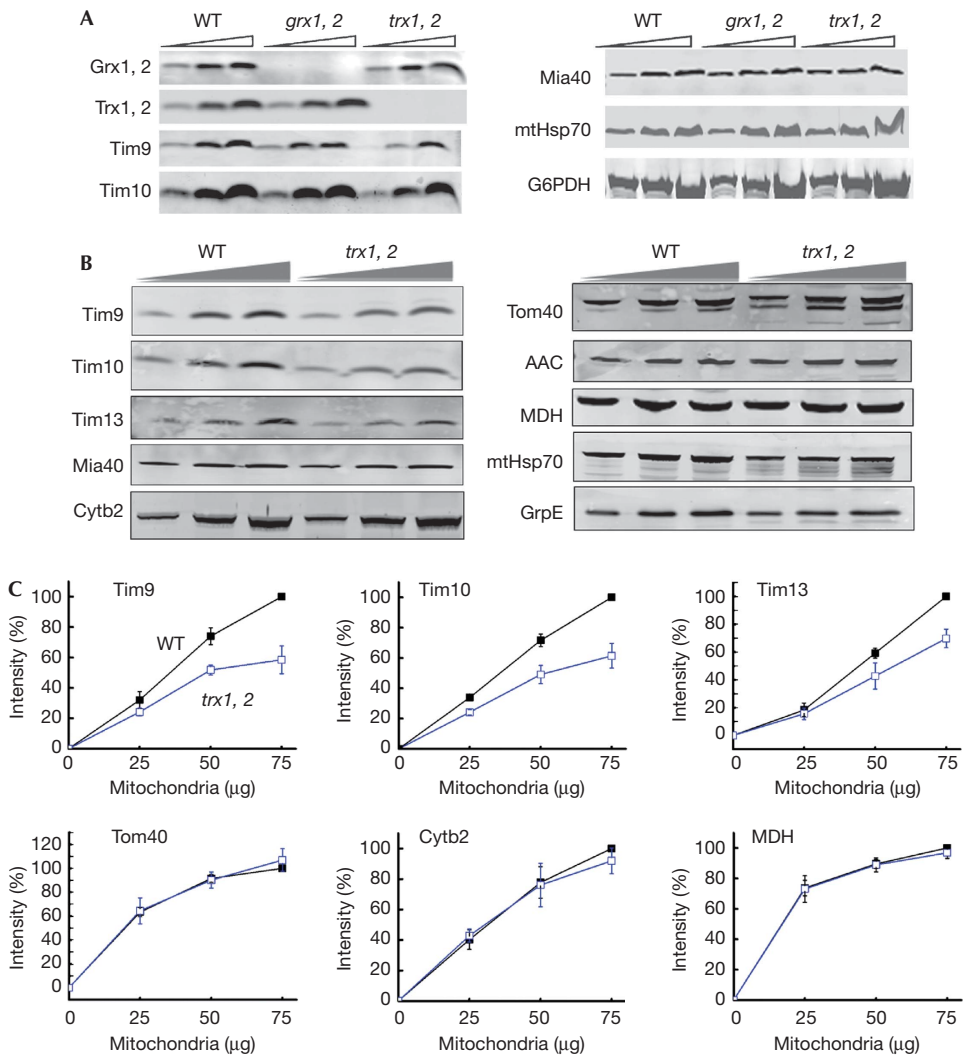

Fig 2 | Effects of the Trx system on protein expression level. (**A**) Western blots of cellular extracts from the wild-type (WT) and mutant cells. Yeasts were grown to exponential phase in YPEG medium, then lysed and analysed using antibodies against the indicated proteins. Cytosolic protein G6PDH was used as a loading control. (**B**) Western blots with mitochondria isolated from the WT and mutant cells. The WT and *trx1 trx2* yeast cells were grown in YPD to OD_{600} of 10 and shifted to YPEG for 6 h. Then mitochondria were isolated and analysed using antibodies against the indicated proteins. 25, 50 and 75 µg mitochondria were loaded. The IMS proteins (Tim9, Tim10, Tim13 and Cytb2); Mia40: IMS/IM anchored; the outer membrane Tom40; IM AAC; and matrix protein malate dehydrogenase (MDH), mtHsp70 and co-chaperone GrpE were analysed. (**C**) Quantification of proteins in the mitochondria isolated from the WT (black solid squares) and *trx1 trx2* (blue open squares) cells as described in **B**. The levels of the small Tim proteins were significantly different (by Student's *t*-test: Tim10 $P<0.05$ at all points, Tim9 and Tim13 $P<0.05$ at 50 and 75 µg), and not significantly different for the marker proteins. Error bars represent s.e. ($n=3$). grx, glutaredoxin; IM, inner membrane; IMS, intermembrane space; Trx, thioredoxin.

affected by the addition of the components of Trx system in the reactions (Fig 3C), and Mia 40 was mainly in the oxidized state as shown previously [20]. Taken together, these results indicate that (i) the Trx system selectively facilitates the import of the redox-sensitive precursors of mitochondrial IMS proteins, and (ii) the general mitochondrial import machineries are not affected by the presence of the Trx system.

The Trx system keeps small Tims in reduced forms

We anticipated that the mechanism of enhanced import of the small Tim proteins was that the Trx system can maintain the precursors in a reduced form. To confirm this idea, following the import assay described above, the redox state of the remaining un-imported proteins was analysed using the AMS thiol-modification assay (Fig 4A). The results indicate that while all the un-imported proteins were oxidized in the control (lane 1), the Trx1 system can maintain a large fraction of the proteins in a reduced form (lane 2). A small fraction of reduced proteins also existed in the reaction containing Trx1 (lane 4), but not Trr1 alone (lane 3). The same result was obtained for both Tim9 and Tim10.

Our results indicate that the presence of the Trx system causes an increased level of reduced precursors, and improved import of

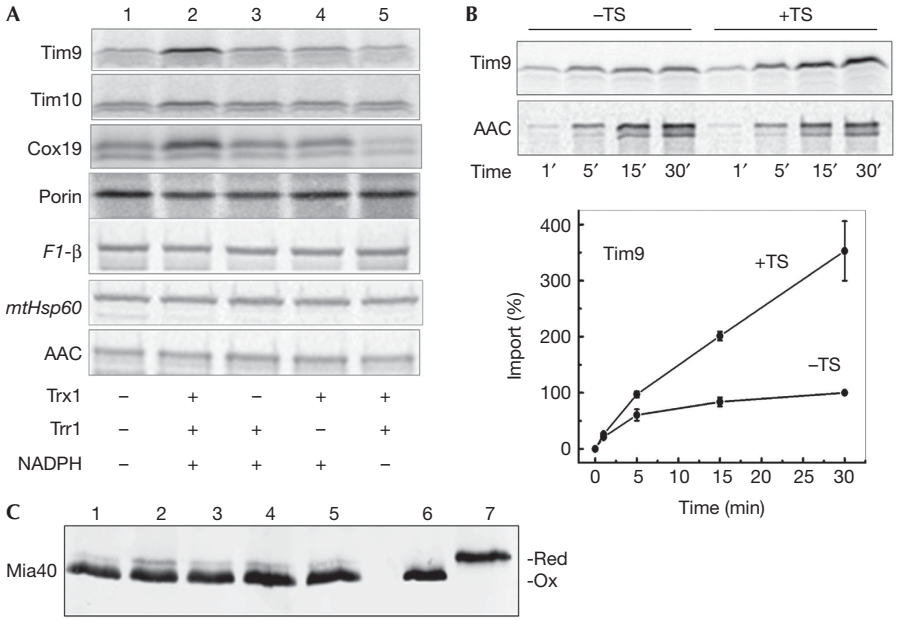

Fig 3 | The Trx system facilitates the import of MIA substrates. (**A**). Effects of Trx system on the mitochondrial import. *In vitro* translated radioactive precursor proteins as indicated were incubated with isolated mitochondria in the presence or absence of the purified Trx system at 25 °C for 30 min, followed by trypsin treatment to remove un-imported proteins. Then, all mitochondrial imports were analysed by SDS–PAGE and autoradiography. (**B**) Time course of Tim9 and AAC import in the presence (+TS) or absence (−TS) of the Trx system, and the qualification for Tim9 (bottom, −TS, 30 min as 100%). Error bars represent s.e. ($n >= 3$). (**C**) Western blot of 4-acetamido-4′-maleimidylstilbene-2,2′-disulfonic acid assay of Mia40 after incubating with components of Trx system at 25 °C for 20 min. Lanes 1–5 as in **A**, lanes 6 and 7 were oxidized (Ox) and reduced (Red) controls. MIA, mitochondrial import and assembly; NADPH, nicotinamide adenine dinucleotide phosphate; TS, Trx system; Trr, thioredoxin reductase; Trx, thioredoxin.

these precursors. However, as the mitochondrial import system contains many components, it remained possible that our results could be because of an indirect effect of the Trx system on some of these components. To address this, we asked whether the Trx system can directly reduce disulphide bonds of the small Tim proteins. Purified oxidized Tim10 was incubated with purified Trx1 in the presence and absence of purified Trr1 for 10 min, followed by the AMS assay. The results showed that a fraction of Tim10 was reduced by the presence of the Trx1 system (Fig 4B, lane 3), suggesting that Tim10 is a substrate of the Trx1 system. Consistently, the small Tim proteins cannot be reduced by Trx1 or Trr1 alone (lanes 2 and 4; note that in the absence of Trr1, Trx1 was in the oxidized inactive form). Thus the small Tim proteins can be reduced by the Trx system directly. However, only a fraction of the protein was reduced under these experimental conditions, indicating that the fully oxidized proteins might not be very good substrates of the Trx1 system.

Small Tims proteins are good substrates of Trx system

There are two intramolecular disulphide bonds in Tim9 and Tim10 formed between the Cys residues of the twin CX3C motif in juxtaposition (C1–C4, and C2–C3). Previous work showed that oxidative folding of the small Tim proteins occurs through formation of single disulphide–bonded intermediates and that these intermediates are also import-incompetent [7]. Thus, we asked whether the Trx system can reduce these folding intermediates more efficiently. For this, double Cys mutants with each disulphide bond mutated to Ser (C1,4S and C2,3S) were used. As shown in Fig 4C, all the Cys mutants can be fully reduced by the Trx1 system, and a time-course analysis confirmed that reduction of the mutants was very rapid. While only about 10% of native Tim10 was reduced after 10 min, all of the single disulphide–bonded mutants were reduced within 1 min (Fig 4D). Thus, reduction of the single-disulphide intermediates by the Trx1 system is at least 100-fold faster than that of the fully oxidized proteins.

To obtain more quantitative results, the reactions were measured by following absorption changes at 340 nm because of NADPH oxidation (Fig 5A), and the results were analysed using the Michaelis–Menten equation (Fig 5B). The catalytic constant k_{cat} and Michaelis constant K_m were determined to be 23 min^{-1} and 6.0 μM for Tim10C1,4S, and 29.0 min^{-1} and 5.3 μM for Tim10C2,3S, respectively, and the substrate efficiency (k_{cat}/K_m) was 3.8×10^6 M^{-1} min^{-1} for Tim10C1,4S, and 5.5×10^6 M^{-1} min^{-1} for Tim10C2,3S. This substrate efficiency is similar to that of the well-characterized substrates of Trx, such as ribonucleotide reductase, arsenate reductase and insulin [21–23]. This result confirms that both single-disulphide intermediates are excellent substrates of the Trx system, supporting our conclusion that the Trx system maintains the small Tim proteins in a reduced form in the cytosol and thus facilitates their mitochondrial import.

To understand why the Cys mutants, but not the WT proteins, are excellent substrates of the Trx system, overall folding of

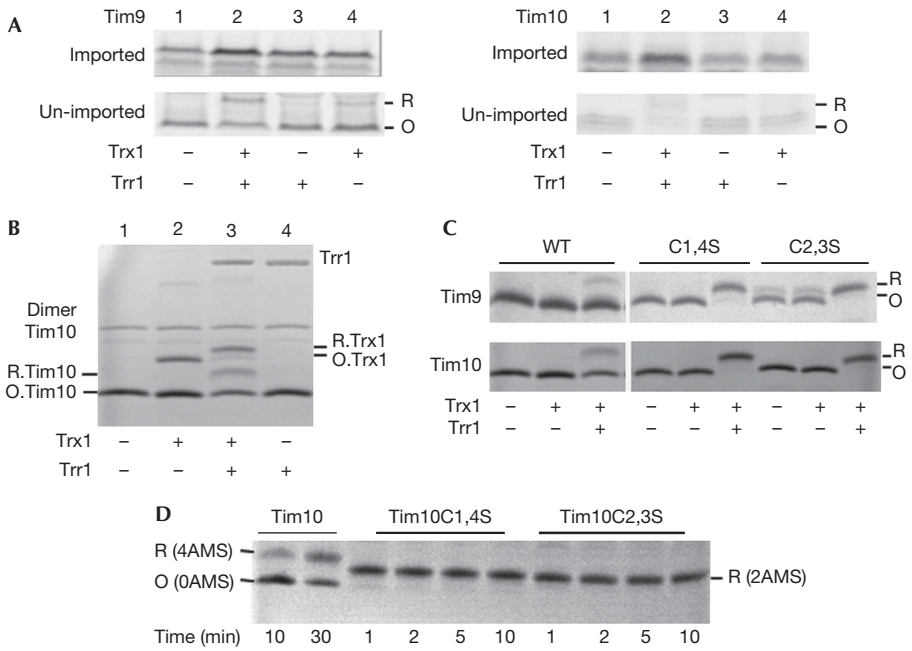

Fig 4 | Effects of Trx system on the redox state of Tim9 and Tim10. (**A**) Import and the redox state of un-imported small Tim proteins. The proteins were imported in the presence or absence of Trx system (TS: 1.5 μM Trx1, 0.5 μM Trr1 and 0.6 mM NADPH) at 25 °C for 30 min, and then each reaction was divided into two. One treated with trypsin for import analysis (top panels), the other was centrifuged and the supernatant was treated with AMS (bottom panels). (**B**) The Trx system reduces disulphide bonds of purified Tim10. Tim10 (10 μM) was incubated with 0.6 mM NADPH in the presence and absence of Trx1 (1.5 μM) and/or Trr1 (0.5 μM) at 25 °C for 10 min. Then the redox state was analysed by AMS assay. (**C**) AMS assay of the WT and double Cys mutant of Tim9 and Tim10 as described in **B**. (**D**) Time course of the reduction of WT and mutant Tim10 by the Trx system. (**B–D**), SDS–PAGE with Coomassie staining. The reduced (R) and oxidized (O) states are indicated. AMS, 4-acetamido-4′-maleimidylstilbene-2,2′-disulfonic acid; NADPH, nicotinamide adenine dinucleotide phosphate; Trr, thioredoxin reductase; Trx, thioredoxin; WT, wild-type.

these proteins was studied using far-ultraviolet circular dichroism (CD; Fig 5C). As shown previously, the WT proteins are folded with α-helical structure, which becomes unfolded on addition of a reducing agent, Tris(2-carboxyethyl)phosphine (TCEP). Clearly, both double Cys mutants of Tim10 display significantly lower CD signals than the oxidized WT protein (Fig 5C curves a, b and c). Oxidized Tim10C1,4S seems to be as unfolded as the reduced protein, and there is no obvious spectrum change on addition of TCEP (curves b and e). In comparison to the WT protein, Tim10C2,3S is partially folded and becomes unfolded on addition of TECP (curves c and f). Thus, together with the above enzyme kinetic study, our results revealed that the Trx enzymes preferably react with Tim10 in an unfolded or partially folded state. In other words, the Trx enzymes react with the folding intermediates preferably and effectively rather than the folded small Tim proteins, indicating a stereoselective control mechanism. This result is consistent with the fact that all the well-known substrate proteins of the Trx enzymes have a solvent-exposed disulphide bond. Such a stereoselective mechanism will not only allow the enzyme to recognize a wide range of substrates, but also to reduce disulphide bonds effectively at an early stage of protein folding. We presume that apart from the small Tim proteins, many more redox-sensitive proteins can be maintained in a reduced state through the redoxin system by preventing the formation of early folding intermediates.

CONCLUSION

In summary, whereas the MIA pathway is used for import and oxidative folding of many Cys-containing IMS proteins inside mitochondria, here we provide the first evidence that the cytosolic Trx system is required to keep the precursors in a reduced form in the cytosol and thus to facilitate their mitochondrial import. The Trx system specifically facilitates the import of redox-sensitive IMS proteins without affecting matrix and membrane proteins, through an efficient disulphide bond transfer reaction that could be reconstituted using purified proteins. Further, we show that single-disulphide folding intermediates of the small Tim proteins are excellent substrates of the Trx system. The Trx enzyme preferentially recognizes unfolded or partially folded Tim10, and thus catalyses the reduction of the folding intermediates rather than the fully oxidized small Tim proteins. Our findings provide important insight into the initial steps of mitochondrial protein biogenesis, specifically how mitochondrial precursors are maintained in an import-competent form in the cytosol.

METHODS

Materials. 4-Acetamido-4′-maleimidylstilbene-2,2′-disulfonic acid were obtained from Invitrogen Molecular Probes. EDTA was from BDH Co, and all other chemicals were obtained from the Sigma at the highest grade. The *yeast* strains used in this study were the isogenic derivatives of W303 as described previously [18].

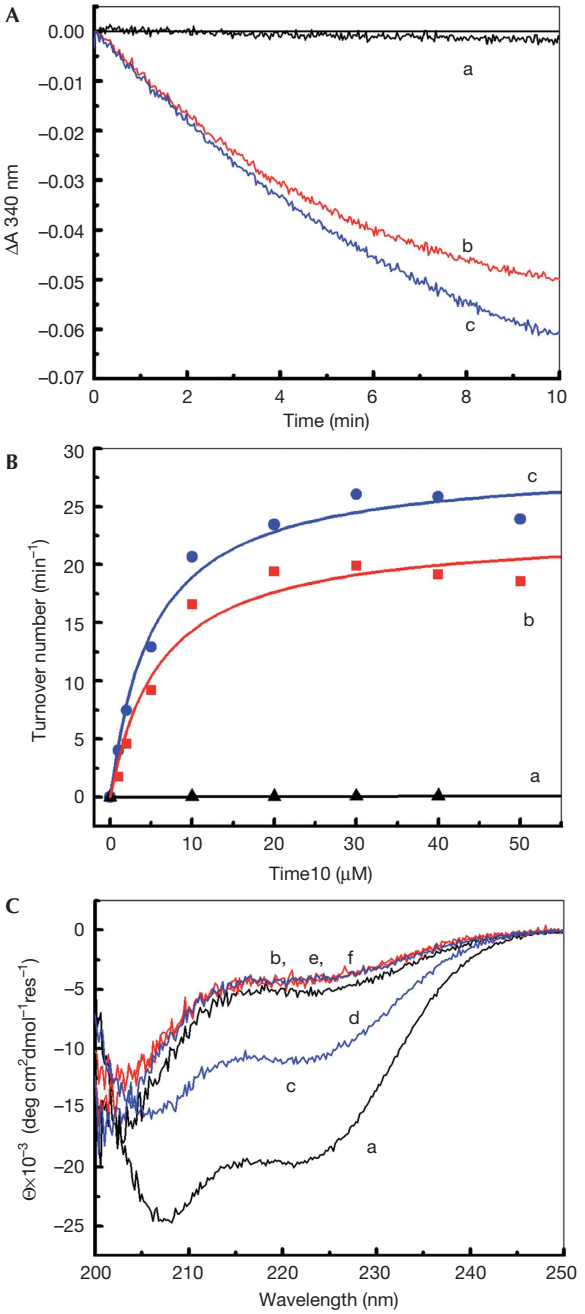

Fig 5 | Kinetic and structural analysis of the WT and mutant Tim10. (**A**) Time course of absorption change at 340 nm for 10 μM Tim10 WT (a), Tim10C1,4S (b) or Tim10C2,3S (c) in the presence of 0.1 μM Trx, 0.1 μM Trr1 and 140 μM NADPH, after subtraction of blank reaction in the absence of Tim10. (**B**) Michaelis–Menten plots of the WT (a), Tim10C1,4S (b) and Tim10C2,3S (c) as studied in **A**. The k_{cat} and K_m were determined to be 23 min^{-1}, 6.0 μM for Tim10C1,4S, and 29.0 min^{-1}, 5.3 μM for Tim10C2,3S, respectively. (**C**) Far-ultraviolet circular dichroism spectra of the WT Tim10 (a, d), Tim10C1,4S (b, e) and Tim10C2,3S (c, f), in the absence (a–c) or presence (d–f) of 1 mM TCEP at 25 °C for 1 h. NADPH, nicotinamide adenine dinucleotide phosphate; Trr, thioredoxin reductase; Trx, thioredoxin; WT, wild-type.

Protein preparations. Oxidized WT and mutant Tim10 were purified as described previously in buffer AE (50 mM Tris, pH 7.4, 150 mM NaCl, 1 mM EDTA) [10,24]. Trx1 and Trr1 were purified as described previously [25], and followed by gel filtration (Superde × 200 column). Flavin adenine dinucleotide was added to Trr1 before gel filtration. Trx1 concentration was determined using extinction coefficient of 10,095 $M^{-1} cm^{-1}$ at 280 nm, and Trr1 concentration was determined based on extinction coefficient of 11,300 $M^{-1} cm^{-1}$ for flavin adenine dinucleotide at 450 nm.

Miscellaneous. All experiments were carried out at 25 °C in buffer AE unless stated. AMS assay was performed as described in [7]. CD spectra were recorded as described in [14]. Mitochondria isolation and protein import analysis were performed as described previously [26,27]. All import reactions were performed in the presence of 2 mM EDTA. For steady-state levels of mitochondrial protein analyses, the WT and *trx1 trx2* yeast cells were first grown in YPD until OD_{600} of 10 and then, cells were isolated by centrifugation, washed twice with autoclaved milli-Q water, then shifted to grow in YPEG for 6 h before the mitochondria were isolated. For the Trx enzyme kinetic analysis, WT or mutant Tim10 (1–50 μM) was mixed with 0.1 μM Trx and 140 μM NADPH, and the reaction was initiated by adding 0.1 μM Trr1. The oxidation of NADPH was followed at 340 nm using a Cary300 spectrophotometer (Varian Ltd).

ACKNOWLEDGEMENTS

We thank to N. Pfanner, K. Hell and M. Pool for protein constructs; to M. Spiller for reading manuscript and helpful comments. H.L.'s research is supported by the Royal Society, Biotechnology and Biological Sciences Research Council and Leverhulme Trust.

Author contributions: H.L. designed the study. R.D., Q.W., E.C.P., C.M.G. and H.L. all designed and performed experiments. R.D., E.C.P. and H.L. analysed the experimental results. H.L. wrote the manuscript with input from C.M.G.

REFERENCES

1. Schmidt O, Pfanner N, Meisinger C (2010) Mitochondrial protein import: from proteomics to functional mechanisms. *Nat Rev Mol Cell Biol* **11:** 655–667
2. Chacinska A, Koehler CM, Milenkovic D, Lithgow T, Pfanner N (2009) Importing mitochondrial proteins: machineries and mechanisms. *Cell* **138:** 628–644
3. Herrmann JM, Hell K (2005) Chopped, trapped or tacked—protein translocation into the IMS of mitochondria. *Trends Biochem Sci* **30:** 205–211
4. Herrmann JM, Kauff F, Neuhaus HE (2009) Thiol oxidation in bacteria, mitochondria and chloroplasts: common principles but three unrelated machineries? *Biochim Biophys Acta* **1793:** 71–77
5. Lu H, Allen S, Wardleworth L, Savory P, Tokatlidis K (2004) Functional TIM10 chaperone assembly is redox-regulated *in vivo*. *J Biol Chem* **279:** 18952–18958
6. Mesecke N, Terziyska N, Kozany C, Baumann F, Neupert W, Hell K, Herrmann JM (2005) A disulfide relay system in the intermembrane space of mitochondria that mediates protein import. *Cell* **121:** 1059–1069
7. Morgan B, Lu H (2008) Oxidative folding competes with mitochondrial import of the small Tim proteins. *Biochem J* **411:** 115–122
8. Tokatlidis K (2005) A disulfide relay system in mitochondria. *Cell* **121:** 965–967
9. Hell K (2008) The Erv1-Mia40 disulfide relay system in the intermembrane space of mitochondria. *Biochim Biophys Acta* **1783:** 601–609
10. Lu H, Woodburn J (2005) Zinc binding stabilizes mitochondrial Tim10 in a reduced and import-competent state kinetically. *J Mol Biol* **353:** 897–910

11. Tienson HL, Dabir DV, Neal SE, Loo R, Hasson SA, Boontheung P, Kim SK, Loo JA, Koehler CM (2009) Reconstitution of the mia40-erv1 oxidative folding pathway for the small tim proteins. *Mol Biol Cell* **20:** 3481–3490
12. Hu J, Dong L, Outten CE (2008) The redox environment in the mitochondrial intermembrane space is maintained separately from the cytosol and matrix. *J Biol Chem* **283:** 29126–29134
13. Ostergaard H, Tachibana C, Winther JR (2004) Monitoring disulfide bond formation in the eukaryotic cytosol. *J Cell Biol* **166:** 337–345
14. Ivanova E, Ball M, Lu H (2008) Zinc binding of Tim10: Evidence for existence of an unstructured binding intermediate for a zinc finger protein. *PROTEINS: Struct Func Bioinf* **71:** 467–475
15. Lu H, Golovanov AP, Alcock F, Grossmann JG, Allen S, Lian LY, Tokatlidis K (2004) The structural basis of the TIM10 chaperone assembly. *J Biol Chem* **279:** 18959–18966
16. Holmgren A (1989) Thioredoxin and glutaredoxin systems. *J Biol Chem* **264:** 13963–13966
17. Meyer Y, Buchanan BB, Vignols F, Reichheld JP (2009) Thioredoxins and glutaredoxins: unifying elements in redox biology. *Annu Rev Genet* **43:** 335–367
18. Garrido EO, Grant CM (2002) Role of thioredoxins in the response of *Saccharomyces cerevisiae* to oxidative stress induced by hydroperoxides. *Mol Microbiol* **43:** 993–1003
19. Dietmeier K, Honlinger A, Bomer U, Dekker PJ, Eckerskorn C, Lottspeich F, Kubrich M, Pfanner N (1997) Tom5 functionally links mitochondrial preprotein receptors to the general import pore. *Nature* **388:** 195–200
20. Terziyska N, Grumbt B, Kozany C, Hell K (2009) Structural and functional roles of the conserved cysteine residues of the redox-regulated import receptor Mia40 in the intermembrane space of mitochondria. *J Biol Chem* **284:** 1353–1363
21. Zahedi Avval F, Holmgren A (2009) Molecular mechanisms of thioredoxin and glutaredoxin as hydrogen donors for Mammalian s phase ribonucleotide reductase. *J Biol Chem* **284:** 8233–8240
22. Messens J, Van Molle I, Vanhaesebrouck P, Limbourg M, Van Belle K, Wahni K, Martins JC, Loris R, Wyns L (2004) How thioredoxin can reduce a buried disulphide bond. *J Mol Biol* **339:** 527–537
23. Holmgren A (1979) Thioredoxin catalyzes the reduction of insulin disulfides by dithiothreitol and dihydrolipoamide. *J Biol Chem* **254:** 9627–9632
24. Ivanova E, Jowitt TA, Lu H (2008) Assembly of the mitochondrial Tim9-Tim10 complex: a multi-step reaction with novel intermediates. *J Mol Biol* **375:** 229–239
25. Mukhopadhyay R, Shi J, Rosen BP (2000) Purification and characterization of ACR2p, the *Saccharomyces cerevisiae* arsenate reductase. *J Biol Chem* **275:** 21149–21157
26. Meisinger C, Pfanner N, Truscott KN (2006) Isolation of yeast mitochondria. *Methods Mol Biol* **313:** 33–39
27. Morgan B, Ang SK, Yan G, Lu H (2009) Zinc can play chaperone-like and inhibitor roles during import of mitochondrial small Tim proteins. *J Biol Chem* **284:** 6818–6825